

Molecular understanding of cytoneme-based Wnt trafficking

Zur Erlangung des akademischen Grades eines

DOKTORS DER NATURWISSENSCHAFTEN

(Dr. rer. nat.)

von der KIT-Fakultät für Chemie und Biowissenschaften
des Karlsruher Instituts für Technologie (KIT)

genehmigte

DISSERTATION

von

Benjamin Mattes

1. Referent: Assoc. Prof. Dr. Steffen Scholpp

2. Referent: Prof. Dr. Martin Bastmeyer

Tag der mündlichen Prüfung: 17.10.2018

Erklärung der Urheberschaft

Ich erkläre hiermit an Eides statt, dass ich die vorliegende Arbeit selbstständig und ohne Benutzung anderer als der angegebenen Hilfsmittel angefertigt habe. Die aus fremden Quellen direkt oder indirekt übernommenen Gedanken sind als solche gekennzeichnet. Des Weiteren habe ich die Satzung der Universität Karlsruhe (TH) zur Sicherung guter wissenschaftlicher Praxis in der jeweils gültigen Fassung beachtet. Diese Arbeit wurde bisher weder in gleicher noch in ähnlicher Form einer anderen Prüfungsbehörde vorgelegt und auch nicht veröffentlicht.

Ort und Datum:

Unterschrift:

Karlsruhe,

.....

.....

(Benjamin Mattes)

Abstract

Cell-to-cell communication by signaling proteins is essential to orchestrate development and tissue homeostasis in all multicellular organisms. The highly conserved family of Wnt proteins are important guiding cues to control these processes. Fundamental to this complex signaling network are relatively small and defined signaling centers in a given tissue that produce and distribute Wnt proteins. Adjacent, larger groups of cells respond to these spatial and temporal information in a concentration-dependent manner and adjust their transcriptional program. However, a regulated sequence of morphogen activity is required to generate a fine-tuned communication network. Therefore, a controlled propagation machinery must ensure accurate signal distribution from the source to the surrounding tissue to initiate the correct developmental path.

In this thesis, I consolidated the knowledge of the molecular machinery controlling cytoneme formation in zebrafish development. I expanded this principle to other aspects of Wnt signaling such as cancer growth and tissue homeostasis. Via a screening approach, I identified the receptor tyrosine kinase Ror2 as a promoting factor for cellular protrusions in general and particularly for Wnt8a cytonemes in cultured cells and *in vivo*. Consistently, I described the novel ligand-receptor pair Wnt8a and Ror2 by measuring the affinity for membrane accumulations and by biophysical imaging applications such as fluorescence correlation spectroscopy. Subsequently, functional interaction and transduction of the Wnt/PCP pathway was demonstrated during zebrafish convergence and extension and during non-canonical reporter activation in *Xenopus*. Wnt8a and Ror2 are considered to act in mutually repressive pathways, although the autocrine interplay for cytoneme formation to facilitate paracrine Wnt/ β -catenin dissemination seems to be conserved. Thus, the model can be applied to other systems: The transcriptional β -catenin level and resulting proliferation of gastric cancer cells can be regulated by Ror2, thereby only disrupting the signal transmitting transport machinery in the source cells. Furthermore, I provided evidence of an *ex vivo* human stem cell organoid system, where growth and survival require cytoneme-mediated Wnt proteins from isolated myofibroblasts. Remarkably, this setup resembles an innovative approach for stem cell maintenance in the murine intestinal crypt and expands the potential roles of cytonemes in development, tissue homeostasis and diseases.

Acknowledgements

I'm very grateful to Dr. Steffen Scholpp for providing me with the possibility to work on this fascinating project. I want to thank him for his guidance, encouragement, and scientific advice throughout all these years.

I would like to thank Prof. Dr. Martin Bastmeyer to accept as my second referent and for evaluating my PhD thesis.

I would like to thank Dr. Thomas Dickmeis and Dr. Gary Davidson for helpful advice and discussions as part of my TAC committee.

I would like to thank all my previous Lab members who accompanied me in all the time at the ITG. I would especially thank Sabrina Weber, Dr. Bernadette Boesze, Dr. Eliana Stanganello, Dr. Simone Geyer, and Yonglong Dang for a great and fun time together and a productive work atmosphere. Particularly, I would like to thank Bernadette for her advice on this thesis.

I would like to thank Dr. Lucy Brunt, Lauren Porter, Simone Schindler and Jenna Corcoran for an amazing last period of my PhD in Exeter and for both helpful discussions and physical balance.

I would like to thank my collaboration partners. I would like to thank Prof. Suat Özbek and Dr. Lilian Kaufmann for the intriguing insight into the *Xenopus* model, Prof. Ulrich Nienhaus and Dr. Benedikt Prunsche for FCS support, and Prof. David Virshup and Dr. Gediminas Greicius for their remarkable organoid addition.

I would like to express a special gratitude to my parents, all my friends, and especially my wife Daniela, who gave me the strength and endurance I needed to always continue and accomplish this work.

List of publications

Mattes, B., Y. Dang, G. Greicius, L.T. Kaufmann, B. Prunsche, J. Rosenbauer, J. Stegmaier, R. Mikut, S. Özbek, G.U. Nienhaus, A. Schug, D.M. Virshup, and S. Scholpp. 2018. Wnt/PCP controls spreading of Wnt/ β -catenin signals by cytonemes in vertebrates. *Elife*. 7:1–28.

Brinkmann, E.M., **B. Mattes**, R. Kumar, A.I.H. Hagemann, D. Gradl, S. Scholpp, H. Steinbeisser, L.T. Kaufmann, and S. Özbek. 2016. Secreted Frizzled-related Protein 2 (sFRP2) redirects non-canonical Wnt signaling from Fz7 to Ror2 during vertebrate gastrulation. *J. Biol. Chem.* 291:13730–13742.

Stanganello, E., A.I.H. Hagemann, **B. Mattes**, C. Sinner, D. Meyen, S. Weber, A. Schug, E. Raz, and S. Scholpp. 2015. Filopodia-based Wnt transport during vertebrate tissue patterning. *Nat. Commun.* 6:5846.

Mattes, B., S. Weber, J. Peres, Q. Chen, G. Davidson, C. Houart, and S. Scholpp. 2012. Wnt3 and Wnt3a are required for induction of the mid-diencephalic organizer in the caudal forebrain. *Neural Dev.* 7:12.

Mattes B, Scholpp S. Emerging role of contact-mediated cell communication in tissue development and diseases.

The manuscript has been submitted to *Histochemistry and Cell Biology*.

Rosenbauer J, **Mattes B**, Reinartz I, Wedgwood K, Schindler S, Sinner C, Scholpp S, Schug A. Modeling of Wnt-mediated Tissue Patterning in Vertebrate Embryogenesis

The manuscript has been submitted to PNAS.

Table of Contents

ABSTRACT.....	VII
ACKNOWLEDGEMENTS	IX
LIST OF PUBLICATIONS	X
TABLE OF CONTENTS	XI
FIGURE INDEX.....	XIV
ABBREVIATIONS.....	XVI
1. INTRODUCTION.....	1
1.1. DEVELOPMENT OF MULTICELLULAR ORGANISMS	1
1.2. ROLE OF MORPHOGENS DURING DEVELOPMENT	1
1.3. MORPHOGENS ORIGINATE FROM LOCAL ORGANIZING CENTERS.....	3
1.4. THE WNT SIGNALING PATHWAY	5
1.4.1. <i>Wnt signaling in development and disease</i>	5
1.4.2. <i>Molecular mechanism of Wnt signal transduction</i>	7
1.4.3. <i>Canonical Wnt/β-catenin pathway</i>	8
1.4.4. <i>The Wnt/β-catenin pathway during neural plate pattern formation</i>	10
1.4.5. <i>Non-canonical β-catenin independent pathway</i>	12
1.5. ROR-FAMILY RECEPTOR TYROSINE KINASES.....	15
1.5.1. <i>Domain architecture</i>	15
1.5.2. <i>Ror-family RTKs in development</i>	16
1.5.3. <i>Ror2 function as a Wnt receptor and its role in Wnt signal transduction</i>	17
1.6. WNT PROTEINS: STRUCTURE, MATURATION AND SECRETION	19
1.7. ACTIVE DISTRIBUTION MECHANISMS OF WNT MOLECULES	22
1.7.1. <i>Restricted diffusion by HSPGs</i>	23
1.7.2. <i>Free diffusion facilitated by Wnt binding proteins</i>	24
1.7.3. <i>Exovesicles as morphogen carrier</i>	25
1.7.4. <i>Contact-dependent signaling</i>	25
1.7.5. <i>Cargo transfer by tunneling nanotubes</i>	27
1.8. MORPHOGEN TRANSPORT BY CYTONEMES	29
1.8.1. <i>Discovery of cytonemes</i>	29
1.8.2. <i>Cytonemes in vertebrates</i>	30
1.8.3. <i>The role of Wnt Cytonemes during zebrafish neural plate patterning</i>	31
1.9. ZEBRAFISH AS A MODEL ORGANISM.....	33

1.11.	AIM OF THIS WORK.....	35
2.	MATERIAL AND METHODS.....	36
2.1.	MATERIALS	36
2.1.1.	<i>Equipment and tools</i>	36
2.1.2.	<i>Chemicals</i>	36
2.1.3.	<i>Solutions</i>	38
2.1.4.	<i>Kits</i>	39
2.1.5.	<i>Molecular tools and enzymes</i>	39
2.1.6.	<i>Nucleotides</i>	40
2.1.7.	<i>Plasmids</i>	41
2.1.8.	<i>Fish strains</i>	42
2.1.9.	<i>Cell lines</i>	42
2.1.10.	<i>Microscopes</i>	43
2.1.11.	<i>Software</i>	43
2.2.	METHODS	43
2.2.1.	<i>Molecular cloning</i>	43
2.2.2.	<i>Zebrafish maintenance</i>	45
2.2.3.	<i>Zebrafish microinjections</i>	46
2.2.4.	<i>Quantitative real-time PCR</i>	47
2.2.5.	<i>Whole mount in situ hybridization</i>	48
2.2.6.	<i>Cell culture experiments</i>	49
2.2.7.	<i>Organoid formation of intestinal crypt cells</i>	51
2.2.8.	<i>Automated filopodia analysis software</i>	52
2.2.9.	<i>Dual-color line-scanning fluorescence correlation spectroscopy</i>	53
2.2.10.	<i>Luciferase reporter assay in Xenopus embryos</i>	53
2.2.11.	<i>Image acquisition</i>	53
2.2.12.	<i>Statistical analysis</i>	54
3.	RESULTS.....	55
3.1.	KINASE SCREEN AND AUTOMATED IMAGE-ANALYSIS IDENTIFIES THE RECEPTOR TYROSINE KINASE ROR2 AS A POTENTIAL CYTONEME REGULATOR.	55
3.2.	TYROSINE KINASE ROR2 REGULATES FILOPODIA EMERGENCE <i>IN VITRO</i> UPSTREAM OF CDC42.....	58
3.3.	WNT/PCP COMPONENTS FEATURE OVERLAPPING EXPRESSION DOMAINS IN THE DORSAL MARGINAL ZONE DURING EARLY GASTRULATION.	60
3.4.	CLUSTER FORMATION OF WNT8A AND ROR2 IS DEPENDENT ON THE CRD DOMAIN.....	62

3.5.	WNT8A AND ROR2 CO-MIGRATION AND PROTEIN BINDING IN SIGNALING CLUSTERS	66
3.6.	WNT8A/ROR2 SIGNALING ACTIVATES THE B-CATENIN-INDEPENDENT PLANAR CELL POLARITY (..... PCP) PATHWAY	68
3.7.	IMAGING SETUP AND QUANTITATIVE ANALYSIS OF WNT-CYTONEMES DURING ZEBRAFISH GASTRULATION.....	75
3.8.	ROR2 PRESENTS WNT8A TO THE TARGET CELL TO INDUCE LIGAND-RECEPTOR CLUSTER..	77
3.9.	ROR2 INDUCES WNT-CYTONEMES DURING ZEBRAFISH NEURAL PATTERNING.....	83
3.10.	ROR2 REGULATES PARACRINE B-CATENIN SIGNALING BY AUTOCRINE Wnt/PCP- MEDIATED CYTONEMES.....	85
3.11.	ROR2 DEPENDENT CYTONEMES OPERATE IN GASTRIC CANCER CELL PROLIFERATION..	90
3.12.	ROR2-DEPENDENT Wnt CYTONEMES ARE REQUIRED IN MURINE INTESTINAL CRYPT HOMEOSTASIS.....	95
4.	DISCUSSION	97
5.	APPENDIX	114
6.	REFERENCES.....	124

Figure Index

Figure 1: Schematic of the “French flag model” proposed by Lewis Wolpert 1962.	3
Figure 2: Dynamic range of Wnt signaling during development and adulthood.	6
Figure 3: A classic overview of the canonical Wnt signaling pathway in OFF and ON state.	9
Figure 4: Schematic overview of the Wnt-mediated antero-posterior CNS pattern formation during gastrulation.....	12
Figure 5: Comparison of canonical and non-canonical Wnt signaling pathways.	14
Figure 6: Domain architecture and binding regions of Ror-family RTKs.	16
Figure 7: The structure of <i>Xenopus</i> Wnt8a binding to the mouse Fzd8-CRD derived from the X-ray crystallography.....	20
Figure 8: Overview of the Wnt maturation and secretion pathway.	21
Figure 9: Models for paracrine Wnt transport.....	23
Figure 10: Contact-dependent cell-cell communication.	28
Figure 11: Overview of Wnt cytoneme structure and function during zebrafish neural plate patterning.	31
Figure 12: Kinase library screen with automated image-analysis identifies the RTK Ror2.	57
Figure 13: In-depth analysis of the role of Ror2 in filopodia formation in PAC2 fibroblasts.	60
Figure 14: Expression pattern of the Wnt ligand <i>wnt8a</i> and Wnt PCP receptors <i>ror2</i> and <i>fzd7a</i> during early gastrulae stages.	62
Figure 15: Confocal analysis and intensity profiles highlights Wnt8a/Ror2 cluster formation in the cell membrane dependent on the CRD.	64
Figure 16: Evaluation of Wnt8a/Ror2/Fzd7a cluster formation and Dvl2 recruitment to the membrane.	65
Figure 17: Line scanning-fluorescence correlation spectroscopy (ls-FCS) analysis of zebrafish embryos at 8 hpf.....	67
Figure 18: Ror2 over-expression induces a concentration-dependent PCP phenotype.....	69
Figure 19: CRISPR/Cas9 gene silencing approaches for Ror2 and Ror1.	70
Figure 20: Analysis of a Wnt/PCP-mediated C&E defect by evaluation of the <i>ntl</i> expression.	72
Figure 21: Synergistic Wnt PCP activation during C&E by Wnt8a and Ror2 affects cell shape of notochordal cells.	73
Figure 22: AFT2 reporter assay in <i>Xenopus</i> embryos to measure Wnt/PCP activation.	74
Figure 23: Imaging setup and cytoneme quantification of single cells in a 3D confocal volumes.....	76
Figure 24: Visualization of cytonemal Wnt transport <i>in vivo</i>	79
Figure 25: Dissecting cytonemal Wnt transport: Analysis of the Lrp6-response in receiving cells.	80
Figure 26: Dissecting cytonemal Wnt transport: Involvement of the Wnt receptor Fzd7a in cluster formation and filopodia induction.....	82

Figure 27: In-depth analysis of cytonemes in zebrafish embryos *in vivo*. 84

Figure 28: Gene expression of marker genes to highlight changes in pattern formation..... 87

Figure 29: Ror2 enhances paracrine Wnt- β -catenin signaling in HEK293T co-culture. 89

Figure 30: Ror2 augments paracrine Wnt- β -catenin distribution in zebrafish embryo clones. 90

Figure 31: Analysis of cell extensions in the gastric cancer cell lines AGS and MK28..... 92

Figure 32: Analysis of cytonemal Wnt spreading in the gastric cancer cell lines AGS and MKN28. . 93

Figure 33: Importance of Ror2 dependent cytonemes in gastric cancer cell proliferation. 94

Figure 34: Intestinal crypt cell organoids requires Ror2-positive supportive myofibroblasts. 96

Figure 35: The influence of Ror2 levels on paracrine Wnt/ β -catenin distribution and my presented applications for Wnt cytoneme transport. 110

Abbreviations

AGS	Primary gastric adenocarcinoma
AP	Antero-posterior
aPKC	Atypical protein kinase C
Bmp	Bone morphogenetic protein
cDNA	Complementary deoxyribonucleic acid
Cas9	CRISPR associated protein 9
CNS	Central nervous system
CRISPR	Clustered Regularly Interspaced Short Palindromic Repeats
DAPI	4',6-diamidino-2-phenylindole
DIG	Digoxigenin
Dvl	Dishevelled
DMSO	Dimethyl sulfoxide
Dpp	Decapentaplegic
DV	Dorso-ventral
EGF	Epidermal growth factor
FGF	Fibroblast growth factor
FNL α	FilaminA
FITC	Fluorescein isothiocyanate
MO	Morpholino antisense oligomers
mRNA	Messenger ribonucleic acid
ORF	Open reading frame
PCR	Polymerase chain reaction
PFA	Paraformaldehyde
sFRP	Secreted frizzled-related protein
Wnt	Wingless-integrated
APC	Adenomatous polyposis coli
ARP2/3	Actin related proteins 2/3

ATF2	Activating transcription factor 2
Cdc42	Cell division control protein 42 homolog
CK1	Casein kinase 1
CRD	Cysteine rich domain
Dpp	Decapentaplegic
Dvl	Dishevelled
ECM	Extracellular matrix
Evi	Eveness interrupted
Fzd	Frizzled
GAP	GTPase activating protein
Gbx	Gastrulation brain homeobox
GPI	Glycosylphosphatidylinositol
Gsc	Goosecoid
GSK3	Glycogen synthase kinase-3
HEK	Human embryonic kidney
Hh	Hedgehog
HSPG	Heparan sulphated proteoglycan
I-BAR	Inverted Bin/amphiphysin/Rvs
IRSp53	Insulin Receptor tyrosine kinase Substrate p53
JNK	C-Jun N-terminal kinase
Lef	Lymphoid enhancer factor
Lrp	Low density lipoprotein receptor related proteins
MKN	Gastric tubular adenocarcinoma liver metastasis
MyoX	Myosin X
Otx	Orthodenticle homeobox
PCP	Planar cell polarity
Porcn	Porcupine
Rac	Ras-related C3 botulinum toxin substrate
Rho	Ras homolog gene family

Ror2	Receptor tyrosine kinase-like orphan receptor 2
RTK	Receptor tyrosine kinase
Shh	Sonic hedgehog
TCF	T-cell factor
TK	Tyrosine kinase
Tkv	Thickveins
TNT	Tunneling nanotube
UTR	Untranslated region
Wg	Wingless
Wl	Wntless
Wnt	Wingless/Integrated

1. Introduction

1.1. Development of multicellular organisms

The embryogenesis of multicellular organisms requires a tight coordination in a wide range of biological processes. Guiding every aspect of development is a massive challenge, but our understanding of this event has been greatly enriched in recent decades. In a very limited amount of time during early development, all cells must divide, migrate and acquire distinct cell fates to form a functioning three-dimensional patterned embryo. It is fascinating, that most of these important cellular decisions come down to constant cell-cell communication facilitated by a minority of specialized cells within a tissue. These signaling centers transmit spatial and temporal information to guide cellular fates during the course of development. Astonishingly, the main body plan is established by only a countable amount of secreted signals, so-called morphogens that initiate a cascade of intracellular signaling events in a concentration-dependent manner. Morphogens, such as the highly conserved family of Wnt proteins, are secreted from signaling centers and are fundamental to orchestrate early events of diversification. Morphogens generate cellular responses by specific ligand-receptor interactions in the recipient tissue and are generally dependent on the distance to the source of production. However, a regulated sequence of morphogen activity is required to generate a fine-tuned communication network. Therefore, a controlled propagation machinery must ensure accurate signal distribution from the source to the surrounding tissue to initiate the correct developmental program. Wnt proteins are essential to guide cell decisions and tissue homeostasis, and therefore perturbations in Wnt signaling are highly connected to both human degenerative diseases and cancer.

1.2. Role of morphogens during development

Cell fates define the properties and the behavior of cells. They originate from complex changes in gene expression and the epigenetic code. Yet in development, cells operate not only as individuals, but also in large scale systems such as cell layers, organs or even organisms. Therefore, in the context of developmental biology, the process of an initially similar cell population to adapt a diverse cell fate and anatomy according to space and time is known as patterning and a fundamental aspect during embryogenesis (Gurdon *et al.*, 1994). The observation of several key events during development predicted the existence of special signaling substances that could govern pattern formation (Gilbert, 1993). Positional

information can be established by these so-called morphogens (Turing, 1952), which are secreted proteins with a signaling function to facilitate a concentration gradient across a tissue.

The Scottish mathematical biologist D'Arcy Wentworth Thompson investigated the principles of self-organization that lead to pattern formation in his book "*On Growth and Form*" (Thompson, 1992). He observed similarities in the anatomical features of related species and correlated these with an underlying biological order, explained by early mathematical models. Alan Turing was animated by this work and hypothesized an advanced model that would revolutionize the perspective of pattern formation by suggesting the existence of secreted and diffusible substances that operate in a self-organized system (Turing, 1952). He observed several patterns in nature, which could be all explained by a counter-gradient of two substance with different physical properties. In Turing's reaction-diffusion system, a slow diffusing activator would compete against a fast-spreading inhibitor, giving rise to periodic patterns over a larger propagation distance. By adjusting the parameters of the individual parameters, the model can generate a wide variety of spatial patterns, including the pigment stripe pattern of zebrafish (Kondo and Miura, 2010). In terms of morphogen gradients and self-organized systems, the "French flag" model of Lewis Wolpert is seen as a milestone in the explanation of tissue patterning. He postulated the existence of positional information by a chemical gradient that induces a change of cell fates according to their position in this morphogenic field (Wolpert, 1969, 1989). Cells within this morphogen gradient can sense differences in molecule content and interpret them by responding to them in a concentration-dependent manner. The resulting cellular response is conceptually termed the "French flag model", represented by the three-colored French flag, where each color would represent a concentration threshold which the cell is able to sense and adopt to that respective cell type (Figure 1). The French flag model is applicable even in modern biology and explains several processes that are reliant on a morphogenic gradient, for example the establishment of the body axis. Morphogen gradients determine the anterior-posterior (AP), dorsal ventral (DV), and left-right body axis during embryogenesis (Heller and Fuchs, 2015), one of the first and fundamental challenges of a new life. A famous example of concentration gradients provides the patterning of *Drosophila* embryos. Bicoid (bcd) protein forms a gradient along the anteroposterior axis and this positional information is directly translated into certain cellular fates (Driever and Nusslein-Volhard, 1988). The alteration of proper bcd gradient distribution would result in the shift of the corresponding

anterior or posterior embryonic structures, highlighting the relevance of gradients with a developing tissue.

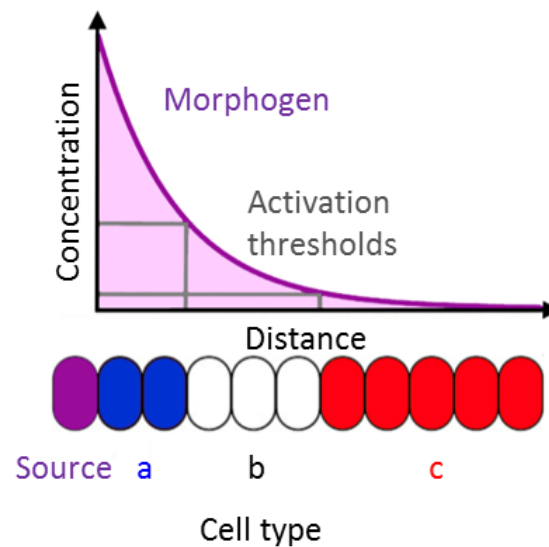


Figure 1: Schematic of the “French flag model” proposed by Lewis Wolpert 1962. A secreted morphogen is distributed over a tissue in a concentration-dependent manner. Cells respond to the diffusible signal and acquire certain cell fates depending on the signal concentration and activation threshold. The resultant cellular identities are represented in colorization of the French flag in blue, white and red.

1.3. Morphogens originate from local organizing centers

A crucial aspect of morphogens is the existence of specialized signaling centers, distinct organizing tissues responsible for production and release. The transplantation experiments of Spemann and Mangold in 1924 established the concept of local organizers during development. They provided first evidence that vertebrate neural tissue and subsequently the induction of the nervous system is induced in the ectoderm by signals from the dorsal mesoderm (De Robertis, 2006; De Robertis and Kuroda, 2004; Spemann and Mangold, 2001). Also, the transplantation of the dorsal pole of amphibian gastrula embryos to the ventral side of a host embryo induced a second body axis which led to the discovery of basic principles of local organizers (De Robertis, 2006): These defined cell populations produce molecules that affect the surrounding cells. Furthermore, ectopic induction of this signal by organizer translocation is able to mimic the main function of the organizer in the receiving tissue (Martinez Arias and Steventon, 2018; Hatta and Takahashi, 1996). Similar regions with organizing function were further discovered shortly after such as the Nieuwkoop center (Nieuwkoop and Nigtevecht, 1954) in amphibians, which induces the Spemann’s organizer. Equivalent tissues were observed in vertebrates as well as the teleost shield (Oppenheimer,

1936) and the Hensen's node in birds and mammals (Waddington, 1936), all of them with the ability to induce ectopic neural tissue when transplanted into a more ventral located area.

Furthermore, the discovery of the Spemann's organizer also grounded the principle of a two-step model of neural induction and subsequent patterning. According to the "default model" of neural induction, ectodermal cells have an inherent tendency towards the neural lineage (Munoz-Sanjuan and Brivanlou, 2002). However, constitutive bone morphogenetic proteins (Bmp) signaling prevents ectodermal cells from realizing their neural fate by inducing an epidermal fate. This tendency of neuralization can be observed in dissociated *Xenopus* animal caps of gastrula-stage embryos (Grunz and Tacke, 1989; Born *et al.*, 1989), which re-aggregate to establish neural tissues if no Bmp signals are present. The cells destined to form neural tissue must therefore be protected from the inhibitory substance. Three gene families were discovered to be responsible for counteracting the mesodermal factors that are locally produced in the Spemann's organizer. *Noggin*, *chordin* and *folliculin* are genes encoding for antagonizing binding partners of several transforming growth factor beta (TGF β)-related factors such as Bmp to protect the neural tissue in its default state (Lamb *et al.*, 1993; Hemmati-Brivanlou and Melton, 1994; Sasai *et al.*, 1994). The default model is a simple and tempting explanation for neural induction, yet there are several unanswered question and it appears to be more complex than initially proposed (Stern, 2005). In a second step, the protected neural tissue acquires a certain neural fate. Similarly, in amphibians, after initial establishment of neural identity by the organizer a second transforming factor govern the subsequent differentiation. In terms of the Spemann's organizer, posteriorizing factors are released to confer progressive posterior identity in a concentration gradient across the tissue to establish defined neural fate and grade the neuro ectoderm into anterior forebrain to dorsal spinal cord (Nieuwkoop, 1997; Sasai and De Robertis, 1997).

Despite the establishment of the body plan by pattern formation of morphogens being a versatile process, it is astonishing that only handful types of signaling molecules are required. Most of the key aspects in biology are based on morphogens such as members of the Hedgehog (Hh), Fibroblast growth factor (FGF), Epidermal growth factor (EGF), and Wnt families. The latter mentioned group of Wnt proteins will be in the main focus of this work and regulates amongst other things the subdivision of the vertebrate central nervous system (CNS) by establishing AP positional information within the developing neural plate (Green *et al.*, 2015; Wilson and Houart, 2004; Mattes *et al.*, 2012).

1.4. The Wnt signaling pathway

1.4.1. Wnt signaling in development and disease

For a precise developmental program, a spatial and temporal feed of information is a substantial obligation. Accurate cell-cell communication is crucial for development during embryogenesis and subsequent maintenance. Decades ago, it was postulated that a gradient of signaling molecules regulates key events during development (Wolpert, 1969). Since then, signaling molecules such as Wnt proteins and their respective transduction pathways have been intensively studied and have been shown to have tremendous impact on embryogenesis. The investigation of these pathways has elucidated not only their role in several aspects of development, but also their involvement in cancer if these cues are maliciously executed (Clevers, 2006).

The Wnt family was independently discovered in the late 20th century. Groundwork in mouse identified the *int-1* (subsequently *wnt1*) gene, a proto-oncogene causing mammary carcinomas upon stimulation by the mouse mammary tumor virus (MMTV) (Nusse and Varmus, 1982; McMahon and Bradley, 1990). At the same time, the segment polarity gene *wingless* (*wg*) was identified in *Drosophila* that manifests a variable misdevelopment of the adult wing. The subsequent name “Wnt” is derived from a combination of *wingless* and *int-1* as both genes were found to encode homologous proteins which belong to a large and conserved superfamily of signaling molecules that can be found in all branches of the animal kingdom (Nusse *et al.*, 1991). Since this first discovery, 19 Wnt proteins have been described in human.

The Wnt signaling pathway orchestrates a multitude of fundamental events during development and adulthood (Figure 2). During embryogenesis, Wnt directs important cell fate decisions, cell proliferation and cell polarity to ensure the precise formation of a generally undefined sheet of cells into structured tissues and ultimately into a complex organism. In adults, Wnt maintains tissue homeostasis, is required for regeneration after injury, is vital to control stem cell operations and for the continued renewal of the stem cell pool (Logan and Nusse, 2004). Due to the relevance of Wnt signaling throughout the lifetime of the organism, it is therefore not surprising that dysregulation of this pathway can lead to severe malfunctions and diseases.

Uncoupling of the tightly regulated downstream activity resulting from Wnt signaling leads to a variety of malicious effects, especially as most tissues are dependent on Wnt for their normal homeostasis, self-renewal or repair. To date, any disruptions that interfere with this balanced regulation, whether it be a mutation that causes a constitutive active or repressed Wnt signaling pathway, has had dire consequences (Figure 2). The Wnt transduction cascade is centered on the regulation of the core component β -catenin. The most famous and most studied disease related to Wnt is familial adenomatous polyposis (FAP), induced by mutations in the *adenomatosis polyposis coli* (*APC*) gene which causes aberrant β -catenin levels (Kinzler *et al.*, 1991; Nishisho *et al.*, 1991). These adenomatous lesions are an autosomal dominant inherited mutation causing the occurrence of hundreds of polyps in the colon as a result of limitless cell proliferation. *Axin2* mutations, another factor controlling β -catenin, are related to tooth defects as well as display a higher tendency for colon cancer (Lammi *et al.*, 2004). Conversely, loss of Wnt signaling can also cause severe disorders such as tetra-amelia, a condition which is described by the absence of limbs. This misdevelopment is assigned to a loss of a single Wnt ligand Wnt3 (Niemann *et al.*, 2004). Furthermore, impaired bone density and defects in eye vascularization (exudative vitreoretinopathy, FEVR) can also be caused by mutations targeting the receptors of the Wnt pathway. A single substitute amino acid in the LRP5 co-receptor leads to an insensibility towards DKK inhibition and subsequent infinite Wnt signaling in this tissue (Logan and Nusse, 2004).

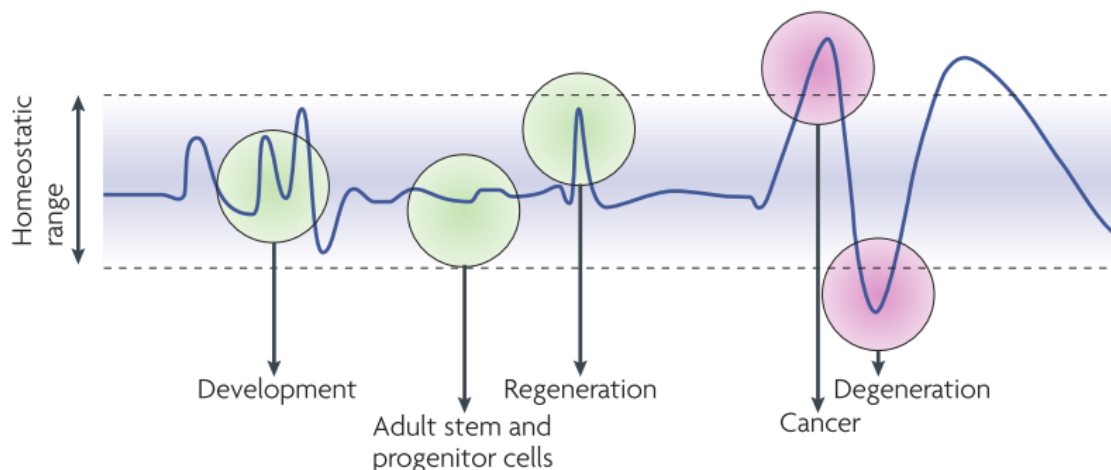


Figure 2: Dynamic range of Wnt signaling during development and adulthood. Wnts are kept in a finely regulated homeostatic range. During embryogenesis, high and precise Wnt- β -catenin levels are required in various developmental contexts. Later in time, Wnt is particularly relevant in stem cell differentiation, maintenance, and is upregulated following acute injury. However, disturbance of this regulatory grid on both ends cause diseases such as cancer or degenerative conditions. Figure from Angers and Moon, 2009.

1.4.2. Molecular mechanism of Wnt signal transduction

Wnt signaling depends on a complex web of interactions with a multitude of regulatory elements. The Wnt family consists of secreted glycoproteins associated in short- and long-range cell-cell signaling (Willert and Nusse, 2012). Their inherent function as morphogens allows them to mediate highly specific cell responses in distant tissues that range from influencing small movement changes of a cell to fundamental cell fate decisions in multicellular organisms. The mode of action can be simplified into two essential layers: The first involves the binding of the Wnt ligands to a variety of receptors, co-receptors and further interaction partners on the cell surface (Kikuchi *et al.*, 2009). The definite composition of ligand-receptor pairs shapes the generated signal, which can lead to context-specific signaling in different cells depending on ligand and receptor presence. One of the most notable binding partners is the Wnt receptor frizzled (Fzd), a seven-segment transmembrane receptor with a binding motif in form of a cysteine-rich domain (CRD) (Bhanot *et al.*, 1996), which connects the extracellular reception of the ligand with the trigger of the downstream transduction cascade. To date, there are 19 mammalian Wnt family members activating ten distinct Fzd receptors and additional co-receptors, and various membrane-bound or extracellular co-activators or repressors (Yu and Virshup, 2014). This dazzling amount of combinations defines the received signal on the ligand-receptor level. The second layer of Wnt signaling results from the mediated downstream response which depends on the ligand-receptor signal itself but is also modulated by a variety of available intracellular factors. Different classes of pathways have been assigned to specific activities. This subdivision of Wnt pathways was founded on the basis of ectopic axis induction in *Xenopus* embryos as well as the transformation of the mouse mammary epithelial cell line C57MG (McMahon and Moon, 1989), both events that are based on β -catenin levels and subsequent change in gene expression. The β -catenin dependency led to the classification into “canonical” and “non-canonical” pathways, and has been firmly maintained since then even though this strict division is not as concordant with today’s knowledge (van Amerongen and Nusse, 2009). The best studied Wnt response is the initiation of the Wnt/ β -catenin pathway characterized by the degradation of β -catenin and the activation of TCF transcriptional complexes. However, further Wnt responses include β -catenin independent pathways which rely on partially similar intracellular components but also completely different receptors such as Ror2 and Ryk (related to receptor tyrosine kinase), signal transducers including JNK and Src kinases, small Rho GTPases family members, and even calcium fluxes (Gordon and Nusse, 2006). The

various pathways are often studied and displayed as separate linear responses, however, horizontal crosstalk and shared pathway elements point to a more and more integrated Wnt signaling network (van Amerongen and Nusse, 2009). The context-specificity and the almost infinite combinations create one of the challenges in exploring Wnt signaling and dissecting singular molecular functions.

1.4.3. Canonical Wnt/ β -catenin pathway

After decades of intensive research, the canonical Wnt/ β -catenin pathway is the most studied and best understood branch of the signaling network. It resembles the main transduction cascade as a vital regulator of cell proliferation, cell fate decisions as well as tissue and stem cell homeostasis.

Cytoplasmic β -catenin levels emerged to as the deciding factor of canonical Wnt signaling, which ultimately decides if the Wnt pathway resembles an OFF or ON state (Figure 3). Free β -catenin is kept on a low level by a constant degradation via a multiprotein complex, the so-called destruction complex consisting of the scaffold proteins Axin, adenomatosis polyposis coli (APC), protein phosphatase 2A (PP2A), glycogen synthase kinase 3 (GSK3), and casein kinase 1 α (CK1 α) (Voronkov and Krauss, 2013). In this condition, the lymphoid enhancer-binding factor/T cell-specific (LEF/TCF) transcription factor in the nucleus is associated with Groucho and represses the expression of Wnt target genes. A Wnt ON state can be induced by binding of a canonical Wnt ligand to the respective set of membrane receptors. Wnt ligands have been classically divided into two groups on the basis whether an effect on changing β -catenin levels – which is exhibited through the downstream potential to induce a secondary axis upon ectopic expression – it can be classed as a canonical Wnt ligand. Wnt1, Wnt3, Wnt3a, Wnt7a, Wnt7b, Wnt8 are common members of canonical Wnt signaling with axis duplication potential as mentioned (Du *et al.*, 1995; Wong *et al.*, 1994). In concordance with this, Wnt ligands without these characteristics such as Wnt2, Wnt4, Wnt5a, Wnt6, and Wnt11 are assigned to several different Wnt pathways, even though there is overlap depending on the cellular context and organisms.

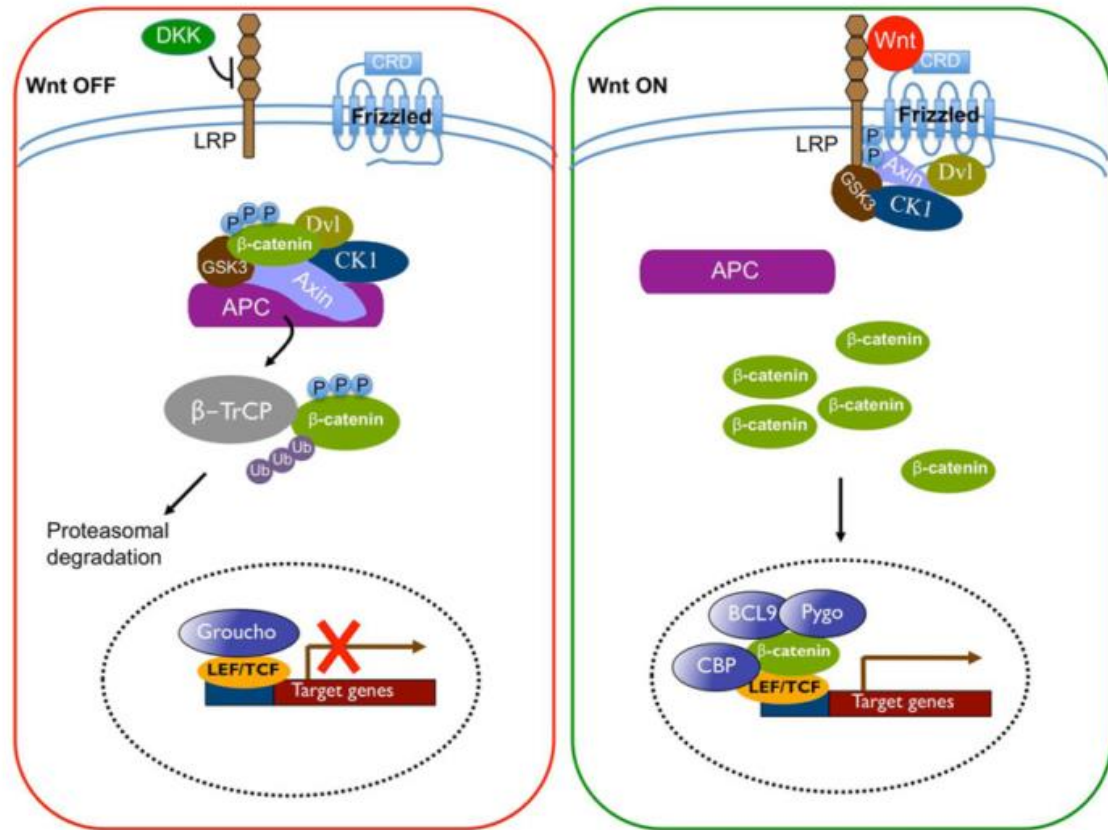


Figure 3: A classic overview of the canonical Wnt signaling pathway in OFF and ON state. In its Wnt OFF state, β -catenin is consistently subjected to proteasomal degradation by the Wnt destruction complex composed of APC, Axin, Dvl, GSK3, and CK1. To activate the pathway, canonical Wnt ligands bind to Fzd and LRP5/6 receptor. Subsequent complex formation initiates a wave of downstream events to prevent β -catenin degradation. Stable β -catenin translocates to the nucleus to activate LEF/TCF-mediated Wnt target gene expression. Figure from Yu and Virshup, 2014.

Signal transduction starts with the establishment of Wnt ligand-receptor complexes consisting of the seven-transmembrane receptor Fzd and the low density lipoprotein receptor related proteins 5 LRP5/6 co-receptor (Logan and Nusse, 2004; He *et al.*, 2004). The topology of Fzd receptors resembles that of G-protein coupled receptors (GPCR) which features seven membrane segments in addition to typical phosphorylation and glycosylation sites for cyclic AMP-dependent protein kinase (PKA), protein kinase C (PKC) and casein kinase 2 (CK2) (Angers and Moon, 2009), but lacking conserved GPCRs characteristics such as the Asparagine-Arginine-Tyrosine motif crucial for G-protein coupling. LRP5/6 is believed to be another key component assigning the resulting ligand-receptor complex into a canonical branch. LRP5 and LRP6 show partially redundant functions in mouse gastrulation, but LRP6 was shown to perform a more vital role during embryogenesis whereas LRP5 is

crucial in bone homeostasis (He *et al.*, 2004). Nevertheless, Wnt/Fzd/LRP5/6 complexes initiates a series of events that subsequently change the β -catenin levels of the cells. Following this change, downstream transducers such as Axin and Dvl are recruited to form multi-protein receptor aggregates defined as signalosomes (Hagemann *et al.*, 2014; Bilic *et al.*, 2007). Dvl is a modular protein that is used in between different Wnt pathways and contains three unique structural domains allocated to the distinct path and becomes activated upon direct phosphorylation. It contains a DIX, PDZ and DEP domain, whereas the DIX and PDZ are required for canonical Wnt signal transduction (Wallingford and Habas, 2005). Upon Wnt/Fzd/LRP clustering, Dvl becomes activated. (Wong *et al.*, 2003). The dynamic polymerization of Dvl features a high affinity for Axin. Consequently, the whole Axin destruction complex is recruited to the plasma membrane (Gammons and Bienz, 2018). Membrane localization phosphorylates the cytoplasmic tail of LRP5/6, mediated by CK1 γ , which serves as a direct competitor to GSK3. In the active form, the Dvl-signalosome inhibition of GSK3 disrupts the functionality of the destruction complex (Gordon and Nusse, 2006). Without Wnt pathway activation, GSK3 and CK1 α phosphorylate cytoplasmic β -catenin. That leads to ubiquitination by the E3 ubiquitin ligase β -transducin repeats containing protein (β -TrCP) and subsequent proteasomal degradation (Kitagawa *et al.*, 1999). Now inactive, β -catenin is protected from degradation and accumulates in the cytoplasm (Hatsell *et al.*, 2003). A subset of β -catenin translocates to the nucleus. This translocation process itself it poorly understood. β -catenin does not contain a nuclear localization sequence (NLS). It has been proposed that Ras signaling could be an important element for its nuclear import (Obrador-Hevia *et al.*, 2010). Once β -catenin accumulates in the nucleus it binds to a large number of binding partners to initiate target gene expression, the best characterized is the TCF/LEF DNA-binding transcription factors. In this process, β -catenin displaces Groucho and recruits additional member as B-cell lymphoma 9 protein (BCL9), Pygopus, and histone modifier CREB binding protein (CBP). This complex is able to turn the transcriptional repressor function of LEF/TCF to an activator and enables context-specific gene expression (Cadigan and Waterman, 2012).

1.4.4. The Wnt/ β -catenin pathway during neural plate pattern formation

The patterning of the zebrafish neural plate is an explicit example for the role of Wnt/ β -catenin signaling during development. Once neuroectoderm is induced, it must be graded into different subdomains along the antero-posterior body axis. The two-step activation/transformation model by Nieuwkoop in 1952 proposes that after the initial neural

induction, there is a transforming signal, which converts the initially specified anterior neuroectoderm to more posterior fates (Kim *et al.*, 2002; Sasai and De Robertis, 1997; Nieuwkoop and Nigtevecht, 1954). The zebrafish CNS arises from a simple sheet of neuroectoderm cells; however, by the end of somitogenesis, it is graded into distinct morphological structures as forebrain, midbrain, hindbrain and spinal cord. Key players of this process are the caudalizing factors, secreted from posterior located marginal organizers, such as Wnt, Fgf, Nodals, and retinoic (Green *et al.*, 2015). Combined activity of these signaling pathways is necessary to establish a crude AP pattern in the forming neural tube which is subsequently compartmentalized into further CNS subdivisions (Kiecker and Niehrs, 2001).

Wnt proteins released from the mesendoderm progenitors at the blastoderm edge (referred as the marginal zone organizer) feature a very early expression during patterning of the anterior neural plate (ANP) (Kiecker and Niehrs, 2001; Nordstrom *et al.*, 2002; Rhinn *et al.*, 2005). The significance of Wnt/ β -catenin signaling during AP patterning is demonstrated by zebrafish mutants such as *headless (hdl)* or *masterblind (mbl)*, which carry mutations in their *tcf3* or *axin1* gene and produce severe patterning defects (Kim *et al.*, 2000; Heisenberg *et al.*, 2001). During gastrulation, a gradient of Wnt/ β -catenin is established, whereas a source of Wnt antagonists at the animal located anterior neural border (ANB) protects the most anterior located neural plate from Wnt caudalizing properties (Houart *et al.*, 2002) by establishing a second counter-gradient of potent Wnt antagonists (Figure 4). The extracellular Wnt antagonists of the family of secreted frizzled related proteins (sFRP) Sfrp1a and Frzb counter balance Wnt/ β -catenin signaling and shape the Wnt gradient within the ANP (Wilson and Houart, 2004). The dose-dependent response to the gradient within the neural plate leads to the elaboration of gene expression domains to establish the forebrain, midbrain, and hindbrain primordia (Rhinn *et al.*, 2006). Several Wnt proteins such as Wnt3, Wnt3a, Wnt4a, Wnt5b, Wnt8b, Wnt10b, and Wnt11 are present in the marginal zone between four to seven hpf with variations in their time of onset (Lu *et al.*, 2011). One of the first and most crucial Wnt/ β -catenin signals confined in the marginal zone is Wnt8a. Wnt8a is proposed to be the main factor for early posteriorization in zebrafish at this stage (Lekven *et al.*, 2001; Kelly *et al.*, 1995; Erter *et al.*, 2001). Consistently, ectopic Wnt8a expression in the embryo represses forebrain identity while inducing hindbrain marker *gbx1* in a dose dependent manner (Fekany-Lee *et al.*, 2000).

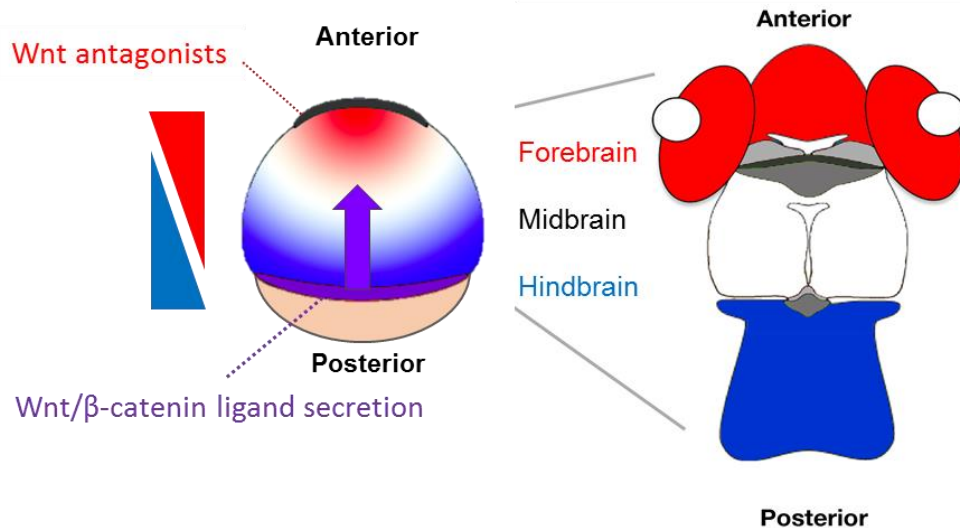


Figure 4: Schematic overview of the Wnt-mediated antero-posterior CNS pattern formation during gastrulation. Early morphogen gradients (represented at 8 hpf) grade the embryo and result in a diversification into distinct neural brain identities highlighted at 24 hpf. The purple stripe of cells represents the dorsal marginal zone organizer and is the predominant source of Wnt proteins during gastrulation. A gradient of released Wnt/ β -catenin protein provides positional information across the neuroectodermal cell sheet. Wnt antagonists of the sFRP family refine the gradient from the anterior animal pole. Cells respond in a dose-dependent manner and acquire forebrain, midbrain and hindbrain fate according to the Wnt/ β -catenin levels.

1.4.5. Non-canonical β -catenin independent pathway

Besides the canonical Wnt pathway, Wnt can also operate in additional routes which do not rely on β -catenin levels or GSK3 β activity. These Wnt pathways were termed non-canonical or β -catenin independent pathways and describe several different branches that are far from understood. Additionally, cross-talk between individual pathways has been reported and complicates the classification (Grumolato *et al.*, 2010). Interestingly, non-canonical signaling is stimulated by a different subset of Wnt ligands with the most prominent members being Wnt5a and Wnt11 (Niehrs, 2012). A common theme is that these pathways do not generally lead to a transcriptional alteration to determine cell fates. Instead, the transduction cascade often causes morphogenetic cell movements and polarity by influencing cytoskeletal elements (Croce and McClay, 2008). The pathway structure is highly diverse and can include Fzd receptor-mediated ligand binding (Sato *et al.*, 2010) or Fzd-independent pathway activation by single-pass transmembrane receptor tyrosine kinases Ror2 or Ryk (Green *et al.*, 2014). The Wnt planar cell polarity (Wnt/PCP), Wnt/ Ca^{2+} , and Wnt/atypical protein kinase C (Wnt/aPKC) pathways have undergone the most research because they have been found to be crucial in several developmental aspects and diseases.

Binding of non-canonical Wnts to Fzd receptors can influence intracellular Ca^{2+} levels and act through three calcium sensitive components: the calcium/calmodulin-dependent protein kinase II (CamK2), the phosphatase calcineurin, and the protein kinase C (Kestler and Kühl, 2008). It is also believed that the initial Wnt ligand-receptor signal is transduced through heterotrimeric G-proteins (Kuhl *et al.*, 2000b). The sudden influx of Ca^{2+} ultimately activates the nuclear factor of activated T-cells (NF-AT) transcription factors (Veeman *et al.*, 2003). Wnt/ Ca^{2+} signaling regulates the proliferation and migration of cells (Veeman *et al.*, 2003) and promotes ventral cell fates in *Xenopus* (Kuhl *et al.*, 2000a). Furthermore, Wnt5a activation of CamK2 and PKC (Weeraratna *et al.*, 2002) and the mediation of epithelia to mesenchymal transition (EMT) (Dissanayake *et al.*, 2007) in melanoma cells implicates its role in cancer progression. Ryk kinases interact with Wnt ligands with a domain similar to the secreted Wnt inhibitor WIF. They have been shown to modulate Wnt signaling during *Drosophila* neurogenesis (Yoshikawa *et al.*, 2003). Derailed (Drl, the *Drosophila* Ryk homolog) is required for axonal guidance out of the posterior commissure by interacting with Dwnt5. Thereby, Drl mutants feature similar deficiencies as Dwnt5 mutants.

The best understood β -catenin independent pathway to date is the Wnt/PCP pathway, also referred as Wnt/JNK (c-Jun -terminal kinase) (Oishi *et al.*, 2003) or Wnt/Ror2 (Yuan *et al.*, 2011). Signal transduction is mediated by Fzd receptor binding (Adler, 2002), Dvl activation (Nishita *et al.*, 2010b) and a varying set of co-receptors including Ror2 (Nishita *et al.*, 2006) and Van Gogh like 1 and 2 (Vangl1 and Vangl2) (Gao *et al.*, 2011). Interestingly, several Fzd independent functions have been reported with Wnt5a and Ror2 which might suggest a classification as an individual pathway (Schambony and Wedlich, 2007), which is described in more detail in a later chapter of this work (Figure 5). Dvl, a central relay station for distinct Wnt pathways, the DIX and the DEP domains were found to be indispensable for PCP signaling (Nishita *et al.*, 2010b). Consistently, depending on ligand and receptor composition, Wnt complex formation induces a specific downstream signal cascade that involves several kinases such as Phosphoinositide 3 kinase (PI3K) and several mitogen-activated protein kinases (MAPK) that subsequently activate JNK and the small RhoGTPases such as Ras-related C3 botulinum toxin substrate (Rac1), Ras homolog gene family A (RhoA), and cell division control protein 42 homolog (Cdc42) (Schlessinger *et al.*, 2009). Activated JNK is able to phosphorylate c-Jun leading to activating transcription factor-2 (ATF-2) mediated gene transcription (Schambony and Wedlich, 2007). The expression of *Xenopus* paraxial protocadherin (XPAPC) that is required for proper convergent extension

movements is the most famous target gene to date. Furthermore, activated RhoGTPases feature transcriptional independent effects to influence cytoskeleton rearrangements, tissue polarity, and cell migration (Nishita *et al.*, 2010a; Hikasa *et al.*, 2002; Schambony and Wedlich, 2007).

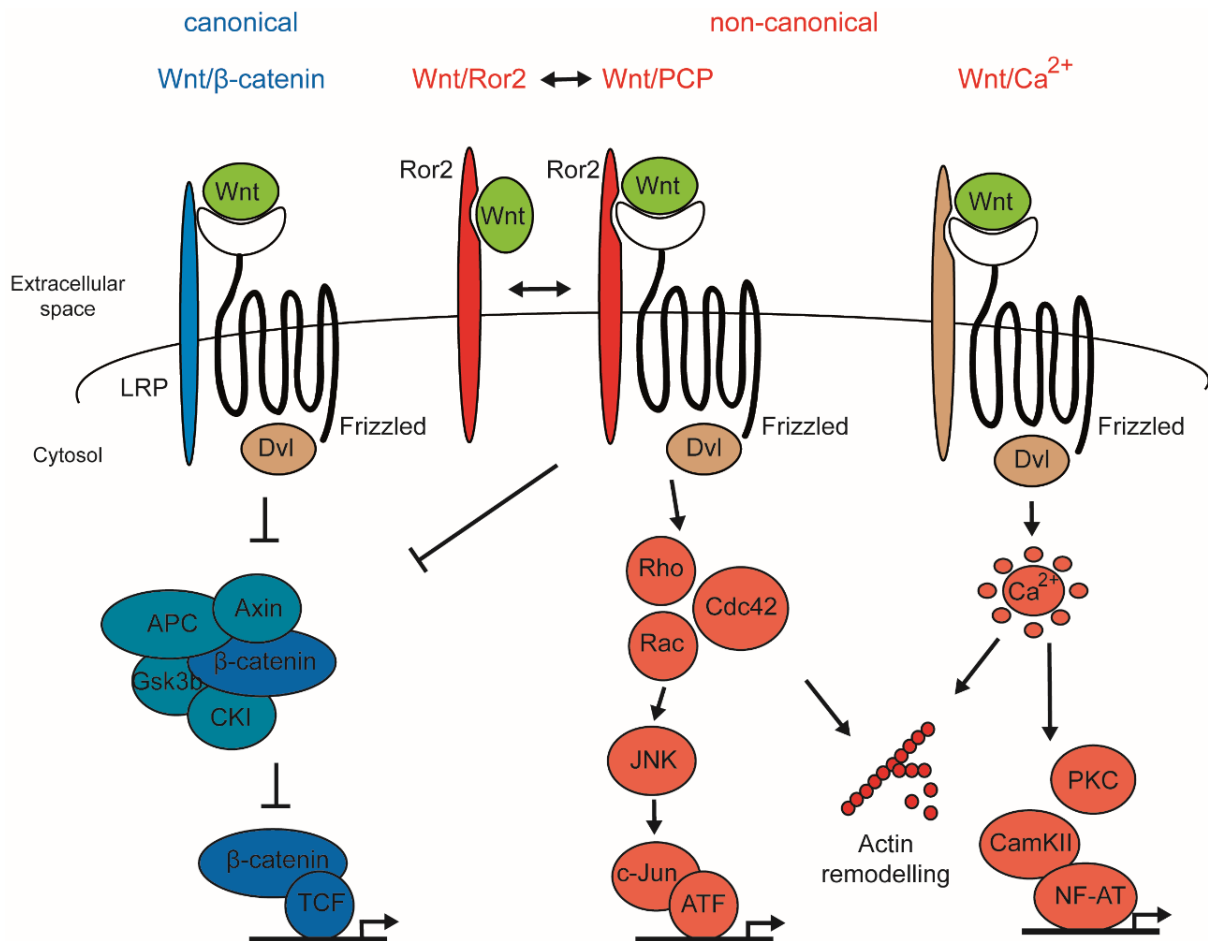


Figure 5: Comparison of canonical and non-canonical Wnt signaling pathways. In addition to the canonical Wnt pathway, there are β -catenin independent pathways which display a large degree of heterogeneity. The cellular response depends on the ligand and receptor composition that leads to downstream events including transcriptional activation of target genes and cytoskeleton rearrangements. In this process, the RTK Ror2 is described as a co-receptor in the Wnt/PCP pathway or as an independent receptor associated in a separate Wnt/Ror2 pathway.

The PCP pathway has emerged as a fundamental mechanism with various roles in development. Wnt5a and Wnt11 regulate mammalian anterior-posterior axis elongation, patterning of the neural tube and somites and regulation of EMT in axial and paraxial mesodermal precursors (Andre *et al.*, 2015). Additionally, Wnt5a and Wnt11 operate in different aspects of convergent extension movements in *Xenopus* in a non-redundant manner, with Wnt11 polarizing the dorsal mesodermal cells while Wnt5 is required for collective cell

migration (Wallkamm *et al.*, 2016). Consistently, Ror2 and Wnt11 regulate convergence and extension movements in zebrafish (Bai *et al.*, 2014) and disruption of Ror2 function resembles the phenotype of *silberblick slb/wnt11* mutants (Heisenberg *et al.*, 2000). Furthermore, Wnt5a cooperates with Ror2 to stimulate filopodia formation and cell migration (Nishita *et al.*, 2006) and is also highly linked to tumorigenesis (Nishita *et al.*, 2010a). Wnt/Ror2 promote gastric cancer proliferation by activating the CXCL16–CXCR6 axis (Takiguchi *et al.*, 2015), mammary tumor progression (Roarty *et al.*, 2017), and induces tumor invasiveness by regulating Golgi transport through intraflagellar transport 20 (IFT20) (Nishita *et al.*, 2017).

1.5. Ror-family receptor tyrosine kinases

1.5.1. Domain architecture

The Ror-family of receptor tyrosine kinases (Ror2-RTK) plays a crucial role in a variety of cellular functions such as differentiation, proliferation and angiogenesis during development as well as in adult organisms (Green *et al.*, 2008; Stricker *et al.*, 2017). As a result of this multitude of functions, it is not surprising that dysfunctional Ror RTKs lead to critical defects during development such as skeletal deformities and leukaemia. Historically, Ror RTKs were first isolated in 1992 in the human neuroblastoma cell line SH-SY5Y owing to their homology to another family of RTKs, the RTK family of neurotrophin receptors (NTRK) (Masiakowski and Carroll, 1992). NTRKs have a prominent function in nervous system development. The NTRK family was expanded with the identification of the Ror2 RTKs. In a wider view the superfamily of RTKs in mammals contains 58 members distributed in 20 superfamilies up to this date, one of which is the Ror2-family of receptor tyrosine kinases. Furthermore, the Ror-family of RTK only includes the two members Ror1 and Ror2, which are characterized by similar structural features (Stricker *et al.*, 2017).

Both Ror1 and Ror2 RTKs are single pass type I transmembrane proteins that share the same domain architecture (DeChiara *et al.*, 1996). On the extracellular site, they consist of one Immunoglobulin-like (Ig-like) domain, one cysteine rich domain (CRD) and one Kringle domain (Figure 6). The extracellular part of Ror is well known for its function as a membrane receptor, binding a multitude of interacting proteins, but it has a preference for Wnt proteins due to the similarities to the Wnt binding domain found in the Wnt receptor Frizzled (Billiard *et al.*, 2005).

The intracellular domain of all vertebrate Ror proteins consists of a tyrosine kinase domain, one Proline-rich region surrounded by two serine/threonine-rich domains for interaction with internal factors and transduction of signaling cues. Ror proteins are evolutionary conserved and can be found in vertebrates and even in protostomes (Bainbridge *et al.*, 2014). Some domains vary between different species. However, the CRD, Kringle and TK domain seem to be of most importance for its function and are conserved amongst all Ror orthologs (Minami *et al.*, 2010).

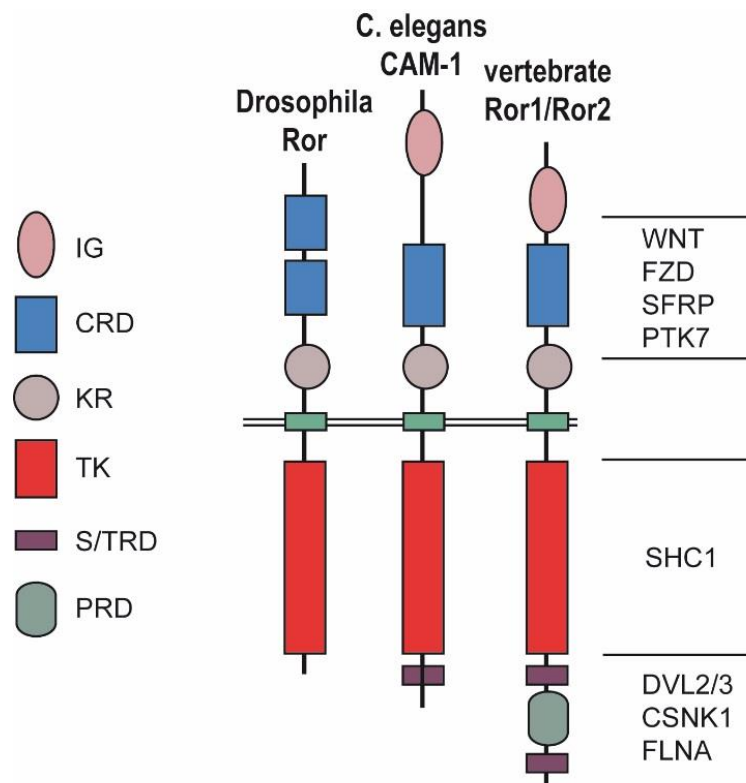


Figure 6: Domain architecture and binding regions of Ror-family RTKs. Ror domains of selected vertebrate and invertebrate Ror family proteins. Domain architecture is largely conserved between all species except for the variation of the S/TRD and PRD in all invertebrates and the split CRD in the *Drosophila* ortholog. On the right, prominent interaction partners and binding motifs are listed to the respective regions of Ror2. IG: Ig-like domain; CRD: Cysteine rich domain; KR: Kringle domain; TK: Tyrosine kinase; S/TRD: Serine/Threonine-rich domain; PRD: Proline-rich domain. Figure adapted from Stricker *et al.*, 2017.

1.5.2. Ror-family RTKs in development

Despite the strong domain similarities of Ror RTKs in vertebrates, they exhibit pronounced disparities in their expression pattern and its allocated function. *Drosophila* Ror1 (Dror) and Ror2 (DNrk) orthologs are first expressed at germ band stage and subsequently maintained in the neural ectoderm throughout embryogenesis highlighting a role in neural

development (Wilson *et al.*, 1993). The *C.elegans* Ror2 (CAM-1) shows a broader spectrum of expression, but it is also present in neural tissue where it contributes to a multitude of functions such as neural cell migration, axon guidance and the orientation of the anterior nerve ring (Mentink *et al.*, 2014). Vertebrate Ror function has been studied in zebrafish, chicken, frog and mouse. The zebrafish Ror2 expression is maintained throughout embryonic development consisting of maternally derived Ror2 transcript and spiking peaks of expression at various embryonic stages (Bai *et al.*, 2014; Young *et al.*, 2014). During gastrulation, Ror2 becomes ubiquitous with a dense occurrence in neural tissue and is a crucial regulator of mesoderm and neuroectoderm cell migration during convergence and extension (C&E) and body axis formation (Bai *et al.*, 2014; Keller *et al.*, 2000). These cell-guiding and regulatory roles of Ror2 during development mainly support its function as a receptor for Wnt5a and Wnt11, which is described further below.

Mouse Ror has a widespread temporal and spatial expression including lung, early limb bud, central nervous system and in cartilage (DeChiara *et al.*, 2000). Both receptors show redundancy in their expressed location but are highly exclusive when it comes to their function. Ror2 is the most prominent of both Ror RTKs, as it is linked to various human diseases. Mutations in human Ror2 cause severe skeletal defects such as recessive Robinow syndrome and brachydactyly type B, manifesting short-limbed dwarfism and deficient digits respectively (Green *et al.*, 2008). The role of Ror2 mutations in development has been studied extensively in mouse as the skeletal defects of mutant mRor2 mice resemble the diseased state of human Ror2 including dwarfism, shortened limbs and facial deformities (Takeuchi *et al.*, 2000; Minami *et al.*, 2010).

1.5.3. Ror2 function as a Wnt receptor and its role in Wnt signal transduction

The most prominent functions of Ror2 RTKs have been attributed to act as Wnt receptors with their vital role in Wnt signal transduction (Green *et al.*, 2014). Ror receptors were initially named as orphan receptors due to the uncertainty of their respective ligand. However, in the last years, Ror family receptors ascended as vital receptors for Wnt proteins and to guide important aspects of this signaling pathway (Green *et al.*, 2008). Ror2 receptors are mainly associated with binding the non-canonical Wnt ligand Wnt5a via its CRD domain causing homodimerization and autophosphorylation (Oishi *et al.*, 2003; Liu *et al.*, 2007). Consistent with the skeletal abnormalities of Ror2 knock-out mice, Wnt5a mutant mice

resemble a strikingly related phenotype by presenting dwarfism, short limbs and respiratory dysfunction which can lead to neonatal lethality (Oishi *et al.*, 2003; Ho *et al.*, 2012). Similarities of Ror2 and Wnt5a mutant mice suggest a functional relationship in development. Wnt5a as a ligand for Ror2 – described as a context specific independent receptor or as a co-receptor in combination with the Wnt receptor Frizzled – has been solidified. Wnt5a induces the complex formation between Ror2 and Frizzled with a resulting downstream activation of the non-canonical Wnt pathway leading to variable and context dependent signal cues including gene transcription, polarized cell movements, cytoskeleton rearrangements, and tumor invasion (Nishita *et al.*, 2006; Brinkmann *et al.*, 2016; Schlessinger *et al.*, 2009; Schambony and Wedlich, 2007).

To fulfill its role, Ror2 can interact with a multitude of proteins to modulate signaling output on the extracellular C-terminal part. The collagen triple-helix repeat containing protein 1 (Cthrc1) augments the formation of Frizzled/Ror2 aggregates by working as a linking adapter between receptor pairs (Yamamoto *et al.* 2008). The Frizzled-like CRD is the main binding site for Wnt proteins, most prominently for Wnt5a. Other Wnt proteins in various different organisms and *in vitro* cultures have been reported to interact with Ror2 such as Wnt1, Wnt2, Wnt3 and Wnt3A, Wnt4, Wnt5A and Wnt5B, Wnt6, Wnt7A, Wnt8, Wnt11 (Stricker *et al.*, 2017). Also, Wnt antagonists such as secreted Frizzled-related proteins sFRP are also capable of interacting with Ror2's CRD domain and obstruct the binding effectiveness to other ligands. It was also suggested that sFRPs could act as a switch for distinct non-canonical signaling branches by stabilizing Ror2 complexes and blocking Fzd7 endocytosis (Brinkmann *et al.*, 2016).

The intracellular N-terminus forwards the transduction cascade by operating with various effector proteins. Several activities are being associated with its function as an active TRK. Wnt5a binds to Ror2 and induces homo-dimerization and transduction cascade activation (Liu *et al.*, 2008). Furthermore, tyrosine phosphorylation can also be observed by forced dimerization of Ror2, while ligand binding can either induce tyrosine or serine/threonine phosphorylation (Grumolato *et al.*, 2010). Interesting, Ror1 might act as a pseudo-kinase as it was reported to fail kinase activity, which could explain its discrepancy in biological function compared to Ror2 (Gentile *et al.*, 2011). N-terminal interaction partners (Figure 6) include further Wnt/PCP components such as phosphorylated Dvl and Frizzled for AP1 and RhoGTPase activation, casein kinase 1 (CSNK1) interaction to induce Vangl phosphorylation as well as the actin-binding protein FilaminA (FNLA) (Nomachi *et al.*, 2008; Nishita *et al.*,

2006). Association with FNLa was shown to be indispensable for Ror2-mediated filopodia formation, as the formation of these cell protrusions requires the presence of FNLa in several melanoma cell lines (Nishita *et al.*, 2006). It is important to note that Ror2 can also influence the Wnt/ β -catenin pathway by interacting with and phosphorylation by CK1 epsilon (CSNK1E) and GSK3, two fundamental kinases of canonical Wnt signaling (Kikuchi *et al.*, 2007; Grumolato *et al.*, 2010). Ror2-mediated and Wnt/ β -catenin signaling are mostly known as mutual repressive (Winkel *et al.*, 2008). However, dependent on the biological context and receptor composition, Ror2 was shown to stimulate Wnt/ β -catenin signaling. There is evidence that Ror2 may modulate canonical Wnt signaling in lung epithelial cells by cooperation with Fzd2, but not Fzd7 (Li *et al.*, 2008). Ror2 has also been shown to positively regulate Wnt/ β -catenin in human breast cancer which underlines its versatile operations dependent on available binding partners and downstream factors (Henry *et al.*, 2014).

1.6. Wnt proteins: Structure, maturation and secretion

To fulfill the function of a secreted morphogen, Wnt proteins require a complex maturation process that includes glycosylation, palmitoylation and subsequent transport to the plasma membrane (Langton *et al.*, 2016; Port and Basler, 2010; Takada *et al.*, 2017).

The structural properties of Wnt proteins resemble 22-24 highly conserved cysteine residues which form intramolecular disulfide bridges to maintain the secondary structure. The analysis of the first discovered Wnt unveiled features such as glycosylation, secretion and a strong attachment to the cell membrane (Nusse *et al.*, 1991), latterly shown to be conditional on covalent acylation (Willert *et al.*, 2003). However, due to the low solubility of Wnt proteins, purification and subsequent analysis of the structure and especially interaction to their particular receptors proved to be challenging. After decades of Wnt research, the structure of Wnt and its binding behavior with the Fzd receptor was elucidated. Crystal structure analysis of *Xenopus* Wnt8a binding to the mouse Fzd8-CRD revealed two unusual amino structures of xWnt8a resembling an “index finger and a thumb” to associate with Fzd8 at two binding positions (Figure 7) (Janda *et al.*, 2012). The thumb represents the N-terminal domain (NTD) and is composed of several α -helices building five disulfide bridges by the conserved cysteine residues and extends the highly conserved palmitoleic acid modification at serine 187, which was shown to be indispensable for Wnt activity. The tip of the Wnts thumb reaches deep into a hydrophobic groove of the Fzd8-CRD. The second binding by the C-terminal index-finger features two β -sheets preserved by six disulfide bridges. Contact is

mainly achieved by hydrophobic amino acid contacts to Fzd8-CRD (Janda *et al.*, 2012). Interestingly, some binding positions on Fzd8 vary in other Fzd family proteins and could explain the specificity for certain Wnt/Fzd combinations.

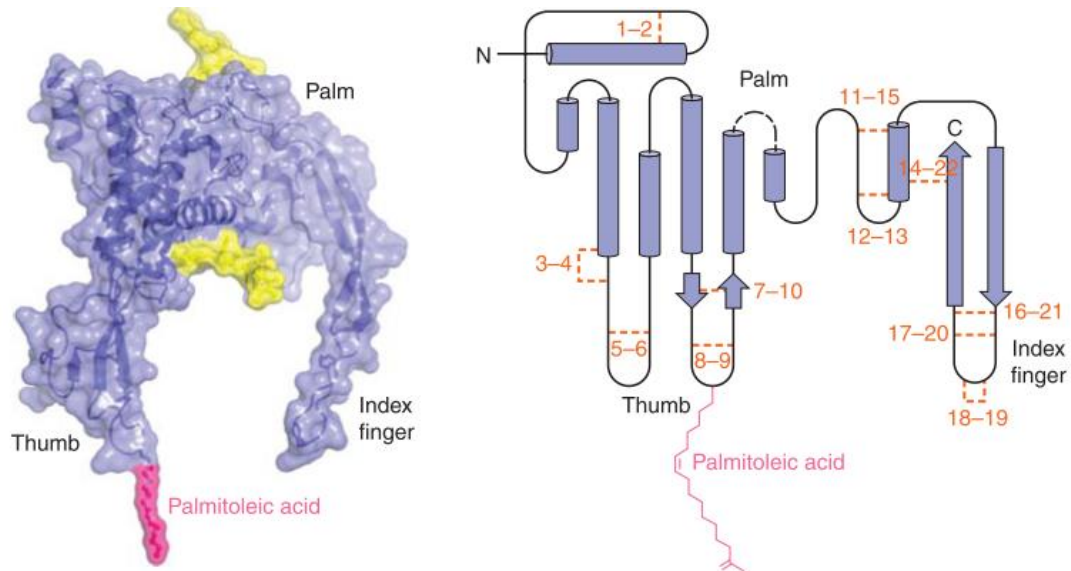


Figure 7: The structure of *Xenopus* Wnt8a binding to the mouse Fzd8-CRD derived from the X-ray crystallography. The secondary structure contains 22 cysteines with disulfide bridges, establishing the N-terminal domain (NTD) thumb and C-terminal index-finger structures which interact with the Fzd receptor. Figure adapted from Willert and Nusse, 2012.

For the maturation process, all Wnt proteins must undergo post-translational modifications (except *Drosophila* WntD) in the endoplasmic reticulum (ER) and Golgi apparatus after translation (Figure 8). The glycosylation of Wnts varies between the family members. Wnt1 is glycosylated on four residues and Wnt1 carries only two N-linked glycosylations, while the WntD homolog contains none (Ching *et al.*, 2008). The function of the glycosylation is not yet completely understood. Glycosylation was shown to be important for proper secretion (Komekado *et al.*, 2007), while other reports propose a rather dispensable function (Tang *et al.*, 2012). Unlike the lipidation, glycosylation was suggested to be less important for signaling activity (Kurayoshi *et al.*, 2007). Wnt proteins are further post-translationally modified with one monosaturated fatty acid at a single serine residue in the ER by Porcupine (Takada *et al.*, 2006). Porcupine is a membrane associated O-acyl transferase (MBOAT) and catalyzes the attachment of the palmitoylate moiety to Wnt. This lipid modification is crucial for its interaction to Wnt receptors and therefore for signaling activity (Janda *et al.*, 2012; Takada *et al.*, 2006). Porcupine modifies the serine residue S209 in Wnt3a. Consequently, mutations of serine 209 prevent lipidation and the majority of

secretion (Nile and Hannoush, 2016). Acetylation with a lipid anchor supports further modification and processing through the secretion pathway. Porcupine is a central requisite for Wnt protein maturation, therefore it is not surprising that a *porcupine* mutation has severe consequences due to reduced Wnt signaling. Loss of Porcupine is associated to Focal dermal hypoplasia (FDH), a X-chromosomal developmental disorder that attributes male lethality, dermal hypoplasia or skeletal and dental malformations (Grzeschik *et al.*, 2007; Wang *et al.*, 2007). Wnt with its palmitoylate addition is transported from the ER to the Golgi to undergo protein sorting and forwarding into the secretory machinery. Another core component directs this step of Wnt secretion. The chaperone Wntless (WLS; Also known as Evi) is a membrane bound receptor that shuttles Wnt to the cell surface (Bartscherer and Boutros, 2008). WLS is dependent on the prior palmitoylation by Porcupine (Bänziger *et al.*, 2006; Bartscherer *et al.*, 2006). Consistent with *porcupine* loss of function, WLS knockdown in mice generates a similar embryonic lethal with deficiency in body axis formation (Fu *et al.*, 2009).

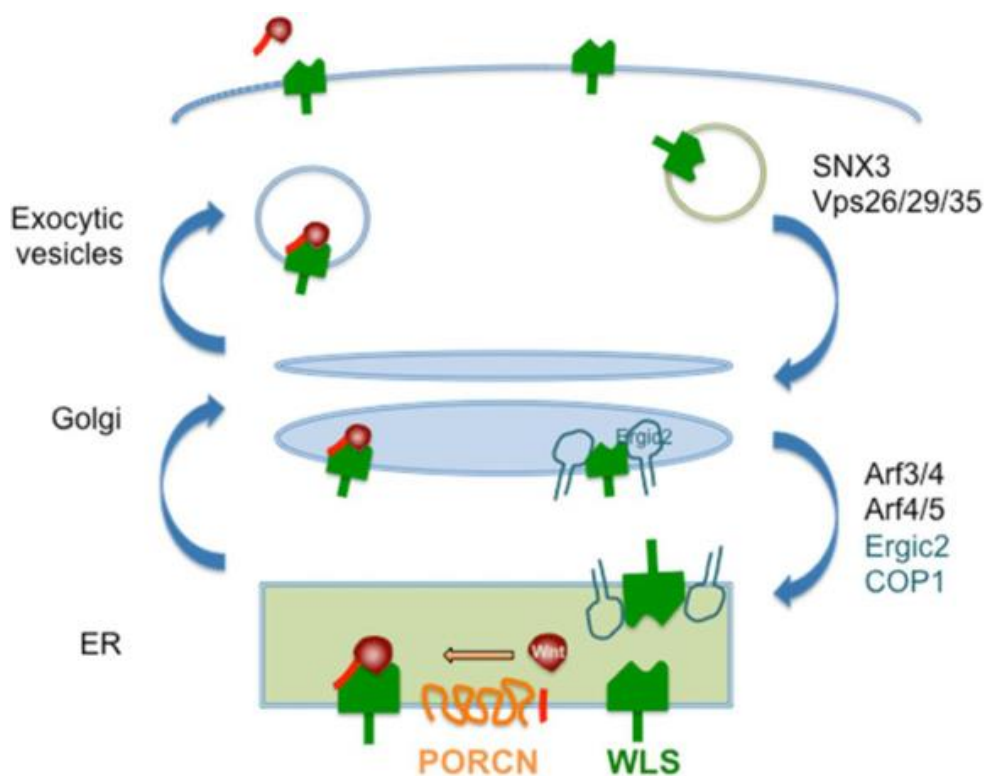


Figure 8: Overview of the Wnt maturation and secretion pathway. Wnt palmitoylation is facilitated by the O-acyl transferase Porcupine (PORCN) in the ER. The chaperone Wingless (WLS) binds and shuttles Wnt to the cell surface to enable its dissemination. WLS is recycled back to the Golgi via clathrin-mediated endocytosis and the retromer complex, and further to the ER by COP1 depended transport. Figure from Yu and Virshup, 2014.

Upon arrival at the plasma membrane, Wnt is disassociated from WLS to allow secretion and trafficking. However, Wnt proteins were shown not to rely on the secretory pathway alone to travel between cells (Bartscherer and Boutros, 2008; Harterink and Korswagen, 2012). Instead, a specialized transport machinery is required to guide the membrane-attached Wnt proteins to their destination as further described in the following chapter (Port and Basler, 2010; Stanganello and Scholpp, 2016). WLS undergoes a clathrin-dependent recycling process (Port *et al.*, 2008) to ensure consistent availability of WLS shuttle proteins for Wnt dissemination (Figure 8). WLS is endocytosed in endosomes and directed to the *trans* Golgi network by the retromer complex, composed of two vacuolar protein sorting (Vps) containing subcomplexes for cargo selection (Vps35p, Vps29p, Vps26p) and structure subunits (Vps5p, Vps17p) (Seaman, 2005). WLS is transported back to the ER in a second step involving the COP1 transport machinery in addition to the GTPases ARF4/4 and ARF4/5 and Ergic2 (Yu *et al.*, 2014). Dysfunction of WLS retrograde transport from the Golgi to the ER can lead to phenotypes comparable to loss of Wnt as discovered in a *C.elegans* vps-35 mutation (Coudreuse *et al.*, 2006).

1.7. Active distribution mechanisms of Wnt molecules

Since the observation of Porcupine-mediated acylation by palmitoyl to Wnt proteins (Takada *et al.*, 2006; Willert *et al.*, 2003), researchers have undertaken vigorous effort to elucidate the mechanism of Wnt transport (Takada *et al.*, 2017; Stanganello and Scholpp, 2016). Free diffusion through the extracellular space, the basic principle of morphogen distribution, is impaired by the strong membrane affinity of Wnt (Harterink and Korswagen, 2012). Even so, in some contexts Wnt signals need to be delivered ≥ 20 cell diameters away from the source of production to bind the respective receptors and activate target gene expression (Zecca *et al.*, 1996). Intriguingly, a forced membrane-tethering of the *Drosophila* Wnt Wingless would not cause aberrant development and is able to pattern the imaginal wing disc accordingly (Alexandre *et al.*, 2014), which led to the proposal that the lipid attachment is not removed after secretion. On the other hand, the requirement of secretion and lipidation can be context-dependent, as evidence of *porcupine*-deficient zebrafish embryos suggests, where ectopic Wnt5b dissemination was hindered, while embryos with Wnt3a were less affected (Chen *et al.*, 2012). Furthermore, polarity is another crucial factor in Wnt secretion because ectopically expressed Wnt11 is released apically in a WLS-dependent manner in cultured epithelial cells, while Wnt3a is secreted basolaterally. Several examples demonstrate the heterogeneity in Wnt secretion and propagation machinery and hint on a complex

context-dependent transport mechanism. In fact, several Wnt possible dissemination types have been elucidated so far including transport by cell division (Farin *et al.*, 2016), binding to lipid-binding transport proteins (Mulligan *et al.*, 2012), restricted diffusion by ECM interactions (Yan and Lin, 2009), membranous extracellular vesicles (McGough and Vincent, 2016), and by extension of cellular protrusions (Huang and Kornberg, 2015; Stanganello *et al.*, 2015) (Figure 9). All of them illustrate valid concepts for Wnt spreading and have been presented essential as Wnt traveling in the respective tissue or biological process. The best-characterized examples are described in the following.

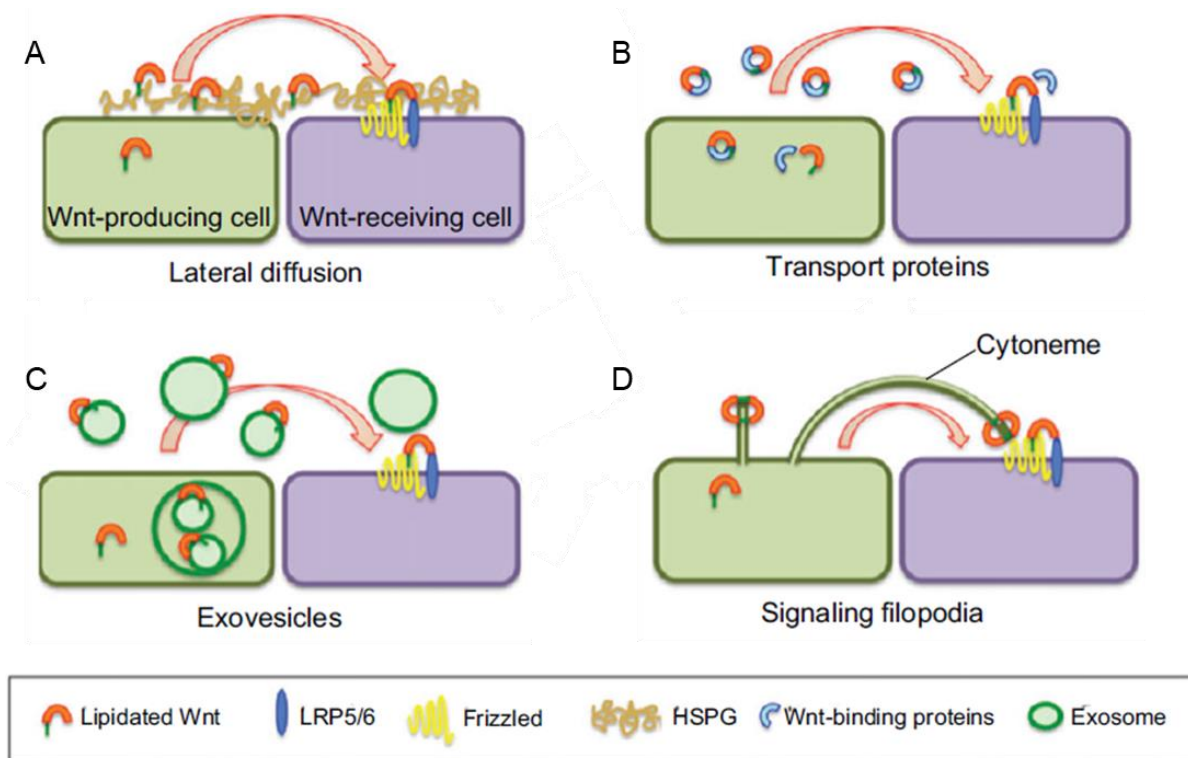


Figure 9: Models for paracrine Wnt transport. (A) Wnt moves through interaction with a heparan sulfate proteoglycans (HSPG) matrix. (B) The hydrophobic lipid modification of Wnt is covered by extracellular Wnt binding proteins such as sFRPs or secreted Wg-interacting molecule (Swim) to enable extracellular space travelling. (C) Wnt is associated to the surface of an extracellular vesicles such as exosomes and lipoprotein particles. (D) Cellular extensions shuttle Wnt proteins to target cells in a contact-dependent manner. Figure adapted from Stanganello and Scholpp, 2017.

1.7.1. Restricted diffusion by HSPGs

As described before, the lipid anchor of Wnt associates it to the cell membrane but is also fundamental for Wnt-Fzd receptor interaction (Janda *et al.*, 2012). The properties and composition of the extracellular matrix modulate the trafficking potential of extracellular proteins (Figure 9A). The interaction of Wnt proteins with heparan sulfate (HS)

proteoglycans (HSPGs), defined by the substitution with several HS glycosaminoglycan (GAG) polysaccharide chains, is one example of modifying Wnt trafficking post-secretion (Yan and Lin, 2009). The binding of Wg to heparin was proposed to regulate the amount of Wnt proteins available on the plasma membrane (Chakrabarti *et al.*, 1992). The HSPGs (Division abnormally delayed protein) Dally and Dally-like protein (Dlp) in *Drosophila* shape the Wg gradient by enabling Wg spreading (Han *et al.*, 2005), despite having been related to the opposing effects. Dally expression stimulates Wnt signaling by elevating Wg presentation to the Fzd receptor dFzd2 (Lin and Perrimon, 1999). However, Dally reduces Wnt signaling in adjacent tissues but promotes long-range Wnt activation (Han *et al.*, 2005; Yan and Lin, 2009). Modifications of extracellular HSPGs also affect Wnt trafficking and Wnt signaling activity (Fellgett *et al.*, 2015). The heparan-sulfate-specific 6-O-Sulfatase 1 (Sulf1) modulates HSPGs by attaching HS modifications. Sulf1 affect the bio-availability of the Wnt ligands Wnt3a, Wnt8a, and Wnt11b in *Xenopus* by altering their membrane localization and extracellular protein levels. Interestingly, Sulf1 acts in a ligand-dependent manner and has controversial effects on different Wnt ligands in both canonical and non-canonical signaling, because Sulf1 decreases Wnt8a activity while Wnt11b activity is enhanced (Fellgett *et al.*, 2015).

1.7.2. Free diffusion facilitated by Wnt binding proteins

Extracellular molecules can cover the hydrophobic moiety of Wnt to allow migration through an aqueous extracellular environment (Figure 9B). The secreted Wg-interacting molecule (Swim) was shown to promote extracellular Wg diffusion. Swim is an extracellular transport protein of the Lipocalin family and can interact with the Wg lipid addition. In the *Drosophila* wing disc, reduction of endogenous Swim expression impairs long-range Wg gradient formation and signaling (Mulligan *et al.*, 2012), however, a similar function of lipocalin in vertebrates has not been observed yet. Overexpression, however, does not improve Wg diffusion but reduces its signaling potential by interfering with ligand-receptor interactions. Likewise, secreted Frizzled-related proteins (sFRPs) are secreted Wnt inhibitors but were also shown to facilitate Wnt spreading in a tissue. Two members of the sFRP family in *Xenopus*, Frzb and crescent, expand the delivered range of Wnt8 (Mii and Taira, 2009). Consistently, a loss of sFRP1 and sFRP2 in mice causes a disruption in Wnt11 transport and consequently a deficiency in Wnt/ β -catenin in the embryonic optic cup (Esteve *et al.*, 2011). Additionally, ectopic sFRP1 expression in the *Drosophila* wing disc extend Wg distribution to preferably stimulate long-range targets instead of short range genes (Esteve *et al.*, 2011).

Even though the ability to bind Wnt proteins was demonstrated in various contexts, the biological relevance for this distribution mechanism is still disputable and needs to be further elucidated.

1.7.3. Exovesicles as morphogen carrier

Instead of protecting the hydrophobic moiety with a single protein, Wnt proteins can use their lipid anchor to associate with membranous extracellular vesicles as a secretion and dispersion system (Figure 9C). *Drosophila* Wg was documented first on extracellular lipoprotein particles described as argosomes (Greco *et al.*, 2001), apolipoprotein-containing phospholipid monolayers containing the *Drosophila* homolog of apolipoprotein lipophorin. These lipoprotein vesicles were important for forming the Wg gradient, because reduced lipophorin restricts the range of Wg diffusion and the overall extracellular Wg levels (Panáková *et al.*, 2005). Consistently, Wnt3a was isolated in high-density lipoproteins (HDL) particles in mammalian *in vitro* culture (Neumann *et al.*, 2009). Furthermore, Wnt can be shuttled by association on exosome particles (Gross and Boutros, 2013). Exosomes are released by fusion of multi-vesicular-body (MVB) with the plasma membrane. Wnts are loaded onto MVBs by help of the cargo receptor Evi/WLS. Several lines of evidence demonstrate Wnt protein trafficking over large distances via exosomes independent of lipoprotein particles and can induce active Wnt signaling activity in *Drosophila* and human cells (Gross *et al.*, 2012). Active Wnt5b associated on exosomes was reported in several cancer cell lines to promote paracrine cell migration and proliferation (Harada *et al.*, 2017). Furthermore, fibroblast-derived exosomes enabled axonal regeneration in the injured CNS. Exosomes recruit Wnt10b toward lipid rafts in neurons to drive autocrine mTOR via GSK3 β . Remarkably, exosome application rescued axonal regeneration in Wnt10b-deleted animals (Tassew *et al.*, 2017). In terms of Wg gradient formation, *Drosophila* S2 cells secrete Wg exosomes in the wing disc. However, The Wnt gradient was unaffected by those Wnt containing exosomes (Beckett *et al.*, 2013).

1.7.4. Contact-dependent signaling

Contact-dependent cell to cell communication systems such as cytonemes or tunneling nanotubes (TNTs) are facilitated by membranous extensions that share striking similarities with filopodia (Sougata Roy, 2015; Austefjord *et al.*, 2014). Filopodia are actin-rich membrane protrusions that extend from cells (Mattila and Lappalainen, 2008; Jacquemet *et al.*, 2015). These finger-like structures are thin with a diameter of about 100-300 nm.

Filopodia contain parallel-oriented, tight filamentous F-actin bundles allowing quick extension and retraction within minutes. Functionally, filopodia are involved in many essential tasks.

In general, filopodia have most often been associated with changes in cell shape or in migration of cells and tissues (Ridley *et al.*, 2003). For example, filopodia are necessary for neurite formation and axon guidance in neurons. During cell migration, filopodia form initial adhesion sites, which can later be transformed into stable, mature focal adhesions. Finally, tissue migration and wound healing is a further common event during embryonic development. Filopodia project at the edges of epithelial cells and have an important role during the movement of these epithelial cell sheets. Cell adhesion molecules allow the ‘tentacles’ to stick to the substrate or to neighboring cells to promote migration. However, it is nearly impossible to assign a specific function to filopodia, because selective removal is not possible without compromising the integrity of the cell.

The dynamic nature of filopodia have also suggested an additional sensory role. Filopodia have been described as ‘antenna’ of the cell, used to probe their environment. Signals from the environment sensed by filopodia influences their cell behavior. Indeed, filopodia contain receptors for a huge variety of signaling molecules and extracellular matrix proteins. For example, a bidirectional signaling interaction of the EphrinB1 ligand on filopodia of hepatic progenitors and the EphB3b receptor on filopodia of cells of the lateral plate mesoderm is important for positioning the liver (Cayuso *et al.*, 2016). Consequently, filopodia may act as sites for signal transduction. The length and the dynamics of these ‘fishing rods’ make them ideal signal receivers crucial for the development of a tissue. In some circumstances, the signal can also be passed on by filopodia. Filopodia on macrophages have been suggested to relay signals in such a way. In zebrafish, pigment cells project filopodia with signal-containing vesicles at their tips and deposit these in the tissue. These vesicles are taken up by macrophages and subsequently re-distributed to the target cells (Eom and Parichy, 2017).

Two main modes of contact-dependent signal transport have been elucidated over the past years. Both are accepted cell-cell communication systems but operate in slightly different scope of actions: Tunneling nanotubes (TNTs) (Rustom *et al.*, 2004) and cytonemes (Ramírez-Weber and Kornberg, 1999) (Figure 10).

1.7.5. Cargo transfer by tunneling nanotubes

Contact-dependent long-range signaling requires the formation of thin membranous, cytoplasmic connections to transmit various types of information. Tunneling nanotubes were initially discovered by the group of Hans-Hermann Gerdes in 2004. In the following years, many types of cargo were found to be transported in or on TNTs. For example, these intercellular bridges enable the mobilization of cargos of various sizes, from signaling proteins to cellular organelles including endosomal vesicles, mitochondria (Rustom *et al.*, 2004, Kadiu and Gendelman, 2011a ; Smith *et al.*, 2011, Wang & Gerdes, 2015), lipid droplets (Astania *et al.*, 2015), pathogens (Onfelt *et al.*, 2006; Sowinski *et al.*, 2008), prions (Gousset *et al.*, 2009; Zhu *et al.*, 2015) and electrical signals (Wang *et al.*, 2010).

These versatile cell connections were originally described in primary rat pheochromocytoma (PC12) cultures which build nanotubular bridges that can reach up to several cell diameters to exchange membrane vesicles and organelles (Rustom *et al.*, 2004). Like cytonemes, TNTs are actin-and tubulin-based protrusions, but possess some unique features: once established, TNTs form stable bridges between cells with a seamless membrane connectivity (Figure 10). Electron micrographs demonstrated a continuous channel that connects the cytoplasm of both cells allowing lateral diffusion of cytoplasm and bi-directional transport of cargo (Rustom *et al.*, 2004). High-resolution structural analysis yielded accurate insights into the molecular features of these cellular conduits. Broadly speaking, TNTs are categorized in two groups (Onfelt *et al.*, 2006): short and thin nanotubes with a diameter of tens of nanometers and a length below 50 μm , which transport smaller cargo such as proteins. The second class are longer and thicker TNTs with a diameter over 700 nm and span over hundreds of micrometers. These intracellular bridges can be used to mobilize larger cargo such as organelles.

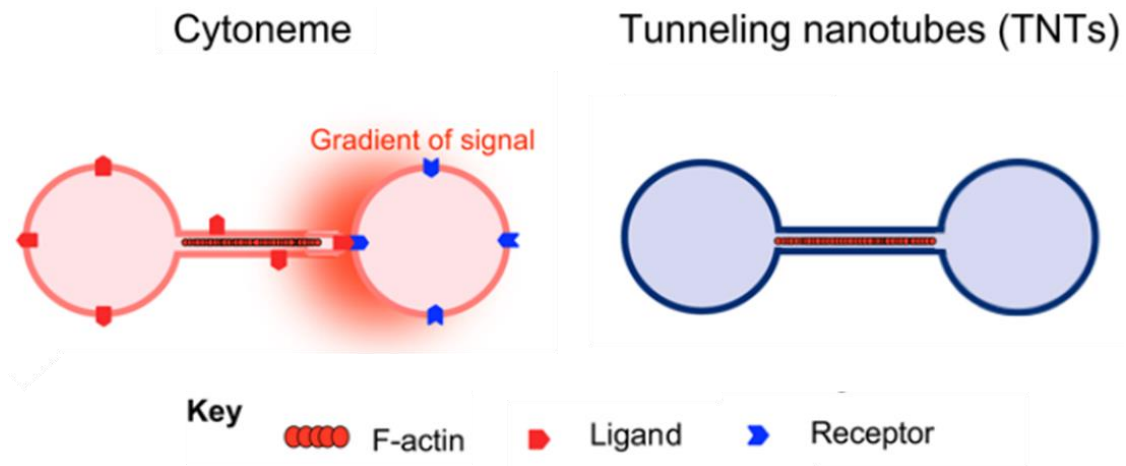


Figure 10: Contact-dependent cell-cell communication. Both cytonemes and TNTs are fine cellular connections between cells composed of mainly F-actin. Cytonemes were reported to facilitate ligand-receptor interactions and can generate a signaling gradient across a tissue. TNTs build persistent connections and transfer both small and large cargo in a bi-directional manner through the seamless membrane channels. Figure from Abounit and Zurzolo, 2012

In vitro, TNTs were shown to be involved in a multitude of processes, but until recently there was a shortage of data available to underline their relevance *in vivo*. With improvements in fixation methods and live imaging, TNTs could be described in several tissues. Neural crest cells in chick embryos show TNTs linking two cells by a continuous membrane tether, which is maintained during migration. If broken, it causes a cue for a directional change (Teddy, 2004). These bridges actively exchange cytoplasmic material in a bi-directional manner to gain positional information (McKinney *et al.*, 2012). Intercellular bridges were also reported in gastrulating zebrafish embryos that share striking similarities to TNTs (Caneparo *et al.*, 2011). They are different from the cytoneme-like protrusions because these bridges are established and then maintained in daughter cells after cell division. Additionally, transfer of cytosolic and membrane-tethered fluorescent proteins was reported, suggesting there is a seamless transition from one cell to the other which could mediate cell-cell communication during gastrulation. This continuous membrane tube tethers cells for several hours and can extend up to 350 μm . In cancers, TNTs play a further pivotal role in the exchange of information within a tumor. TNTs connect tumor cells of patient-derived malignant pleural mesothelioma to enable a bi-directional transfer of organelles and other cytosolic components (Lou *et al.*, 2012), highlighting a role in mammalian cancer cell pathogenesis and invasion. Similar to TNTs in the cornea, these TNTs of invasive malignant

mesothelioma cells are formed *de novo* to communicate with surrounding cells. TNTs between stromal mesenchymal cells or endothelial cells and cancer cells were also reported in 3D anchorage-independent spheroids and tumor explants (Pasquier *et al.*, 2013). These findings suggest that TNTs play a role in cell-cell communication in the metastatic niche.

1.8. Morphogen transport by cytonemes

TNTs were shown to transport cargo in a bi-directional fashion (Lou *et al.*, 2012; Teddy, 2004; Rustom *et al.*, 2004) permitted by the open-ended protrusion and broad amount of diverse functions and modes of delivery. However, another kind of contact-dependent cell-cell communication system, cytonemes, can transmit signals. Cytonemes operate as a one-way road and rely mainly on ligand-receptor interactions between a producing and a receiving tissue. Their signaling purpose and generation of a morphogen gradient stands out as a vital criterion (Pröls *et al.*, 2016). In various contexts, these cytonemes allowing the spreading of signaling proteins as well as in reception, by extending with cellular projections over a wide field of tissue. This allows a short to long range signal transport in various tissues such as the air sac primordium in the tracheal system, eye and wing imaginal discs or in the abdominal epidermis. Additionally, cytonemes were shown to be important for a multitude of signaling pathways, such as Dpp, Hh, EGF, and FGF and Wnt.

1.8.1. Discovery of cytonemes

A special type of long cellular extension connected to signaling events was first noted in *Drosophila* wing imaginal disc cells by the lab of Thomas Kornberg. These protrusions orient uniformly towards the disc midline where the morphogen signaling protein Decapentaplegic (Dpp) is expressed (Ramírez-Weber and Kornberg, 1999). The Dpp receptor Thickveins (Tkv) is present in motile puncta in these extensions suggesting that they are used to transport Dpp across the disc (Hsiung *et al.*, 2005). Based on this initial finding, filopodia, which are involved in signal distribution by containing ligands or receptors, have been termed cytonemes (Figure 10). Further to this initial finding, cytonemes could also be observed in various other *Drosophila* tissues. For example, the Egf receptor (EgfR) is present in clusters in the cytonemes that orient to the morphogenetic furrow where the ligand Spitz Spi/Egf is expressed (Roy *et al.*, 2011). Cytonemes have also been suggested to deliver Hh signaling in the *Drosophila* embryo. In both wing disc and abdominal histoblasts, cytonemes from Hh-producing cells extend across its morphogenetic gradient (Bischoff *et al.*, 2013). Hh cytonemes extend and retract dynamically and act as conduits for ligand dispersion mainly at

the basal plane of the epithelium. Hh proteins associate with vesicles, which are transported along these cytonemes (Gradilla *et al.*, 2014). Consistently, cytonemes similarly emanate from the ligand-receiving cells (González-Méndez *et al.*, 2017). Essential Hh signaling components of the receiving cell localize to these cytonemes, including the canonical Hh receptor Patched. Formation of the sending and the receiving cytonemes depends on the composition of the extracellular matrix. Cytonemes require heparan sulphate proteoglycans such as Dally and Dally-like protein for proper extension. Especially for cytonemes decorated with receptors, it appears there is a high level of signal-specificity. In tracheal cells, cytonemes carry either the receptor to the *Drosophila* fibroblast growth factor protein, Branchless (Btl), or they hold the dpp receptor Tkv (Roy *et al.*, 2011; Hsiung *et al.*, 2005). Furthermore, cytonemes are modular in response to changing amounts of signaling protein. Overexpressed GFP-labelled EGF receptor in the eye disc reduces the range and effectiveness of cytonemes ranging from the EGF Spitz morphogen source. Cells must possess a complex intrinsic mechanism of morphogen sensing and a way to subsequently reconfigure cytonemes to balance signal uptake and ensure normal development.

1.8.2. Cytonemes in vertebrates

There is accumulating evidence that vertebrate cells have a similar ability to form signaling filopodia. In transformed mammalian cell lines, filopodia are associated with the transduction cascade for EGF signaling (Lidke *et al.*, 2005) and FGF signaling (Koizumi *et al.*, 2012). They have been observed extending from B cells (Gupta and DeFranco, 2003) and from mast cells induced by chemokines (Fifadara *et al.*, 2010). Furthermore, cytonemes have also been described regulating distribution of pigment cells in zebrafish (Inaba *et al.*, 2012). A recent report describes cytonemes as an essential trafficking mechanism for Shh in the chick limb bud (Sanders *et al.*, 2013). The Shh ligand is transported in the anterograde direction in cytonemes with a length of 200 μm . Structurally, Shh cytonemes are characterized by the existence of microtubules at the proximal base. Accordingly, transport of Shh – with a maximum velocity of anterograde particle movement of 120 nm/s – is consistent with actin-based myosin motors. Cytonemes also formed by these chick mesenchymal cells carry the Shh co-receptors Cdo and Boc and connect to the Shh positive cytonemes. This allows the distribution of the Shh protein over a distance of several hundreds of micrometers in the chick limb bud. In the context of Wnt signaling, epithelial cells in chicken embryos feature Wnt receptor Fzd7 containing cytonemes responsible for retrograde trafficking of Wnt proteins. These cytonemes are suggested to mediate signaling events by establishing a

morphogen gradient between distant epithelial cells during embryonic development. Consistently, several Wnt proteins have been preferably linked to cytonemes in various systems and developmental contexts. (Holzer *et al.*, 2012; Luz *et al.*, 2014; Stanganello *et al.*, 2015; Sagar *et al.*, 2015; Stanganello and Scholpp, 2016). One prominent example is the function of Wnt/ β -catenin signaling during CNS patterning.

1.8.3. The role of Wnt Cytonemes during zebrafish neural plate patterning

For a complex structure such as the neural plate with sharp boundaries, a fine-tuned spatial and temporal sequence of morphogen activity in a migrating and proliferating cell population of neuro-ectodermal cells is required. Recent evidence highlighted the role of Wnt cytonemes during zebrafish neural AP patterning (Stanganello *et al.*, 2015; Stanganello and Scholpp, 2016). In zebrafish embryonic development, Wnt morphogens are transported from a local signaling source to pattern the central nervous system during gastrulation. Cytonemes originate from a Wnt expressing local organizer, the dorsal marginal zone (Figure 11A) and extend preferably to the animal pole. Wnt8a protein clusters decorate the tips of specialized actin-based filopodia on signal-transmitting cells.

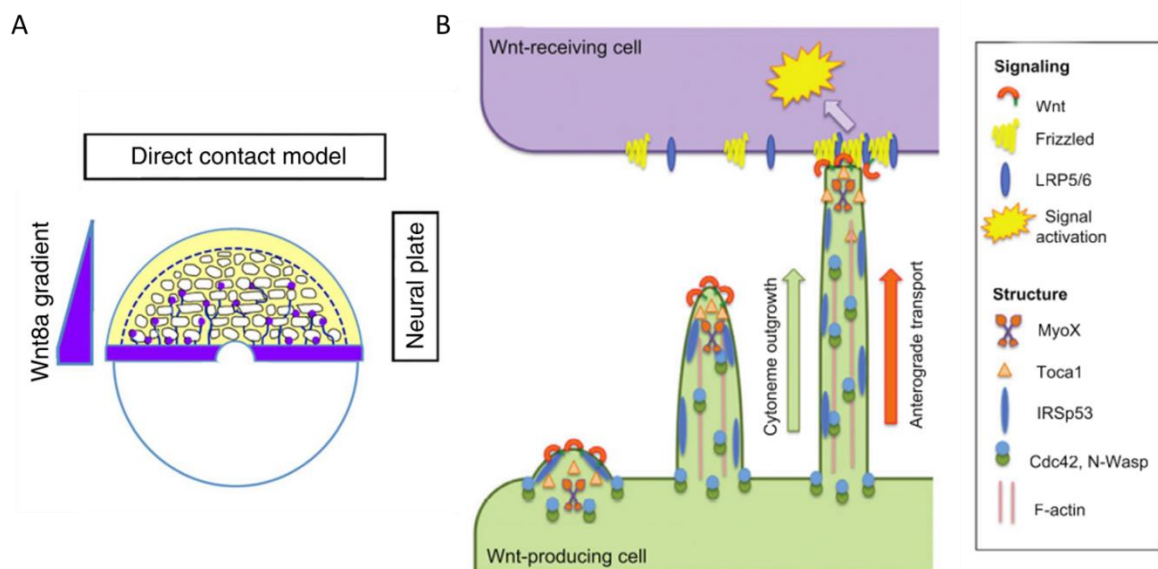


Figure 11: Overview of Wnt cytoneme structure and function during zebrafish neural plate patterning. (A) A morphogenic Wnt8a gradient is mediated by cytonemes emerging of Wnt8a-producing marginal zone cells (purple). Cytonemes span several cell diameters and are decorated by Wnt8a proteins on the distal filopodia tip. Wnt8a is deposited to neuro-ectodermal cells upon cell contact to guide cell fate decisions respective to the signal concentration. (B) Structure of a zebrafish Wnt8a-cytoneme and resulting receptor-

complex formation on target site. Nucleation and elongation of cytonemes depend on the actin machinery. Wnt8a clusters are found on the filopodia nucleation area and on cytoneme tips. Wnt8a forms Fzd/Lrp6 signalosomes in recipient tissue and activation of the Wnt/ β -catenin signaling pathway. Figure adapted from (A) Stanganello *et al.*, 2015 and (B) Stanganello and Scholpp, 2016.

The Cdc42 machinery was found to be a requirement for a functional cytoneme delivery system, and operates in combination with the neural Wiskott-Aldrich syndrome protein (N-Wasp), the Rho family GTPase effector Insulin Receptor tyrosine kinase Substrate p53 (IRSp53), and the transducer of Cdc42-dependent actin assembly 1 (Toca1) (Stanganello *et al.*, 2015). These cell protrusions extend up to 50 μ m and are able to activate the Wnt/ β -catenin signal transduction cascade, demonstrated by analyzing the relative expression levels of the target genes *axin2* and *lef1*, in the neighboring signal-receiving cells at the contact point of the filopodia to the cell body (Figure 11B). Cytoneme contact to the receiver cell features classical properties of Wnt signaling because a Wnt/Fzd/Lrp6 signalosome is established upon contact, a classic indicator of Wnt signaling activation (Niehrs, 2012; Hagemann *et al.*, 2014). Pruning of the cytoneme follows target finding and initial cell contact, retaining the Wnt8a/receptor cluster in the target plasma membrane. The attached Wnt cluster is endocytosed to mediate subsequent pathway activation. Furthermore, this propagation mechanism has been shown to be crucial for the generation of a proper morphogenic field (Stanganello *et al.*, 2015): Dysfunctional cytoneme delivery by inhibition of general actin-based protrusions caused severe patterning defects, verified by the position of the distinct neural patterning genes *otx2* and *gbx1*, which mark respectively the forebrain and the midbrain anlage or the developing hindbrain area (Rhinn *et al.*, 2005). Furthermore, requisition for cytonemes was verified in a Monte-Carlo simulation approach based on the measured experimental parameters.

In summary, delivery by cytonemes allows a highly tunable configuration for Wnt morphogen propagation in a system of highly dynamic tissue movements as in gastrulation. Signaling intensity can be regulated by the range and the amount of cytonemes, the morphogen concentration on the cytoneme tip, contact frequency and persistence of Wnt/receptor clusters on target cells. Additionally, context specific interpretation of receptor composition in the receiving tissue permits further regulation. However, specific regulation mechanisms to control the properties of Wnt cytonemes apart from broad actin-regulators are yet to be elucidated.

1.9. Zebrafish as a model organism

The zebrafish (*Danio rerio*) is a flourish vertebrate model organism for biological researches by unifying excellent embryology and versatile genetic manipulation (Nüsslein-Volhard and Dahm, 2002). As a vertebrate model is shares several developmental features with mammals, applicable to understand physiological and disease related conditions. Developmental principles such as pattern formation and the establishment of the body axis are evolutionary well conserved. Consistently, the zebrafish genome contains orthologs of most of the human genes, even though genome duplication has occurred deep in the ancestry of teleost fish (Postlethwait *et al.*, 2000). This genomic equivalence and conserved basic mechanisms are a great benefit especially in biomedical translated applications compared to classic invertebrate models as *Drosophila melanogaster* or *C. elegans*, which shine for their determined genetic developmental program and easy genetic manipulation, respectively. Zebrafish embryos have many unique features that make it ideal for developmental studies. For a start, a large number and easily accessible offspring develops *ex utero* and can be used for research immediately after fertilization, an enormous advantage compared to the mammalian mouse model *Mus musculus*. Zebrafish embryos are relatively large in size and transparent during the first 24 hours of their development (Kimmel *et al.*, 1995), allowing easy observation for morphological alterations and exceptional fluorescent microscopy techniques to visualize cellular processes, monitor reporter expressions, or for utilization in bio sensing approaches in living embryos. Another convenient aspect is rapid embryonic development. The general vertebrate specific body features can be seen after around two days and are nearly complete after five days. This includes compartmentalization of the brain, eyes and other internal organs. Another decisive advantage is the easy possibility for genetic manipulation and large-scale mutagenesis screens, making zebrafish suited for gene identification. As with other model organisms, the number experimental approaches for zebrafish have increased over the past years. Classic embryological techniques reach from mRNA or DNA microinjection to drive the inherent production of proteins, interference of protein translation by morpholinos (Nasevicius and Ekker, 2000), conditional cell-specific expression systems as the Gal4/UAS (Halpern *et al.*, 2008), through to transplantation of cells from a donor embryo. The range of the molecular toolset to manipulate gene expression and perform genome engineering took a big leap as well. Genome engineering developed from uncontrolled integration by the Tol2 transposase system to zinc finger nucleases (ZFNs), transcription activator-like effector nucleases (TALENs) leading to the fine-tuneable

machinery with CRISPR/Cas9 (clustered regularly interspaced short palindromic repeats/CRISPR associated protein 9) that allows nucleotide-specific disruption and insertion events into the genome (Albadri *et al.*, 2017).

1.11. Aim of this work

Wnt signaling is fundamental to establish the main body plan of complex organism by directing cell fate decisions during patterning. To operate as morphogens, Wnt proteins must form a concentration gradient across a tissue to activate a precise cellular program. Wnt proteins are palmitoylated, and consequently strongly attached to the cell membrane, which restrain passive diffusion.

I hypothesize, Wnts require an active transport machinery to reach the responsive tissue. Previous work revealed a filopodia-based propagation mode for Wnt molecules to directly contact the responsive cell to deliver Wnt proteins, activate Wnt-Signalosome formation and activate target gene expression. Wnt-cytonemes sprout from the Wnt producing marginal zone to propagate these signaling molecules over the prospective neural plate to facilitate AP patterning.

The aim of this work was to elucidate the molecular basis of Wnt-cytoneme formation and the delivery in vertebrate cells. Therefore, I intended to identify factors that specifically drive and regulate cytonemes. Subsequently, these molecular cues for cytonemes should be dissected to reveal the underlying molecular principles. Eventually, insight on cytoneme transport can be transferred to other signaling systems to assess gradient formation.

By probing for a cytoneme regulator, the tyrosine kinase and Wnt receptor Ror2 was identified to combine essential characteristics such as association with Wnt signaling, control of cytoskeleton elements, and upstream factor of the Rho GTPase Cdc42. A line of evidence suggested Ror2 to stimulate filopodia formation in various contexts. However, Ror2 acts in the mutually repressive Wnt/PCP pathway in contrast to the patterning-mediating Wnt/ β -catenin pathway. The involvement of Ror2 was investigated *in vitro* in various cell culture models as well as *in vivo* during zebrafish gastrulation. By breaking down the operations for sending and recipient cells, I was deciphering a model for Wnt-cytoneme regulation. In the end, this adjustable contact-dependent model was reviewed for its effectiveness during zebrafish AP patterning and applied to another system such as in mouse intestinal crypt homeostasis and human gastric cancer proliferation.

2. Material and Methods

2.1. Materials

2.1.1. Equipment and tools

Name	Description
35mm Cell culture dishes with ventilation	ThermoFisher Scientific
ABI StepOnePlus	ThermoFisher Scientific
Capillary holder	World Precision Instruments
Dissection forceps	World Precision Instruments
Microinjector with integrated pressure supply	FemtoJet
Flaming/Brown Microcapillary Puller P-97	Sutter Instrument
Gel electrophoresis System	Bio-Rad
Glass capillary 1mm/0.75mm OD/ID	World Precision Instruments
Glass-bottom dishes	MatTek
Gradient PCR machine	Eppendorf
Laminar Flow Cabinet	LaboGene
Microloader tips	Eppendorf
NanoDrop	ThermoFisher Scientific
T75 cell culture flasks	ThermoFisher Scientific
Three-axis manual Micromanipulator	World Precision Instruments
Tissue culture incubators	ThermoFisher Scientific
Tungsten needle TGW1510	World Precision Instruments

2.1.2. Chemicals

1-phenyl-2-thiourea (PTU)	Sigma-Aldrich
4',6-diamidino-2-phenylindole	Sigma-Aldrich
Agarose	Peqlab
Ampicillin	Carl Roth
Anti-Digoxigenin-Fab fragments	Roche

Blocking reagent	Roche
Bovine serum albumin (BSA)	PAA
Calcium acetate	Carl Roth
Calciumchloride	Sigma-Aldrich
Chloroform	Sigma-Aldrich
Citric acid	Carl Roth
Dimethylsulfoxide	Sigma-Aldrich
Dulbecco´s modified Eagle´s medium (DMEM)	ThermoFisher Scientific
Ethanol	Carl Roth
Ethidiumbromide	Carl Roth
Ethylenediaminetetraacetic acid (EDTA)	Roth
Fetal bovine serum (FBS)	ThermoFisher Scientific
Formamide	Carl Roth
Glycerol	Carl Roth
Glycine	Carl Roth
Heparin	Roche
HEPES	Roche
Hydrochloric acid (HCl)	Merck
Isopropanol	Carl Roth
Kanamycin	ThermoFisher Scientific
Leibovitz´s L-15	ThermoFisher Scientific
Low melting agarose	Carl Roth
Methanol	Carl Roth
Methylene blue	Sigma-Aldrich
Midori Green	Biozym
NBT/BCIP solution	Roche
Paraformaldehyde	Merck
Penicilin/Streptomycin	ThermoFisher Scientific
Phalloidin, Tetramethylrhodamine B isothiocyanate	Sigma-Aldrich

(TRITC)	
Phenol red (Phenolsulfonphthalein)	Sigma-Aldrich
Phosphate buffered saline (PBS)	ThermoFisher Scientific
Pronase	Carl Roth
Proteinase K	Sigma-Aldrich
RPMI-1640	ThermoFisher Scientific
Sodium acetate (NaAc)	Carl Roth
Sodium chloride (NaCl)	Carl Roth
Sodium hydroxide (NaOH)	Carl Roth
tricaine	Sigma-Aldrich
Tris-base	Carl Roth
Tris-HCl	Carl Roth
Triton-X-100	Carl Roth
Trizol	ThermoFisher Scientific
Trypsin 0.25% (w/v)-EDTA	ThermoFisher Scientific
Tween 20	Carl Roth

2.1.3. Solutions

1x MESAB	400 mg tricaine powder, 2.1 ml 1 M TRIS (pH 9.0) in 100 ml H ₂ O, pH 7.0
Calcium free Ringer	116 mM NaCl, 2.9 mM KCl, 5 mM HEPES, pH 7.2
E3 zebrafish medium	5 mM NaCl, 0.17 mM KCl, 0.33 mM CaCl ₂ , 0.33 mM MgSO ₄ , 0.1% methylene blue
HYB-	50% formamide, 5x SSC (pH=6.0) , 0.1% Tween-20
HYB+	HYB- with 5 mg/ml torula (yeast) RNA, 50 µg/ml heparin
HYB+	500 ml Formamide , 250 ml 20x SSC (pH 6), 0.1% Tween20, 0.5 mg/ml torula (yeast) RNA, 50µg/ml Heparin
MABT	100 mM Maleic acid, 150 mM NaCl, 0.1% Tween-20, pH 7.5
NTMT	100 mM NaCl, 100 mM Tris pH 9.5, 1% Tween20

PBST	1 x PBS + 0.1% Tween20
PFA	4% paraformaldehyde in 100 mM phosphate buffer pH 7.4
PTU	0.003% 1-phenyl-2-thiourea in 10% Hank's saline
SSCT	8,7g NaCl, 4,41g Na3Citrate per L, pH 6.0 + 0.01% Tween-20

2.1.4. Kits

Name	Description
Direct-zol RNA Mini Prep Kit	Zymo Research
FuGene HD Transfection Kit	Promega
Illustra ProbeQuant G-50 Microcolumns	GE Healthcare Europe
In-Fusion HD Cloning Kit	Clontech
mMESSAGE mMACHINE Transcription (Sp6,T3,T7)	ThermoFisher Scientific
peqGold Gel Extraction Kit	Peqlab
QIAGEN Plasmid Purification Kit	Qiagen
SuperScript® III First-Strand Synthesis System	ThermoFisher Scientific
SYBR green qPCR Kit	ThermoFisher Scientific
TOPO TA and Blunt Cloning Kit	ThermoFisher Scientific

2.1.5. Molecular tools and enzymes

Name	Description
Anti-Digoxigenin-AP fab fragments	Roche
Anti-Fluorescein-AP fab fragments	Roche
DIG RNA Labeling Mix	Roche
DNase I	Ambion
FITC RNA Labeling Mix	Roche
GeneRuler DNA ladder mix	Fermentas
GoTaq-Polymerase	Promega
GTPase Inhibitor ML141	Merck Millipore
LifeAct Actin Stain	ThermoFisher Scientific
MMLV Reverse transcriptase	Promega

One Shot TOP10 Chemically Competent <i>E.coli</i>	ThermoFisher Scientific
Pfu DNA Polymerase	Promega
Phalloidin, Fluorescein Isothiocyanate Labeled	Sigma-Aldrich
Restriction enzymes	New England Biolabs and Fermentas
Shrimp Alkaline Phosphatase	Promega
Sp6 RNA polymerase	ThermoFisher Scientific
T4 Ligase	Promega
T7 RNA polymerase	ThermoFisher Scientific
Wnt inhibitor IWR-1	Sigma-Aldrich

2.1.6. Nucleotides

Name	Description	Sequence
<i>ror2</i> Morpholino	Gene Tools	(5'- CAGTGTAACAACCTTCCAAACTCTC C -3')
TrueGuide Synthetic 2-piece gRNA system	ThermoFisher Scientific	
<i>ror2</i> gRNA ORF #1	ThermoFisher Scientific	(5'- TACAACTGGAGCTCATCTGG-3')
<i>ror2</i> gRNA ORF #2	ThermoFisher Scientific	(5'- CTTGCAGAGGCCCAAAGTGG-3')
<i>ror2</i> gRNA UTR #1	ThermoFisher Scientific	(5'- GTGCACACTTGAGACTTTGG-3')
<i>ror1</i> gRNA ORF #1	ThermoFisher Scientific	(5'- AATCTGGACACCACAGACAC-3')

Primer

DNA primer for cloning	Metabion or Eurofins
DNA sequencing	Eurofins

RT-qPCR

primers

<i>actb1</i>	Metabion	(5'-CCTTCCTTCCTGGGTATGG-3'; 5'-GGTCCTTACGGATGTCCAC-3')
<i>axin2</i>	Metabion	(5'-CAATGGACGAAAGGAAAGATCC-3'; 5'-AGAAGTACGTGACTACCGTC-3')
<i>lef1</i>	Metabion	(5'-CAGACATTCCCAATTTCTATCC-3'; 5'-TGTGATGTGAGAACCA ACC-3')

Antisense RNA probes

<i>axin2</i>	<i>ntl (tbxta)</i>
<i>fgf8a</i>	<i>pax6a</i>
<i>Fzd7a</i>	<i>Wnt8a</i>
<i>hgg1 (ctslb)</i>	

2.1.7. Plasmids

Name	Description
dCas9	Provided by Robert Wilkinson, Medical School, University of Sheffield.
Dvl2	(Hagemann <i>et al.</i> , 2014)
Fzd7aWT	(Hagemann <i>et al.</i> , 2014)
Fzd7aΔC	(Hagemann <i>et al.</i> , 2014)
Fzd7aΔN	(Hagemann <i>et al.</i> , 2014)
GPI-anchored CFP	(Hagemann <i>et al.</i> , 2014)
hLrp6	(Stanganello <i>et al.</i> , 2015)
IRSp534K	(Casella <i>et al.</i> , 1981)
mRor2- ΔCRD-GFP	Mouse Ror2 with truncated CRD
pcDNA3-EGFP-Cdc42T17N	Addgene #12976
pCS2+ GAP43-GFP	(Okada <i>et al.</i> , 1999)

pCS2+ H2B-RFP	provided by the lab of Scott E. Fraser, California Institute of Technology.
pCS2+ hLrp6-GFP	Provided by Gary Davidson, KIT, Karlsruhe (Chen <i>et al.</i> , 2014).
pCS2+Fz7a-CFP	(Hagemann <i>et al.</i> , 2014)
pCS2+GPI-anchored mCherry	(Scholpp <i>et al.</i> , 2009)
pCS2+xRor2	xRor2-mCherry was inserted in the ClaI/XhoI site of pCS2+.
pCS2+xRor2 ^{3I}	(Hikasa <i>et al.</i> , 2002)
pCS2+xRor2-mCherry	(Feike <i>et al.</i> , 2010)
pCS2+xWnt5a-GFP	(Wallkamm <i>et al.</i> , 2014)
pCS2+zfCas9	Codon optimized Cas9 for zebrafish provided by Joachim Wittbrodt, COS, Heidelberg.
pCS2+zfWnt5b	Addgene #21282
pCS2+zfWnt8aORF1	Addgene #17048
pCS2+zfWnt8aORF1-GFP	(Rhinn <i>et al.</i> , 2005)
pCS2+zfWnt8aORF1-mCherry	(Stanganello <i>et al.</i> , 2015)
pDest7xTCF-nucRFP	(Moro <i>et al.</i> , 2012)
pmKate2-f-mem	Evrogen # FP186

2.1.8. Fish strains

Name	Description
AB ₂ O ₂	Institute of Toxicology and Genetics
AB ₂ O ₃	Institute of Toxicology and Genetics
WIK	University of Exeter
tg(-6gsc:EGFP-CAAX)	Smutny <i>et al.</i> , 2017

2.1.9. Cell lines

PAC2 zebrafish fibroblasts
Gastric tubular adenocarcinoma liver metastasis cells (MKN28)

human embryonic kidney cells (HEK293T; CRL-1573)

primary gastric adenocarcinoma cells (AGS)

2.1.10. Microscopes

Leica DMI6000 SD

Leica SP5 X confocal microscope with dip-in objective

Leica SP8 X confocal microscope with dip-in objective

Olympus SZX16 equipped with a DP71 digital camera

Olympus SZX16 equipped with a DP71 digital camera

2.1.11. Software

Name	Description
Adobe Photoshop CS5	Adobe systems
Cell D imaging software	Olympus
Fiji	ImageJ
Imaris 9.1	Bitplane AG
LAS AF imaging software	Leica
Matlab	The MathWorks, Inc.
SnapGene Sequence Viewer 4.1	SnapGene

2.2. Methods

2.2.1. Molecular cloning

2.2.1.1. Extraction of mRNA and cDNA synthesis for molecular cloning

To create a cDNA library of zebrafish embryos, the RNA of approximately 100 AB₂O₃ embryos at 8, 14 and 24 hpf was collected. After dechoriation, TRIzol reagent was added

and they were immediately crushed with a crucible and vortexed to homogenize. Then embryos were shaking on a heat block for 10 minutes at 37°C, chloroform was added and incubated at RT for 5 minutes before centrifugation. To the supernatant Isopropanol was added, incubated again 10 minutes on ice and centrifuged for 10 minutes. The supernatant was discarded, and the pellet was washed with ice-cold EtOH and again centrifuged for 5 minutes. The RNA pellet was dried and resuspended in 15µl dH₂O and stored at -80°C before further use. For cDNA synthesis Super Script III Super Mix (Life Technologies) was used and the cDNA was stored at -20°C.

2.2.1.2. Polymerase Chain Reaction (PCR)

PCR was performed to amplify selected target gene coding sequences out of the generated zebrafish cDNA. A GoTaq DNA Polymerase 50µl reaction mix was prepared according to the manufacturer protocol. The PCR product in green GoTaq buffer was immediately used for agarose gel electrophoresis with 0.5 - 1.5% agarose dependent on fragment size and afterwards purified with peqGOLD Gel Extraction Kit.

2.2.1.3. Digestion, ligation and transformation

The purified PCR product was digested with restriction enzymes specific for the PCR-inserted restriction sites, while the corresponding vector was digested equally with both restriction enzymes to ensure sticky end insertion without relegation of the vector. For single restriction enzyme approaches, vector was treated with Shrimp Alkaline Phosphatase (SAP) for 15 min to ensure unwanted relegation of the vector backbone. Digested PCR product and vector were once again purified by the peqGOLD Gel Extraction Kit and afterwards ligated with Rapid DNA Ligation Kit. For Transformation *Escherichia coli* TOPTEN chemically competent cells were heat shocked with 2 µl of the cloned plasmid for 90 seconds at 42°C and rested for 5 minutes on ice. 250 µl of 1x LB medium was added and incubated on a shaker at 37°C for 1 hour, streaked on 2% agarose LB-plates containing 100 µg/ml ampicillin or 50 µg/ml kanamycin, and incubated at 37°C O/N. Additionally Blue/white selection was performed if the backbone was applicable for it.

2.2.1.4. Plasmid preparation

Regularly, five to ten colonies were picked of the LB plate and 5 ml to 500 ml of 1x LB was inoculated. After shaking incubation on 37°C O/N of the bacterial culture the plasmid was extracted and purified by plasmid preparation was performed by using Qiagen Plasmid Mini, Midi or Maxi Kit. For plasmids intended to microinject into zebrafish embryos as

DNA, the Qiagen Plasmid Midi Endotoxin-free kit was used instead. The pellet was resuspended in 30-50 µl H₂O and concentration was measured with a photometer.

2.2.1.5. DNA sequencing

The cloned plasmids were sequenced using the Barcode Economy Run Service of Microsynth or the Custom DNA Sequencing Service of Eurofins Genomics. Therefore, 1.2 µg of plasmid in a 15 µl reaction mixed were sent according to the user guidelines. For pCS2+ sequencing, company supplied Sp6 primer and custom pCS2+-specific T7 primer were used for forward and reverse sequencing, respectively. Sequencing results were analyzed using the SnapGene sequence viewer and online BLAST (Nucleotide BLAST and blastx) feature on www.ncbi.nlm.nih.gov.

2.2.1.6. Capped *in vitro* mRNA synthesis

Plasmids for overexpression in zebrafish were linearized 3' of the ORF following poly-A domain and mRNA was transcribed using the mMessage mMachine SP6/T3/T7 Kit protocol, dependent on the plasmid promoter, and purified by a LiCl precipitation according to the protocol.

2.2.2. Zebrafish maintenance

2.2.2.1. Zebrafish husbandry

The data I present in this study was acquired with wild-type zebrafish (*Danio rerio*) (AB2O2) as well as with the transgenic zebrafish line tg(-6gsc:EGFP-CAAX) (Smutny *et al.*, 2017). All animal work (zebrafish husbandry and experimental procedures) were undertaken in accordance with the German law on Animal Protection approved by Local Animal-Protection Committee (Regierungspräsidium Karlsruhe, Az.35-9185.64) and the Karlsruhe Institute of Technology (KIT), and under project and personnel licenses granted by the UK Home Office under the United Kingdom Animals (Scientific Procedures) Act, in accordance with the University of Exeter's ethical policies and approved by the University of Exeter's Animal Welfare and Ethical Review Body.

2.2.2.2. Zebrafish husbandry

Zebrafish were maintained at 28°C on a 14 h light/10 h dark cycle (Brand, M.G. and C, 2002). For breeding, zebrafish were placed into a spawning in a 2:1 ratio one day before mating. With the start of the next light cycle, male and female zebrafish were allowed to mate by removal of the separator. Embryos were collected in 30 min intervals to ensure

homogenous batch of embryonic stages and transferred into a Petri dish containing E3 embryo medium. Embryos were raised at 28°C in zebrafish E3 media. To prevent pigment formation, embryos were raised in 0.2 mM 1-phenyl-2-thiourea (PTU, Sigma, St Louis, MO 63103 USA) after 24 hpf. Embryos were stages according to (Kimmel *et al.*, 1995). At the designated stage, the embryos were used for microinjection, mounted for live imaging or fixed by 4% PFA for *in situ* hybridization and kept at 4°C.

2.2.3. Zebrafish microinjections

2.2.3.1. Injection setup

Glass capillaries with filament (1mm/0.75mm OD/ID) were prepared on a Flaming-Brown Microcapillary puller. Injection needles were filled using Eppendorf microloader tips, fastened on a microcapillary holder fixed on a three-axis manual micromanipulator next to an Olympus stereomicroscope and opened up by breaking the fine tip using dissection forceps. Zebrafish embryos were lined up in a plain Petri dish, or in a 1.5% agarose coated Petri dish with patterned slots if zebrafish embryos were injected without chorion. Zebrafish embryos were injected using a FemtoJet Microinjector plus integrated pressure supply with a foot trigger.

2.2.3.2. Microinjection procedure for OE, knock-down and knock-out of gene expression

For altering gene expression *in vivo* by microinjection, a morpholino knockdown approach or mRNA overexpression was performed. Morpholinos (MO) are synthetic oligonucleotides of ~25 bp length which bind on complementary mRNA. They can be directed against the start codon (ATG) of the mRNA and by this block its translation or they are directed against an intron-exon boundary, which inhibits the splicing of the pre-mRNA. In both ways the protein is not made and therefore the gene is knocked down. Unlike DNA, bases of the Morpholino-oligomers are bound to a morpholine backbone instead of deoxyribose rings and are linked through phosphorodiamidate groups, which increase their stability in the organism due to slower degradation. For a transient gene overexpression, *in vitro* transcribed and capped mRNA or endotoxin-free plasmid DNA was injected. These exogenous implemented mRNA is translated into the designated protein by the cell innate machinery, usually with an addition of a fluorescent tag to help visualization and to study protein function.

The injection of DNA, mRNAs, gRNA or Morpholino oligomers were performed at different time points between into the yolk or in one of 8/16 blastomeres to generate distinct patterns of expression according to the experimental needs (see the figure legends for the mode of injection in individual experimental setups). Ror2 MO was used in a 0.5mM concentration (5'-CAGTGTAACAACCTCCAAACTCTCC -3') (Gene Tools, Philomath, OR 97370 USA), mRNA concentrations were used ranging between 25 ng/ μ l and 300 ng/ μ l, while DNA was commonly injected in 50 ng/ μ l concentrations. For CRISPR/Cas9, sgRNA target sequence in either ORF or 5'UTR of a gene locus was designed in <http://chopchop.cbu.uib.no/>: zRor2 gRNA Exon1 (5'- TACAACCTGGAGCTCATCTGG-3'); zRor2 gRNA Exon2 (5'- CTTGCAGAGGCCCAAAGTGG-3'); zRor2 gRNA 5'UTR (5'- GTGCACACTTGAGACTTTGG-3'); zRor1 gRNA Exon2 (5'- AATCTGGACACCACAGACAC-3'). Ready-to-use custom designed TrueGuide Synthetic gRNA was ordered and annealed with crRNA according to manufacturer's guidelines. 300 ng/ μ l codon-optimized zCas9 or dCas9 mRNA was injected with 50 ng annealed sgRNA in one-cell stage embryos for a CRISPR/Cas9 knock-out or CRISPR-Interference mediated knock-down, respectively.

Subsequent microinjection, embryos were incubated at 28°C until subjected for image acquisition or fixed for whole-mount mRNA in situ hybridization at indicated time points.

2.2.4. Quantitative real-time PCR

For quantitative real-time PCR (qRT-PCR), successful microinjection was verified by fluorescent dye-co-injection. Afterwards, 50 embryos each were lysed in 1 ml TriZol, and total RNA was prepared using Direct-zol RNA Mini Prep Kit from Zymo Research. cDNA was prepared using MMLV reverse transcriptase from Promega and analyzed in a 96-well Real-Time PCR system from LifeTechnologies (ABI StepOnePlus). qRT-PCR primers were designed for a 50-100 bp amplicon size, checked for no secondary structures or unspecific binding and a 50-60% GC content with a T_m of 60°C. Furthermore, primer region was designed to span an exon-exon junction to avoid amplification of any genomic DNA contamination. Results were analyzed using the $\Delta\Delta$ CT method.

2.2.5. Whole mount in situ hybridization

2.2.5.1. Transcription of DIG and FITC labelled ISH probes

Plasmid templates were linearized prior to the 3' start of the sense ORF by restriction enzymes (Promega). Antisense transcription was performed containing 4 μ l 5x transcription buffer, 2 μ l 10x DIG or FITC RNA labeling mix (Roche), 1 μ l RNase inhibitor, 5 μ l linearized plasmid, 2 μ l T7 or SP6 DNA polymerase and dH₂O to 20 μ l. Reaction mix was transcribed for 3 hours at 37°C and then stopped by adding 2 μ l 0.2M EDTA pH 8 and 28 μ l dH₂O to the reaction. The reaction mix was put on a G50 column (GE Healthcare), and after one minute of incubation, centrifuged at 6000 rpm for 1 minute and diluted in 300 μ l Hyb+ solution. For further usage in the in-situ hybridization, the labeled probes were diluted in a 1:10 to 1:20 concentration in Hyb+.

2.2.5.2. Hybridization with labeled RNA probes

Embryos were dechorionated in PBST either manually by forceps or by enzyme digestion with Protease (10 mg/ml, Sigma-Aldrich). Embryos were fixed overnight in 4% PFA at the desired developmental stage. The Embryos were dehydrated in 100% MeOH for at least 30 minutes at -20°C. Embryos got rehydrated in PBST and re-fixed in 4% PFA. ProteinaseK (5 mg/ml) digestion was applied for embryos 24 hpf or older. Embryos were prehybridized in Hyb+ at 68°C until the DIG- or FITC-labelled antisense RNA probe was applied overnight.

2.2.5.3. Detection by alkaline phosphatase conjugated antibodies

Probe-mix was removed and several washing steps were carried out in solutions at 68°C, including Hyb-, SSCT, and MABT. Embryos were blocked in 2% DIG-Block for at least 1 hour and then incubated 4 hours in anti-DIG-antibodies diluted 1:2000 in 2% DIG-Block. Antibodies were removed and embryos were washed with MABT and stored over night at 4°C. For staining, embryos were transferred to a 24-well-plate and consecutively washed with MABT. The staining solution NBT-BCIP was diluted 5:1000 in NTMT and applied on the embryos. The developing time for the intensity depends on the probes. After staining, embryos were washed and re-fixed and subsequently transferred into 70% Glycerol. Embryos were stored until further preparations for image acquisition in Glycerol/PBST at 4°C.

2.2.6. Cell culture experiments

Cell lines (AGS, MKN7, MKN28) were provided by Toby Phesse, ECSCRI, Cardiff Cell line HEK293 was obtained from American tissue culture collection, ATTC, Wesel, Germany. PAC2 fibroblasts were derived from 24 h old embryos and maintained in Leibowitz-15 media and supplemented with 15% fetal bovine serum and 5% embryo extract, generously provided by Nicholas Foulkes (KIT).

2.2.6.1. Maintenance of PAC2 culture

Zebrafish PAC2 fibroblasts were cultivated in Leibowitz-15 media (supplemented with 10% fetal bovine serum, 1% L-Glutamine (2 mM) and 1% Penicillin/Streptomycin) at 28°C without additional CO₂ supply.

2.2.6.2. Maintenance of HEK293T culture

Human Embryonic Kidney HEK293T (HEK293T; CRL-1573) cells were cultivated in DMEM media (supplemented with 10% fetal bovine serum, 1% L-Glutamine (2 mM) and 1% Penicillin/Streptomycin) at 37°C and with 5% CO₂ supply.

2.2.6.3. Maintenance of AGS, MKN7 and MKN28 culture

Primary gastric adenocarcinoma cells (AGS), Gastric tubular adenocarcinoma liver metastasis cells (MKN28 and MKN7, derived from different patients; Motoyama *et al.*, 1986) were cultivated in RPMI 1640 media (supplemented with 10% fetal bovine serum, 1% L-Glutamine (2 mM), 1% Penicillin/Streptomycin and 0.1% Gentamicin) at 37°C and with 5% CO₂ supply.

2.2.6.4. Passaging and seeding of cells

For routine cell culture, cells were transferred into new sterile T75 cell culture flasks once they reach 90% confluency. HEK293T, AGS, MKN7 and MKN28 were passaged at least twice a week, while PAC2 cells were split once a week due to their slower metabolism and proliferation rate. For passaging, the old medium was removed by aspiration. Cells were washed with PBS once incubated at 37°C by a 0.25% Trypsin-solution until cells start to detach from the flask. The resuspension in fresh culture medium prevents further effect of Trypsin. Re-suspended cells were seeded into new cell culture flasks and into appropriate culture dishes for experimental usage.

2.2.6.5. Cell freezing and thawing

Cells were frozen for long term storage. Therefore, cells were de-attached and suspended as described above, followed by a gentle centrifugation to collect the cells and re-suspension in a designated freezing media containing 10% DMSO. Cell number was determined by a Neubauer counting chamber and 1×10^6 cells were transferred into each cryogenic vial for short term storage at $-80\text{ }^{\circ}\text{C}$ or long-term storage in liquid nitrogen.

To recover cells from a frozen stock, cryogenic vials were thawed in a 37°C water bath. Pre-heated media was added, cells were centrifuged and the re-suspended with cell culture media containing all supplements. Cells were transferred into smaller T20 culture flasks to ensure growth, before passaging them into T75 flasks for routine passaging.

2.2.6.6. Transient transfection

For transfection experiments FuGENE HD Transfection Reagent (Promega) was used on cells at 80% confluency in designated culture or imaging plates. For quantitative purposes, 5×10^5 cells were seeded the day before in all repetitions. Depending on application and upright/inverse microscope usage, cells were transfected in a 30mm standard culture dish or in MatTek glass-bottom dishes to optimize subsequent imaging. The FuGENE HD Transfection mix consists of 100 μl growth media, 1 μg of total plasmid DNA (equally split in co-transfections) and 4 μl of FuGENE HD Transfection Reagent. The reaction mix was incubated for 15 minutes at room temperature before it was added dropwise into the wells. Transfected cells were incubated appropriately and washed every 24 hours until image acquisition 48 hours post transfection or fixation by 4% PFA.

2.2.6.7. Co-culture procedure and reporter assays

Assays for SuperTOPFlash (STF) TCF/Wnt reporter expression and proliferation required initial co-cultivation of two distinct cell populations. For co-culture experiments, individual transfected cells were incubated for 24 hours, detached by Trypsin-EDTA and incubated in a mixed population for another 48 hours before image acquisition. The newly heterogeneous cell population was esteemed to be 80% confluent to ensure enough area for filopodia growth.

2.2.6.8. Wnt reporter assay and proliferation assay

Both assays require initial co-culture of two distinct cell populations as described previously. After 48 hours of co-culture, images were acquired on similar position in all samples. Image locations were saved by the Mark&Find microscope feature to reproduce

similar scanning setups. For the Wnt reporter activation assay using the 7xTCF-nucRFP plasmid, for one replication, seven 10x magnification images were taken per sample with identical laser intensities and exposure time. Fluorescent nuclei were processed using the Dot-Plugin in Imaris and the average grey value of the nuclei was determined. Total cell number was used as a reference by DAPI staining. The proliferation assay used a similar approach. However, fluorescent nuclei were counted instead of the intensity measurement.

2.2.6.9. Small molecule chemical treatment

For the chemical treatment, cell cultures were treated with GTPase Inhibitor ML141 10 mM (Merck Millipore) or 50 μ M IWR-1 (Sigma) to antagonize the Wnt signaling pathway. Inhibitor stock solutions were diluted in DMSO according to the manufactures protocol. Experimental setups with chemical treatment always include equal DMSO treatment to the control group if not otherwise stated.

2.2.6.10.F-Actin and nuclei staining

Cells were stained to visualize their morphology and detect cellular protrusions. Therefore, cells were fixed for 30 minutes with 4% PFA at room temperature, and then gently washed with PBS to keep cell protrusions unimpaired. Cells were incubated with 50 μ g/ml phalloidin (P1951, Sigma) and 10 μ g/ml DAPI (D9542, Sigma) for one hour, washed twice with PBS und subjected to image acquisition.

2.2.7. Organoid formation of intestinal crypt cells

Organoid formation was performed in collaboration with Prof. Dr. David Virshup (Duke-NUS Medical School, Singapore). Myofibroblasts were prepared from C57BL/6-*Tg(Pdgfra-cre)IClc/J /Rosa^{mTmG}* mice and cultured as previously described (Kabiri *et al.*, 2014). As confluence of cultured cells was reaching 80%, they were transfected with respective siRNA (Dharmacon mouse ROR2 siRNA pool Cat#LQ-041074-00-0002, four siRNAs combined in equal parts at 10nM) using siRNAmix reagent (Invitrogen Cat#13778-030). On day 2 post-transfection, myofibroblasts were mixed with *Porcn* deficient intestinal epithelial cells and cultured using RSPO1 supplemented medium. Organoid counting was performed at the time point when group containing no stromal cells had no surviving organoids left (end of day 3-beginning of day 4 of co-culture). siRNA transfected cells were imaged using OlympusLive Imaging system IX83. Acquired 3D image stacks were de-convoluted using cellSens Dimension (Olympus) and are presented as maximum intensity projections.

2.2.8. Automated filopodia analysis software

The analysis software was designed by Johannes Stegmaier and Prof. Dr. Ralf Mikut (Karlsruhe Institute of Technology). Cells and their attached filopodia were automatically detected in the RFP channel (mem-mCherry) of the acquired images. The images were initially filtered using a Gaussian low-pass filter ($\sigma^2 = 1$) and subsequently used to detect the cell body as well as the cell's filopodia. For the filopodia detection an objectness filter ($\sigma = 1, \alpha = 1, \beta = 1, \gamma = 0.003, N = 2$) was used that emphasized line-like structures based on the eigenvalues of the Hessian matrix at each pixel location (Antiga *et al.*, 2007). The obtained edge-enhanced image was then binarized using a local adaptive threshold filter that set pixels to foreground if their intensity value was larger than a regional mean intensity minus a multiple of the regional intensity standard deviation and otherwise to background (window radius = 200, std. dev. multiplier = 1). To segment the cell body, the local adaptive threshold (window radius = 200, std. dev. multiplier = 1) was applied on the smoothed input image and subsequently used a morphological opening operation (kernel radius = 2) to get rid of noise and remaining filopodia. The cell body was given by the largest connected component in the opened binary image. The segmentation mask of the cell body including filopodia was then constructed by combining the binarized edge-enhanced image with the binary cell body image. The combined cell image was subsequently skeletonized to identify potential filopodia tips at the end points of the skeleton. All above-mentioned preprocessing steps were implemented in the open-source software tool XPIWIT (Bartschat *et al.*, 2016).

The preprocessing results were then imported to a dedicated MATLAB tool that was developed to validate, correct and analyze this kind of images. In order to automatically trace filopodia from the identified tips to the cell body, an adapted livewire algorithm was used (Barrett and Mortensen, 1997). The output of the objectness filter was used as an edge map on which the livewire algorithm tried to find a maximally scoring path from the tip of the filopodium to the center of the cell body. Based on the segmentation of the cell body, the automatic tracing was stopped as soon as the cell body was reached. The interactive user interface was then used to add, remove and correct both segmentation masks and detected filopodia on a per-cell basis. For each cell's filopodia, the Euclidean distance was calculated along the path from the tip to the cell body. The same image preprocessing and tracing was applied to semi-automatically extract filopodia in 3D confocal images. However, for the 3D case, start and end points of the filopodia were provided by the user via a graphical user interface and the livewire approach was applied twice. First on an axial maximum intensity

projection (z) to obtain the lateral path (xy). Subsequently, the axial positioning of the filopodium was obtained by searching for the highest scoring path between the provided start and end points solely in the z-direction. Multiple automatically traced filopodia can then be exported and used to obtain average statistics of all filopodia of interest.

2.2.9. Dual-color line-scanning fluorescence correlation spectroscopy

For the 2c-lsFCS measurements, a home-built confocal microscope was used as previously described (Dörlich *et al.*, 2015), with slight modifications. We used a water immersion objective (HCX PL APO CS 63x /1.2, Leica, Wetzlar, Germany) instead of an oil immersion objective; the multimode fiber, which acts as a confocal pinhole, was modified accordingly to ensure a pinhole size of 1 AU. Data were collected for 390 s by continuously scanning the focus perpendicularly through the membrane. Each scan line consisted of 100 pixels, with a step size of 100 nm. eGFP was excited with a 488 nm continuous wave (cw) laser and mCherry with a 561 nm cw laser. After splitting the fluorescence signal into two color channels by using a 555 nm dichroic filter, 525/50 (eGFP) and 600/37 (mCherry) band pass filters were used for detection. To avoid artefacts in the correlation curves caused by scanner flyback and wavelength switching, the membrane was always kept in the center of the field of view. The intensity data were arranged as an *x-t* pseudo image, and the intensities of those pixels containing membrane fluorescence were integrated to obtain an intensity time trace for correlation analysis, as described earlier (Dörlich *et al.*, 2015).

2.2.10. Luciferase reporter assay in *Xenopus* embryos

For the ATF2 luciferase reporter assay, 4-cell stage *Xenopus* embryos were injected into both animal ventral blastomeres with the 100 pg ATF2-Luciferase reporter plasmid in combination with 10 pg TK-Renilla-Luciferase reporter plasmid. The reporter plasmids were injected alone or in conjunction with 500 pg of the respective synthetic mRNAs. Luciferase reporter assays were carried out from triplicates of five gastrula stage (st.12) embryos lysed to measure Luciferase activity using the Dual luciferase system (Promega).

2.2.11. Image acquisition

For confocal analysis, live embryos were embedded in 0.7% low melting agarose (Sigma-Aldrich) dissolved in 1x Ringer's solution. Images of cells and embryos were obtained with a Leica TCS SP5 X or SP8X confocal laser-scanning microscope using 20x or 63x dip-in objectives. A Leica DMI600SD with 20x objective was used for the kinase library screen. Image processing was performed with Imaris 9.1 software. Filopodia and cytoneme

measurements from confocal z-Stacks of living embryos were performed via the semi-automated filopodia analysis software described before. Cell culture quantifications were carried out by using Fiji software. Roundness of notochordal embryo cells was determined by calculating the width to length ratio per cell in Fiji.

2.2.12. Statistical analysis

All experiments were carried out at least in biological triplicates if not indicated otherwise. Significance was calculated by Student's t-test while asterisks represent the following p-values: * = $P \leq 0.05$; ** = $P \leq 0.01$; *** = $P \leq 0.001$. Box plots: Centre lines show the medians; box limits indicate the 25th and 75th percentiles as determined by R software; whiskers extend 1.5 times the interquartile range from the 25th and 75th percentiles, outliers are represented by dots.

3. Results

3.1. Kinase screen and automated image-analysis identifies the receptor tyrosine kinase Ror2 as a potential cytoneme regulator.

Evidence indicates that Wnt signal molecules are lipidated and remain associated with membranes during secretion, action and degradation (Nusse and Clevers, 2017). Our previous work demonstrated that Wnt molecules can be distributed over 100 μm through a tissue via cytonemes (Stanganello *et al.*, 2015). Manipulation of filopodia led to alterations in Wnt mediated tissue patterning and malformations of the zebrafish embryo.

Therefore, I hypothesized that formation, emergence, and maintenance of cytonemes are tightly controlled. Our previous understanding indicated a process involving the actin skeleton regulation by a RhoGTPase Cdc42-dependent process (Stanganello *et al.*, 2015). Inhibition of filopodia formation and Cdc42 activity reduced the ability of cells to form filopodia and Wnt cytonemes and subsequently reduced the signaling range, even though the amount of available Wnt ligand was not altered. Consequently, neural plate patterning displayed a Wnt-loss phenotype indicated by an anterior shift of the midbrain hindbrain boundary (MHB) position and a reduced *FEZ family zinc finger 2 (fezf2)* positive anterior forebrain primordium.

However, Cdc42 is a downstream effector protein for a wide range of processes. The signal that regulates Cdc42 activation to facilitate cytonemes is still unknown. To test this hypothesis and to elucidate potential cytoneme regulators, a cell-culture based genetic screen was performed. In PAC2 cells, a cDNA clones from a Medaka cDNA library consisting of 229 kinases (Chen *et al.*, 2014; Souren *et al.*, 2009) was arrayed. As the regulation of cell protrusions is a fast and dynamic process in general, I expected it to involve proteins that can actively drive cellular processes. In that regard, kinases are critical in cellular processes involving movement, transport and signaling. The kinase library was co-expressed with membrane-bound mCherry (memCherry) to visualize the cell and its protrusion while the co-expression of Wnt8a-GFP is expected to stimulate the cell to form Wnt8a-cytonemes. 24 h post transfection, the length and number of signaling filopodia per cDNA sample was quantified using an automated filopodia detection software designed in close collaboration with the group of Prof. Dr. Mikut, IAI, KIT (Figure 12A).

The cytoneme quantification software automatically extracts filopodia using the memCherry channel of the acquired images. The raw image was initially smoothed with a Gaussian low-pass filter to reduce image noise for facilitated processing (Figure 12B). To emphasize filopodia in the image, an objectness filter was used that emphasizes line-like structures based on the eigenvalues of the Hessian matrix and binarized the resulting edge image using local adaptive thresholding. The obtained skeleton image allows in turn extracting potential filopodia tips at the end points of the skeleton. The identified cell body (cyan outline) and the potential filopodia tips (magenta dots) are shown in (Figure 12B). A live wire approach was then used to automatically trace filopodia from the tips to the cell body (red lines).

The acquired data of the kinase screen was normalized to transfection controls and relative filopodia number per cell (Figure 12C) or relative filopodia length (Figure 12D) are shown in a graded diagram where every bar on the x-scale represents an individual kinase. A line of the 85% percentile mark was included to highlight high-performing kinases.

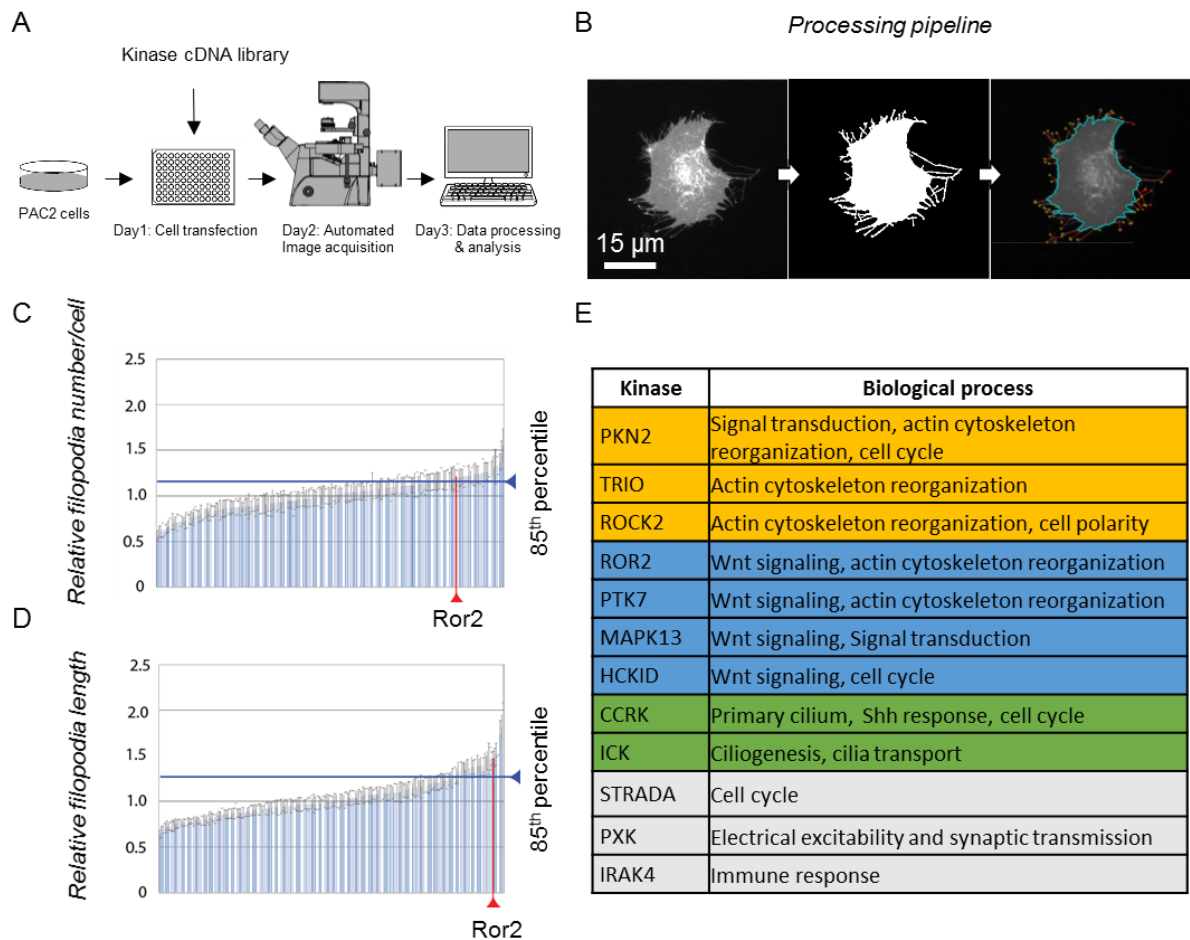


Figure 12: Kinase library screen with automated image-analysis identifies the RTK Ror2 (A) Schematic workflow of the cDNA kinase screen. Wnt8a-GFP and a membrane bound mCherry was co-transfected with medaka kinase genes in a 96-well plate format. Images were acquired automatically and analyzed for filopodia length and numbers by a filopodia detection software. (B) Automated Image analysis software detects and counts filopodia of single cells using the memCherry signal and quantifies their length by automatically tracing the tips back to the cell body. (C, D) Diagram illustrating transfected kinase genes on the x-axis and their relative filopodia number/cell (C) or length (D). Each bar represents one of 229 kinases, sorted ascending by its value. The blue line indicates the 85th percentile. The position of Ror2 in the diagram is highlighted by the red line. (E) Summary table of selected best performing kinases regarding stimulation of filopodia number or length. The color represents different groups, sorted for similar biological functions.

Remarkably, the best performing results regarding a stimulating effect for filopodia length or number can be classified into three main groups with similar biological functions (Figure 12E; for a list of all other cDNA kinases, see Appendix). As cytonemes appear to be actin rich protrusions, it is rather expected to detect key regulators for actin cytoskeleton remodeling as top candidates. Rho-associated protein kinase 2 (ROCK) and TRIO work tightly together with RhoGTPases as RHO, RAC or CDC42 while other hits as the

Serine/threonine-protein kinase N2 (PKN2) regulate processes as cell polarization and cell adhesion. Interestingly, several main candidates have overlapping function in Wnt signaling, most prominently in the non-canonical PCP pathway. Casein kinase I isoform delta (HCKID) regulates diverse cellular growth and survival processes including Wnt signaling by phosphorylation of DVL2 and DVL3. Mitogen-activated protein kinase 13 (MAPK13) is one of the MAPKs which play an important role in the Wnt responses leading to transcription factor activation such as ATF2. Furthermore, genes for alternative protrusions such as cilia were also found. Cyclin dependent kinase 20 (CCRK) and Serine/threonine-protein kinase ICK (ICK) are involved in ciliogenesis, required for SHH responses and transport of SHH pathway components to the ciliary tip. Also, biological processes such as electrical excitability and synaptic transmission in axons or neurite outgrowth by PX domain-containing protein kinase-like protein (PXX) shows the similarities between different kind of cellular projections and the relevance of this screen in general. One gene draws keen interest, as it is involved in both of the main processes, Wnt signal transduction as well as in actin cytoskeleton regulation. Ror2 combines these molecular tasks and was found to stimulate both, the filopodia number per cell as well as average filopodia length above the 85th percentile (Figure 12C,D). Aside from the exceptional potential for filopodia dynamics, Ror2 is upstream of a signaling cascade functioning on a receptor level, thence, presumably upstream of other candidates such as ROCK2, TRIO or MAPK13 and therefore superior to consider as a key regulator for cytonemes and subjected for a following in-depth analysis.

3.2. Tyrosine kinase Ror2 regulates filopodia emergence *in vitro* upstream of Cdc42.

To validate the screening results, I repeated the Ror2 transfection in a high-quality approach with increased sample sizes, more precise microscopy and included well-known filopodia regulators to elucidate Ror2's role in the whole process of filopodia formation. I co-transfected PAC2 fibroblasts with a zebrafish full-length Ror2 expression construct and GPI-mCherry as a membrane marker. The number and length of filopodia was measured in living cells (Figure 13) and the cumulative filopodia length was determined to associate length and numbers of filopodia into a single factor. A specific length of cytonemes is required to reach target cells. Furthermore, more cytonemes represents a higher capacity to release signaling molecules. Therefore, combining them into a single value shows the possible signaling output via cytonemes on a more qualitative level.

Ror2 expression significantly increased the average number and length of filopodia per cell (Figure 13). Ror2 requires homodimerization for trans-autophosphorylation and subsequent downstream signaling (Liu *et al.*, 2007), which can be inhibited by over-expressing a kinase-dead construct. Transfection of the dominant-negative mutant Ror2³¹ (Hikasa *et al.*, 2002), caused a reduction in the cumulative length, consistent with an essential role of the Ror2 kinase activity in filopodia induction in PAC2 fibroblasts. The Rho GTPase Cdc42 is crucial for organizing the actin cytoskeleton to stabilize Wnt cytonemes (Stanganello *et al.*, 2015) and is thought to be a downstream target of the Wnt/Ror2 pathway regulating filopodia (Schambony and Wedlich, 2007). To determine whether Ror2-induced filopodia require Cdc42 function for assembling an actin scaffold I co-transfected Ror2 stimulated fibroblasts with dominant-negative Cdc42^{T17N} (Nalbant *et al.*, 2004). Blockage of Cdc42 function reduced filopodia formation (Figure 13B). BAR-domain containing proteins mold membranes into tube-like filopodia. Insulin receptor tyrosine kinase substrate p53, IRSp53, is a BAR protein, as well as a Cdc42 effector, which connects filopodia initiation and maintenance by assembling the actin scaffold (Yeh *et al.*, 1996). IRSp53^{4K} contains four lysine residues mutated to glutamic acid in the actin-binding sites, inhibiting Cdc42-mediated filopodia formation (Disanza *et al.*, 2013; Kast *et al.*, 2014). IRSp53^{4K} expression, like Cdc42^{T17N} transfection, blocks Ror2-induced filopodia formation (Figure 13B). Treatment of Ror2 expressing cells with ML141, a GTPase inhibitor for Cdc42/Rac1 (Surviladze Z , Waller A, 2010), also caused a substantial reduction in cumulative length of filopodia.

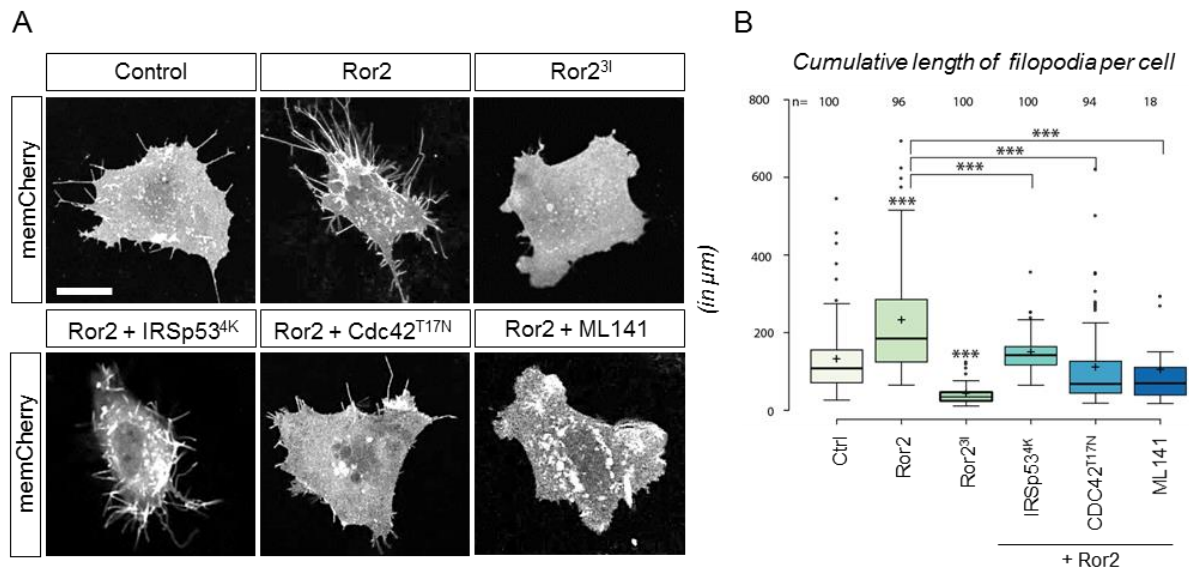


Figure 13: In-depth analysis of the role of Ror2 in filopodia formation in PAC2 fibroblasts. (A) Quantification of filopodia in PAC2 cells 24h after transfection or inhibitor treatment. MemCherry was transfected together with indicated constructs. Scale bar represents 10 μm (B) Boxplot for cumulative filopodia length of cells transfected with indicated constructs measured by ImageJ. Centre lines show the median; box limits indicate the 25th and 75th percentiles as determined by R software; whiskers extend 1.5 times the interquartile range from the 25th and 75th percentiles, outliers are represented by dots. n displays the number of counted cells.

These results validate the kinase screen, as Ror2 is indeed a potent filopodia stimulator by increasing the number of protrusions as well as the length. Furthermore, Ror2 is required for normal filopodia formation as interference in protein function with the kinase dead mutant Ror2³¹ leads to a reduction below control levels. Blocking potential downstream factors revealed that Ror2 acts upstream of a Cdc42-mediated actin process crucial for filopodia outgrowth and maintenance. It is still up to investigate what factors on a receptor level are involved and whether this principle can be validated for cytonemes *in vivo* involved in neural plate patterning.

3.3. Wnt/PCP components feature overlapping expression domains in the dorsal marginal zone during early gastrulation.

The possibility of Ror2 as a crucial cytoneme regulator *in vivo* would require all components of the corresponding process to interact in the same tissue. In the case of Wnt8a-cytonemes during neural plate patterning, several cytoneme-stimulating factors must be

present in the source cells given there are no secreted molecules involved. Considering Ror2's function in the non-canonical Wnt/PCP pathway, the first task to reveal *in vivo* interaction is to compare the expression domains of *ror2* with other general Wnt or PCP genes. In the following, an *in situ* hybridization of whole mount zebrafish embryos was performed at 40% and 75% of epiboly (5 and 8 hpf, respectively) as the process of neural plate patterning is believed to set an early pre-pattern, which is expanded over the time course of early gastrulation (Stanganello *et al.*, 2015). Here, Wnt8a facilitates the patterning of the prospective neural plate (Kelly *et al.*, 1995; Rhinn *et al.*, 2005; Lekven *et al.*, 2001). Expression of the β -catenin Wnt ligand *wnt8a* is confined to the embryonic margin (Figure 14A,B) during zebrafish gastrulation and is the main dorsal determinant in zebrafish at this stage (Lu *et al.*, 2011). This ring-shaped tissue represents the Wnt source cells, nearly surrounding the embryo except at the position of the dorsal shield organizer. Also, other canonical as well as non-canonical Wnt such as Wnt3a, Wnt5b, Wnt8b, and Wnt11 are expressed in the marginal zone with variations in their time of onset. Ror2 has a strong and ubiquitous expression during early gastrulation (Figure 14C,D). This is consistent with sources that document that zebrafish *ror2* expression peaks in early development between 2 and 9 hpf (Bai *et al.*, 2014). Furthermore, *fzd7a* as a Wnt receptor involved in non-canonical Wnt signaling shows an overlapping expression in the dorsal marginal zone as well. Surprisingly, the predominant *fzd7a* expression is very specific in the marginal zone at 40% epiboly during the phase of pre-patterning and translates to a more ubiquitous expression pattern at 75% epiboly (Figure 14E,F).

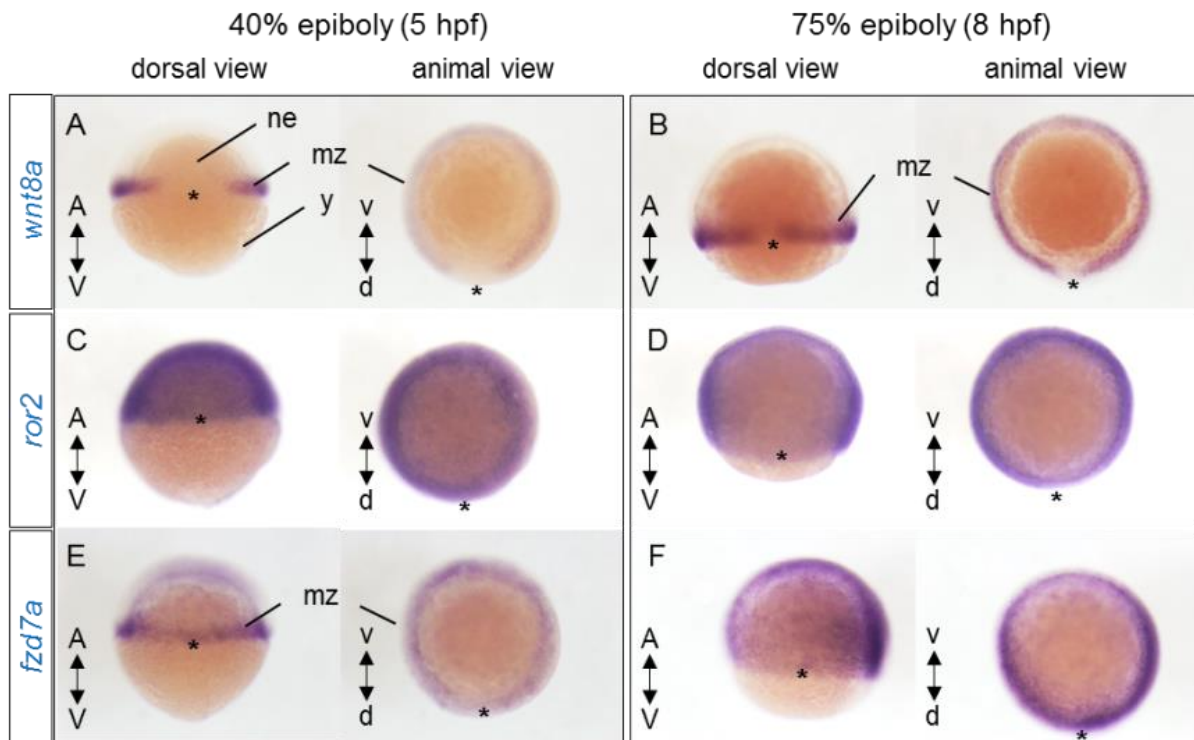


Figure 14: Expression pattern of the Wnt ligand *wnt8a* and Wnt PCP receptors *ror2* and *fzd7a* during early gastrulae stages. Whole mount *in-situ* hybridization images visualize expression of *wnt8a* (A,B), *ror2* (C,D) and *fzd7a* (E,F) from a dorsal or animal view (asterisk marks the position of the dorsal shield organizer) at indicated time points. A, anterior; d, dorsal; mz, marginal zone; ne, neural ectoderm; v, ventral; V, vegetal; y, yolk.

Thus, Ror2 could potentially interact with PCP receptors such as Fzd7a and participate in Wnt ligand binding and signal transduction, as those factors are combined in the dorsal marginal zone as a central signaling compartment. Further investigation is needed regarding direct physical interaction of these ligand and receptor pairs, pathway activation as well as any involvement in the process of cytoneme formation and Wnt protein dissemination, but the condition of *in vivo* interaction is inherent.

3.4. Cluster formation of Wnt8a and Ror2 is dependent on the CRD domain.

Ror2 as a major candidate in the kinase screen proved to be a crucial organizer for filopodia in PAC2 cell culture and has overlapping expression domains with PCP components during early neural ectoderm patterning. Next, Ror2's function regarding Wnt interaction, specifically Wnt8a, has to be deciphered. Ror2 is known as a tyrosine kinase receptor that binds Wnt5a via its extracellular cysteine-rich domain (CRD) (Hikasa *et al.*,

2002) and serves as a β -catenin independent Wnt co-receptor activating the PCP signaling pathway (Schambony and Wedlich, 2007). To investigate the interaction between Ror2 and the β -catenin ligand Wnt8a, I expressed fluorescently tagged Wnt8a and Ror2 proteins in the zebrafish embryo during gastrulation (Figure 15A). Confocal microscopy on live specimens revealed that Wnt8a-GFP displays a punctate pattern in the cytoplasm and at the membrane, including cytoneme tips (Figure 15A,B), whereas Ror2-mCherry without Wnt present is uniformly distributed in the cell membrane (Figure 15B). When Wnt8a-GFP and Ror2-mCherry are co-expressed in the same cell, Ror2-mCherry accumulates in punctae along the membrane (Figure 15B). To demonstrate potential protein-protein interaction, I performed an imaged-based analysis approach to determine co-localization in a defined 3D confocal volume. The Pearson correlation-coefficient determines the co-localization of two fluorescent proteins ranging from 0 to 1, with no overlapping localization to fully identical, respectively. Wnt8a-GFP in combination with Ror2-mCherry indicated a high Pearson correlation-coefficient (PCC) of 0.66, which demonstrates a high co-localization potential (Figure 15A). Even though Wnt8a-GFP is membrane localized, the PCC of 0.21 indicates less interaction, similar to Ror2 with a disrupted Wnt binding site (0.28). To exclude non-specific clustering of fluorescent fusion proteins, I used a Ror2 construct with a deletion in the Fzd-like CRD. The CRD of Ror2 is crucial for interaction with Wnt ligands (Hikasa *et al.*, 2002; Mikels *et al.*, 2009). This approach measures co-localization in the entire confocal volume. As my interest lied primarily in the ligand-receptor interaction directly at the membrane, I performed another assay which investigates correlated fluorescence intensity patterns directly on membrane accumulations. Correlated fluorescence intensity patterns of Wnt8a-GFP and Ror2-mCherry suggest both proteins co-localize intensively in membrane associated clusters, as both the Wnt8a-GFP and the Ror2-mCherry curve peak on cluster occurrence (Figure 15C). I observed that Ror2- Δ CRD-GFP can still localize to the cell membrane and with Wnt8a-mCherry forming clusters therein, although they appear to be less and smaller. Image profile analysis showed a marked reduction of the intensity peaks at the cluster site, indicating that Ror2-CRD is required for the interaction with Wnt8a (Figure 15C).

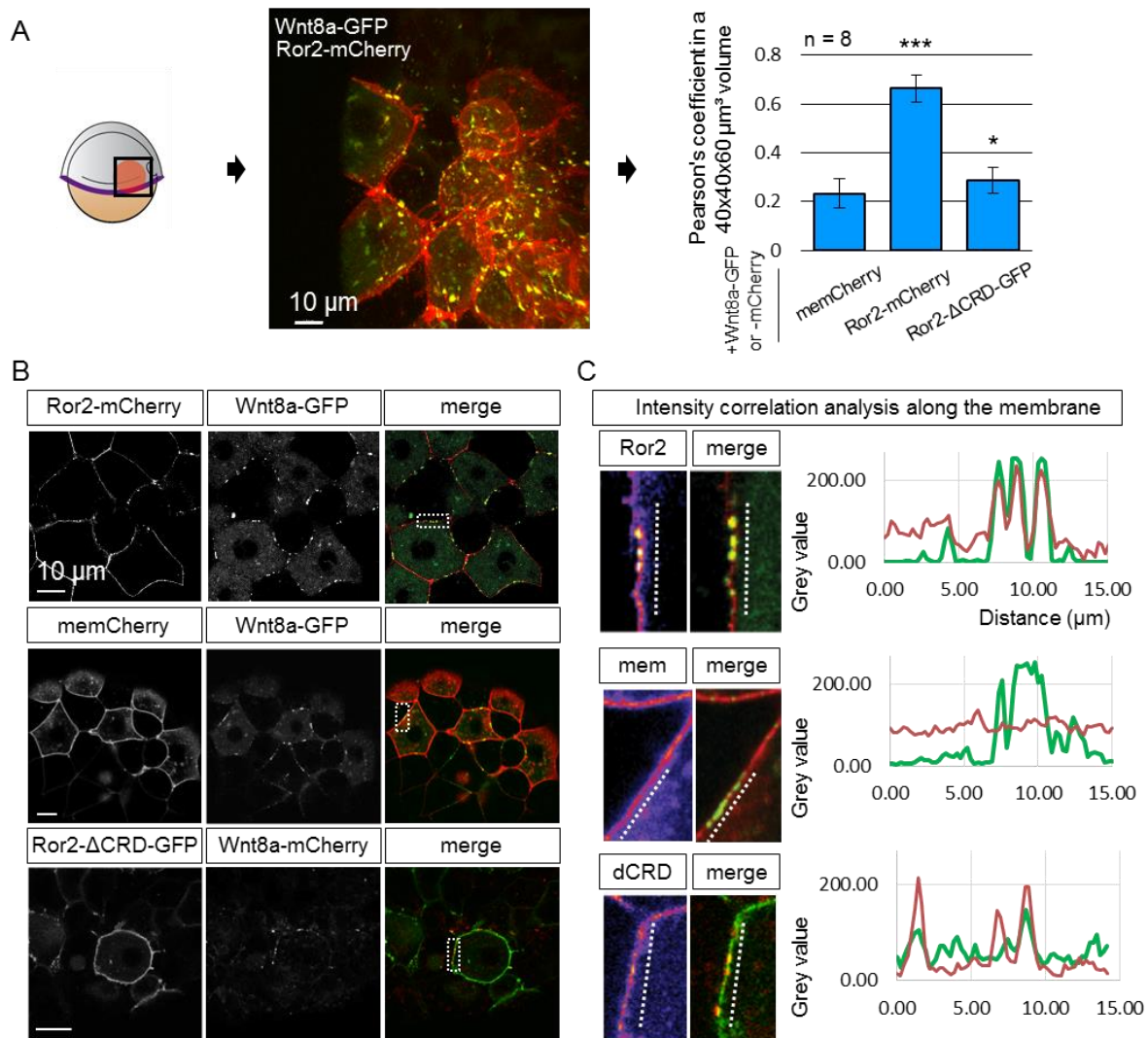


Figure 15: Confocal analysis and intensity profiles highlights Wnt8a/Ror2 cluster formation in the cell membrane dependent on the CRD. (A) At the 8–16-cell stage, single blastomeres of zebrafish embryos were microinjected with mRNA of indicated constructs to generate cell clones at 50% epiboly for confocal microscopy analysis. 3D confocal volumes were subjected to Pearson correlation coefficients assessment in Imaris. The PC coefficient ranges from 0 (no co-localization) to 1 (full co-localization). (B) Imaging visualizes co-localization of proteins at a single confocal plane. (C) Magnified section as highlighted in B showing the single Ror2 or membrane channel by fire LUT, the merge picture and the intensity plot profile as generated in ImageJ. The plot profile shows the grey value and was drawn on standardized confocal images along 15 μ m cell membrane containing spots of Wnt-ligand, highlighted by the dashed line in the enlarged images.

We have previously shown that Fzd7 also interacts with Ror2 and enhances Ror2-mediated signaling during *Xenopus* gastrulation (Brinkmann *et al.*, 2016), suggesting Fzd7a could be a part of the Wnt8a/Ror2 cluster. To test this, I overexpressed Ror2-mCherry, Fzd7a-CFP, and Wnt8a-GFP and observed a profound membrane-spanning cluster formation of all components (Figure 16A) and coherent correlated fluorescence intensity pattern in cell

membrane accumulations (Figure 16B). Further investigation was carried out by a Pearson correlation in a defined volume. As Wnt and Fzd7a are partly membrane associated, the coefficient compared to the membrane marker memCherry gives a baseline of co-localization between two membrane associated proteins without inherit interaction (0.21 for memCherry/Fzd7a and 0.24 for memCherry/Wnt8a) (Figure 16C). Next, Wnt8a, Ror2, and Fzd7a were co-expressed to enable signalosome formation. Person-correlation-coefficient is limited to correlating two proteins at once. Therefore, to observe all options, three correlations were calculated. Interestingly, all cases showed a similar coefficient of over 0.4 indicating all proteins are represented in the same membrane accumulations, which show already a very decisive co-localization in the membrane and even on cytoneme tips as it is described in a later chapter of this thesis (Figure 26).

Analysis of Wnt8a/Ror2 interaction was extended by involving downstream factors of the Wnt pathway. Dvl is recruited to the cell membrane upon Wnt/ β -catenin as well as Wnt/PCP pathway activation, although different domains are activated to transmit a diverse signal (Gao and Chen, 2010). Quantification of Dvl2-GFP membrane accumulations allows to draw conclusions about Wnt pathway activation. Interesting, both Wnt8a and Ror2, but not Wnt5a, were able to recruit a statistically high number of Dvl2 cluster to the membrane (Figure 16D).

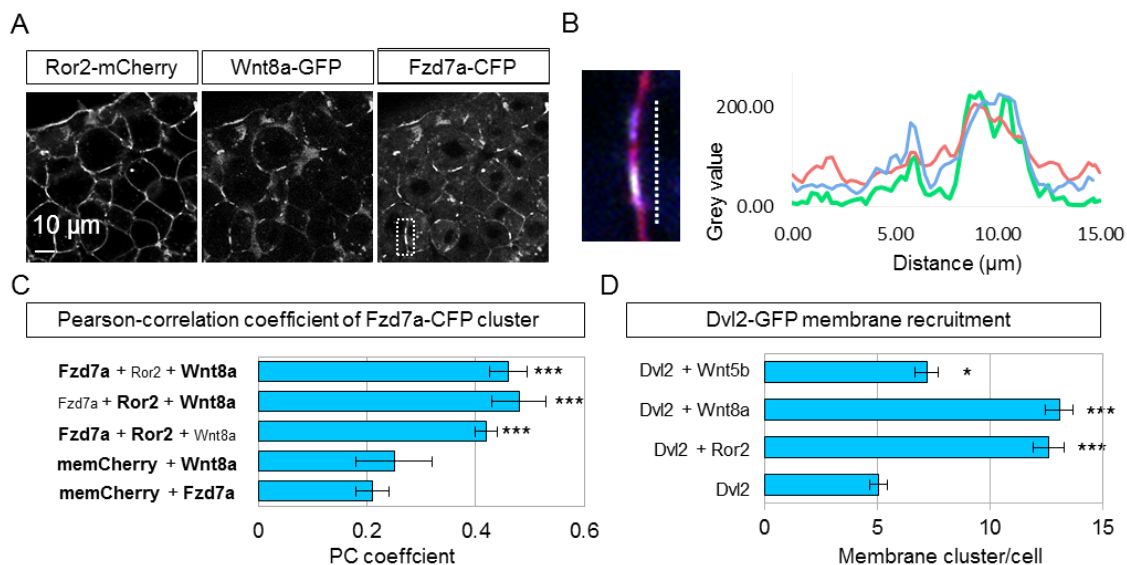


Figure 16: Evaluation of Wnt8a/Ror2/Fzd7a cluster formation and Dvl2 recruitment to the membrane.

(A) Zebrafish embryos were microinjected with mRNA of indicated constructs for confocal microscopy analysis. Image visualizes co-localization of proteins at a single confocal plane. Wnt8a/Ror2/Fzd7a demonstrate wide membrane-spanning cluster. (B) Intensity plot profile were generated in ImageJ. The plot profile shows the

grey value of all three over-expressed proteins and was drawn on standardized confocal images along 15 μm cell membrane containing spots of Wnt-ligand, highlighted by the dashed line in the enlarged images. (C) The Pearson-correlation efficient calculated for two proteins each (shown in bold) of several 30 μm confocal stacks by using Imaris co-localization plugin. The PC coefficient ranges from 0 (no co-localization) to 1 (full co-localization). (D) Dvl2-GFP membrane clusters of single cells were counted in confocal z-stacks. Signalosome formation was monitored by observing recruitment of Dvl2-GFP to the membrane in embryos injected with indicated constructs.

Confocal image analysis suggested a strong association between Wnt8a and Ror2 that might also involve other receptors such as Fzd7a. Both, while expressed in the same cell, co-localize in potential signaling clusters which could explain Dvl2 recruitment to the membrane. Furthermore, the data proposes that Wnt8a interacts with Ror2 by binding to its CRD. However, these clusters seem to be very dynamic and only still pictures were evaluated. Thus, high-quality analysis tools regarding protein-protein binding and co-migration were conducted next.

3.5. Wnt8a and Ror2 co-migration and protein binding in signaling clusters

Based on the results above, I hypothesize that Wnt8a binds to Ror2. To further characterize Wnt8a/Ror2 protein-protein interactions *in vivo*, I used line-scanning fluorescence correlation spectroscopy (lsFCS), which measures concentrations and diffusion coefficients of ligands and receptors in the presence of a membrane (Figure 17A) (Dörlich *et al.*, 2015). A specific region of interest (ROI) is scanned for a set period of time with alternating excitation wavelengths enabling the detection and subsequent correlation of two fluorescent proteins. A cross correlation of both proteins involves a binding and mutual motion, with the amplitude of the curve depending on the ligand-receptor cluster concentration. I performed lsFCS analysis in two different spots in living zebrafish specimen during early gastrulation, at a Ror2 positive membrane domain (spot 1) or at a Wnt8a/Ror2 membrane cluster (spot 2; Figure 17B). A focused laser spot was scanned across the membrane for 390 s while the intensity was measured as a function of time. After compensation for membrane fluctuations, the intensity time traces were time-correlated. In spot 1, I found intensity fluctuation from Ror2-mCherry emission (Figure 17C). A fit of the autocorrelation function revealed a receptor concentration (area density) of $C_r = (37 \pm 3) \mu\text{m}^{-2}$. The diffusion coefficient, $D = (0.28 \pm 0.03) \mu\text{m}^2 \text{s}^{-1}$, is similar to values found for LRP6 receptors in the plasma membrane (Dörlich *et al.*, 2015). There was no clear emission from

Wnt8a-GFP molecules in spot 1. By contrast, lsFCS on spot 2 revealed clear autocorrelations in both color channels (Figure 17D), indicating the presence of both Wnt8a-GFP and Ror2-mCherry at this site. Additionally, a dual-color cross-correlation between Wnt8a-GFP and Ror2-mCherry indicated concerted intensity fluctuations in both color channels, which arise from their co-diffusion in the plasma membrane due to binding.

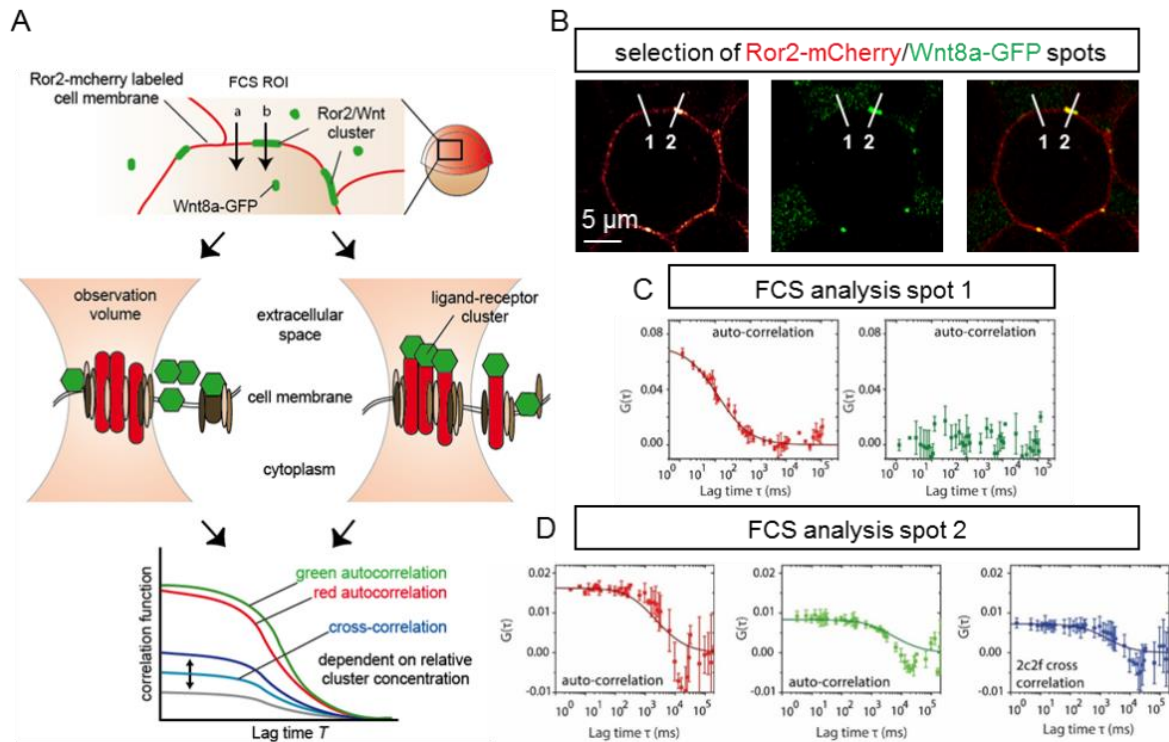


Figure 17: Line scanning-fluorescence correlation spectroscopy (ls-FCS) analysis of zebrafish embryos at 8 hpf. (A) Simplified schematic of FCS scanning and the resulting correlation function. (B) Living embryos injected with Wnt8a-GFP and Ror2-mCherry were mounted in agarose prior to FCS scanning. Close-up of a 8 hpf zebrafish cell represents schematically the lsFCS data acquisition. Data was taken by laser scanning perpendicular to the membrane (white lines). Analysis was conducted in the absence (spot 1) or presence (spot 2) of Wnt8a-GFP. Ror2-mCherry image is presented in fire-LUT to emphasize the membrane accumulation. (C) Autocorrelation functions of Ror2-mCherry (red) and Wnt8a-GFP (green) (symbols) and model fit (line) measured in spot 1. The total time of the measurements was 390 seconds. Importantly, there is no Wnt8a-GFP at this position as shown by the lacking autocorrelation in the green channel. Error bars represent standard deviations from two measurements. (D) Autocorrelation functions of Ror2-mCherry (red) and Wnt8a-GFP (green) and the dual-color cross-correlation (blue) (symbols) and model fits (lines) measured in spot 2. Here, Wnt8a-GFP is measurable, and the blue cross-correlation amplitude indicates binding of Ror2-mCherry and Wnt8a-GFP. Error bars indicate standard deviations from two measurements.

Therefore, the cross-correlation lsFCS data provide clear evidence of complex formation between Wnt8a and Ror2. Furthermore, the low diffusion coefficient of the bound species, $D = (0.02 \pm 0.01) \mu\text{m}^2 \text{s}^{-1}$, indicates that the complexes diffuse presumably as large clusters in

close steric contact with other components. The data suggest Wnt8a and Ror2 co-migrate and form dense protein clusters. The most vital aspect subsequently is to elucidate whether these signal complexes can transmit a Wnt signal; and if so, to which Wnt pathway they belong as Wnt8a and Ror2 are traditionally classified on two mutual antagonistic sides of the Wnt network.

3.6. Wnt8a/Ror2 signaling activates the β -catenin-independent Planar Cell Polarity (PCP) pathway

PCP signaling plays a role in regulating tissue migration during gastrulation (Tada and Heisenberg, 2012). PCP signaling via Ror2 activation regulates collective cell migration towards the embryonic midline, which is most pronounced in the mesodermal germ layer in zebrafish (Bai *et al.*, 2014). I hypothesized that manipulation of Ror2 causes defects in collective cell migration by impairing proper PCP signaling. To test this hypothesis, I altered Ror2 function by over-expression and knock-down as well as knock-out approaches.

First, controllable Ror2 over-expression and the effect on embryogenesis is evaluated in a concentration-dependent manner and compared to available data. Interestingly, Ror2 mRNA injection concentrations of 50 ng/ μ l or below demonstrated no distinguishable morphological alterations compared to the control (Figure 18). As of 100 ng/ μ l Ror2 mRNA or higher, embryos featured concentration-dependent Wnt/PCP phenotypes. In later approaches, mild over-expression with 25 ng/ μ l was used to test for synergistic interactions with Wnt ligands.

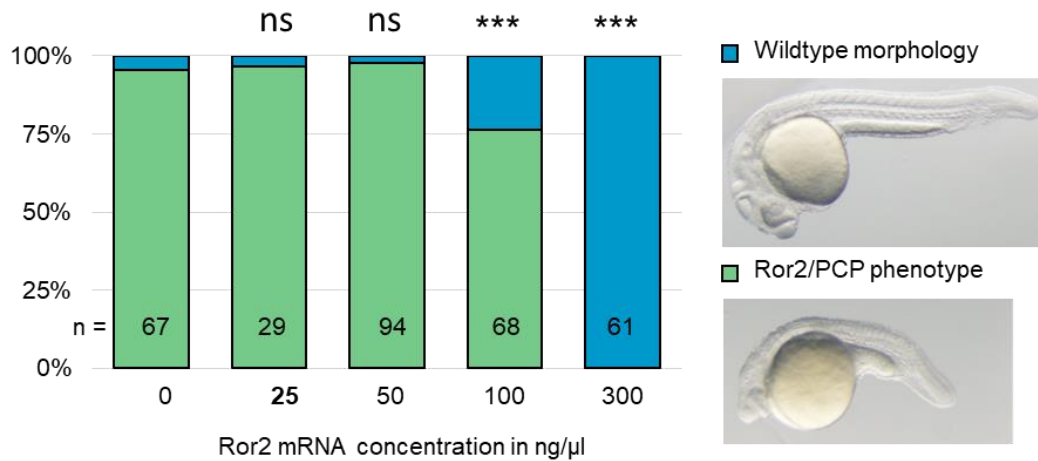


Figure 18: Ror2 over-expression induces a concentration-dependent PCP phenotype. Microinjection of Ror2 mRNA in rising concentrations and classification of phenotypes into groups representing developmental alterations at 24 hpf. Chi-squared test was performed to determine p-values.

Next, Ror2 function in zebrafish was evaluated in a knock-down and knock-out approach utilized by the Class 2 Clustered Regularly Interspaced Short Palindromic Repeat/ CRISPR associated protein 9 (CRISPR/Cas9) system (Irion *et al.*, 2014; Jao *et al.*, 2013). The CRISPR/Cas9 setup is illustrated in Figure 19C. Ror2 gRNA targeting exon2 and exon3 were simultaneously used in combination with a zebrafish codon-optimized Cas9 to cause cleavage and non-homologous end joining (NHEJ) of the *ror2* locus to give rise to small indels in the target DNA resulting in amino acid deletions, insertions, or frameshift mutations to disrupt the open reading frame (ORF) of the targeted gene. *Ror1* was targeted by a gRNA designed for exon2. Another method for *ror2* gene silencing was performed with CRISPR-Interference (CRISPR-I) (Larson *et al.*, 2013; Gilbert *et al.*, 2013). I designed two gRNAs targeting the promoter elements and transcription start site (TSS) of *ror2* in the 3'UTR and co-injected an mRNA encoding for a Cas9 protein with truncated cleavage activity. Mode of action for this system depends on the blocking initiation as the dCas9 molecule retains the ability to bind to target DNA that leads to a reduced expression without permanently modifying the genome (Figure 19C).

Effect on development was analyzed by convergence and extension defects in F0 generations: The angle between the anterior and posterior ends of the embryo in ventral view, the proper convergence of the embryonic midline in Tg(*gsc*:GFP-CAAX) embryos in dorsal view, and the complete phenotype at 28 hpf. Tg(*gsc*:GFP-CAAX) embryos express a membrane bound GFP in notochordal *gsc*-positive cells. Both, *ror2* CRISPR and CRISPR-I cause profound C&E defects in F0. The angle of anterior and posterior ends is widened while

the convergence to the midline is disrupted (Figure 19A). Ror1 knockdown leads to less severe morphological changes. By analyzing effects on the entire body plan at 28 hpf, Wnt/PCP defects are detectable similar to Ror2 over-expression (Figure 19B). Intriguingly, an effect on anterior head formation was detected as well, which should be unaffected by non-canonical Wnt signaling and could hint to implications in β -catenin signaling and AP patterning. In the following, Ror2 is further characterized for its PCP potential, especially by interaction with distinct Wnt ligands, while the involvement in β -catenin is considered in the later chapters of this thesis.

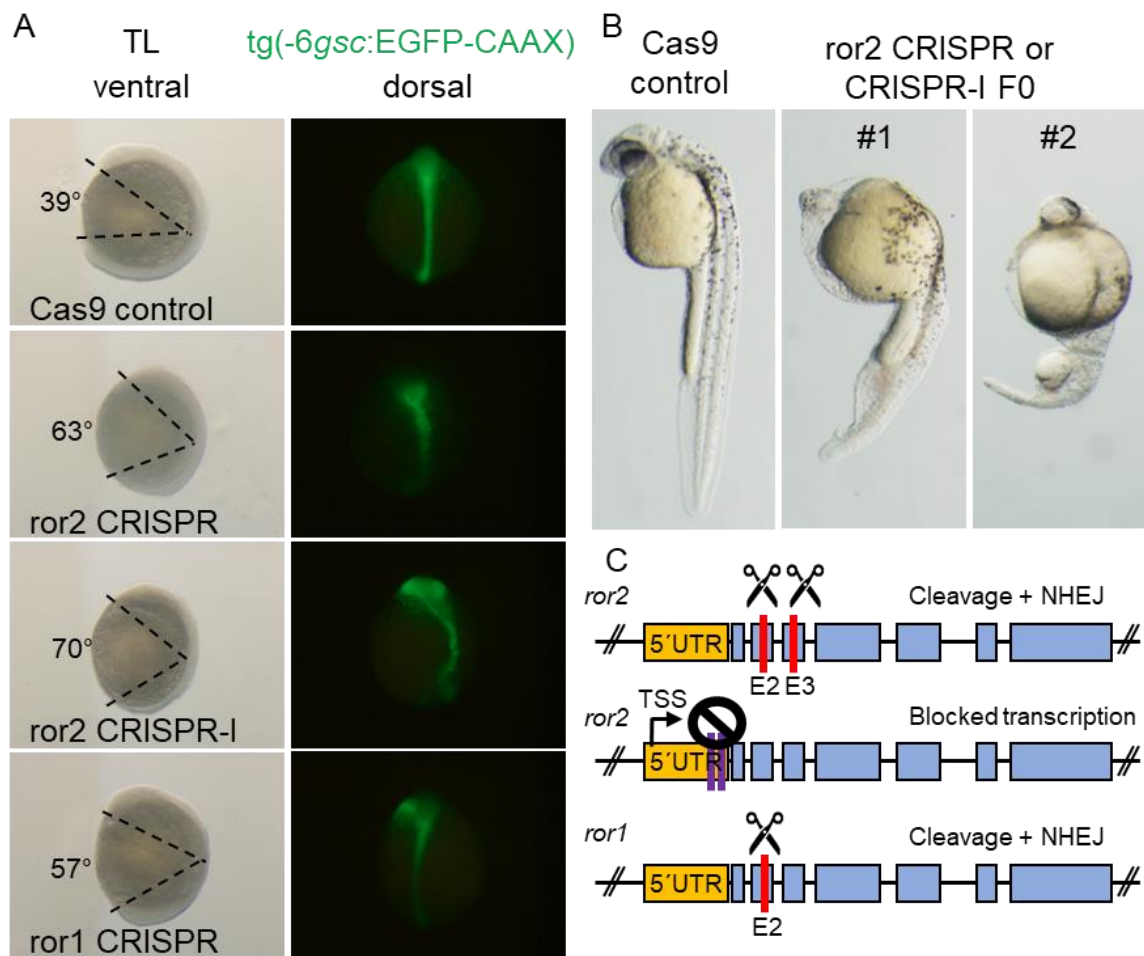


Figure 19: CRISPR/Cas9 gene silencing approaches for Ror2 and Ror1. (A) Measurement of the angle between the anterior and posterior ends of the embryo in ventral view and the proper convergence of the embryonic midline in *Tg(gsc:GFP-CAAX)* embryos in dorsal view of injected F0 embryos at 14 hpf. (B) Resulting phenotype of CRISPR and CRISPR-I injected embryos. Images highlight only two selected severe phenotypes. (C) Schematic design of this CRISPR and CRISPR-I approach. Ror2 or Ror1 ORF-gRNAs (red) cut the DNA in combination with Cas9, while UTR-designed gRNAs (purple) in combinations with dCas9 aim for a blocked transcription without inducing double strand breaks.

By binding the classically canonical Wnt ligand to a Wnt/PCP receptor the question arises which signal is transmitted. As the receptors of signal complexes - here Ror2 and Fzd7a - activate the downstream cascade by phosphorylation and recruitment of pathway proteins it is most advised to investigate their signaling route in more detail. Therefore, the interaction of Wnt8a with Ror2 could trigger non-canonical PCP signaling via the Ror2 pathway. I utilized the classical PCP controlled process of collective cell migration towards the embryonic midline to observe the involvement of Wnt8/Ror2 in non-canonical signaling. C&E can be visualized by condensation of the *no tail a* (*ntl*; also known as *T-box transcription factor Ta*, *tbxta*) positive notochordal plate at the embryonic midline at 11 hpf (Figure 20A). By dorsal view on this distinct stripe of *ntl*-positive cells, any PCP effect is known to disrupt its precise formation. Co-staining for *hatching gland* (*hgg*, also known as *cathepsin Lb*, *ctslb*) marks the most anterior structure to help its positioning with its most dorsal *ntl* expression facing the camera. To this end, I over-expressed the Ror2 receptor, which alone had a very small effect on the establishment of the *ntl* expression domain (Figure 20A,C; for classification see Figure 20B). However, over-expression of Wnt8a leads to a broadening and shortening of the *ntl* expression domain. This phenotype is reminiscent of Wnt5b activation. A similar phenotype was observed when Wnt8a and Ror2 were co-expressed. Categorization of the phenotypes suggests that the co-activation of Ror2/Wnt8a or Ror2/Wnt5b have similar effects (Figure 20A,C), but synergistically intensified due to Ror2 presence (Figure 20C). Inhibition of Ror2 function by either Ror2³¹ expression or Ror2 morpholino knockdown also led to C&E defects.

For a more comparative readout for C&E disruption in different sample setups, the width of *ntl-a* expression was measured (Figure 21A) as represented by the arrows in Figure 21B. As Fzd receptors mediate a signal transduction in a variety of different pathways, I wondered whether Fzd has a role in my observed Wnt8a/Ror2 interaction. I found an enhanced broadening of the embryonic midline of Wnt8a/Ror2 overexpression compared to the single injections, but a severe broadening if Wnt8/Fzd7a and Wnt8a/Fzd7a/Ror2 were overexpressed (Figure 21D). Even Fzd7a alone lead to a striking phenotype. This suggests that endogenous Ror2 is expressed at high levels already, as observed before (Figure 14C,D), and the available Wnt ligand concentration and Fzd7a availability is the key quantity-controlling step in this context of PCP signaling during zebrafish C&E. Nevertheless, the data provides first evidence of functional Wnt8a/Ror2 synergy.

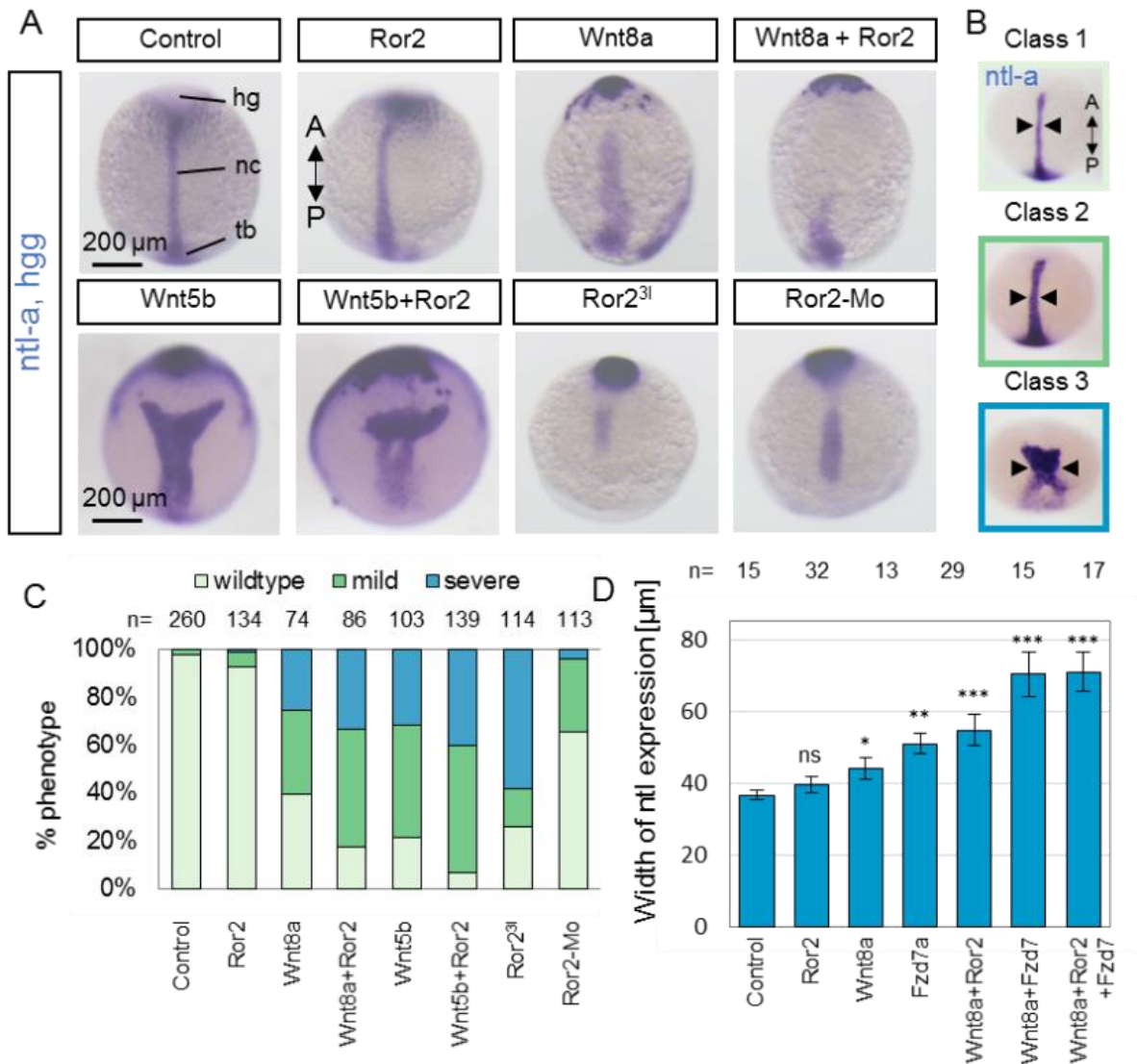


Figure 20: Analysis of a Wnt/PCP-mediated C&E defect by evaluation of the *ntl* expression. (A) Embryos at 11 hpf were fixed and subjected to *in situ* hybridization against *hgg/ntl*. Image shows a dorsal view. A, anterior; hg, hatching gland; nc, notochord; tb, tail bud; P, posterior. (B,C) Classification of embryos into 3 groups of phenotypes (wildtype, mild, severe) depending on their *ntl* expression shown in B. (D) Quantification of the *ntl* width. Location of measurement is shown in (B) (black arrows) and the bar diagram represents average width with SEM.

During C&E, cells intercalate in the notochordal plate (convergence), push previously adjacent cells apart, and lengthen the field along the AP axis (extension) (Glickman, 2003). I investigated the shape of the notochord cells in 11 hpf embryos with ectopically expressing Wnt or Ror2 signaling components. Tg(*gsc*:GFP-CAAX) embryos express a membrane bound GFP in notochordal *gsc*-positive cells. Fixed specimens were positioned in dorsal view (Figure 22A) to determine the influence on their cell shape by PCP signaling. A width to length ratio was calculated subsequently. I found that the cells had a less bipolar shape and

displayed a more circular form in embryos with Wnt8/Ror2 signaling, reminiscent of Ror2 activation by Wnt5a (Figure 22B,C), suggesting that mediolateral narrowing of axial mesoderm is reduced. Impact of low levels of Ror2, Wnt8a or Wnt5b without a co-expressed counterpart was very mild compared to the change in cell shape if both are present. This data shows clearly the synergistic operation of Wnt8a/Ror2, however, no statement can be made about either activation or inhibition, as both conditions would lead to PCP alterations and therefore alter cell migration and C&E movements.

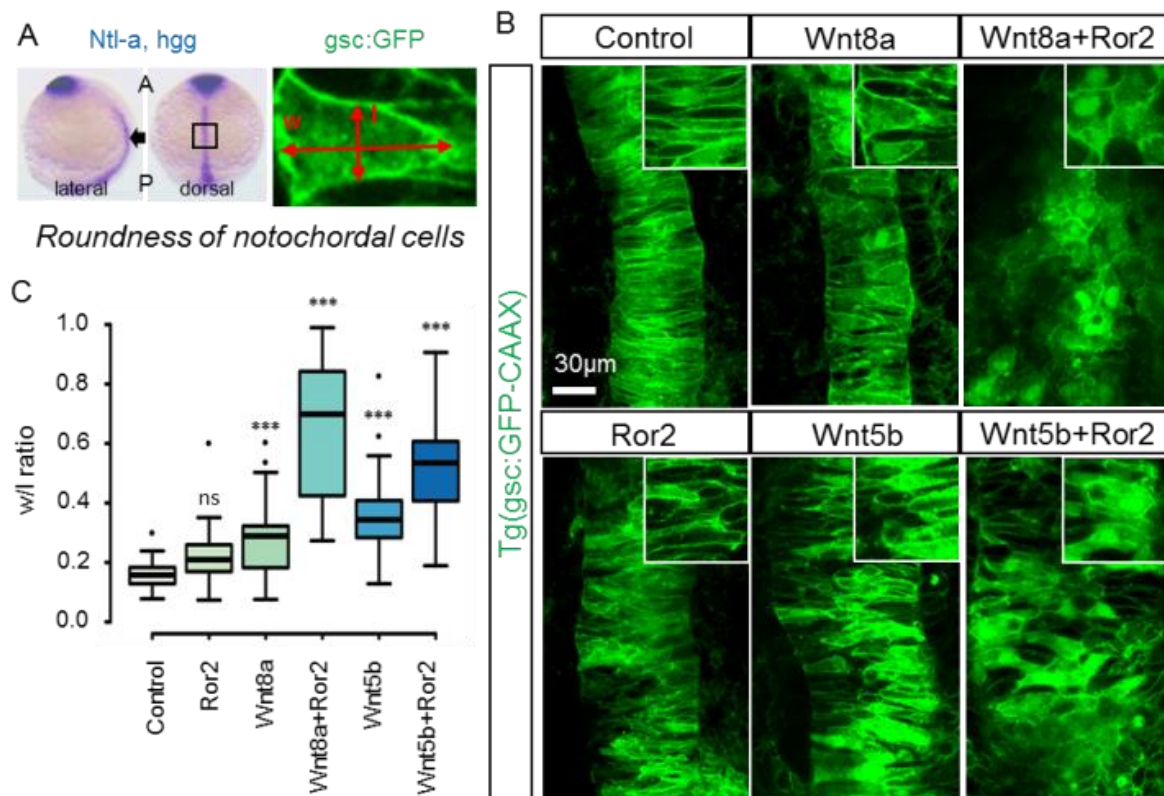


Figure 21: Synergistic Wnt PCP activation during C&E by Wnt8a and Ror2 affects cell shape of notochordal cells. (A) Tg(*gsc:GFP-CAAX*) embryos were microinjected with indicated constructs, fixed at 11 hpf, and a defined z-stack was imaged by confocal microscopy. ISH image stained for *ntl-a* and *hgg* represents the position of the notochord and the area of the image acquisition to determine the cell roundness. Image on the right shows the width/length ratio determination of notochordal cells marked by membrane associated GFP. A, anterior; P, posterior. (B). Confocal stack shows the notochord marked by *gsc:GFP-CAAX* from a dorsal orientation. Magnified inset highlights the shape of notochord cells. (C) Analysis of notochordal cell roundness. Boxplot shows the width/length ratio of 20 notochordal cells each. Circularity ranges from 0 (infinitely elongated polygon) to 1 (perfect circle).

Activation and inhibition of the PCP signaling pathway leads to a similar phenotype (Tada and Heisenberg, 2012). Therefore, with previous setups it cannot be distinguished how

Wnt8a/Ror2 alters PCP signaling. During *Xenopus* gastrulation, Wnt5A activates Ror2 downstream signaling, leading to Cdc42 activation, JNK phosphorylation, and, ultimately, the enhancement of ATF2 transcription (Hikasa *et al.*, 2002; Schambony and Wedlich, 2007). To test whether zebrafish Wnt8a is able to activate or repress Ror2 signaling, a reporter assay with an ATF2 responsive element was used driving luciferase expression in *Xenopus* embryos (Brinkmann *et al.*, 2016; Ohkawara and Niehrs, 2011) to back up our system with another well-known quantitative PCP readout which perfectly complements previous results. *Xenopus* embryos can be transiently modified in the same manner as zebrafish. Injection of both the ventral and dorsal blastomeres lead to overexpression of the ATF2 responsive element plus zebrafish Wnt8a in various setups (Figure 22A), before luciferase reporter assay was carried out of full embryo lysates. Wnt8a co-expressed with Ror2 produced a greater than five-fold induction of the ATF2 reporter in *Xenopus* (Figure 22B). Co-expression of Wnt5A/Ror2 led to a similar activation of reporter expression, whereas expressed Ror2 without a co-expressed ligand did not alter expression of the ATF2 reporter. I determined whether the kinase domain of Ror2 is required for Wnt8a dependent activation of the PCP pathway by overexpressing Wnt8a together with dominant-negative Ror2³¹. I observed a reduction of ATF2 reporter activation compared to activation of Wnt8a/Ror2.

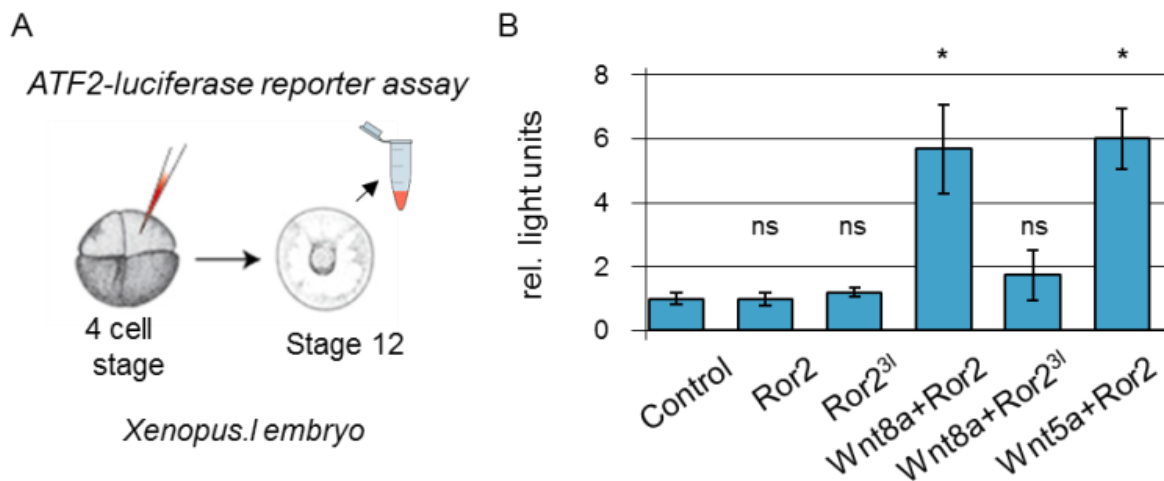


Figure 22: ATF2 reporter assay in *Xenopus* embryos to measure Wnt/PCP activation. (A) Summary of *Xenopus* injection and luciferase assay procedure performed in collaboration with Lilian Kaufman, Heidelberg. At four cell stage, embryos were injected into both ventral and dorsal blastomeres and subjected to a luciferase reporter assay at stage 12. (B) ATF luciferase reporter assay of pooled *Xenopus* gastrulae injected with indicated constructs and both the ATF2 firefly luciferase and renilla luciferase reporter. Bar diagram shows the mean with S.D. of three independent experiments.

Taken together, the data indicates that Wnt8a serves as a ligand for the receptor Ror2 and induces PCP signaling upon binding. Thus, ectopic over-expression of Wnt8a modulates cell movements and cell morphology in zebrafish and gene transcription in *Xenopus*. Replacing Ror2 by a signaling-truncated Ror2 in presence of Wnt8a proves the importance and specificity for subsequent pathway activation.

3.7. Imaging setup and quantitative analysis of Wnt-cytonemes during zebrafish gastrulation.

I already provided detailed evidence of Wnt8a/Ror2 interaction, cluster formation and signaling output that greatly influences C&E in zebrafish and *Xenopus* target gene expression. I hypothesize the observed influence of PCP signaling cause alterations in Wnt cytoneme formation.

Therefore, the following study is focused on observing Ror2 regarding Wnt8a-cytonemes in single zebrafish cells *in vivo* and further tissue culture systems. Cytonemes are very small and dynamic structures and observation of single cells as well as their dynamic over small timeframes adds an immense amount of understanding. However, the complexity of studying fluorescent tagged proteins on delicate structures such as cytonemes in living organism over minutes or hours required the adaptation and optimization of the process of sample preparation, subsequent detection and processing. Precise microinjection of tagged constructs into 8-or 16-cell blastomeres zebrafish embryos generates a distinctive cell population in the developing embryo (Figure 23A). As it grows, cells intermingle and by chance, single labeled living cells are surrounded by unlabeled wildtype cells which are extremely important when studying cell-cell communication by protrusions. Equally labeled cells next to the source would conceal protrusions. Figure 23C presents two cells positive for Wnt8a-GFP and memCherry in their innate *in vivo* environment. Cells can be observed interacting with their surroundings. Furthermore, Wnt8a-GFP-positive tips (Figure 23C, white arrows) mark the corresponding protrusion as Wnt-cytonemes, while the Wnt8a cluster is deployed over time to unlabeled signal-receiving cells. After generation of sample data in a 3D volume, processing by a semi-automatic segmentation software using a live wire approach (Barrett and Mortensen, 1997) was used for quantification (Figure 23B). The earlier PAC2 kinase screen used a preliminary form that was dedicated now to a complex 3D surrounding (Figure 12). As these 3D imaging stacks were very diverse, start and end points are manually set by

the user and the operation itself was less automatic than in 2D in order to be less error susceptible and more precise.

Overall, this setup was dedicated to unravel cytoneme biology in zebrafish and served as a robust procedure to observe and measure Wnt cytonemes in all subsequent experiments.

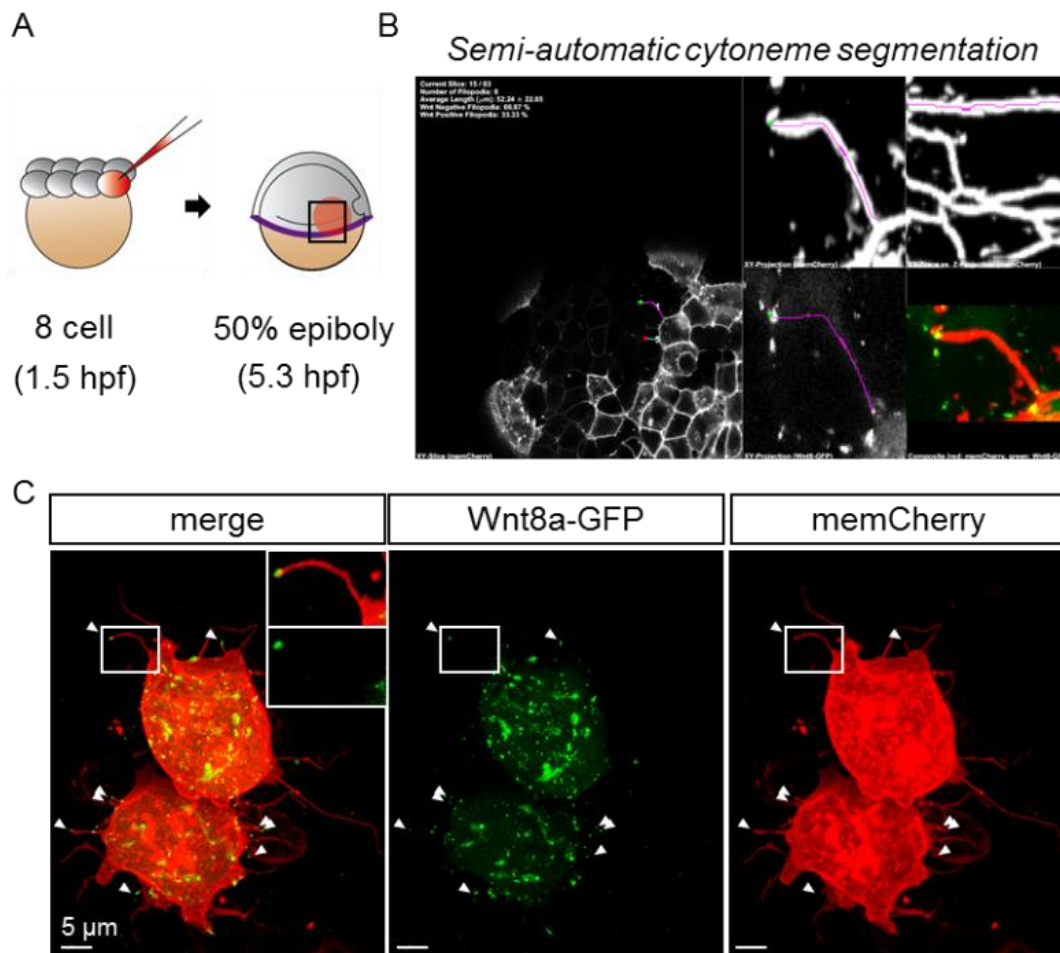


Figure 23: Imaging setup and cytoneme quantification of single cells in a 3D confocal volumes. (A) Representation of injection and scanning procedure. Zebrafish embryos were injected in one of eight or sixteen blastomeres to generate a defined cell clone during gastrulation. Confocal images near the dorsal site of the marginal zone (purple line) were acquired for quantitative or qualitative purposes. (B) Cytonemes were traced in 3D using a semi-automatic approach optimized for confocal image stacks. Left: Software displays the XY-plane of a confocal volume in which filopodia start and end points are manually set by the user. Right, top row: XY-Projection and XY-Trace vs Z-Projection of memCherry. Right, bottom row: XY-Projection of Wnt8a-GFP and composite image. (C) 3D confocal image of a cell clone at 50% epiboly expressing Wnt8a-GFP and memCherry *in vivo* surrounded by undetectable untransfected cells at 50% epiboly. Wnt8a-GFP is mainly located intracellular or membrane bound in accumulations and is also displayed on cytoneme tips (highlighted by white arrows).

3.8. Ror2 presents Wnt8a to the target cell to induce ligand-receptor cluster.

The understanding of cytonemal Wnt8a-GFP transport during neuro-ectoderm patterning is far from complete. Thus, I wanted to observe the dynamics of Wnt8a and Ror2 during cytoneme formation in a complex environment.

A role for Ror2 might be revealed during observation of live cytonemes and the interplay with other signaling components in the same source cell, but also with proteins in signal receiving cells. Cluster formation of Ror2 with Wnt8a, Wnt/Ror2-mediated PCP signaling and filopodia outgrowth in zebrafish PAC2 cell culture already indicate a striking involvement of Ror2 in cytoneme biology. I hypothesize, that protein dynamics, when co-expressed with fluorescent labels in dorsally located cells of an embryo during gastrulation, enhance the understanding of cytonemal Wnt8a delivery in presence of Ror2.

The question arises how Wnt8a and Ror2 interact to facilitate cytoneme-mediated transport. Therefore, I performed a high-resolution imaging approach in the developing zebrafish embryo by over-expressing fluorescence-tagged constructs that feature correct cell localization and retain biological activity. The high-sensitivity of the image-based approach allowed reducing the expression levels of the tagged construct and microscope laser intensity significantly while still maintaining full fluorescent capacity up to at least 30 minutes of constant confocal laser scanning. Photo bleaching, photo toxicity and morphological alterations of the embryonic phenotype were not observed at 24 hpf.

By a time-lapse analysis, formation and transport of Wnt8a-GFP cluster on cytonemes in presence of Ror2-mCherry were captured. The early formation of cytonemes was studied first. Wnt is supposed to be transported to the membrane and subsequently deposited on a newly formed cytoneme. Confocal time-lapse scans with 30 s framerates of 3D volumes of up to 30 μm in z-direction allowed tracking single Wnt cluster in living zebrafish gastrulae. After recruitment, Wnt8a co-localizes with Ror2 at the plasma membrane suggesting Wnt8a-Ror2 cluster induction (Figure 24A; 1:30) as previously described (Figure 15). Interestingly, a newly formed cytoneme with the observed Wnt8a/Ror2 cluster arises shortly after (Figure 24A; 3:00) and is elongated over time. The observed timeframe could be the first documentation of a Wnt8a cluster, initiating its own dissemination via Ror2/PCP-mediated

signaling and cytoneme induction in real time, although individual steps have to be analyzed in more detail.

Furthermore, it is still uncertain which events follow cytonemal Wnt transport and Lrp6 receptor binding at the target cell. In another real-time tracing of a Wnt-cytoneme, I observed novel insights in signal processing (Figure 24B). First, a Wnt8a-cytoneme is elongated while scouting for a receiving cell (0:00 – 9:30). The cytoneme tip merges with the target cell membrane (9:30), where it remains for presumably signalosome formation and downstream signaling as described before (Stanganello *et al.*, 2015). The cytoneme prunes back shortly after (10:00) while completely committing the Wnt/Ror2-positive cytonemal cluster to the receiving cell. Within minutes, the clusters are endocytosed into the target cell (11:30) before the Wnt8a-GFP signal completely vanishes at 12:00. The remaining endocytosed Ror2-mCherry signal excludes the possibility of the cluster escaping the imaging area. Therefore, it suggests a downstream mechanism specifically affecting the Wnt8a-GFP. This might expand the established knowledge of cytonemal transport as the sequences of action in the signal receiving cells are still far from complete.

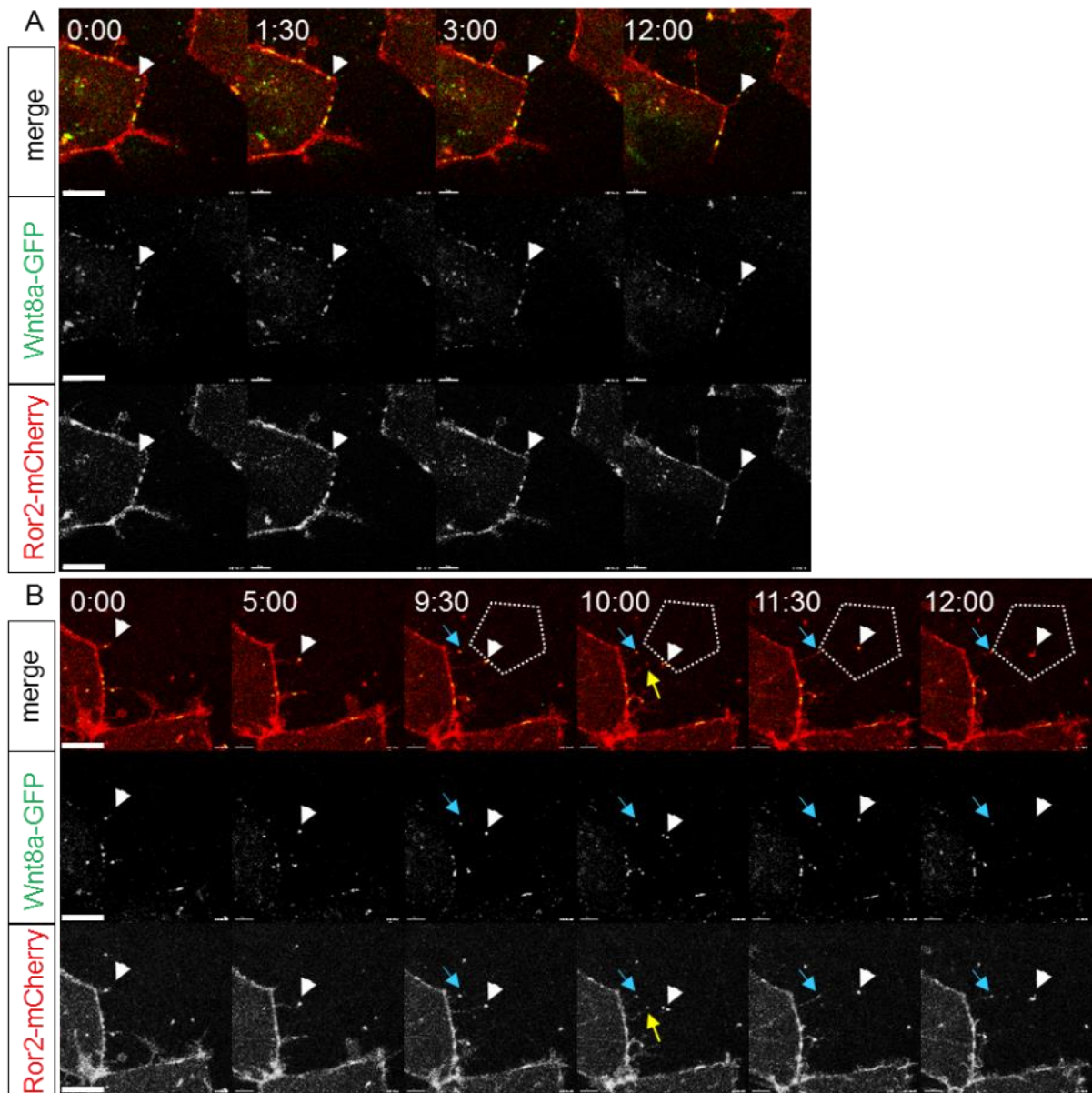


Figure 24: Visualization of cytonemal Wnt transport *in vivo*. Still pictures of indicated time points, taken at a 30 s frame rate. (A) A Wnt8a-GFP cluster is recruited to the plasma membrane and subsequently transported on a newly formed cytoneme tip. Cytoneme merges directly at the Wnt/Ror2 cluster position. White arrow points to the Wnt8a/Ror2 cluster. (B) Dynamic of a Wnt8a/Ror2 cluster on a cytoneme (white arrow) transported to a receiving cell. Cytoneme breaks and prunes back at 10:00 (yellow arrow). Subsequently, Wnt8a/Ror2 cluster is endocytosed and Wnt8a-GFP signal disappears at 12:00, while Ror2-mCherry persists. A second cytoneme targeting the same cell is emphasized by a blue arrow.

I was wondering whether Wnt8a-Ror2 induces the Wnt signaling cascade in the target cell. Therefore, I performed a test to visualize the first requirement for paracrine signal activation: Wnt ligand-receptor complex formation. However, sending and responding cells must be labelled differently. To obtain a separation in producing and secreting cell, the

double-blastomere microinjection approach was utilized as described in Figure 25B. This allows generation of two separate cell populations in close proximity with a unique expression of fluorescent proteins to study paracrine signal transmission (Figure 25C).

Next, I analyzed Lrp6-signalosome formation at the plasma membrane of the target cell. Cytonemal Wnt8a-mCherry induces Lrp6-GFP cluster formation at the membrane of the target (Figure 25A). I hypothesize that the source cell presents Wnt8a by clustering the ligand on Ror2 positive cytonemes. Indeed, Lrp6-GFP clusters at the contact points of Ror2-positive cytonemes (Figure 25C). Therefore, I conclude that Ror2 clusters on cytoneme tips to act as a platform to present Wnt8a to the target cell and induce the Wnt signaling cascade therein.

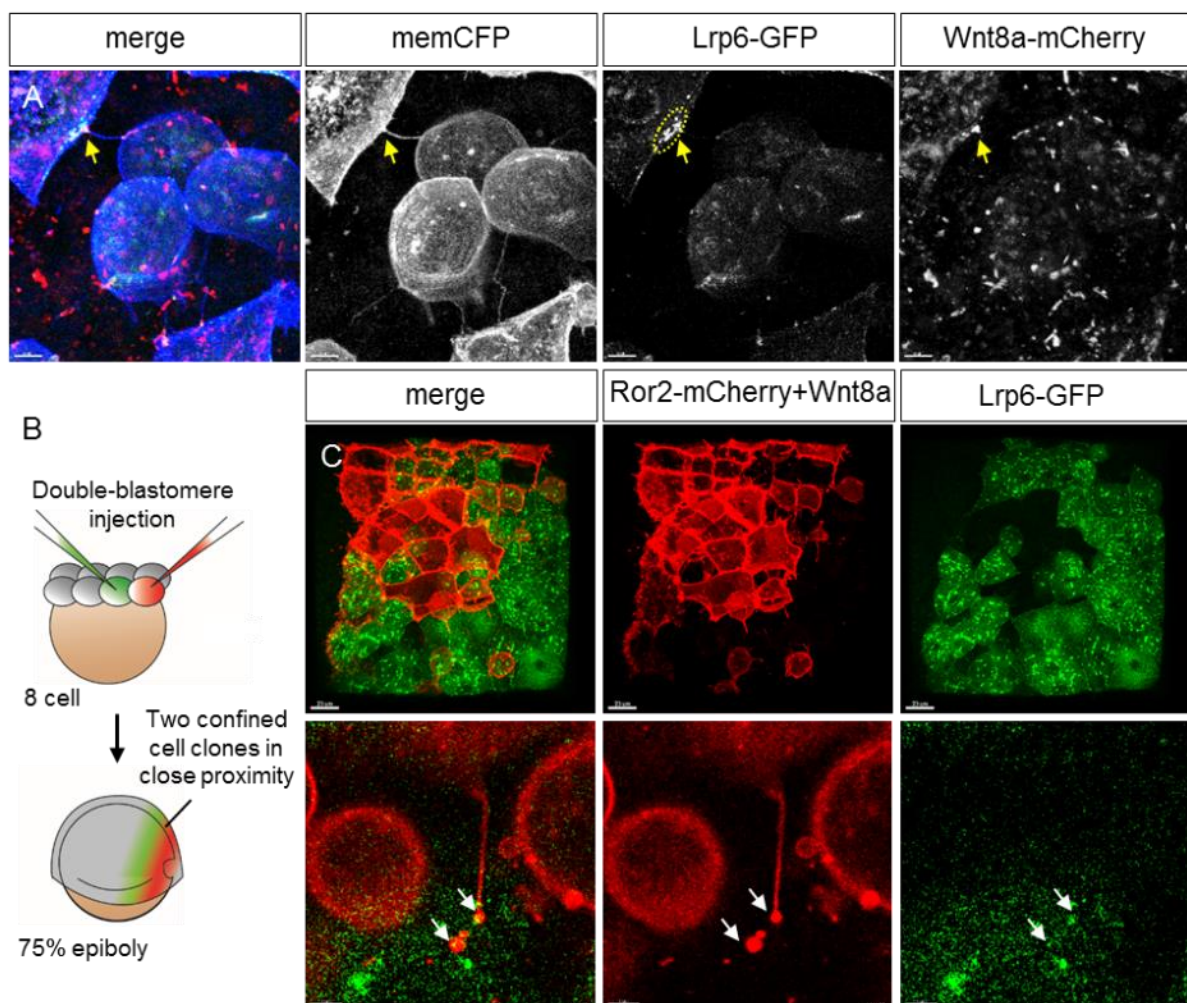


Figure 25: Dissecting cytonemal Wnt transport: Analysis of the Lrp6-response in receiving cells. (A) Maximum projection of injected zebrafish cells *in vivo*. Wnt8a-GFP cytoneme leads to Lrp6-GFP membrane cluster on cytoneme contact point (yellow arrow). (B) Schematic principle of a double injection approach into 8-cell stage zebrafish embryos to generate two distinctive and separate cell populations in close proximity. (C) This double injection approach was used to study Wnt8a/Ror2-mCherry cytoneme interaction with Lrp6-GFP

positive receiving cells (maximum projection in top row). Single plane magnification (bottom row) displays Lrp6-GFP/Ror2-mCherry co-localization on a cytoneme tip and a previously delivered vesicle.

Furthermore, other essential Wnt signal components such as the Fzd7a receptor have been shown previously to be impactful for Wnt8a/Ror2 operations (Figure 20D). Therefore, I wanted to gain additional insight utilizing high resolution imaging and Fzd7a deletion constructs. Co-expression of Fzd7a-CFP, Wnt8a-GFP and Ror2-mCherry supports tremendous cluster formation especially on membrane sections in contact with adjacent cells and on enlarged cytoneme tips (Figure 26A). The substantial specificity was further evaluated in regards of Wnt8a-GFP cluster capabilities. Fzd7a constructs Fzd7a Δ C and Fzd7a Δ N exhibit depletions in the extracellular or intracellular domain, respectively (Figure 26B). The full-length Fzd7a^{WT} in presence of Ror2-mCherry leads to the previously observed consolidated cluster formation (Figure 26C). Fzd7a Δ C appears to have an increased Wnt8a-GFP clustering with Wnt8a-GFP decorating almost the entire cell membrane (Figure 26C). Even though the extracellular Wnt-binding domain is unaltered, lack of downstream signaling and recycling upon Wnt binding could explain the augmented Wnt8a occurrence in the membrane. In contrast, Fzd7a Δ N reduces Wnt8a-membrane cluster significantly. Wnt8a-GFP appears to be less membrane associated and present in inner cell compartments. I suspect the lack of the Wnt-binding CRD prevents Wnt8a-GFP binding to detain it at the membrane. The question arises how more or less Wnt8a-clustering by Fzd7a affects filopodia formation. Therefore, the established filopodia assay in PAC2 cells was utilized as shown previously and their length were assessed. It is particularly interesting that depletions of the Δ C or Δ N domain both reduce the induction filopodia in presence of Ror2 as a stimulating factor (Figure 26D), even though only Fzd7a Δ N had a visible effect on Wnt8a-GFP cluster formation. Thus, not only cluster formation, but also the downstream cascade by frizzled is required for proper filopodia formation in Fzd7a/Wnt8/Ror2 signaling complexes.

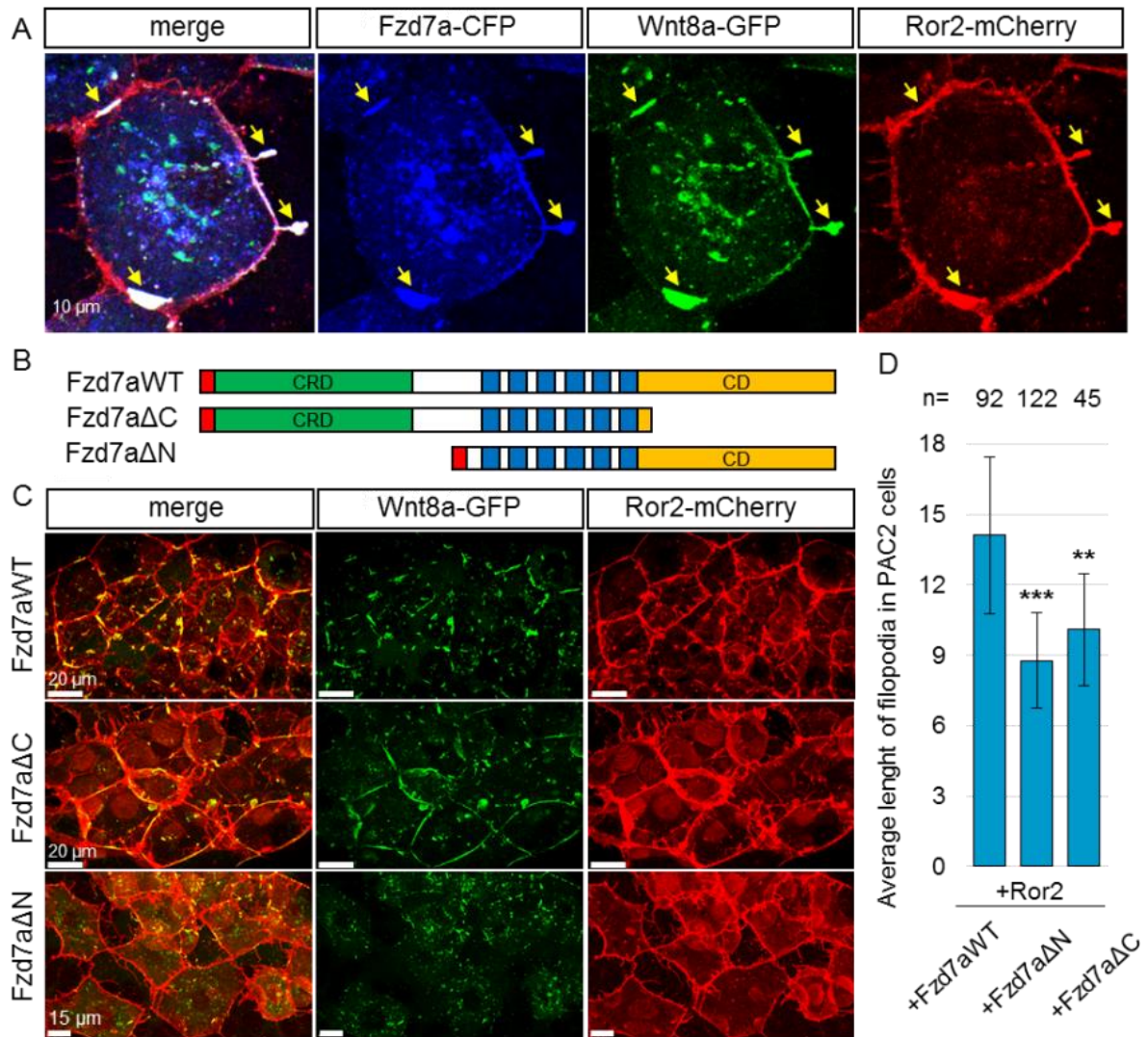


Figure 26: Dissecting cytonemal Wnt transport: Involvement of the Wnt receptor Fzd7a in cluster formation and filopodia induction. (A) Single image plane of zebrafish cells *in vivo* injected with indicated mRNA at eight-cell stage. Co-localization of Fzd7a-CFP, Wnt8a-GFP, and Ror2-mCherry can be seen at the plasma membrane to neighboring cells and on cytoneme tips (highlighted by yellow arrows). (B) Structure of Fzd7a wildtype or mutant constructs with missing N-terminal or C-terminal domains of the protein. CRD, Cysteine-rich domain; CD, Cytosolic domain; Signal peptide and 7x transmembrane domain is shown in red and blue respectively. (C) Investigation of Fzd7a cluster formation in confocal volumes. Co-expression of Wnt8a-GFP, Ror2-mCherry, with either Fzd7aWT, Fzd7aΔC, or Fzd7aΔN demonstrates cluster formation. Absence of long membrane accumulations with Fzd7aΔN indicates a dependency of the N-terminal domain for Wnt8a membrane accumulations. (D) Bar diagram with SEM for filopodia length in PAC2 cell culture transfected with indicated constructs. n displays the number of cells measured.

In vivo imaging expands the total understanding of how Wnt8a ligands transmit signals and act with their respective receptors. Further steps are required to fully dissect the complex mechanism of cytonemal transport into the individual building blocks of cytoneme formation,

ligand transport and ligand transfer. Here, valuable live data represents the cytoneme process and documents not only the involvement of Wnt8a/Ror2 cluster in cytoneme induction and subsequent ligand handover, but also reveals information about the time span. Cytoneme target finding was observed in several minutes, while ligand transmission, endocytosis, and potential degradation occurred in seconds to minutes.

3.9. Ror2 induces Wnt-cytonemes during zebrafish neural patterning.

The findings indicated that Ror2 might have a lead role in cytoneme formation. I hypothesize, Ror2 actively regulate the occurrence of cytonemes and that I can modulate cytoneme properties if mis-expressed. To test this hypothesis, Ror2's role in general filopodia formation was evaluated first and in a second approach, in context with Wnt8a-GFP cytonemes.

To study the dynamics of filopodia formation in the Wnt8a positive germ ring during normal development in zebrafish I quantified Wnt-negative protrusions or Wnt signaling filopodia during gastrulation in live embryos using a semi-automatic live wire approach as described previously (Figure 27).

I found the number as well as the lengths of filopodia significantly increase from 5 – 7 hpf, which comprises the neural plate patterning phase (Figure 27A). This coincides with increasing Ror2 expression levels during zebrafish development (Bai *et al.*, 2014). I wondered whether formation of these filopodia was dependent on Ror2 function. I manipulated Ror2 signaling and measured germ ring cell filopodia number at 6 hpf. Only a modest increase of filopodia number was found if Ror2 was activated, suggesting Ror2 itself is not the rate-limiting factor. However, when Ror2 function was reduced by over-expression of Ror2^{3I}, a significant reduction in filopodia number was observed (Figure 27B). I conclude that Ror2 signaling is required for filopodia induction and maintenance of embryonic marginal cells during zebrafish development as it regulates the number of protrusions. In contrast to PAC2 cell culture, no significant effect of Ror2 on filopodia length was observed, demonstrating the relevance to compare tissue culture results in *in vivo* systems.

I continued to visualize Wnt8a-cytonemes by generation of cell clones at the embryonic margin expressing Wnt8a-GFP and memCherry. Wnt8a-GFP clusters were seen in the cell membrane and cytoneme tips of germ ring cells. A profound increase in cytonemes carrying

Wnt8a-GFP clusters on their tips were detected upon Ror2 overexpression (Figure 27C). Conversely, I found a significant reduction in the number of cytonemes in Ror2 deficient marginal cells. Filopodia without detectable Wnt8a seemed to be unaffected by Ror2 signaling in zebrafish as numbers of Wnt-negative protrusions are unaffected by Ror2 overexpression or depletion (Figure 27C). This suggests that Ror2 regulates a specific subset of cytonemes, those carrying Wnt8a *in vivo*.

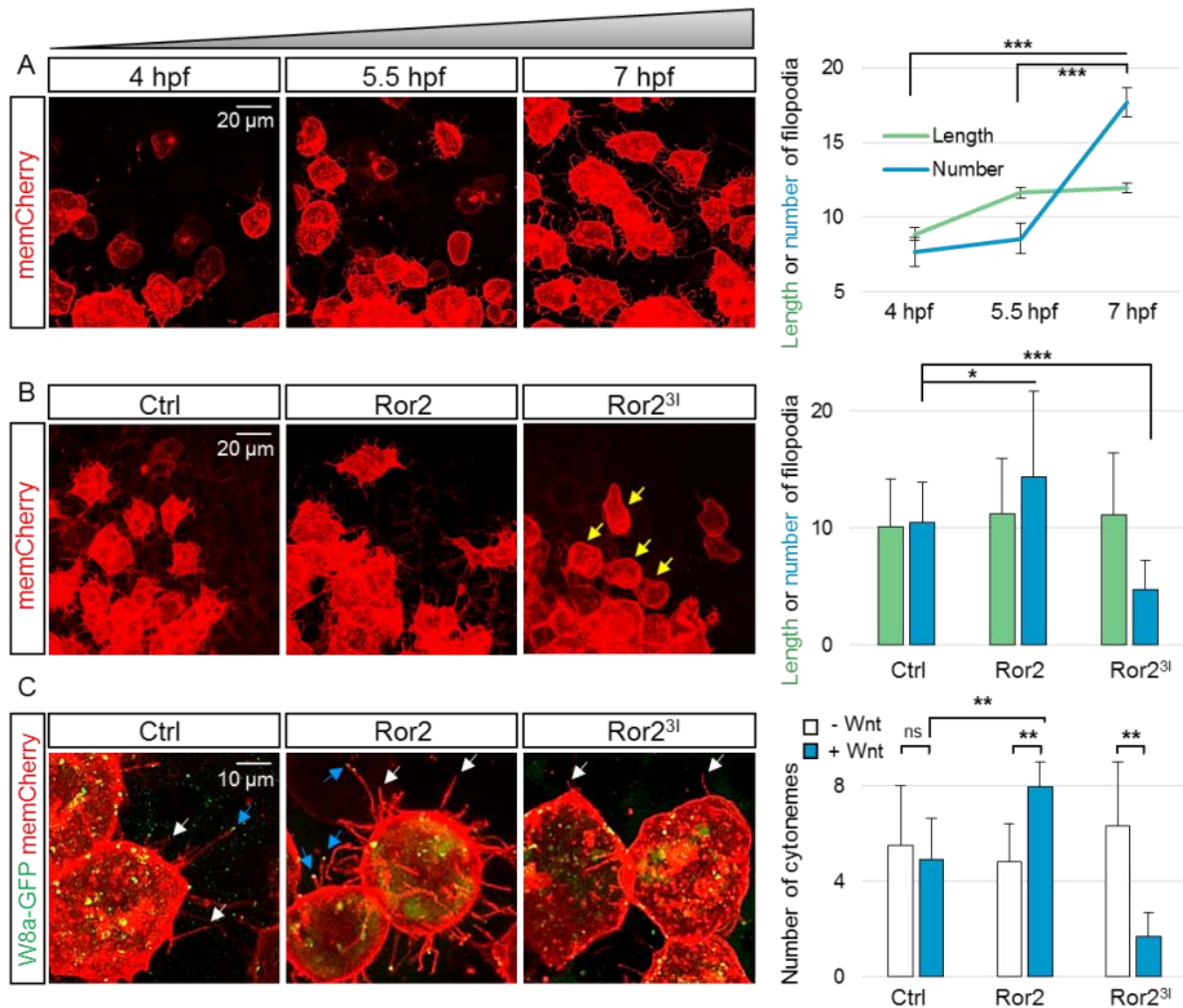


Figure 27: In-depth analysis of cytonemes in zebrafish embryos *in vivo*. (A) Live confocal microscopy analysis for filopodia dynamics over time. Mosaic expression of memCherry was utilized to quantify the protrusions of single cells at positions as indicated. The image shows the same cells with a maximum projection at different time points during zebrafish gastrulation. Filopodia of cells were measured by a semi-quantitative segmentation software (see Figure 23B). Quantification illustrates the mean filopodia length and number per cell with SEM at different time points. (B) Effect of Ror2 on filopodia length and number. Live confocal microscopy analysis for filopodia of embryos injected with Ror2 or Ror2^{3l} mRNA. Diagram shows mean filopodia length and number per cell with SEM. (C) Analysis of Wnt cytonemes during live imaging. Embryos were microinjected at 16 cell stage to generate a cell clone expressing Wnt8a-GFP and memCherry to visualize cytonemes. Confocal images were taken of single cells and subjected to filopodia length/number measurement.

Bar diagram displays number of filopodia without Wnt8a-GFP (white) or with Wnt8a-GFP (= Wnt-cytonemes, blue) on the tip of the protrusion.

Based on these findings, I hypothesized that Ror2 function in the Wnt source cells is crucial for Wnt dissemination via cytonemes. These data suggest that Ror2 signaling specifically regulates the number of Wnt positive cytonemes *in vivo* and thus represents a cytoneme specific regulator. Thus, I predict a decrease in Wnt signal activation in the neighboring tissue if Ror2 function is compromised in Wnt8a source cells which is subject to investigation in the following chapters.

3.10. Ror2 regulates paracrine β -catenin signaling by autocrine Wnt/PCP-mediated cytonemes

I speculated that Ror2 signaling may have a function in Wnt ligand trafficking and, consequently, in paracrine β -catenin signaling during zebrafish gastrulation. To test this, I analyzed its effect on C&E processes and, simultaneously, on neural plate patterning during embryogenesis.

Monitoring the development provides an immense amount of knowledge on the large-scale function of a protein. Here, crucial steps of embryogenesis were selected to interpret and reconstruct Ror2 function. By *in situ* hybridization (ISH), mRNA levels and position during several stages of development highlight important landmarks of neuro-ectodermal patterning. ISH against *axin2*, *fibroblast growth factor 8 (fgf8)* and *paired box gene 6a (pax6a)* were performed at 8, 9 and 24 hpf, respectively (Figure 28A-C). The displayed schematic helps to compare the regular gene expression. *Axin2* serves as a Wnt target gene and reflects Wnt activation in the neuroectodermal tissue (Jho *et al.*, 2002). Consequently, it presents a wedge-shaped expression surrounding the Wnt-positive marginal zone except at the most ventral margin and the dorsal shield organizer (Figure 28A). On the other hand, the expression of *fgf8* and *pax6a* highlight prominent landmarks of embryonic structures to validate a correct progression of embryogenesis. The two-striped expression domain of *fgf8* marks the prospective position of the midbrain-hindbrain boundary (MHB) (Rhinn *et al.*, 2005), a profound structure dividing midbrain and hindbrain area with subsequent organizer function, thus serving as another Wnt source later on in development (Figure 28B). *Pax6a* is a transcription factor involved in various aspects during development. In this study, *pax6a* is merely used by reason of its informative expression domain that displays individually all of the most anterior major brain structures at 24 hpf (Figure 28C).

Over-expression of Ror2 by injection of low levels of mRNA did not induce severe morphological changes in zebrafish embryos, consistent with the findings that Ror2 without a suitable ligand only mildly impacts on PCP mediated processes (Figure 18). Solely, *axin2* expression appears to be further expanded which could indicate an increased reach for Wnt transport, however, the 24 hpf phenotype don't account for increased Wnt signaling (Figure 28D). Over-expression of Wnt8a resulted in a substantial alteration in neural plate patterning as described above, with β -catenin signaling being activated in the entire neural plate, marked by ubiquitous *axin2* expression at 6 hpf (Figure 28D). As a consequence, I observed posteriorization of the developing nervous system, observed as an anterior shift of the *fgf8a* positive MHB at 9 hpf and a loss of the anterior *pax6a* positive forebrain at 24 hpf. In embryos co-expressing Wnt8a together with Ror2, there is still a posteriorization phenotype in the neural plate was observed - although sparsely minimized - and, in addition, I found that C&E is compromised, as the neural plate does not converge to the midline and, consequently, the expression domains of *fgf8a* at the MHB showed a pronounced gap. I compared these observations to embryos expressing the β -catenin independent ligand Wnt5a, and Wnt5a together with Ror2 (Figure 28D). Ror2 mediated Wnt5a signaling induces C&E in *Xenopus* (Hikasa *et al.*, 2002) and represses β -catenin signaling in mouse embryos (Mikels *et al.*, 2009). In both settings, a strong effect on C&E movement in the zebrafish embryo was observed. In addition, Wnt5a/Ror2 over-expression led to reduced β -catenin signaling, causing a reduction in target gene expression (*axin2*) and anteriorization of the neural plate, leading to a posterior shift of *pax6a* expression in the forebrain (Figure 28D).

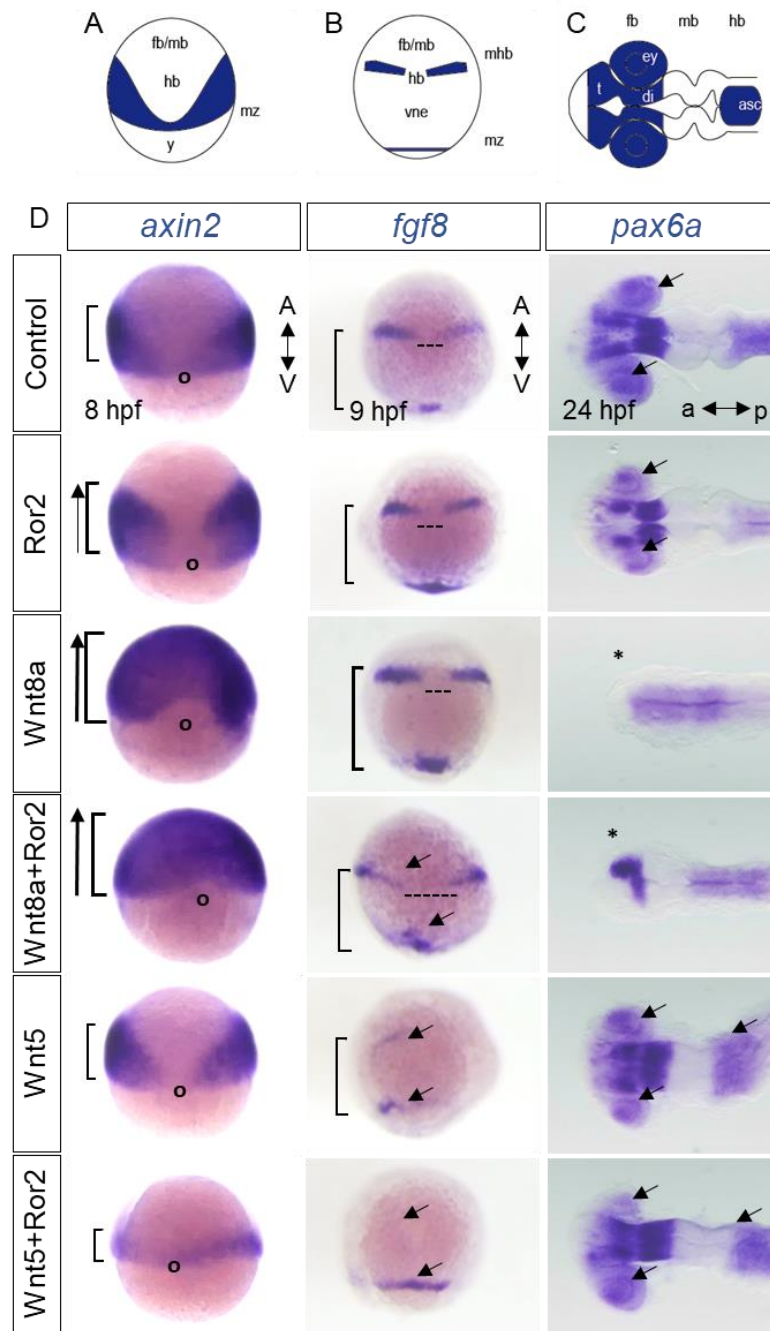


Figure 28: Gene expression of marker genes to highlight changes in pattern formation. (A) Illustration of important expression domains and landmarks in *in-situ* hybridizations for *axin2*, *fgf8* or *pax6a*. fb, forebrain; mb, midbrain; hb, hindbrain; y, yolk; mz, axial marginal zone; mhb, midbrain-hindbrain boundary; vne, ventral neuroectoderm; t, telencephalon; di, diencephalon; ey, eye; asc, anterior spinal cord. (B) Microinjected embryos at indicated stages were fixed and subjected to *in situ* hybridization against the Wnt target gene (*axin2*) or markers for brain patterning (*fgf8a*, *pax6a*). Dorsal view. Yolk of *pax6a*-stained embryos was removed prior image acquisition. Position of the dorsal shield organizer is shown by the circle. Brackets indicate expansion of Wnt target gene expression (*axin2*), distance of *fgf8* expression domains or forebrain territory (*pax6a*), while the asterisk indicates a lack of forebrain tissue. A, animal; v, vegetal; a, anterior; p, posterior.

I conclude that Wnt8a activates β -catenin signaling, and induces PCP signaling via the Ror2 receptor during zebrafish development. By contrast, Wnt8/Ror2 ubiquitous in all tissues lead to slightly less Wnt activation in total, presumably by Wnt8a/PCP inhibition, while the range of Wnt-active tissue might be expanded due to stimulated Wnt-cytosomes. I showed that Wnt5b/Ror2-mediated PCP signaling represses Wnt/ β -catenin signaling in an autocrine manner. We hypothesized that Wnt8a function depends on the route of secretion. However, global over-expression did not differentiate between autocrine and paracrine Wnt8a signaling mechanisms and on subsequent downstream activation. In further trials the autocrine Wnt/Ror source is going to be separated from the receiving population.

To separate Wnt-producing from Wnt-receiving cells, I performed a co-cultivation assay using HEK293T cells, which are typically Wnt-Off due to low endogenous expression of Wnt ligands (Voloshanenko *et al.*, 2017). Cytosome regulators were transfected into HEK293T source cells (representing Wnt-producing cells) and co-cultivated with HEK293T cells expressing the SuperTOPFlash Wnt reporter (Wnt receiving cells). Seven TCF responsive elements (7xTRE) drive a nuclear-mCherry expression (Moro *et al.*, 2012) (Figure 29A). Upon Wnt pathway activation on a transcriptional level, stimulated transcription factors bind the TCF responsive elements and produce a measurable nucleus localized mCherry signal. To start this process however, receiving HEK293T cells require Wnt ligands. Therefore, the amount of mCherry signal depends on the capabilities of the source cells Wnt-transport machinery.

Co-cultivation of 7xTRE-nucRFP cells, sensitized for Wnt signaling with Irf6 co-expression, determined the baseline of nuclear mCherry signal. Total cell number detected by DAPI staining was uniform throughout the samples, while nuclear mCherry expression depends on transfection of indicated constructs (Figure 29B). Ror2 transfection into source cells did not significantly alter the induction of 7xTRE-nucRFP in the receiving cells (1.3x fold; Figure 29B,C), due to the unavailability of Wnt ligands. However, Wnt8a-producing cells lead to 15-fold activation of signaling activity in the HEK293T reporter cells. Reporter expression was further enhanced to 22-fold (147.3% compared to Wnt8a transfected source cells) when Wnt-producing cells co-expressed Wnt8a and Ror2, indicating a synergistic interaction between Wnt8a and Ror2 (Figure 29B,C). Co-transfection of Wnt8a with dominant-negative Ror2³¹ resulted in a 34.6% decrease in reporter activation, compared to Wnt8a transfected source cells. Wnt5b has no β -catenin activity, either alone or co-expressed with Ror2.

Increase in β -catenin activity demonstrates that Ror2 can potentiate paracrine signaling, presumably by boosting Wnt ligands transferred to a receiving tissue. I suspect the Wnt increase is due to Wnt8a transmission via Ror2 dependent cytonemes in HEK293T cells, while Wnt5b and Wnt5b/Ror2 transfections were unable to activate the β -catenin signaling reporter in neighboring cells (0.78- and 0.98-fold respectively; Figure 29B,C).

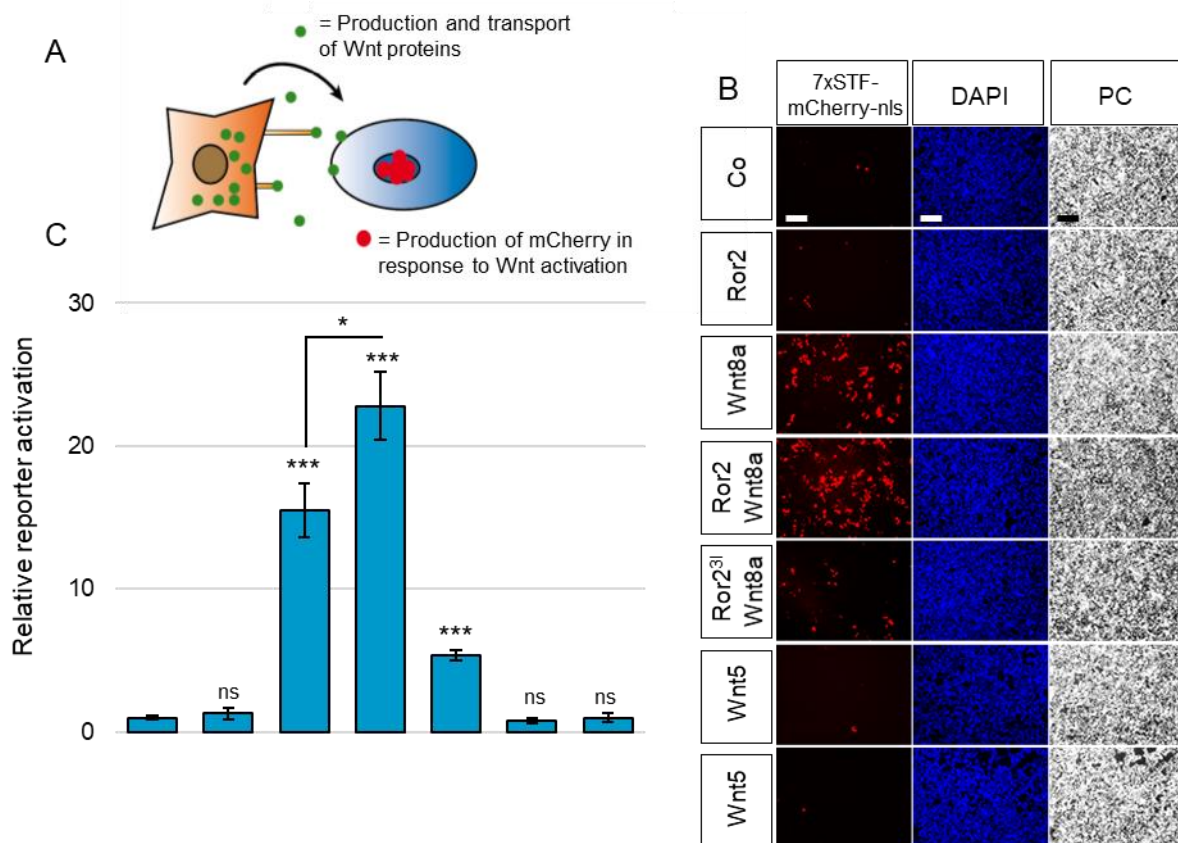


Figure 29: Ror2 enhances paracrine Wnt- β -catenin signaling in HEK293T co-culture. (A) Principle of the co-culture reporter gene assay in HEK293T cells. Wnt reporter population was transfected with the 7xSTF-nucRFP Wnt responsive element together with lrp6 and co-cultured with a Wnt-source population as indicated in a second step. (B) After 48 h of co-cultivation, fluorescence images were taken to quantify reporter activation while DAPI staining documents a constant cell number in all samples (DAPI quantification now shown). Scale bar represents 200 μ m. (C) Relative reporter activation by measuring the nuclear mCherry signal. Bar diagram represents the mean value with SEM of 3 independent experiments.

To test whether Ror2-mediated Wnt cytonemes affect β -catenin dependent target gene activation in neighboring cells *in vivo*, I generated small-source clones by microinjecting cytoneme regulator mRNAs at the eight-cell stage (Figure 30A). By mid-gastrulation, the source cells were distributed over an area of the embryo and intermingled with WT host cells, generating many responding cells around a few source cells. At 6 hpf, I analyzed the

transcriptional profile of the embryos for the β -catenin target genes *axin2* and *lef1*. Embryos containing few cells over-expressing Ror2 or Ror2³¹ showed no significant alteration in *axin2* or *lef1* expression (Figure 30B). However, source cells over-expressing Wnt8a resulted in a significant increase in β -catenin dependent target gene expression, which was not further enhanced by Ror2 addition. However, blockage of cytoneme formation in the Wnt8a source cells by co-expression of Ror2³¹ led to a significant reduction of β -catenin target gene induction in neighboring cells (Figure 30B). Blockage of filopodia *per se* by over-expression of the dominant-negative form of IRSp53^{4K} caused a similar reduction of activation of *axin2* and *lef1* expression in embryos.

This suggests that, during zebrafish gastrulation, the majority of Wnt8a protein is transmitted via cytonemes and that the formation of these Wnt cytonemes is Ror2 dependent. Consistent with the previously shown Ror2 effect on cytonemes in zebrafish, knockdown of Ror2 function has a more striking effect due to Ror2's ubiquitous availability in the *in vivo* system.

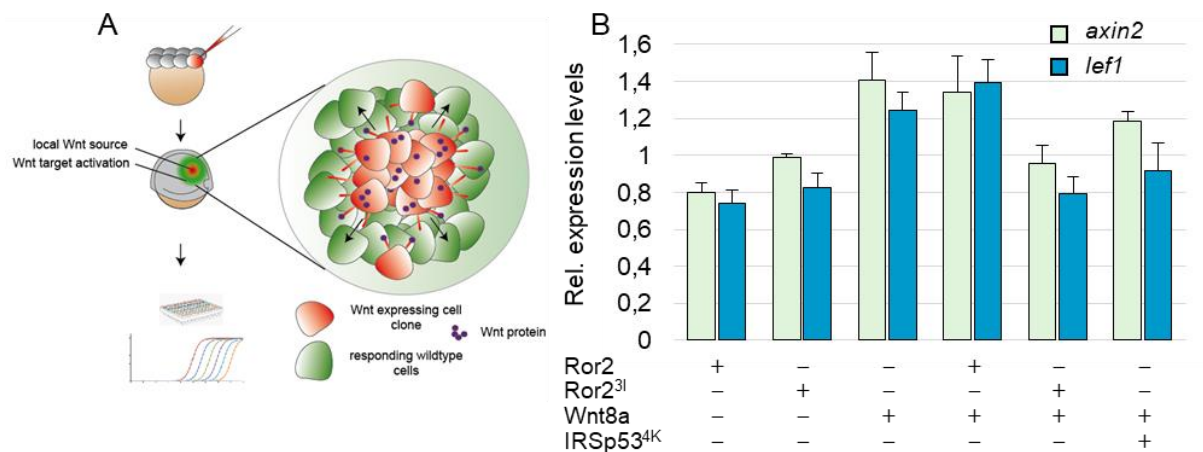


Figure 30: Ror2 augments paracrine Wnt- β -catenin distribution in zebrafish embryo clones. (A) Workflow of clonal injection to induce a local Wnt source with following RTqPCR analysis of target genes in responding cells. The cell clone spreads Wnt signal and activates target genes in neighboring cells. (B) Graph shows relative $\Delta\Delta$ Ct value in comparison with control embryos (set at 1.0) of the Wnt/ β -catenin target genes *axin2* and *lef1*. Target genes were normalized to the housekeeping gene *actb1*.

3.11. Ror2 dependent cytonemes operate in gastric cancer cell proliferation

Over-activation of canonical Wnt/ β -catenin signaling can be identified in one-third of gastric cancers (Chiurillo, 2015). β -catenin signaling is essential for self-renewal of gastric

cancer stem cells, leading to Wnt-mediated resistance to apoptosis, which may be responsible for recurrences in these tumors. The Wnt/ β -catenin-independent branch plays a similarly important role in cancer progression: The key ligands Wnt5a and Ror2 are upregulated in various gastric cancers (GC) regardless of the histological phenotype. To ask whether Wnt ligands are transported on cytonemes between gastric cancer cells, I used gastric tubular adenocarcinoma liver metastasis cells (MKN7 and MKN28) and primary gastric adenocarcinoma cells (AGS).

Based my previous data I hypothesized that Ror2 act as a key component in cytonemal Wnt signaling and its implication could be a conserved principle. In order to prove this concept in an applied context, I studied cytonemes in GC cells and transferred the cytoneme-concept on Wnt-dependent processes as proliferation and finally organoid formation of intestinal crypt cells.

The first requirement for the GC cell model was to prove the existence of filopodia and moreover cytonemes. Transfected membrane bound mCherry or F-actin staining by LifeAct localized filopodia in GC cell lines (Figure 31). AGS cells appear to grow in a spread single-cell manner and display a fascinatingly high amount of filopodia. A high magnification of the protrusions reveals large bulges on the proximal filopodia tips, a promising indicator of potential protein clusters located on them (Figure 31A). Forced expression of Ror2-mCherry marks the membrane and protrusions as reported in PAC2 cells before. Interestingly, I observed stable filopodia attached to an untransfected cell in close proximity (Figure 31B, yellow arrows). Furthermore, this targeted AGS cell contained a large quantity of Ror2-mCherry clusters (Figure 31B, red arrows) originating from a Ror2-positive cell and was potentially delivered via cytonemes. MKN28 and MKN7 GC cells (MKN7 data not shown) proliferate in a group of cells clustered together. Although they possess a significantly lower content of filopodia, Ror2-mCherry cluster were distributed to neighboring un-transfected cells (Figure 31C, red arrow). Surprisingly, over-expression of Ror2 greatly increased filopodia occurrence, thus, Ror2-positive cells can be easily distinguished (Figure 31C, yellow arrow).

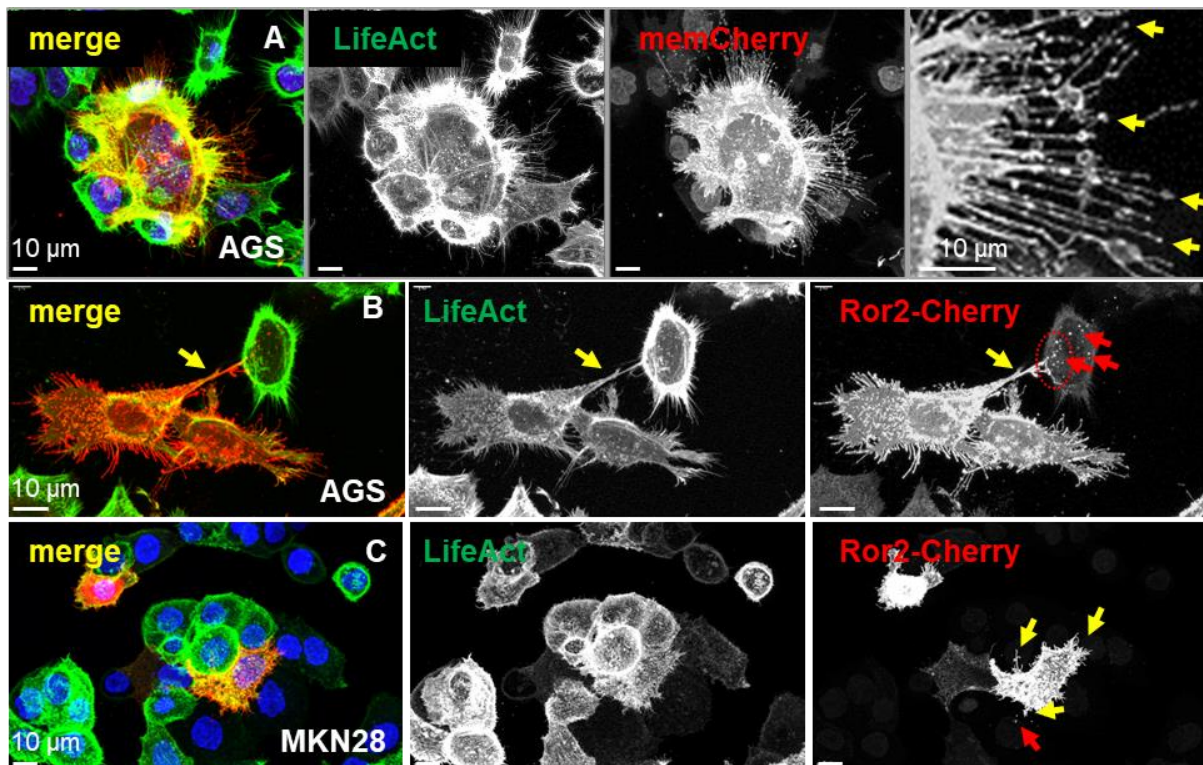


Figure 31: Analysis of cell extensions in the gastric cancer cell lines AGS and MK28. Confocal z-projections of fixed or live cells. (A-C) AGS or MKN28 cells transfected with memCherry and stained with LifeAct. (A) AGS cells feature a multitude of filopodia with broadened filopodia tip structures. (B,C) Yellow arrow marks filopodia connections of AGS (B) or MKN28 (C) cells to adjacent cells and red arrow highlights delivered Ror2-mCherry clusters to a non-transfected adjacent cell.

Next, I assessed the formation of Wnt-cytonemes in AGS and MKN28 GC cells by co-expression of Wnt8a-mCherry in live GC cells. Surprisingly, AGS cells were actively transporting Wnt in the cell, associating Wnt in cluster at the cell membrane, and moreover, it was also detected on a large amount of cytoneme tips (Figure 32A, yellow arrows). The Wnt-cytoneme output of AGS cells appears to be very vigorous, as some cells exhibit a halo-like Wnt8a-mCherry ring. This ring-shaped accumulation of Wnt8a originates from the cell while it might stick to the plastic properties of the cell culture base. Fascinatingly, the distance of the Wnt8-mCherry accumulation to the cell body approximately represents the average length of cytonemes (Figure 32A, red arrows). MKN28 cells hold more inconspicuous cytonemes, as they are often covered by the tight connection to the neighboring cells (Figure 32B). On the other hand, they don't require elongating as far to reach the approximate cells. However, even by absence of long visible protrusions, Wnt8a-mCherry is transported to un-transfected cells in close proximity (Figure 32B, red arrows).

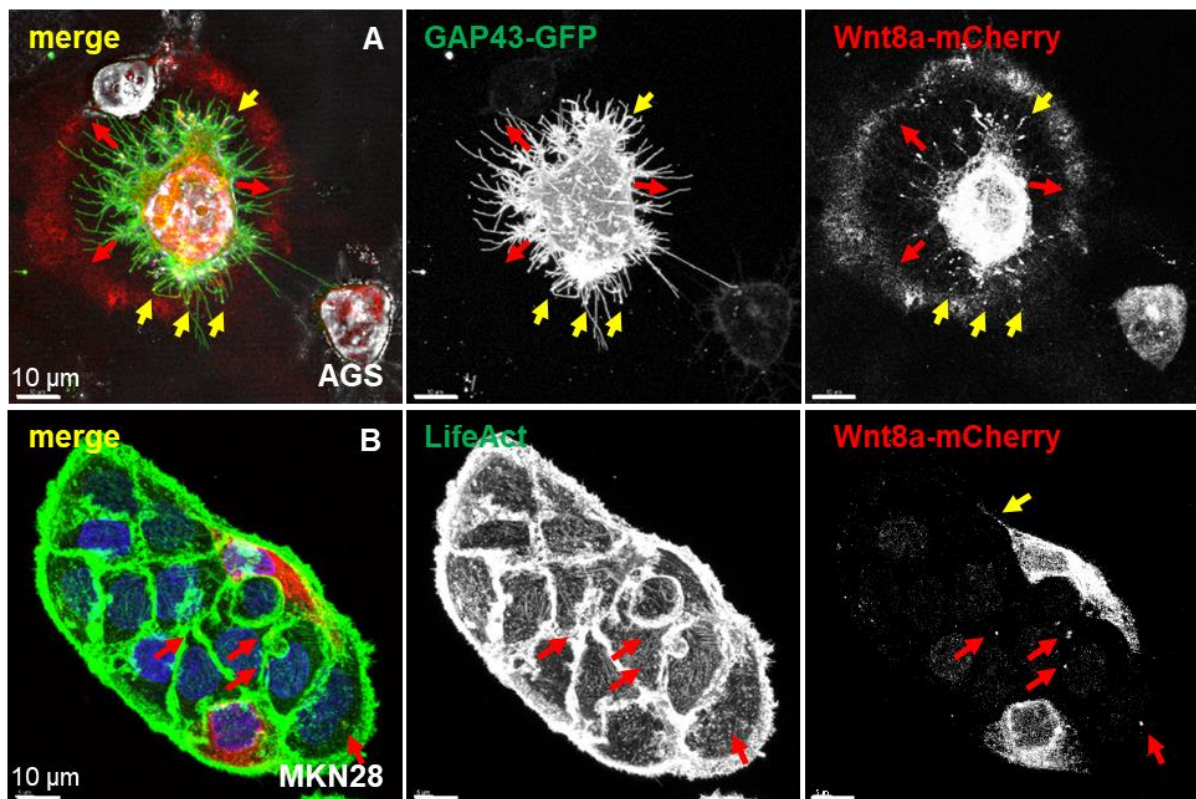


Figure 32: Analysis of cytonemal Wnt spreading in the gastric cancer cell lines AGS and MKN28. Confocal z-projections of fixed or live cells. (A) Confocal images of live AGS cells transfected with GAP43-GFP and Wnt8a-mCherry. Yellow arrows mark several Wnt8a-mCherry cytonemes and red arrow highlights circular Wnt8a-mCherry spots around the producing cell (B) Fixed MKN28 cell stained with LifeAct-GFP. Wnt8a-mCherry was distributed to neighboring untransfected cells.

Taken together, I provided evidence of the presence of cytonemes in GC cell culture. A large quantity of protrusions and cytonemal Wnt8-mCherry can be found in AGS cells. Furthermore, the existence of membrane particles and Wnt-mCherry cluster in un-transfected cells as well as the Wnt8-mCherry surrounding of producing cells illustrating their high transmission rate of Wnt. Although MKN28 and MKN7 cells have a less active character, Wnt8-mCherry is still delivered.

In the following setup, I focused on AGS cells as they show highly dynamic formation and retraction of cytonemes and are likely receptive to Ror2 manipulation. I assessed the effect of Ror2 on filopodia on a quantitative level. Over-expression of Ror2 led to a mild increase of the number of filopodia in GC cells, whereas, there was a significant reduction of filopodia length in cells expressing dominant-negative Ror2³¹ (Figure 33A). This result indicates that Ror2 also control filopodia formation in GC cells in a similar fashion as shown in PAC2 cells. However, they appear to already contain a profound Ror2/PCP activation as

the over-expression of Ror2 didn't amplify filopodia lengths and number as much as in PAC2 cells. Consequently, these GC cells might contain a high cytonemal Wnt transport already in their natural state. This sets the foundation to observe Wnt-dependent processes as proliferation in GC cells by modification of Ror2-dependent cytonemes.

AGS cells express Wnt1 at constant high levels, and, thus, have high endogenous β -catenin activity, which has been linked to the increased proliferation rate of this cell line (Mao *et al.*, 2014). To assess whether cytoneme-mediated Wnt transport influences AGS cell behavior, and specifically proliferation, I co-cultivated Ror2 transfected cells with cells carrying the nuclear marker nucRFP (Figure 33B). Cells over-expressing Ror2 significantly increase cell proliferation in neighboring AGS cells (Figure 33C). Co-expression of the filopodia-specific inhibitor IRSp53^{4K} with Ror2 led to a strong reduction of Ror2-induced proliferation. Inhibition of Wnt signaling by the tankyrase inhibitor IWR1 (Chen *et al.*, 2009) abrogated the stimulatory effect of Ror2 expression, confirming that the Ror2 effect is due to increased Wnt signaling.

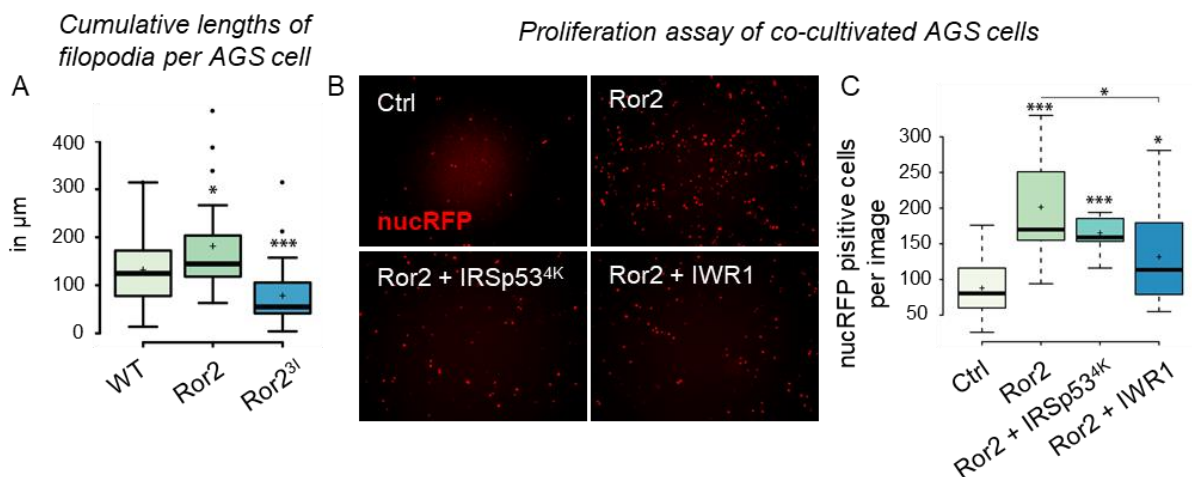


Figure 33: Importance of Ror2 dependent cytonemes in gastric cancer cell proliferation. (A) Boxplot of cumulative filopodia lengths for AGS cells transfected with an empty plasmid, Ror2 or Ror2³¹. (B,C) Proliferation assay of nucRFP transfected AGS cells after a 48 hrs co-cultivation with cells transfected with indicated construct and treated by IWR1 respectively. (B) Fluorescent images were subjected for cell counting. Average nucRFP cells per image are shown in Boxplot C.

I conclude that Wnt is moved on cytonemes between GC cells to stimulate Wnt/ β -catenin signaling and proliferation in neighboring cells. Abrogation of this transport route has a similar consequence as inhibition of Wnt signaling *per se* – it leads to reduced proliferation.

3.12. Ror2-dependent Wnt cytonemes are required in murine intestinal crypt homeostasis.

Finally, to transfer the Ror2-cytoneme model to another system, I asked whether Wnt cytonemes operate in fundamental aspects of Wnt tissue homeostasis such as in the mouse intestinal crypt. The intestinal crypt requires a constant supply of Wnt signaling for tissue maintenance (Beumer and Clevers, 2016; Kuhnert *et al.*, 2004; Pinto *et al.*, 2003; Sailaja *et al.*, 2016). The cellular source of Wnts that maintain the *Lgr5*-expressing intestinal stem cells niche is not completely understood. *In vivo*, it was recently suggested that *Pdgf receptor alpha* (*Pdgfra*) positive subepithelial myofibroblasts provide the major source of physiologically relevant Wnts, which maintain the intestinal crypt *in vivo* (Greicius *et al.*, 2018). It has been proposed that they transmit Wnts to the epithelial stem cells (Kabiri *et al.*, 2014; Valenta *et al.*, 2016).

By the help of Prof. David M. Virshup and his colleagues at the Duke-NUS Medical School in Singapore, experts on the field of *ex vivo* organoid culture and Wnt signaling, we were able to address this question. Myofibroblasts were prepared and cultured from C57BL/6-*Tg(Pdgfra-cre)1Clc/J/Rosa^{mTmG}* mice. Subsequently, they were transfected by Ctrl- or Ror2-siRNA. These myofibroblasts were imaged to assess Ror2-dependent filopodia. The GFP-positive intestinal myofibroblasts form a large amount of long filopodia (Figure 34A). The cumulative length of all filopodia is compared to Ror2 silencing. The formation of filopodia is inhibited by siRNA-mediated knock-down of Ror2 (Figure 34B). Furthermore, an organoid formation assay was used to analyze the requirement of Wnt signaling filopodia in the intestinal crypt. Wnt deficient *Porcn*^{-/-} crypt cells were co-cultivated with Wnt3a-secreting L cells or myofibroblasts to grow Wnt-deficient crypt organoids. As a mutation in *Porcn* shuts down all inherent Wnt production, these cells rely on an external Wnt source to grow and survive. Co-culture of Wnt3a-secreting L cells or WT myofibroblasts with Wnt-deficient crypt cells leads to induction and maintenance of crypt organoids (Kabiri *et al.*, 2014). Interestingly, these myofibroblasts extend filopodia to engulf crypt organoids (Figure 34C). If Ror2 is knocked down in the Wnt-producing myofibroblasts, a substantial decrease in the number of organoids was observed (Figure 34D).

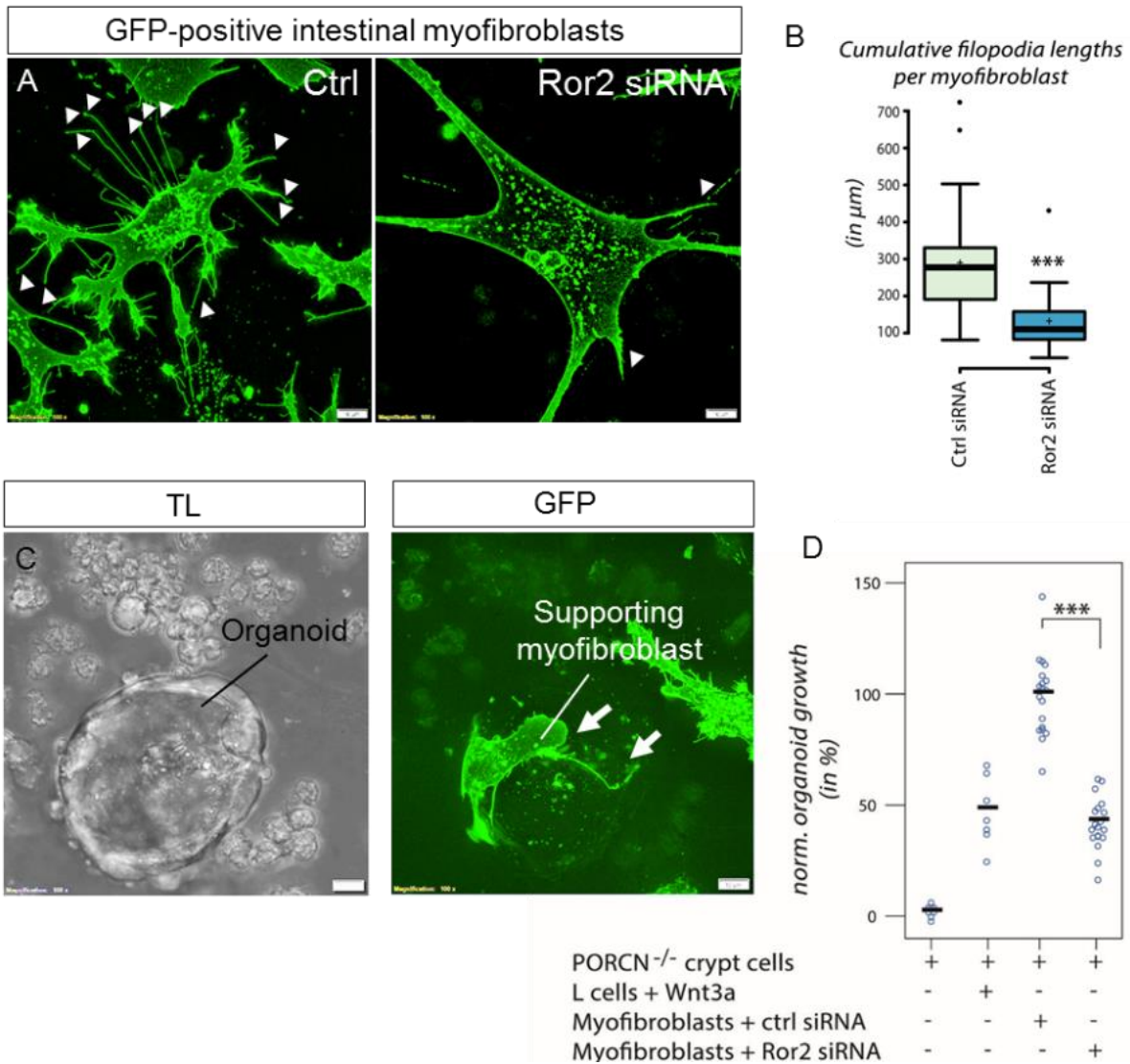


Figure 34: Intestinal crypt cell organoids requires Ror2-positive supportive myofibroblasts. (A) Fluorescent images of purified intestinal myofibroblasts derived from a GFP-positive mouse transfected with control siRNA (n=31) or Ror2 siRNA (n=29). (B) Myofibroblasts were quantified for cumulative filopodia length per cell. (C) Mouse crypt organoid supported by a purified GFP-positive intestinal myofibroblast. Support myofibroblasts display long cell protrusions surrounding the organoids (white arrows). (D) *Ex vivo* organoid formation assay of PORCN deficient intestinal crypt cells co-cultured with indicated cell population for 3-4 days. Organoid survival was normalized to crypt cells transfected with ctrl siRNA.

This suggests that Wnt signaling transport on Ror2-dependent cytonemes from the myofibroblasts is crucial for induction and maintenance of the intestinal crypt. I conclude that cytonemes are vital for Wnt protein dissemination in vertebrates and their appearance is regulated by Ror2-mediated PCP signaling.

4. Discussion

Generation of a Wnt gradient

Wnt/ β -catenin signals shape the body plan of multicellular organisms during embryogenesis. Only a handful of signals give rise to a high complexity of cell fates and complex patterns. This is facilitated by their function as morphogens, secreted by an organizing tissue and disseminated over a longer range. The understanding of pattern formation in biology is a problematic subject, which is not completely understood to date. Pioneers of that field as Alan Turing or Lewis Wolpert revolutionized the understanding of morphogen gradients, by presenting models that are applicable in several aspects in biology (Turing, 1952; Wolpert, 1969).

Almost all classical morphogen models depend on the requirement of a free motion of the inducing factor. As such, the reaction-diffusion system of Turing described a model of counter gradients composed of an activating and repressing factor (Turing, 1952). In fact, the aspect of two competing gradients is nowadays an established concept in biology and can explain patterns such as the pigment stripe pattern of zebrafish (Kondo and Miura, 2010). An example for Wnt counter gradient can be found during zebrafish AP patterning. Wnt inhibitors such as sFRPs are secreted from the opposite site as Wnt proteins, believed in counter acting the signal activity by binding Wnt proteins. Advantage is the regulatory aspect: a variety of patterns can be generated by adjusting the parameters as binding affinity, inhibitory potential or diffusion range. However, a free diffusible morphogen is a necessary requirement for this model.

Classic morphogen models hold true for some aspects in biology, however, ever since the discovery of Wnt palmitoylation, the question arises how a free diffusion could be achieved for highly membrane-associated proteins such as Wnt (Takada *et al.*, 2006; Willert *et al.*, 2003). Wnt proteins are known to induce a developmental program far away from the source of their production. Given the high membrane affinity by the acylation, Wnt proteins are supposed to accumulate in close proximity. However, replacement of Wnt with a membrane-tethered substitution in *Drosophila* does not disrupt the Wnt mediated cellular response of distant cells and established a correct morphogenic pattern with only minor deficiencies in growth (Alexandre *et al.*, 2014). Consistently, Wnt proteins can be observed

spread out from the source. Additionally, long and short-range target genes respond to a Wnt gradient. Consequently, there must exist a cell autonomous machinery to disseminate Wnt proteins over a certain distance.

Wnt spreading accomplished by cell division would not require diffusion and presents a reliable approach to transfer a membrane bound morphogen in a short-range application. However, the spreading from the source in a distance of several hundreds of micrometers is required in long-range functions for Wnt. Interestingly, even though Wnt was believed to be a secreted morphogen, there is almost no profound evidence of diffusible Wnt proteins in vertebrates. Wnt transporter such as Swim were reported in invertebrates as *Drosophila* to promote extracellular trafficking by diffusion (Mulligan *et al.*, 2012). Very recently, the human lipid chaperones Afamin revealed a hydrophobic binding socket modeled to specifically bind the Wnt hydrophobic moiety consistent to the x-ray XWnt8-Fzd8-CRD interaction (Naschberger *et al.*, 2017). The dramatically increased Wnt solubility might enable diffusion.

Active distribution mechanisms have been reported in several different systems and the elucidation of Wnt transport has become a major challenge. Exovesicles shuttle Wnt between cells, form gradients, activate signaling responses, while Wnt proteins are fused to the exosome membrane (Panáková *et al.*, 2005; Gross and Boutros, 2013).

However, the question for the underlying regulation arises. Morphogens need to initiate a in fine-tuned cellular response. But how can a cell ensure an accurate amount of signal to reach the destination? Shuttle proteins and exosomes allow migration through the extracellular space but cannot be guided once they are released.

Cellular extensions enable a cell autonomous function to drastically increase the morphogen transfer by specification of the direction, bypass the distance between cells and consequently specify the signal intensity. Wnt is released of exosome-like vesicles at the *Drosophila* neuromuscular junction to control morphogenesis (Korkut *et al.*, 2009). Trans-synaptic morphogen transmission presents a combinatorial approach of exosomal secretion and cellular extensions, thereby acquiring specificity in Wnt transmission.

My work centers the contact-dependent distribution by cytonemes. By the ability to form direct cell-to-cell contacts, the cell does not rely on a secondary secretion mechanism as

carrier proteins or Exovesicles. Signals can be delivered directly, consequently it reduces the expended resources. Furthermore, by probing the environment, the trafficking of the cellular protrusions and their target finding can be tightly controlled. Even though cytonemes are highly diverse, the general applicable mode of action is the establishment of cell-cell contacts to enable distant ligand-receptor interaction and thereby eliminating the requirement of a diffusible state of the morphogen. Membrane attachments can be even advantageous in terms of recruitment to the cytoneme membrane, maintaining adhesiveness at the cytoneme during target finding and elongation, or by utilizing a stable membrane path as a freeway to effectively reach the destination. With my presented evidence in this thesis, I expand the existing view of cytoneme formation and regulation. I show that cytonemes can be tightly controlled to provide accurate morphogen dissemination in their respective biological context.

Cytonemes distribute Wnt proteins

The idea of filopodia to exchange information goes back to early experiments in sea urchin gastrulae embryos, where thin cell protrusions were detected (Wolpert and Gustafson, 1961). The sensitive nature of these fine structure impaired their further characterization massively and only progress in less disrupting fixation and detection systems, especially the advancement in live imaging, turned the scales. Ever since the discovery of cytonemes in *Drosophila* (Ramírez-Weber and Kornberg, 1999), the reports of cytonemes in different aspects of development and other organisms were rising. Amongst others, several functions in the *Drosophila* imaginal disc, wing-disc-associated tracheal cells, and lymph gland have been observed (Kornberg and Roy, 2014). The direction of transport in invertebrates seems to be highly dynamic and adaptive to the respective tissue or cargo. In vertebrates, most morphogen distribution was observed in anterograde direction so far. However, due to the requirement of differentially labeling of the source tissue, the donor tissue, and the ligand or receptor cargo, the technical challenge is immense and could conceal more roles of cytoneme transport.

A different type of protrusion for cell-cell communication such as TNTs establish intracellular bridges to transport versatile cargos between cells including small soluble molecules to large organelles, pathogens, or even electrical signals (Austefjord *et al.*, 2014). They establish a static cytoplasm-connecting channel for a continuous transfer. Although cytonemes and TNTs share the principle of direct cell contact, they seem to be very diverse

structures in terms of function and even in their underlying molecular mechanism, which was reported to act in opposite to the filopodia-based actin regulatory complex (Delage *et al.*, 2016). The cellular protrusion in my study vary from TNTs in terms of a dynamic property, no membrane continuity and reliance on common filopodia-formation mechanism. Even though it was not shown in this work, a small fraction of cellular protrusions during zebrafish gastrulation was observed to persists in stable contact between cells for tens of minutes to hours. It would be attractive to investigate, whether there is another type of cellular extension besides cytonemes to facilitate a steady exchange of signals in discrete tissues.

The common theme of cytoneme transport during development is the ligand-receptor interaction in conjunction with a subsequent pathway transduction. Cytoneme-mediated delivery of signaling proteins such as EGF (Lidke *et al.*, 2005), FGF (Koizumi *et al.*, 2012), Shh (Sanders *et al.*, 2013), Wnt2b (Holzer *et al.*, 2012) have already been reported in vertebrate tissues, but the identification of the relevant biological context is challenging. We found cytonemal Wnt8a transport in zebrafish gastrulation to be the predominant delivery model in the process of tissue specification (Stanganello *et al.*, 2015), in line with other reports of filopodia-based Wnt distribution (Luz *et al.*, 2014). By activating Fzd/Lrp6 signalosome formation and subsequent Wnt/ β -catenin pathway activation the prospective neural tube is subdivided in antero-posterior direction (Stanganello *et al.*, 2015). The process of early patterning is stretched over several hours in a highly kinetic and proliferative tissue. For that reason, cytonemes require to deliver an adequate amount of signal to the various responding cells to ensure the activation of the correct developmental program. Wnt8a cytonemes have defined parameters such as the number and length of Wnt8a-decorated protrusions, motility of the protrusions, direction to their destination, average time of contact, delivered amount of protein and surely even more undescribed or undetected variables.

But how can Wnt create a long-range gradient in a cell sheet that surpasses the maximum cytoneme length by far? At 8 hpf, the neural plate has a dimension of over 600 μm , while the longest cytonemes rarely extend to 50 – 80 μm .

Eventually, the distribution of Wnt proteins was shown to occur already at 4 hpf, where neural plate cells are in close proximity to the source. Wnt cytonemes reach all cells to set a defined pre-pattern (Stanganello *et al.*, 2015). Later, the resulting long-range gradient is

facilitated by the proliferation- and migration-dependent of an existing gradient in addition to the constant supply of cytonemal Wnt to the nearest cell sheets.

Consistent to the idea of early patterning and tissue expansion, my observations of cytoneme dynamic extend the understanding of the regulatory mechanisms during this phase of Wnt distribution. Cytonemes are present already at 4 hpf, but I could show a drastically increase in their quantity during neural plate elongation. Therefore, the larger the cell sheet becomes, the more effective is the cytoneme machinery to induce posterior fate. I started this work with the expectation to discover an inherent regulatory system to command Wnt source cells to express the accurate set of Wnt cytonemes in the respective timeframe and cellular context. Interestingly, the time of Ror2 expression correlates with the increase in cytonemes during this critical phase of Wnt patterning. In the following, Ror2 is discussed as a regulatory element for cytoneme formation, Wnt transport and subsequent β -catenin activation.

Ror2 signaling directs the actin-based filopodia machinery

An increasing amount of developmental processes are found recently to contain cytoneme transport as mentioned before. While the main interest generally consists in discovering the signal distribution and the biological purpose for the responding tissue, the details about the underlying principle is often unclear. However, the understanding of the molecular processes in the sending cells allows consequently a precise modification of the transport machinery. Accordingly, operations as uncontrolled spreading of molecules during disease conditions could be prevented by intervene in the trafficking event. Therefore, molecular for cytoneme transport should be uncovered by performing a screen for cytoneme effector proteins. A kinase library of 229 cDNAs provided an appropriate starting point to identify proteins with capabilities to actively drive a fast and dynamic downstream signal cascade. Cytonemes change in response to signal protein levels in the cell of production (Sato and Kornberg, 2002; Stanganello *et al.*, 2015). Therefore, the source cell is able to sense and react to its morphogen. Consequently, PAC2 zebrafish fibroblasts were supplied additionally with Wnt8a to sensitize and predetermine the cells for Wnt8a-cytoneme formation. Additionally, the actin-dependent cytonemes rely on the cytoskeleton machinery with Cdc42 to be one of the most prominent driving factors (Stanganello *et al.*, 2015). Therefore, I expected a mechanism that can react to Wnt levels and tightly communicates with the actin-machinery.

I found several intermediates of the Wnt/PCP pathway in the screen: ROCK, TRIO, PKN2 and MAPK13 can be all linked to Wnt/PCP, subsequent pathway transduction, and actin remodeling. Remarkably, ROCK and TRIO indicates involvement of Rho GTPases such as Cdc42, a fundamental element of Wnt cytonemes (Stanganello *et al.*, 2015). The line of evidence indicated Ror2 as the central link with its implication in the actin cytoskeleton machinery and the PCP signal transducing elements. In zebrafish, PCP activation by Ror2/Vangl2 interaction triggers actin remodeling by ROCK downstream of Mcc and JNK (Young *et al.*, 2014). MAPK13 is representative for the consequent Wnt/PCP transduction cascade that ultimately end in ATF2 transcription factor activation and *paraxial protocadherin (papc)* expression in *Xenopus* (Schambony and Wedlich, 2007; Djiane *et al.*, 2000). The mode of action of Ror2 is variable in different tissues, as Ror2 function as a co-receptor in a complex with Fzd (Nishita *et al.*, 2010b), but was also suggested to act independently as a main receptor for XWnt5a in an alternative pathway (Schambony and Wedlich, 2007). In any way, they share a substantial amount of downstream proteins to transmit the respective signal. Interestingly, Ror2 can induce filopodia formation by actin polymerization via coupling of the Ror2-PRD to the actin-binding protein Filamin A (Nishita *et al.*, 2010b).

In the screening approach, Ror2 stimulated filopodia in a Wnt8a-rich environment. Further *in vitro* analysis in the vertebrate cell lines PAC2, AGS, MKN28, and isolated myofibroblasts substantiated the cytoneme-inducing capabilities of the initial screen. Ror2 is a receptor tyrosine kinase and several functions depend on phosphorylation following Wnt binding (Liu *et al.*, 2008; Minami *et al.*, 2010; Mikels *et al.*, 2009). In contrast, it was also suggested that Ror1 and Ror2 kinase domains are catalytically deficient and only function as RTK-like pseudo-kinases (Bainbridge *et al.*, 2014; Gentile *et al.*, 2011). Wnt5a-induced suppression of Wnt3a signal was achievable by the membrane-bound extracellular domain of Ror2. Other structure-function relationship analysis highlights a RTK independent function for Ror2/Wnt5a mediated formation of filopodia and cell migration, while the CRD Wnt binding domain and PRD were found essential (Nishita *et al.*, 2006, 2010a). Interestingly, the RTK was required for the formation of different cell protrusions such as invadopodia (Enomoto *et al.*, 2009). In *Xenopus*, Ror2 mediated morphogenic movements rely on an active RTK function (Hikasa *et al.*, 2002; Djiane *et al.*, 2000). Even though the requirement of the RTK function of Ror2 is controversial in different cellular contexts, I demonstrated a

dependency of the kinase domain in formation of cellular protrusions and subsequent pathway activation. The dominant-negative mutant Ror2³¹ (Hikasa *et al.*, 2002), whose kinase domain contains three point-mutants that replace lysines at position 504 (in the putative ATP-binding motif), 507 and 509 with isoleucine, caused a reduction of filopodia *in vitro* and *in vivo*, reduced Wnt8/Ror2-mediated signal transduction and cytoneme-mediated Wnt8 delivery. In the context of filopodia formation, Ror2³¹ displayed a similar phenotype as the inhibition of the filopodia-machinery itself by IRSp53^{4K} with four lysine residues mutated to glutamic acid in the actin-binding sites, underlining the RTK dependency. Interestingly, Ror2 expression alone is sufficient to induce both length and number in PAC2 cells but can only regulate filopodia number *in vivo* in zebrafish.

I demonstrated that Ror2 facilitates a transduction cascade upstream of Cdc42, a relay station in the formation and maintenance of the actin scaffold, in accordance with the previous Wnt8a-cytoneme model (Stanganello *et al.*, 2015) and published evidence in *Xenopus*: PI3K, Cdc42 and JNK were described as downstream effectors of Wnt/Ror2 signaling (Schambony and Wedlich, 2007). Co-expression of Cdc42^{T17N} rescues Ror2-induced C&E alterations (Hikasa *et al.*, 2002). Thus, my analysis provides a novel link for a regulatory mechanism of cytonemes facilitated by Ror2/PCP pathway activation.

Ror2/Wnt8a binding demonstrates a novel *in vivo* signaling platform

The most prominent role of Ror2 has been attributed to its function as Wnt receptor (Green *et al.*, 2014). It is widely accepted that Ror2 binds Wnt5a to transduce a Wnt/PCP signal that requires homodimerization and autophosphorylation (Oishi *et al.*, 2003; Liu *et al.*, 2007), supported by the striking similarities of Wnt5 or Ror2 mutant mice which both exhibit craniofacial abnormalities, dwarfism, and short limbs (Ho *et al.*, 2012; Oishi *et al.*, 2003). Ror2 is composed of a extracellular Frizzled-like CRD that was reported to interact with other Wnt ligands than Wnt5a in multiple *in vitro* studies (Stricker *et al.*, 2017): Wnt1, Wnt2, Wnt3 and Wnt3A, Wnt4, Wnt5A and Wnt5B, Wnt6, Wnt7A, Wnt8, Wnt11. In contrast, data for *in vivo* interaction in a biological context is less consolidated. Wnt11 is the second-best characterized ligand for Ror2. In zebrafish, Wnt11 is a binding partner of Ror2 to modulate C&E during zebrafish gastrulation. Both, Wnt5a and Wnt11 are required in mouse for PCP-controlled C&E movement and anterior-posterior axis elongation (Andre *et al.*, 2015).

As most of the known binding partners describe non-canonical Wnt ligands, I identified the canonical Wnt8a as a potential binding partner. As the cytoneme screening approach was executed in a Wnt8a-rich environment, testing binding affinity for Wnt8a/Ror2 was obligatory. Indeed, imaging of fluorescent-tagged proteins in culture and *in vivo* revealed interaction in signaling clusters with a similar appearance as described for Wnt5/Ror2 in *Xenopus* (Wallkamm *et al.*, 2014). The very specific co-localization of these aggregates in the cell membrane and on proximal cytoneme tips suggest an implication in signal transduction as signalosomes (Hagemann *et al.*, 2014) as well as in cytonemal Wnt transport (Stanganello *et al.*, 2015). FCS can provide powerful biophysical information about the interaction of two proteins. The system was optimized for live specimens, and was previously shown to provide robust data on Wnt inhibitor Dkk1 and Dkk2 binding to Lrp6 (Dörlich *et al.*, 2015) in HEK293T cells and XWnt5A/Ror2 complexes in *Xenopus*. Similarly, free Ror2-mCherry represented an equal diffusion coefficient of $0.28 \pm 0.03 \mu\text{m}^2 \text{s}^{-1}$ as the membrane co-receptor Lrp6 (Dörlich *et al.*, 2015), which functions in a similar fashion as co-receptor for canonical Wnt signaling. I could determine a strong cross correlation with Is-FCS and thereby co-migration and binding of Wnt8/Ror2 in signal clusters but not in the residual membrane without obvious accumulation. I hypothesized that Wnt8a/Ror2 binding might be facilitated by further factors that attract nearby and free Wnt8 and Ror2 proteins as a signaling platform. This is also in line of evidence by the restricted diffusion curve I consistently measured in FCS. The correlated fitting model and the low diffusion coefficient of $0.02 \pm 0.01 \mu\text{m}^2 \text{s}^{-1}$ suggest a tight interaction in dense multi-protein networks, leading to a sterically impeded diffusion.

Indeed, in further analysis I identified a high affinity for Fzd7a to co-localize and even intensively enlarge Wnt8a/Ror2 clusters. It is debatable, whether over-expression influences their formation. However, there are several arguments that verify their authenticity in a smaller endogenous scale: First of all, *in vivo* availability and biological context of Ror2 and Fzd7a as a binding partner is given as both genes are expressed in the dorsal marginal zone organizer along with Wnt8a, enabling endogenous interaction in Wnt producing source cells during development. Second, I could prove the specific cluster potential, signal transduction by Lrp6 recruitment, and filopodia stimulating activity by using Fzd7a constructs with truncations in extracellular or intracellular domains. Similarly, Fzd7 clustering and Lrp6 polymerization is reported for Wnt5a-induced Ror2 activation in mammalian cell culture

(Nishita *et al.*, 2010b). Canonical Wnt3 triggers Dvl phosphorylation and negative Wnt/ β -catenin signaling in a Ror2-dependent response (Witte *et al.*, 2010). However, modulation of Ror2 alone in the presence of Wnt8a was sufficient to induce cluster formation and subsequent transduction, suggesting that other interaction partner such as Fzd7 are present in signaling complexes but does not seem to be rate limiting for the response if present in endogenous levels. Further signal proteins, which were not included in this work, might contribute to these signaling platforms as well. The extracellular glycoprotein protein collagen triple helix repeat containing 1 (Cthrc1) selectively stabilized Wnt/PCP receptor complexes by enhancing receptor binding and therefore signal transduction (Yamamoto *et al.*, 2008; Kelley, 2008). Additionally, Vangl2 is considered as a core PCP component (Gao *et al.*, 2011). Wnt5a interacts with Vangl2 and Wnt-induced Ror2/Vangl2 receptor complexes regulate mouse limb bud elongation (Qian *et al.*, 2007). Especially the implication of Vangl2 and its role in the control of cellular extensions is a promising factor to pursue: The axon turning event of Type II neurons depend on Vangl2 (Ghimire *et al.*, 2018). During growth cone guidance, Vangl2 is predominantly located in the membrane, on accumulations where filopodia emerge, and on filopodia tips for directional cues (Shafer *et al.*, 2011). Consistently, Vangl2 stabilizes retracting filopodia of facial branchiomotor neurons (Davey *et al.*, 2016). Taken together, active receptor complexes to stimulate cytonemes are certainly composed of multiple different factors. One of the most intriguing proteins to characterize would be Vangl2, which may add positional guidance or stabilization of cytonemes. I hypothesize that other factors and co-receptors are involved in the establishment of a signaling platform and subsequently the composition of the active complex shapes the resulting signal.

Another layer of credibility for Wnt8a/Ror2 interaction was presented by defining the Wnt-attracting CRD domain as the main binding motif. Truncated Ror2- Δ CRD-GFP was not able to establish dense signaling clusters with Wnt8a-GFP as WT-Ror2. The CRD domain was found to be fundamental in several Wnt ligand-receptor pairs. The best characterized resembles the XWnt8a/Fzd8-CRD and it appears to be a very conserved motif amongst all Wnts. X-ray structure analysis demonstrated the Wnt-thumb interplay with the hydrophobic groove of the CRD (Janda *et al.*, 2012). Similarly, the CRD was found vital for Wnt5a binding causing homodimerization and autophosphorylation (Oishi *et al.*, 2003; Liu *et al.*, 2007). Another CRD-containing protein family capable of interacting with Wnt ligands and Ror2 are sFRPs. They were described as Wnt inhibitors (Cruciat and Niehrs, 2013), but novel insight revealed a more specific task as a molecular switch to redirect distinct non-canonical

signaling branches by stabilizing Ror2 complexes and blocking Fzd7 endocytosis (Brinkmann *et al.*, 2016). In *Xenopus*, Fzd7-mediated PCP leads to RhoA and Rac1 activation while sFRP2 potentiates Wnt5a/Ror2 activation that transduces a signal via Cdc42. SFRPs such as Tlc are present at the animal pole during zebrafish gastrulation (Lu *et al.*, 2011), this postulated modulation of Wnt/PCP signaling branches might indeed affect prioritizing Cdc42-mediated Ror2 signaling to facilitate Wnt-cytoskeleton transport.

Ror2/Wnt8a interaction transduces a non-canonical and cytoskeleton-stimulating signal

I demonstrated Wnt8a/Ror2 binding via its CRD. There is a recruitment of several Wnt/PCP components to establish large signaling clusters, however, the requirement for other receptors and the subsequent change in signaling is unclear. Additionally, *Xenopus* Wnt8 was found in physical interaction with the ectodomain of Ror2 (Hikasa *et al.*, 2002) but it is not known whether XWnt8 induces Ror2 signaling. Binding of Wnt ligands to their cognate receptors induces a canonical or non-canonical signal response dependent on the ligand and receptor composition (Niehrs, 2012). According to the conventional classification, Wnt1, Wnt3a, and Wnt8a belong to the β -catenin dependent Wnt signaling proteins, whereas Wnt5a and Wnt11 are representatives of the β -catenin independent Wnt signaling proteins (Kikuchi *et al.*, 2011). In addition, both distinct signaling branches act in a competing and mutually repressive state by inhibition of pathway components but also by the requirement of shared rate-limiting hub proteins (Niehrs, 2012; van Amerongen and Nusse, 2009). For example, it is well established that Wnt5a/Ror2 signaling activates JNK to inhibit β -catenin-mediated TCF/LEF gene expression (Mikels and Nusse, 2006). Furthermore, Wnt5a competes with Wnt3a for the Wnt receptor Fzd2 resulting in β -catenin repression in mammalian cell culture (Sato *et al.*, 2010). In tissue culture, intracellular Ror2 signaling represses β -catenin signaling via its tyrosine kinase activity (Mikels and Nusse, 2006) and interaction with the shared effector protein Dvl (Witte *et al.*, 2010). However, depending on the appropriate receptor composition, the non-canonical ligand Wnt5a is able to activate β -catenin target genes as shown in presence of LRP5 and mFz4 (Mikels and Nusse, 2006).

Binding of zebrafish Wnt8a to Ror2 *in vivo* is a novel functional interaction, and the downstream transduction cascade of the canonical-associated Wnt8a with a Wnt/PCP receptor is unknown. My data presents evidence of a signal transduction in a non-canonical

β -catenin independent manner. I demonstrated a synergistic regulatory effect of morphogenic movements and cell shapes during C&E in zebrafish gastrulation and an RTK-domain dependent activation of ATF2 target genes in *Xenopus*. Interestingly, Wnt8a alone induces C&E defects, suggesting a non-canonical function itself in the presence of the respective endogenous receptors. Similarly, reports in *Hydra* postulated a non-canonical function of *hvWnt8* in initiation and maintenance of bud and tentacle evagination (Philipp *et al.*, 2008). In this context, *hvWnt8*, Fz2 and Dvl stimulate a JNK-mediated pathway. As Wnts are evolutionary conserved, the non-canonical aspect for Wnt8a might be a poorly explored subject that contributes to the magnificent complexity of Wnt pathways.

I further provide evidence that Ror2/PCP-dependent signaling is crucial for cytoneme emergence in Wnt source cells. The three-fold expansion of filopodia occurrence between 4 to 7 hpf during gastrulation highly correlates with the expression onset of several Wnt genes (Lu *et al.*, 2011) and *ror2* (Young *et al.*, 2014). I can show that Ror2 function regulates filopodia number and modulates specifically Wnt8a-GFP cytoneme emergence in dependency of the RTK-domain. The accepted view on cytoneme formation follows the rules of filopodia extension activation of the N-WASP nucleation complex activated by RhoGTPases such as Cdc42, Rac1 or RhoD (Ho *et al.*, 2004; Faix and Rottner, 2006; Stanganello *et al.*, 2015). Subsequently, actin polymerization stimulators such as the Arp2/3 and Ena/VASP complex as well as actin bundling mediated by fascin1 (FSCN1) facilitate the extension of the protrusion. In line with the common model, Ror2 act upstream of the established and inherent actin-machinery to stimulate cytonemes. I provided live data of Wnt8/Ror2 membrane-complexes to facilitate cytoneme formation and maintaining the signal complex on its tip during elongation and target finding. I hypothesize, the same cluster activating the cytoneme machinery is loaded onto the distal cytoneme tip. Thereby, Ror2 would additionally provide directional advice. Consistently, Ror2 was shown to mediate polarization by Wnt5a-induced JNK activation and association with FLNa and aPKC during wound healing of fibroblasts (Nomachi *et al.*, 2008). In *Caenorhabditis elegans*, the axonal projections of neurons respond to Wnt to refine the axial patterning. Remarkably, the Ror family receptor CAM-1 modulates the location of the response and thereby directs patterning (Modzelewska *et al.*, 2013).

My dynamic live data also illustrates Lrp6-signalosome formation in response to Wnt cytoneme contact as previously published (Stanganello *et al.*, 2015), but also the intracellular

uptake of the Wnt ligand. Internalization of the Wnt/receptor complex is a fundamental aspect of Wnt signaling (Kikuchi *et al.*, 2011). The clathrin-dependent transport of ligand to the lysosome is an established route that may attenuate and regulate the response by degradation of an active receptor complex. Endocytosis in the *Drosophila* embryonic epidermis is required for refining the range of Wg signaling and compromising the endocytic pathway causes elevated signaling and distorted epidermal fate (Dubois *et al.*, 2001).

My data highlights a Ror2-accompanied Wnt8a transport from the sending cell up to mutual internalization by the target cell. However, after endocytosis Ror2 and Wnt8a diverge within the first minute of the endocytic route. It was postulated that the ligand-receptor complex and the signal-transmitting transducer complex take separate endocytic routes following endocytosis. While, the Wnt/Fzd/Lrp6 complex takes a Rab-mediated path to degradation and recycling, the transducer-complex is maintained (Hagemann *et al.*, 2014). Similarly, Ror2 and Wnt8a may take different parts in cell response post-internalization. In fact, in the context of a β -catenin response, it is a necessity to separate Ror2 from the other signalosome components. The PCP stimulating effect of Ror2 would counteract the Wnt/ β -catenin activation. However, no Wnt/ β -catenin inhibition by Ror2/PCP was observed, indicating a sorting mechanism or a competence of the responding cell to interpret the delivered signal.

The suggested role of Ror2 in cytoneme regulation was discovered for the ligand-delivery function in the sending cell. In several vertebrate tissues, cytonemes formed by responding cells were described, thereby expanding the possible distance of morphogen transport. Shh and co-receptors Cdo and Boc containing cytonemes in the chicken limb bud can reach up to 150 μm from both sides to cover a morphogenic range of almost 300 μm (Sanders *et al.*, 2013)sanders. If receiving cytonemes play a vital function in neuroectodermal Wnt8a patterning it is not yet consolidated but might increase Wnt spreading or sharpen the gradient by supporting target finding. The molecular mechanism of receiving signaling filopodia is still unknown and whether the same actin machinery regulates this process in a similar fashion. *Ror2* spikes in expression in signal responding neuroectodermal tissue and remains highly expressed in the CNS (Young *et al.*, 2014; Bai *et al.*, 2014) and could potentially navigate a retrograde cytoneme response.

Intermingling of Wnt signaling pathways for β -catenin transmission

The strict separation of sending and receiving population is an essential aspect in investigating paracrine signal transport, as a ubiquitous altered gene expression might interfere with the transport machinery of the source but can also cause an unintentional signal response in target cells. Particularly, as Ror2 acts mutually antagonistic to β -catenin signaling (Oishi *et al.*, 2003; Mikels and Nusse, 2006), sending and responding population must be evaluated individually. I observed collectively Wnt/PCP activation, β -catenin activation, or inhibition in ubiquitous presence of Ror2 and Wnt8a. The joint expression of marker and target genes is explained by intermingling of the respective Wnt signaling branches. As reported, the availability and composition of receptors specifies the signal (Henry *et al.*, 2014; Mikels and Nusse, 2006). Remarkably, I can demonstrate Wnt cytonemes depend on an autocrine Ror2/PCP transduction in the source cell. Indeed, the target gene expression of cells responding to Wnt can be modified concretely by adjusting Ror2 levels only in the source cells in tissue culture and in a zebrafish. Impairing Ror2 function compromises paracrine Wnt/ β -catenin activation, without alteration of Wnt ligand availability.

I postulate autocrine Ror2/PCP activation disseminates Wnt to transduce a Wnt/ β -catenin response in adjacent cells. This was presented for Wnt8a as promoting both autocrine Wnt8a/Ror2 and paracrine Wnt8a/Lrp6 transduction depending on the cellular context. Thus, the same morphogen controls its own dissemination, which could be a novel positive feedback mechanism for the producing cell to sense the morphogen levels and adjust the trafficking response accordingly.

Remarkably, the tight interplay of mutual repressing Wnt signaling pathways demonstrates the requirement to separately investigate the sending and the responding population and highlights new principles in paracrine signal transmission. Cytonemal Wnt transport transduces a β -catenin response in cells contacted by Wnt containing cytonemes. By adjusting the Ror2 levels in the Wnt source, the transferred β -catenin signal can be transformed without disrupting the signal itself (Figure 35).

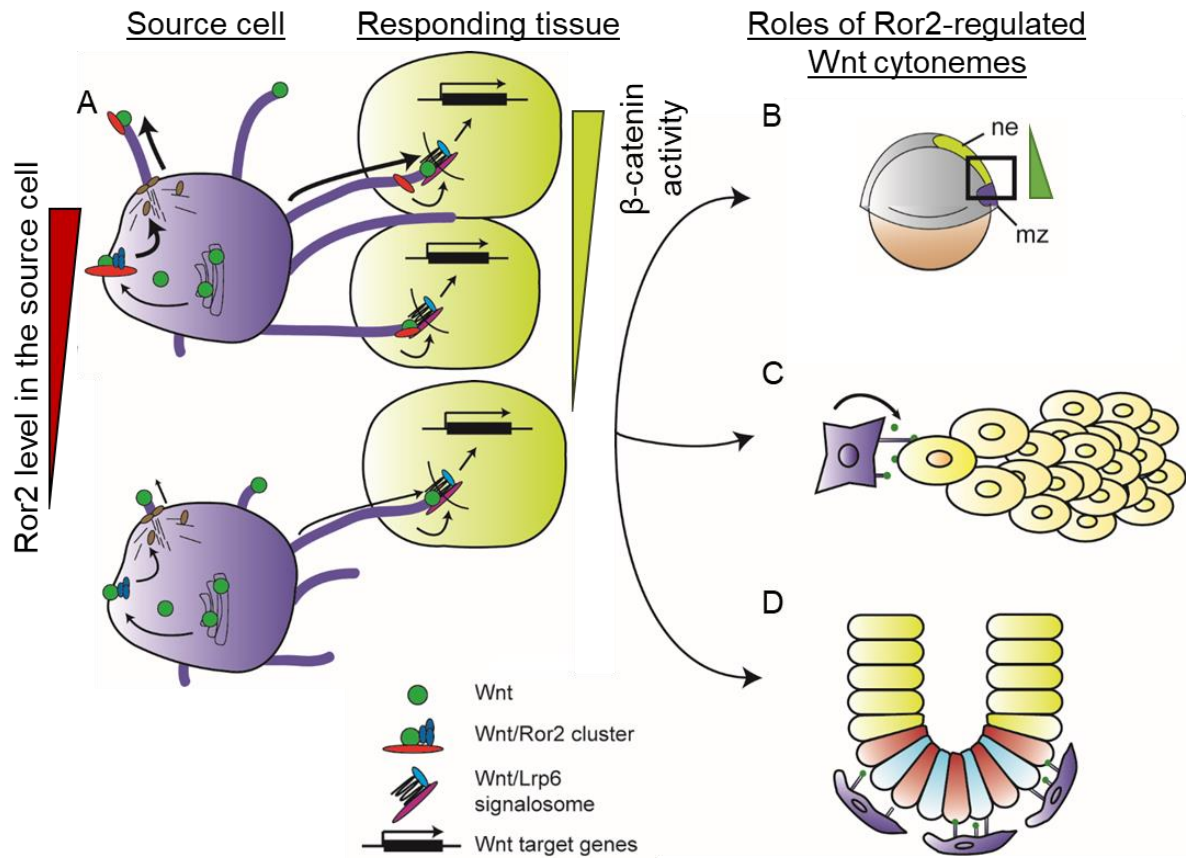


Figure 35: The influence of Ror2 levels on paracrine Wnt/ β -catenin distribution and my presented applications for Wnt cytoneme transport. (A) Autocrine ror2/PCP activation in the Wnt-producing source cell promotes cytoneme formation. Wnt cytonemes transmit a paracrine Wnt/ β -catenin response to neighboring cells. A Ror2-regulated cytoneme model is suggested to play a role in (A) neuroectoderm patterning in zebrafish, (B) gastric cancer proliferation, and (C) intestinal crypt homeostasis represented by *ex vivo* crypt organoid survival.

Cytonemes operate in tissue homeostasis and disease

I provide a profound explanation about autocrine Wnt/Ror2 stimulation that results in Wnt spreading and adjoining β -catenin activation. In this work, I was extensively investigating Ror2-mediated morphogen distribution in the context of zebrafish development and in diverse tissue culture systems.

However, there is also evidence for a more general function of Ror2 in paracrine signal transmission. Ror2 exhibits tumor-promoting activities in several tumor types (Morioka *et al.*, 2009; Enomoto *et al.*, 2009; Wright *et al.*, 2009; O’Connell *et al.*, 2010). Most relate to Wnt5-mediated Ror2 activation, but Ror2 was also found to regulate β -catenin dependent signaling in breast cancer (Henry *et al.*, 2014). Additionally, Wnt-Ror2 positive

mesenchymal cells promote gastric cancer cell proliferation if co-cultivated (Takiguchi *et al.*, 2015). Consistently to that observation, Ror2-mediated cytonemal Wnt distribution might explain the tumor-promoting ability. I demonstrated a Ror2-mediated Wnt delivery in gastric cancer cells promotes cell proliferation. The stimulated proliferative potential was filopodia-dependent and Wnt-mediated. Remarkably, the response was achieved by only modulating the inherent cytoneme machinery to distribute endogenous Wnt. I cannot exclude that other morphogens or growth stimulating factors benefits from the Ror2-transport system, but abrogation of Wnt signaling by the Wnt inhibitor IWR (Huang *et al.*, 2009) implies a Wnt-dependent effect. In accordance to the presented proliferative capabilities, AGS cells express Wnt ligands such as Wnt1 and display a high endogenous β -catenin level (Mao *et al.*, 2014) and are able to autonomously respond to PCP signaling via Ror2 causing reduced β -catenin signaling and proliferation (Yan *et al.*, 2016).

Targeting Wnt/ β -catenin signaling by Wnt-interfering molecules is a common thought in clinical cancer therapy (Nusse and Clevers, 2017). The antitumor agent Salinomycin significantly reduces proliferation and subsequently gastric tumor size by suppression of Wnt1 and β -catenin expression *in vivo* (Mao *et al.*, 2014). Several cancers result from β -catenin or APC mutations and would not respond to Wnt pathway-affecting drugs. Even though their Wnt level is rigid, it is reported that the outgrowth of metastatic lesions and cancer stem cells is still mediated by Wnt itself. Porcupine-targeting drugs such as IWP2, C59, and LGK974 were found promising to circumvent the source-cell Wnt level and focus on the delivery itself (Nusse and Clevers, 2017). In fact, beneficial effects by blocking Wnt maturation and secretion were reported in mouse resulting in a reduction of tumors growth (Madan and Virshup, 2015; Tammela *et al.*, 2017). My approach shares similarities in terms of only disrupting the transfer path of Wnts: Delivery from the area of production is impeded without influencing the endogenous amount of ligand or the source itself. Disabling the cytoneme machinery influences gastric cancer cell growth. Reduction of cytoneme-mediated Wnt transport could be used as a further strategy to inhibit uncontrolled Wnt spreading and proliferation in tumor therapy.

Uncontrolled cell proliferation and tumorigenesis can result in malfunction of accurate tissue homeostasis. As Wnt signaling is implicated in homeostasis and the control of stem cell proliferation and renewal (Logan and Nusse, 2004), I wondered whether the cytoneme model might act in a stem cell niche. Homeostasis in the intestinal crypts requires Wnts to

cooperate continuous maintenance (Beumer and Clevers, 2016; Kuhnert *et al.*, 2004; Pinto *et al.*, 2003; Sailaja *et al.*, 2016). Multiple studies suggested that the stromal compartment could be required, which serve as an essential source for signals including Wnt2b, Wnt5a, Rspo1, and Rspo3 (Aoki *et al.*, 2016). The intestinal stromal compartment consists of a composition of cell types such as hematopoietic cells, fibroblasts, fibrocytes, myofibroblasts, and neural and glial cells (Mifflin *et al.*, 2011). However, if these Wnts are required for crypt maintenance, and how they could be secreted across the basement membrane to reach the stem cells, is controversially discussed. My data show that the protrusions of cultured subepithelial crypt myofibroblasts, a subpopulation of stroma cells, respond to the alteration in Ror2 levels. Furthermore, I provide evidence of an *ex vivo* stem cell organoid system, where growth and survival are maintained by the cytoneme-mediated Wnt supply of isolated crypt myofibroblasts. Remarkably, this setup resembles the intestinal crypt, where *lgr5*-expressing intestinal stem cells rely on Wnt proteins from a source. PORCN^{-/-} deficient crypt cells require Wnt supply from the co-culture myofibroblasts as their individual Wnt machinery is disrupted. I correlate the decrease in Wnt transmission to the reduction in Wnt cytonemes in myofibroblast by loss of Ror2, as previously shown in HEK and AGS cells.

In accordance with my data, it was recently reported that *pdgfra*-positive myofibroblasts are an essential source of both Wnts and RSPO3 in the mouse intestinal crypt (Greicius *et al.*, 2018). It was suggested that these stromal cells transmit Wnts to the epithelial stem cells (Kabiri *et al.*, 2014; Valenta *et al.*, 2016), but the operating principle is not clear. The cytoneme model covers the link between the protrusion-rich stromal cells and the transmission of Wnt signals for homeostasis in the stem cell niche.

Pdgfra-expressing cells are also found to be involved in several other processes and tissues such as in the mesenchyme of lung, gut, and kidney as well as in glial and adipocyte precursors (Roesch *et al.*, 2008; Hoch and Soriano, 2003; Festa *et al.*, 2011). It would be a fascinating to investigate, whether this subpopulation of cells is predestined for a cytoneme-mediated signal transfer and if this presents a general mechanism for tissue dynamics.

Conclusion

Formation of cytoneme-mediated Wnt transport was initially discovered as an essential process during zebrafish neural plate patterning and refined by examination of the cellular response of Ror2 in the Wnt8a producing source. However, my latter observations in cancer proliferation and stem cell homeostasis suggest a more versatile remit for cytonemes (Figure 35). Ligand transfer by cytonemes might be a general mode for Wnt and similar

signaling molecules in vertebrates, in particular for membrane-associated signals such as Shh. I would expect to find a conserved mechanism to promote the formation of respective cytonemes by an autocrine cell response of the ligand. Cytoneme could have a general function in cell types with a profound tendency to form a large quantity of cell protrusions, or in systems where a distinct gap must be overcome to specifically deliver a signal in a controlled manner. The identification of the *pdgfra*-myofibroblasts in the intestine crypt maintenance demonstrates a mechanism of Wnt cytonemes beyond development and will be intriguing to observe whether cytonemes play a relevant role in other tissues where these cells exist. Additionally, disabling the cytoneme machinery influences gastric cancer growth. Even though the approach to impede Wnt distribution is not completely new in cancer therapy, it might be a novel concept to restrict only the transport machinery. My approach shares similarities in terms of only disrupting the transfer path for Wnts: Delivery from the area of production is impeded without influencing the endogenous amount of ligand or the source itself, thereby eliminating potential side effects as healthy Wnt levels might not be affected. Thus, reduction of cytoneme-mediated Wnt transport could be used as a further strategy to inhibit uncontrolled Wnt spreading and proliferation in tumor therapy. Undoubtedly, a wider range of cytoneme mediated processes in development, cancer, and homeostasis are going to be discovered soon and it will be interesting whether the inherent regulatory mechanisms is conserved throughout the different systems.

5. Appendix

Table 1: PAC2 cDNA library screening result for average length of filopodia. n filopodia were measured.

Gene	length	SEM	n
CCRK	11,79	1,03	303
IRAK4	11,19	0,81	419
STRADA	10,67	0,94	258
HCKID	10,03	0,72	474
Novel gene	9,73	0,55	411
TRPM2	9,36	0,73	466
TRIO	9,12	0,63	447
MAPK13	9,04	0,44	530
PKN2	9,03	0,78	511
ULK3	8,90	0,64	526
EPHB2	8,76	0,47	342
STK 25	8,70	0,75	233
MAP2K4	8,59	0,50	517
CDC7	8,56	0,62	384
RAF1	8,55	0,60	406
DAPK2	8,55	0,52	631
Novel gene	8,51	0,85	298
PRKCI	8,48	0,50	682
HSPB8	8,46	0,47	508
RING3 protein	8,44	0,72	284
PKN1	8,41	0,43	729
MAP3K7	8,39	0,58	312
AURKC	8,32	0,68	410
PRKCZ	8,30	0,65	323
SGK2	8,30	0,51	421
VRK1	8,28	0,47	488
CLK2	8,24	0,61	432
SCYL3	8,23	0,60	460
TLK1	8,10	0,76	199
PRKCZ	8,10	0,69	270
ROCK2	7,95	0,47	542
ULK2	7,90	0,58	311
PRPF19	7,73	0,64	377
KALRN	7,62	0,38	307
RIOK3	7,58	0,49	551
Novel gene	7,57	0,56	404
Unknown	7,56	0,42	615
MAPK10	7,54	0,46	433
EPHB3, TYRO6	7,53	0,48	293
Novel gene	7,53	0,52	331

PRPF4B	7,43	0,51	306
TEC	7,42	0,47	465
Novel gene	7,42	0,51	450
ICK	7,42	0,50	554
BMPR2	7,37	0,43	364
PDK2	7,37	0,44	758
PALLD	7,30	0,58	299
Unknown	7,27	0,60	442
Unknown	7,21	0,52	384
CHEK1	7,19	0,44	367
Unknown	7,17	0,41	398
CABC1	7,15	0,79	350
CDC2_ORYLA	7,13	0,41	479
EEF2K	7,10	0,56	395
CDK4	7,08	0,29	484
Unknown	7,06	0,65	205
MYO1C	7,06	0,54	154
Novel gene	7,04	0,40	456
AURKC	7,04	0,80	202
BUB1	7,03	0,43	411
Unknown	6,97	0,54	370
Novel gene	6,92	0,52	413
CDK7	6,88	0,41	470
CHEK1	6,85	0,54	410
CSK	6,81	0,74	257
CDK9	6,78	0,71	407
RIOK3	6,75	0,62	87
BAZ1A	6,75	0,61	335
Novel gene	6,74	0,60	303
GSK3A	6,74	0,58	314
MAP2K6	6,73	0,43	334
BCKDK	6,73	0,50	385
SLK	6,72	0,49	434
MAP3K7	6,71	0,45	391
CAMK2G	6,71	0,51	321
SKR3, ALK-1	6,70	0,38	625
CSNK1E	6,70	0,38	338
TRIM33	6,68	0,39	516
ADCK1	6,65	0,44	424
SRPK1	6,65	0,48	263
YES1	6,64	0,49	504
DAPK3	6,62	0,32	390
Novel gene	6,60	0,31	506
STRADA	6,60	0,54	341

Unknown	6,59	0,54	299
VRK2	6,58	0,44	299
SPCS2	6,57	0,41	549
CDK6	6,56	0,45	397
SCFR, c-kit	6,56	0,52	268
PRKAA1	6,54	0,58	337
PIM3	6,50	0,39	327
Fibroblast growth factor receptor (Fragment)	6,47	0,35	814
ZMYND8	6,47	0,48	344
Unknown	6,43	0,47	379
EPHA2	6,43	0,35	457
CDK2	6,41	0,44	353
TRIB2	6,41	0,44	411
CDK10	6,40	0,52	286
ACVR2B	6,39	0,44	370
ADCK1	6,39	0,50	402
CHUK	6,37	0,31	419
Novel gene	6,35	0,44	554
Membrane guanylyl cyclase	6,22	0,37	594
MAPK12	6,22	0,47	395
Novel gene	6,22	0,42	431
RPS6KB1	6,20	0,58	279
Unknown	6,20	0,41	603
Novel gene	6,17	0,45	397
Novel gene	6,16	0,49	517
CSNK2A2	6,14	0,33	463
SNRK	6,13	0,40	233
PXK	6,13	0,45	458
RIPK2	6,13	0,47	255
FER	6,13	0,49	304
Membrane guanylyl cyclase	6,13	0,35	352
CSNK2A1	6,12	0,41	452
ERN1	6,05	0,21	941
TYRO3	6,05	0,43	287
CDK5	6,05	0,30	572
ABR	6,04	0,48	296
MYOM1	6,04	0,45	257
BRSK2	6,03	0,39	286
MAP4K4	6,00	0,62	311
GSK3A	6,00	0,34	396
ADCK4	5,99	0,53	299
SCFR, c-kit	5,97	0,44	397
HSPB1	5,97	0,33	496
EPHB3	5,97	0,35	388

aPKC	5,96	0,28	563
PLK1	5,96	0,44	391
Novel gene	5,96	0,48	317
EIF2AK1	5,95	0,49	330
PLK4	5,95	0,46	286
ROCK2	5,93	0,41	301
JAK1	5,92	0,22	771
MAPK12	5,88	0,51	259
ERN2	5,88	0,41	480
BMPR2	5,84	0,48	312
MOK, RAGE	5,84	0,40	469
RAF1	5,84	0,56	325
CASK	5,81	0,31	370
ILK	5,81	0,49	297
ABR	5,80	0,44	310
PAK2	5,79	0,59	312
PIK3C2B	5,78	0,46	324
CDK6	5,78	0,48	314
MAP4K4	5,75	0,38	419
MAP3K7	5,75	0,36	659
TRPM1	5,72	0,36	365
Unknown	5,69	0,41	235
PTK7, CCK4	5,68	0,47	274
MKNK1	5,67	0,39	263
MAP2K1	5,66	0,40	278
Novel gene	5,63	0,26	845
Novel gene	5,61	0,34	395
RIOK1	5,61	0,27	475
BRSK2	5,60	0,38	541
ANKHD1	5,60	0,36	372
INSR	5,56	0,38	400
GRK4	5,56	0,34	378
Unknown	5,56	0,34	424
CAMK2G	5,55	0,31	514
Novel gene	5,52	0,36	451
MASTL	5,46	0,30	598
MAPK3	5,45	0,29	454
PKN2	5,44	0,29	374
PXK	5,41	0,26	534
MAPK8	5,40	0,36	449
RIPK1	5,39	0,35	487
Novel gene	5,39	0,34	235
TTK	5,38	0,26	612
MAPK6	5,37	0,26	513

PIK3R4	5,36	0,67	207
CASK	5,35	0,36	333
MAPK9	5,35	0,34	339
CHUK	5,34	0,32	347
CSNK1E	5,32	0,30	422
MELK	5,31	0,31	329
PSKH1	5,29	0,30	500
NRBP1	5,27	0,29	453
Novel gene	5,24	0,45	353
CAMK2G	5,20	0,26	456
PLK1	5,18	0,31	346
PSKH1	5,16	0,29	549
Unknown	5,09	0,29	417
DAPK2	5,05	0,41	512
Unknown	5,04	0,21	566
AKT1	5,02	0,32	442
ACVR2B	5,01	0,43	280
CABC1	5,00	0,46	288
RING3 protein	4,96	0,24	636
ARAF	4,94	0,26	374
PAK4	4,92	0,37	411
MARK1	4,92	0,36	423
PTK7	4,87	0,28	388
Unknown	4,87	0,30	302
PRKAA1	4,87	0,22	422
Unknown	4,85	0,27	351
Unknown	4,85	0,23	556
Unknown	4,84	0,25	415
HUNK	4,84	0,35	395
PRKD3	4,82	0,17	534
HARS2	4,82	0,17	534
TLK1	4,81	0,19	435
MAP2K4	4,74	0,32	241
TGFBR1, ALK-5, SKR4	4,73	0,23	475
MAP4K5	4,71	0,24	399
TRIM71	4,71	0,29	422
CDK9	4,69	0,20	487
GRK4	4,69	0,27	393
RAGE	4,68	0,27	427
STK38	4,65	0,28	414
Unknown	4,63	0,30	533
RIPK4	4,63	0,36	319
Unknown	4,50	0,33	294
CASK	4,48	0,39	290

PIM1	4,48	0,29	319
MAP3K4	4,47	0,27	343
CCT8	4,45	0,39	188
Unknown	4,45	0,26	362
PIK3R4	4,40	0,25	421
ROR1	4,32	0,34	319
Unknown	4,20	0,27	411
FYN	4,07	0,37	320
MARK1	3,94	0,25	290

Table 2: PAC2 cDNA library screening result for average number of filopodia. n cells were counted.

Gene	number	SEM	n
Unknown	46,4	5,5	13
Unknown	41,0	2,8	15
Novel gene	40,2	3,3	21
Unknown	39,7	3,1	14
Novel gene	39,5	5,7	10
PKN2	39,3	5,8	13
PTK7	38,8	4,4	10
ROCK2	38,7	2,5	14
PXK	38,2	2,1	12
Unknown	37,8	3,2	10
ERN1	37,6	2,9	25
Novel gene	37,6	4,5	12
Unknown	37,4	4,9	11
ANKHD1	37,2	2,7	10
Fibroblast growth factor receptor (Fragment)	37,0	2,7	22
ICK	36,9	3,5	15
ERN2	36,9	3,7	13
SKR3, ALK-1	36,8	3,2	17
PSKH1	36,6	2,5	15
DAPK2	36,6	1,6	14
ADCK1	36,6	3,1	11
MAP4K5	36,6	3,7	11
PKN1	36,5	2,6	20
CDK7	36,2	3,5	13
Novel gene	36,1	2,4	14
BRSK2	36,1	2,9	15
GSK3A	36,0	3,0	11
MAPK12	35,9	4,6	11
RAGE	35,6	3,3	12
PLK1	35,6	4,2	11
Unknown	35,5	3,7	15

Unknown	35,3	4,1	12
PRKAA1	35,2	2,4	12
Novel gene	35,1	3,6	13
PIK3R4	35,1	3,3	12
Membrane guanylyl cyclase	34,9	2,9	17
MAPK3	34,9	3,0	13
CDC7	34,9	2,8	11
Unknown	34,9	4,3	11
NRBP1	34,9	2,8	13
CDK9	34,8	3,1	14
RIPK1	34,8	2,6	14
PLK1	34,6	2,7	10
JAK1	34,6	2,7	22
CDK4	34,6	2,7	14
STK38	34,5	2,8	12
PDK2	34,5	2,5	22
TRIO	34,4	2,6	13
MAPK8	34,3	2,6	13
PAK4	34,3	4,0	12
MAPK6	34,2	2,3	15
CHEK1	34,2	3,1	12
PKN2	34,0	3,5	11
MAPK9	33,9	3,7	10
CDK5	33,7	2,4	17
CASK	33,6	4,2	11
Unknown	33,6	3,5	11
YES1	33,6	4,1	15
TLK1	33,5	2,5	13
HARS2	33,4	2,3	16
PXK	33,4	2,7	16
PSKH1	33,3	2,6	15
CASK	33,3	3,5	10
Unknown	33,3	2,8	17
TEC	33,2	3,0	14
SPCS2	33,1	2,6	17
SCFR, c-kit	33,1	3,8	12
EIF2AK1	33,0	3,6	10
MAP3K7	33,0	2,0	20
HUNK	32,9	2,5	12
SCYL3	32,9	2,3	14
EPHA2	32,6	4,5	14
VRK1	32,5	2,9	16
RAF1	32,5	3,2	10
PRKCI	32,5	2,2	21

CSNK1E	32,5	2,2	13
RIOK3	32,4	2,5	17
EPHB3	32,3	3,3	12
Novel gene	32,1	3,6	14
CAMK2G	32,1	2,3	16
CDK2	32,1	2,7	11
Unknown	31,9	2,8	11
CABC1	31,8	3,5	11
Novel gene	31,8	2,8	13
Novel gene	31,7	5,7	10
TGFBR1, ALK-5, SKR4	31,7	2,0	15
BUB1	31,6	2,7	13
TRIB2	31,6	2,8	13
Unknown	31,6	2,8	14
AURKC	31,5	3,1	13
MASTL	31,5	2,0	19
PRPF19	31,4	2,8	12
ZMYND8	31,3	2,7	11
RAF1	31,2	2,0	13
PAK2	31,2	2,5	10
MAP4K4	31,1	2,8	10
TRPM2	31,1	2,4	15
ABR	31,0	2,3	10
SLK	31,0	3,1	14
PTK7, CCK4	30,9	2,9	17
MAPK10	30,9	2,4	14
CSNK2A2	30,9	2,7	15
CSNK1E	30,7	3,8	11
PRPF4B	30,6	2,3	10
TTK	30,6	1,7	20
Novel gene	30,4	3,0	17
EEF2K	30,4	2,2	13
MAP2K6	30,4	4,4	11
RING3 protein	30,3	2,2	21
ADCK1	30,3	3,0	14
Novel gene	30,1	2,7	11
DAPK3	30,0	3,7	13
MAP4K4	29,9	2,7	14
VRK2	29,9	2,8	10
Novel gene	29,8	4,1	10
Unknown	29,8	2,5	14
PIM3	29,7	3,3	11
RIOK1	29,7	2,7	16
ABR	29,6	3,8	10

AKT1	29,5	2,8	15
Novel gene	29,4	1,9	12
PRKCZ	29,4	2,7	11
Membrane guanylyl cyclase	29,3	2,6	12
CAMK2G	29,2	3,5	11
ROR1	29,1	3,1	11
GRK4	29,1	2,8	13
PIM1	29,0	2,8	11
RIPK4	29,0	3,1	11
CHUK	28,9	3,7	12
PRKD3	28,8	2,1	13
Novel gene	28,7	2,7	15
TRIM33	28,7	2,6	18
CDK10	28,6	2,7	10
EPHB2	28,5	2,2	12
Unknown	28,4	2,9	14
RING3 protein	28,4	4,9	10
Novel gene	28,4	2,6	14
CDK6	28,4	3,3	14
ULK2	28,3	2,2	11
MARK1	28,2	2,5	15
CDC2_ORYLA	28,2	2,3	17
TRPM1	28,1	3,7	13
CLK2	28,0	2,4	14
RIOK3	27,9	1,9	14
MAP3K7	27,9	3,5	14
BAZ1A	27,9	2,5	12
Unknown	27,9	3,0	13
MAP2K1	27,8	2,2	10
Unknown	27,7	2,3	15
MOK, RAGE	27,6	4,5	17
Unknown	27,5	2,5	11
MELK	27,4	4,1	12
ROCK2	27,4	2,4	11
ADCK4	27,2	3,8	11
PALLD	27,2	3,3	11
Unknown	27,2	3,1	11
CDK9	27,1	3,0	15
ULK3	27,1	3,0	15
ILK	27,0	3,0	11
PRKCZ	27,0	2,4	10
ARAF	26,7	3,5	14
INSR	26,7	1,7	15
CSNK2A1	26,6	2,4	17

ACVR2B	26,4	1,7	14
MAP3K4	26,4	4,1	13
CHEK1	26,4	2,1	14
MARK1	26,4	2,6	11
CASK	26,4	2,8	11
HCKID	26,3	2,9	18
DAPK2	26,3	2,0	24
STRADA	26,2	2,0	13
GRK4	26,2	2,3	15
CHUK	26,2	2,8	16
CABC1	26,2	1,9	11
GSK3A	26,2	2,1	12
CDK6	26,2	2,0	12
TYRO3	26,1	2,5	11
PLK4	26,0	1,8	11
BRSK2	26,0	2,5	11
FYN	26,0	2,7	12
MAPK12	25,9	2,9	10
MYOM1	25,7	2,8	10
KALRN	25,5	3,4	12
ACVR2B	25,5	2,6	11
RPS6KB1	25,4	2,0	11
Novel gene	25,3	2,5	12
Novel gene	25,2	1,5	22
PIK3C2B	24,9	1,8	13
HSPB1	24,9	1,8	20
MYO1C	24,6	2,9	10
Unknown	24,5	2,8	12
EPHB3, TYRO6	24,4	1,6	12
HSPB8	24,2	1,4	21
Novel gene	24,2	1,9	17
MAPK13	24,1	2,3	22
MKNK1	23,9	3,0	11
TRIM71	23,4	2,2	18
SGK2	23,4	1,5	18
FER	23,4	1,9	13
CSK	23,4	2,9	11
IRAK4	22,9	2,6	17
BMPR2	22,8	1,8	21
BCKDK	22,7	2,2	17
MAP2K4	22,3	1,6	21
BMPR2	22,3	1,4	14
SRPK1	21,9	2,5	12
MAP2K4	21,9	2,8	11

aPKC	21,7	1,6	26
CCRK	21,6	1,8	14
Novel gene	21,4	1,3	11
STK 25	21,2	2,8	11
SNRK	21,2	2,4	11
PRKAA1	21,1	2,0	16
MAP3K7	20,8	1,9	15
PIK3R4	20,7	3,4	10
SCFR, c-kit	20,6	1,8	13
AURKC	20,2	2,4	10
TLK1	19,9	1,9	10
RIPK2	19,6	1,8	13
CAMK2G	19,0	1,4	24
CCT8	18,8	2,0	10
Unknown	18,6	2,4	11
STRADA	18,5	2,1	14
Novel gene	18,1	2,0	21
Unknown	16,8	1,7	14

6. References

- Abounit, S., and C. Zurzolo. 2012. Wiring through tunneling nanotubes - from electrical signals to organelle transfer. *J. Cell Sci.* 125:1089–1098. doi:10.1242/jcs.083279.
- Adler, P.N. 2002. Planar signaling and morphogenesis in *Drosophila*. *Dev. Cell.* 2:525–535.
- Albadri, S., F. Del Bene, and C. Revenu. 2017. Genome editing using CRISPR/Cas9-based knock-in approaches in zebrafish. *Methods.* 121–122:77–85. doi:10.1016/j.ymeth.2017.03.005.
- Alexandre, C., A. Baena-Lopez, and J.-P. Vincent. 2014. Patterning and growth control by membrane-tethered Wntless. *Nature.* 505:180–185. doi:10.1038/nature12879.
- van Amerongen, R., and R. Nusse. 2009. Towards an integrated view of Wnt signaling in development. *Development.* 136:3205–3214. doi:10.1242/dev.033910.
- Andre, P., H. Song, W. Kim, A. Kispert, and Y. Yang. 2015. Wnt5a and Wnt11 regulate mammalian anterior-posterior axis elongation. *Development.* 142:1516–1527. doi:10.1242/dev.119065.
- Angers, S., and R.T. Moon. 2009. Proximal events in Wnt signal transduction. *Nat. Rev. Mol. Cell Biol.* 10:468–77. doi:10.1038/nrm2717.
- Aoki, R., M. Shoshkes-Carmel, N. Gao, S. Shin, C.L. May, M.L. Golson, A.M. Zahm, M. Ray, C.L. Wiser, C.V.E. Wright, and K.H. Kaestner. 2016. Foxl1-Expressing Mesenchymal Cells Constitute the Intestinal Stem Cell Niche. *Cmgh.* 2:175–188. doi:10.1016/j.jcmgh.2015.12.004.
- Astanina, K., M. Koch, C. Jüngst, A. Zumbusch, and A.K. Kiemer. 2015. Lipid droplets as a

- novel cargo of tunnelling nanotubes in endothelial cells. *Sci. Rep.* 5:1–13. doi:10.1038/srep11453.
- Austefjord, M.W., H.H. Gerdes, and X. Wang. 2014. Tunneling nanotubes: Diversity in morphology and structure. *Commun. Integr. Biol.* 7. doi:10.4161/cib.27934.
- Bai, Y., X. Tan, H. Zhang, C. Liu, B. Zhao, Y. Li, L. Lu, Y. Liu, and J. Zhou. 2014. Ror2 receptor mediates wnt11 ligand signaling and affects convergence and extension movements in zebrafish. *J. Biol. Chem.* 289:20664–20676. doi:10.1074/jbc.M114.586099.
- Bainbridge, T.W., V.I. DeAlmeida, A. Izrael-Tomasevic, C. Chalouni, B. Pan, J. Goldsmith, A.P. Schoen, G.A. Quiñones, R. Kelly, J.R. Lill, W. Sandoval, M. Costa, P. Polakis, D. Arnott, B. Rubinfeld, and J.A. Ernst. 2014. Evolutionary divergence in the catalytic activity of the CAM-1, ROR1 and ROR2 kinase domains. *PLoS One.* 9. doi:10.1371/journal.pone.0102695.
- Bänziger, C., D. Soldini, C. Schütt, P. Zipperlen, G. Hausmann, and K. Basler. 2006. Wntless, a Conserved Membrane Protein Dedicated to the Secretion of Wnt Proteins from Signaling Cells. *Cell.* 125:509–522. doi:10.1016/j.cell.2006.02.049.
- Barrett, W.A., and E.N. Mortensen. 1997. Interactive live-wire boundary extraction. *Med. Image Anal.* 1:331–341. doi:10.1016/S1361-8415(97)85005-0.
- Bartscherer, K., and M. Boutros. 2008. Regulation of Wnt protein secretion and its role in gradient formation. *EMBO Rep.* 9:977–982. doi:10.1038/embor.2008.167.
- Bartscherer, K., N. Pelte, D. Ingelfinger, and M. Boutros. 2006. Secretion of Wnt ligands requires Evi, a conserved transmembrane protein. *Cell.* 125:523–533. doi:10.1016/j.cell.2006.04.009.
- Beckett, K., S. Monier, L. Palmer, C. Alexandre, H. Green, E. Bonneil, G. Raposo, P. Thibault, R. Le Borgne, and J.P. Vincent. 2013. Drosophila S2 cells secrete wingless on exosome-like vesicles but the wingless gradient forms independently of exosomes. *Traffic.* 14:82–96. doi:10.1111/tra.12016.
- Beumer, J., and H. Clevers. 2016. Regulation and plasticity of intestinal stem cells during homeostasis and regeneration. *Development.* 143:3639–3649. doi:10.1242/dev.133132.
- Bhanot, P., M. Brink, C.H. Samos, J.C. Hsieh, Y. Wang, J.P. Macke, D. Andrew, J. Nathans, and R. Nusse. 1996. A new member of the frizzled family from Drosophila functions as a Wingless receptor. *Nature.* 382:225–230. doi:10.1038/382225a0.
- Bilic, J., Y.-L. Huang, G. Davidson, T. Zimmermann, C.-M. Cruciat, M. Bienz, and C. Niehrs. 2007. Wnt Induces LRP6 Signalosomes and Promotes Dishevelled-Dependent LRP6 Phosphorylation. *Science (80-)*. 316:1619–1622. doi:10.1126/science.1137065.
- Billiard, J., D.S. Way, L.M. Seestaller-Wehr, R.A. Moran, A. Mangine, and P.V.N. Bodine. 2005. The Orphan Receptor Tyrosine Kinase Ror2 Modulates Canonical Wnt Signaling in Osteoblastic Cells. *Mol. Endocrinol.* 19:90–101. doi:10.1210/me.2004-0153.
- Bischoff, M., A.-C. Gradilla, I. Seijo, G. Andrés, C. Rodríguez-Navas, L. González-Méndez, and I. Guerrero. 2013. Cytonemes are required for the establishment of a normal Hedgehog morphogen gradient in Drosophila epithelia. *Nat. Cell Biol.* 15:1269–81.

doi:10.1038/ncb2856.

- Born, J., J. Janeczek, W. Schwarz, H. Tiedemann, and H. Tiedemann. 1989. Activation of masked neural determinants in amphibian eggs and embryos and their release from the inducing tissue. *Cell Differ. Dev.* 27:1–7. doi:10.1016/0922-3371(89)90039-7.
- Brand, M.G., M., and N.-V. C. 2002. Keeping and raising zebrafish. Oxford University Press, Oxford, UK.
- Brinkmann, E.M., B. Mattes, R. Kumar, A.I.H. Hagemann, D. Gradl, S. Scholpp, H. Steinbeisser, L.T. Kaufmann, and S. Özbek. 2016. Secreted Frizzled-related Protein 2 (sFRP2) redirects non-canonical Wnt signaling from Fz7 to Ror2 during vertebrate gastrulation. *J. Biol. Chem.* 291:13730–13742. doi:10.1074/jbc.M116.733766.
- Cadigan, K.M., and M.L. Waterman. 2012. TCF/LEFs and Wnt signaling in the nucleus. *Cold Spring Harb. Perspect. Biol.* 4. doi:10.1101/cshperspect.a007906.
- Caneparo, L., P. Pantazis, W. Dempsey, and S.E. Fraser. 2011. Intercellular bridges in vertebrate gastrulation. *PLoS One.* 6. doi:10.1371/journal.pone.0020230.
- Casella, J.F., M.D. Flanagan, and S. Lin. 1981. Cytochalasin D inhibits actin polymerization and induces depolymerization of actin filaments formed during platelet shape change. *Nature.* 293:302–305.
- Cayuso, J., A. Dzementsei, J.C. Fischer, G. Karemore, S. Caviglia, J. Bartholdson, G.J. Wright, and E.A. Ober. 2016. EphrinB1/EphB3b Coordinate Bidirectional Epithelial-Mesenchymal Interactions Controlling Liver Morphogenesis and Laterality. *Dev. Cell.* 39:316–328. doi:10.1016/j.devcel.2016.10.009.
- Chakrabarti, A., G. Matthews, A. Colman, and L. Dale. 1992. Secretory and inductive properties of Drosophila wingless protein in Xenopus oocytes and embryos. *Development.* 115:355–369.
- Chen, B., M.E. Dodge, W. Tang, J. Lu, Z. Ma, S. Wei, W. Hao, J. Kilgore, N.S. Williams, G. Michael, J.F. Amatruda, C. Chen, and L. Lum. 2009. Small molecule-mediated disruption of Wnt-dependent signaling in Tissue Regeneration and Cancer. 5:100–107. doi:10.1038/nchembio.137.Small.
- Chen, Q., Y. Su, J. Wesslowski, A.I. Hagemann, M. Ramialison, J. Wittbrodt, S. Scholpp, and G. Davidson. 2014. Tyrosine phosphorylation of LRP6 by Src and Fer inhibits Wnt/ -catenin signalling. *EMBO Rep.* 15:1254–1267. doi:10.15252/embr.201439644.
- Chen, Q., R. Takada, and S. Takada. 2012. Loss of Porcupine impairs convergent extension during gastrulation in zebrafish. *J. Cell Sci.* 125:2224–2234. doi:10.1242/jcs.098368.
- Ching, W., H.C. Hang, and R. Nusse. 2008. Lipid-independent secretion of a Drosophila Wnt protein. *J. Biol. Chem.* 283:17092–17098. doi:10.1074/jbc.M802059200.
- Chiurillo, M.A. 2015. Role of the Wnt/ β -catenin pathway in gastric cancer: An in-depth literature review. *World J. Exp. Med.* 5:84. doi:10.5493/wjem.v5.i2.84.
- Clevers, H. 2006. Wnt/??-Catenin Signaling in Development and Disease. *Cell.* 127:469–480. doi:10.1016/j.cell.2006.10.018.

- Coudreuse, D.Y.M., G. Roel, M.C. Betist, O. Destree, and H.C. Korswagen. 2006. Wnt gradient formation requires retromer function in Wnt-producing cells. *Science*. 312:921–924. doi:10.1126/science.1124856.
- Croce, J., and D. McClay. 2008. Evolution of the Wnt Pathways. 468:173–186. doi:10.1007/978-1-59745-249-6.
- Cruciat, C.M., and C. Niehrs. 2013. Secreted and transmembrane wnt inhibitors and activators. *Cold Spring Harb. Perspect. Biol.* 5:1–26. doi:10.1101/cshperspect.a015081.
- Davey, C.F., A.W. Mathewson, and C.B. Moens. 2016. PCP Signaling between Migrating Neurons and their Planar-Polarized Neuroepithelial Environment Controls Filopodial Dynamics and Directional Migration. *PLoS Genet.* 12:e1005934. doi:10.1371/journal.pgen.1005934.
- DeChiara, T.M., D.C. Bowen, D.M. Valenzuela, M. V Simmons, W.T. Poueymirou, S. Thomas, E. Kinetz, D.L. Compton, E. Rojas, J.S. Park, C. Smith, P.S. DiStefano, D.J. Glass, S.J. Burden, and G.D. Yancopoulos. 1996. The receptor tyrosine kinase MuSK is required for neuromuscular junction formation in vivo. *Cell*. 85:501–512.
- DeChiara, T.M., R.B. Kimble, W.T. Poueymirou, J. Rojas, P. Masiakowski, D.M. Valenzuela, and G.D. Yancopoulos. 2000. Ror2, encoding a receptor-like tyrosine kinase, is required for cartilage and growth plate development. *Nat. Genet.* 24:271–274. doi:10.1038/73488.
- Delage, E., D.C. Cervantes, E. Pénard, C. Schmitt, S. Syan, A. Disanza, G. Scita, and C. Zurzolo. 2016. Differential identity of Filopodia and Tunneling Nanotubes revealed by the opposite functions of actin regulatory complexes. *Sci. Rep.* 6:25–28. doi:10.1038/srep39632.
- Disanza, A., S. Bisi, M. Winterhoff, F. Milanesi, D.S. Ushakov, D. Kast, P. Marighetti, G. Romet-Lemonne, H.M. Müller, W. Nickel, J. Linkner, D. Waterschoot, C. Ampè, S. Cortellino, A. Palamidessi, R. Dominguez, M.F. Carlier, J. Faix, and G. Scita. 2013. CDC42 switches IRSp53 from inhibition of actin growth to elongation by clustering of VASP. *EMBO J.* 32:2735–2750. doi:10.1038/emboj.2013.208.
- Dissanayake, S.K., M. Wade, C.E. Johnson, M.P. O’Connell, P.D. Leotlela, A.D. French, K. V Shah, K.J. Hewitt, D.T. Rosenthal, F.E. Indig, Y. Jiang, B.J. Nickoloff, D.D. Taub, J.M. Trent, R.T. Moon, M. Bittner, and A.T. Weeraratna. 2007. The Wnt5A/protein kinase C pathway mediates motility in melanoma cells via the inhibition of metastasis suppressors and initiation of an epithelial to mesenchymal transition. *J. Biol. Chem.* 282:17259–17271. doi:10.1074/jbc.M700075200.
- Djiane, A., J. Riou, M. Umbhauer, J. Boucaut, and D. Shi. 2000. Role of frizzled 7 in the regulation of convergent extension movements during gastrulation in *Xenopus laevis*. *Development*. 127:3091–3100.
- Dörlich, R.M., Q. Chen, P. Niklas Hedde, V. Schuster, M. Hippler, J. Wesslowski, G. Davidson, and G.U. Nienhaus. 2015. Dual-color dual-focus line-scanning FCS for quantitative analysis of receptor-ligand interactions in living specimens. *Sci. Rep.* 5:10149. doi:10.1038/srep10149.
- Driever, W., and C. Nusslein-Volhard. 1988. The bicoid protein determines position in the

- Drosophila embryo in a concentration-dependent manner. *Cell*. 54:95–104.
- Du, S.J., S.M. Purcell, J.L. Christian, L.L. McGrew, and R.T. Moon. 1995. Identification of distinct classes and functional domains of Wnts through expression of wild-type and chimeric proteins in *Xenopus* embryos. *Mol. Cell. Biol.* 15:2625–2634.
- Dubois, L., M. Lecourtois, C. Alexandre, E. Hirst, and J.P. Vincent. 2001. Regulated endocytic routing modulates wingless signaling in *Drosophila* embryos. *Cell*. 105:613–624.
- Enomoto, M., S. Hayakawa, S. Itsukushima, D.Y. Ren, M. Matsuo, K. Tamada, C. Oneyama, M. Okada, T. Takumi, M. Nishita, and Y. Minami. 2009. Autonomous regulation of osteosarcoma cell invasiveness by Wnt5a/Ror2 signaling. *Oncogene*. 28:3197–3208. doi:10.1038/onc.2009.175.
- Eom, D.S., and D.M. Parichy. 2017. A macrophage relay for long-distance signaling during postembryonic tissue remodeling. *Science* (80-.). 355:1317–1320. doi:10.1126/science.aal2745.
- Erter, C.E., T.P. Wilm, N. Basler, C. V Wright, and L. Solnica-Krezel. 2001. Wnt8 is required in lateral mesendodermal precursors for neural posteriorization in vivo. *Development*. 128:3571–3583.
- Esteve, P., A. Sandonis, C. Ibanez, A. Shimono, I. Guerrero, and P. Bovolenta. 2011. Secreted frizzled-related proteins are required for Wnt/beta-catenin signalling activation in the vertebrate optic cup. *Development*. 138:4179–4184. doi:10.1242/dev.065839.
- Faix, J., and K. Rottner. 2006. The making of filopodia. *Curr. Opin. Cell Biol.* 18:18–25. doi:10.1016/j.ceb.2005.11.002.
- Farin, H.F., I. Jordens, M.H. Mosa, O. Basak, J. Korving, D.V.F. Tauriello, K. de Punder, S. Angers, P.J. Peters, M.M. Maurice, and H. Clevers. 2016. Visualization of a short-range Wnt gradient in the intestinal stem-cell niche. *Nature*. doi:10.1038/nature16937.
- Feike, A.C., K. Rachor, M. Gentzel, and A. Schambony. 2010. Wnt5a/Ror2-induced upregulation of xPAPC requires xShcA. *Biochem. Biophys. Res. Commun.* 400:500–506. doi:10.1016/j.bbrc.2010.08.074.
- Fekany-Lee, K., E. Gonzalez, V. Miller-Bertoglio, and L. Solnica-Krezel. 2000. The homeobox gene bozozok promotes anterior neuroectoderm formation in zebrafish through negative regulation of BMP2/4 and Wnt pathways. *Development*. 127:2333–2345.
- Fellgett, S.W., R.J. Maguire, and M.E. Pownall. 2015. Sulfl has ligand-dependent effects on canonical and non-canonical Wnt signalling. *J. Cell Sci.* 128:1408–1421. doi:10.1242/jcs.164467.
- Festa, E., J. Fretz, R. Berry, B. Schmidt, M. Rodeheffer, M. Horowitz, and V. Horsley. 2011. Adipocyte lineage cells contribute to the skin stem cell niche to drive hair cycling. *Cell*. 146:761–771. doi:10.1016/j.cell.2011.07.019.
- Fifadara, N.H., F. Beer, S. Ono, and S.J. Ono. 2010. Interaction between activated chemokine receptor 1 and FcεRI at membrane rafts promotes communication and F-actin-rich cytoneme extensions between mast cells. *Int. Immunol.* 22:113–128.

doi:10.1093/intimm/dxp118.

- Fu, J., M. Jiang, A.J. Mirando, H.-M.I. Yu, and W. Hsu. 2009. Reciprocal regulation of Wnt and Gpr177/mouse Wntless is required for embryonic axis formation. *Proc. Natl. Acad. Sci. U. S. A.* 106:18598–18603. doi:10.1073/pnas.0904894106.
- Gammons, M., and M. Bienz. 2018. Multiprotein complexes governing Wnt signal transduction. *Curr. Opin. Cell Biol.* 51:42–49. doi:10.1016/j.ceb.2017.10.008.
- Gao, B., H. Song, K. Bishop, G. Elliot, L. Garrett, M.A. English, P. Andre, J. Robinson, R. Sood, Y. Minami, A.N. Economides, and Y. Yang. 2011. Wnt Signaling Gradients Establish Planar Cell Polarity by Inducing Vangl2 Phosphorylation through Ror2. *Dev. Cell.* 20:163–176. doi:10.1016/j.devcel.2011.01.001.
- Gao, C., and Y.G. Chen. 2010. Dishevelled: The hub of Wnt signaling. *Cell. Signal.* 22:717–727. doi:10.1016/j.cellsig.2009.11.021.
- Gentile, A., L. Lazzari, S. Benvenuti, L. Trusolino, and P.M. Comoglio. 2011. Ror1 is a pseudokinase that is crucial for Met-driven tumorigenesis. *Cancer Res.* 71:3132–3141. doi:10.1158/0008-5472.CAN-10-2662.
- Ghimire, S.R., E.M. Ratzan, and M.R. Deans. 2018. A non-autonomous function of the core PCP protein VANGL2 directs peripheral axon turning in the developing cochlea. *Development.* 145. doi:10.1242/dev.159012.
- Gilbert, L.A., M.H. Larson, L. Morsut, Z. Liu, G.A. Brar, S.E. Torres, N. Stern-Ginossar, O. Brandman, E.H. Whitehead, J.A. Doudna, W.A. Lim, J.S. Weissman, and L.S. Qi. 2013. CRISPR-mediated modular RNA-guided regulation of transcription in eukaryotes. *Cell.* 154:442–451. doi:10.1016/j.cell.2013.06.044.
- Gilbert, S. 1993. A Conceptual History of Modern Embryology. Scott Gilbert. *Isis.* 84:175–176. doi:10.1086/356433.
- Glickman, N.S. 2003. Shaping the zebrafish notochord. *Development.* 130:873–887. doi:10.1242/dev.00314.
- González-Méndez, L., I. Seijo-Barandiarán, and I. Guerrero. 2017. Cytoneme-mediated cell-cell contacts for hedgehog reception. *Elife.* 6:1–24. doi:10.7554/eLife.24045.
- Gordon, M.D., and R. Nusse. 2006. Wnt signaling: multiple pathways, multiple receptors, and multiple transcription factors. *J. Biol. Chem.* 281:22429–22433. doi:10.1074/jbc.R600015200.
- Gousset, K., E. Schiff, C. Langevin, Z. Marijanovic, A. Caputo, D.T. Browman, N. Chenouard, F. de Chaumont, A. Martino, J. Enninga, J.C. Olivo-Marin, D. Männel, and C. Zurzolo. 2009. Prions hijack tunnelling nanotubes for intercellular spread. *Nat. Cell Biol.* 11:328–336. doi:10.1038/ncb1841.
- Gradilla, A.-C., E. González, I. Seijo, G. Andrés, M. Bischoff, L. González-Mendez, V. Sánchez, A. Callejo, C. Ibáñez, M. Guerra, J.R. Ortigão-Farias, J.D. Sutherland, M. González, R. Barrio, J.M. Falcón-Pérez, and I. Guerrero. 2014. Exosomes as Hedgehog carriers in cytoneme-mediated transport and secretion. *Nat. Commun.* 5:5649. doi:10.1038/ncomms6649.

- Greco, V., M. Hannus, and S. Eaton. 2001. Argosomes: a potential vehicle for the spread of morphogens through epithelia. *Cell*. 106:633–645.
- Green, D., A.E. Whitener, S. Mohanty, and A.C. Lekven. 2015. Vertebrate nervous system posteriorization: Grading the function of Wnt signaling. *Dev. Dyn.* 244:507–512. doi:10.1002/dvdy.24230.
- Green, J., R. Nusse, and R. van Amerongen. 2014. The role of Ryk and Ror receptor tyrosine kinases in wnt signal transduction. *Cold Spring Harb. Perspect. Biol.* 6:1–12. doi:10.1101/cshperspect.a009175.
- Green, J.L., S.G. Kuntz, and P.W. Sternberg. 2008. Ror receptor tyrosine kinases: orphans no more. *Trends Cell Biol.* 18:536–544. doi:10.1016/j.tcb.2008.08.006.
- Greicius, G., Z. Kabiri, K. Sigmundsson, C. Liang, R. Bunte, M.K. Singh, and D.M. Virshup. 2018. *PDGFR α* ⁺ pericryptal stromal cells are the critical source of Wnts and RSPO3 for murine intestinal stem cells in vivo. *Proc. Natl. Acad. Sci.* 115:201713510. doi:10.1073/pnas.1713510115.
- Gross, J.C., and M. Boutros. 2013. Secretion and extracellular space travel of Wnt proteins. *Curr. Opin. Genet. Dev.* 23:385–390. doi:10.1016/j.gde.2013.02.017.
- Gross, J.C., V. Chaudhary, K. Bartscherer, and M. Boutros. 2012. Active Wnt proteins are secreted on exosomes. *Nat. Cell Biol.* 14:1036–1045. doi:10.1038/ncb2574.
- Grumolato, L., G. Liu, P. Mong, R. Mudbhary, R. Biswas, R. Arroyave, S. Vijayakumar, A.N. Economides, and S.A. Aaronson. 2010. Canonical and noncanonical Wnts use a common mechanism to activate completely unrelated coreceptors. *Genes Dev.* 24:2517–2530. doi:10.1101/gad.1957710.
- Grunz, H., and L. Tacke. 1989. Neural differentiation of *Xenopus laevis* ectoderm takes place after disaggregation and delayed reaggregation without inducer. *Cell Differ. Dev.* 28:211–217. doi:10.1016/0922-3371(89)90006-3.
- Grzeschik, K.-H., D. Bornholdt, F. Oeffner, A. König, M. del Carmen Boente, H. Enders, B. Fritz, M. Hertl, U. Grasshoff, K. Hofling, V. Oji, M. Paradisi, C. Schuchardt, Z. Szalai, G. Tadini, H. Traupe, and R. Happle. 2007. Deficiency of PORCN, a regulator of Wnt signaling, is associated with focal dermal hypoplasia. *Nat. Genet.* 39:833–835. doi:10.1038/ng2052.
- Gupta, N., and A.L. DeFranco. 2003. Visualizing lipid raft dynamics and early signaling events during antigen receptor-mediated B-lymphocyte activation. *Mol. Biol. Cell.* 14:432–444. doi:10.1091/mbc.02-05-0078.
- Gurdon, J.B., P. Harger, A. Mitchell, and P. Lemaire. 1994. Activin signalling and response to a morphogen gradient. *Nature.* 371:487–492. doi:10.1038/371487a0.
- Hagemann, A.I.H., J. Kurz, S. Kauffeld, Q. Chen, P.M. Reeves, S. Weber, S. Schindler, G. Davidson, T. Kirchhausen, and S. Scholpp. 2014. In-vivo analysis of formation and endocytosis of the Wnt/ β -Catenin signaling complex in zebrafish embryos. *J. Cell Sci.* 3970–3982. doi:10.1242/jcs.148767.
- Halpern, M.E., J. Rhee, M.G. Goll, C.M. Akitake, M. Parsons, and S.D. Leach. 2008. Gal4/UAS transgenic tools and their application to zebrafish. *Zebrafish.* 5:97–110.

doi:10.1089/zeb.2008.0530.

- Han, C., D. Yan, T.Y. Belenkaya, and X. Lin. 2005. *Drosophila* glypicans Dally and Dally-like shape the extracellular Wntless morphogen gradient in the wing disc. *Development*. 132:667–679. doi:10.1242/dev.01636.
- Harada, T., H. Yamamoto, S. Kishida, M. Kishida, C. Awada, T. Takao, and A. Kikuchi. 2017. Wnt5b-associated exosomes promote cancer cell migration and proliferation. *Cancer Sci*. 108:42–52. doi:10.1111/cas.13109.
- Harterink, M., and H.C. Korswagen. 2012. Dissecting the Wnt secretion pathway: Key questions on the modification and intracellular trafficking of Wnt proteins. *Acta Physiol*. 204:8–16. doi:10.1111/j.1748-1716.2011.02287.x.
- Hatsell, S., T. Rowlands, M. Hiremath, and P. Cowin. 2003. Beta-catenin and Tcfs in mammary development and cancer. *J. Mammary Gland Biol. Neoplasia*. 8:145–158.
- Hatta, K., and Y. Takahashi. 1996. Secondary axis induction by heterospecific organizers in zebrafish. *Dev. Dyn.* 205:183–195. doi:10.1002/(SICI)1097-0177(199602)205:2<183::AID-AJA9>3.0.CO;2-E.
- He, X., M. Semenov, K. Tamai, and X. Zeng. 2004. LDL receptor-related proteins 5 and 6 in Wnt/beta-catenin signaling: arrows point the way. *Development*. 131:1663–1677. doi:10.1242/dev.01117.
- Heisenberg, C.-P., M. Tada, G.-J. Rauch, L. Saude, M.L. Concha, R. Geisler, D.L. Stemple, J.C. Smith, and S.W. Wilson. 2000. Silberblick / Wnt11 mediates convergent extension movements during zebra @ sh gastrulation. *Nature*. 405:76–81. doi:10.1038/35011068.
- Heller, E., and E. Fuchs. 2015. Tissue patterning and cellular mechanics. *J. Cell Biol*. 211:219–231. doi:10.1083/jcb.201506106.
- Hemmati-Brivanlou, A., and D.A. Melton. 1994. Inhibition of activin receptor signaling promotes neuralization in *Xenopus*. *Cell*. 77:273–281.
- Henry, C., A. Quadir, N.J. Hawkins, E. Jary, E. Llamosas, D. Kumar, B. Daniels, R.L. Ward, and C.E. Ford. 2014. Expression of the novel Wnt receptor ROR2 is increased in breast cancer and may regulate both ??-catenin dependent and independent Wnt signalling. *J. Cancer Res. Clin. Oncol*. 141:243–254. doi:10.1007/s00432-014-1824-y.
- Hikasa, H., M. Shibata, I. Hiratani, and M. Taira. 2002. The *Xenopus* receptor tyrosine kinase Xror2 modulates morphogenetic movements of the axial mesoderm and neuroectoderm via Wnt signaling. *Development*. 129:5227–5239.
- Ho, H.-Y.H., M.W. Susman, J.B. Bikoff, Y.K. Ryu, a. M. Jonas, L. Hu, R. Kuruvilla, and M.E. Greenberg. 2012. Inaugural Article: Wnt5a-Ror-Dishevelled signaling constitutes a core developmental pathway that controls tissue morphogenesis. *Proc. Natl. Acad. Sci*. 109:1–8. doi:10.1073/pnas.1200421109.
- Ho, H.Y.H., R. Rohatgi, A.M. Lebensohn, Le Ma, J. Li, S.P. Gygi, and M.W. Kirschner. 2004. Toca-1 mediates Cdc42-dependent actin nucleation by activating the N-WASP-WIP complex. *Cell*. 118:203–216. doi:10.1016/j.cell.2004.06.027.
- Hoch, R. V, and P. Soriano. 2003. Roles of PDGF in animal development. *Development*.

130:4769–4784. doi:10.1242/dev.00721.

- Holzer, T., K. Liffers, K. Rahm, B. Trageser, S. Özbek, and D. Gradl. 2012. Live imaging of active fluorophore labelled Wnt proteins. *FEBS Lett.* 586:1638–1644. doi:10.1016/j.febslet.2012.04.035.
- Hsiung, F., F.A. Ramirez-Weber, D. David Iwaki, and T.B. Kornberg. 2005. Dependence of *Drosophila* wing imaginal disc cytonemes on Decapentaplegic. *Nature.* 437:560–563. doi:10.1038/nature03951.
- Huang, H., and T.B. Kornberg. 2015. Myoblast cytonemes mediate Wg signaling from the wing imaginal disc and Delta-Notch signaling to the air sac primordium. *Elife.* 4:1–22. doi:10.7554/eLife.06114.
- Huang, S.-M.A., Y.M. Mishina, S. Liu, A. Cheung, F. Stegmeier, G.A. Michaud, O. Charlat, E. Wiellette, Y. Zhang, S. Wiessner, M. Hild, X. Shi, C.J. Wilson, C. Mickanin, V. Myer, A. Fazal, R. Tomlinson, F. Serluca, W. Shao, H. Cheng, M. Shultz, C. Rau, M. Schirle, J. Schlegl, S. Ghidelli, S. Fawell, C. Lu, D. Curtis, M.W. Kirschner, C. Lengauer, P.M. Finan, J.A. Tallarico, T. Bouwmeester, J.A. Porter, A. Bauer, and F. Cong. 2009. Tankyrase inhibition stabilizes axin and antagonizes Wnt signalling. *Nature.* 461:614–620. doi:10.1038/nature08356.
- Inaba, M., H. Yamanaka, and S. Kondo. 2012. Pigment pattern formation by contact-dependent depolarization. *Science.* 335:677. doi:10.1126/science.1212821.
- Irion, U., J. Krauss, and C. Nusslein-Volhard. 2014. Precise and efficient genome editing in zebrafish using the CRISPR/Cas9 system. *Development.* 141:4827–30. doi:10.1242/dev.115584.
- Jacquemet, G., H. Hamidi, and J. Ivaska. 2015. Filopodia in cell adhesion, 3D migration and cancer cell invasion. *Curr. Opin. Cell Biol.* 36:23–31. doi:10.1016/j.ceb.2015.06.007.
- Janda, C.Y., D. Waghray, a. M. Levin, C. Thomas, and K.C. Garcia. 2012. Structural Basis of Wnt Recognition by Frizzled. *Science (80-.).* 337:59–64. doi:10.1126/science.1222879.
- Jao, L.-E., S.R. Wentz, and W. Chen. 2013. Efficient multiplex biallelic zebrafish genome editing using a CRISPR nuclease system. *Proc. Natl. Acad. Sci. U. S. A.* 110:13904–9. doi:10.1073/pnas.1308335110.
- Jho, E., T. Zhang, C. Domon, C.-K. Joo, J.-N. Freund, and F. Costantini. 2002. Wnt/beta-catenin/Tcf signaling induces the transcription of Axin2, a negative regulator of the signaling pathway. *Mol. Cell. Biol.* 22:1172–1183.
- Kabiri, Z., G. Greicius, B. Madan, S. Biechele, Z. Zhong, H. Zaribafzadeh, Edison, J. Aliyev, Y. Wu, R. Bunte, B.O. Williams, J. Rossant, and D.M. Virshup. 2014. Stroma provides an intestinal stem cell niche in the absence of epithelial Wnts. *Development.* 141:2206–2215. doi:10.1242/dev.104976.
- Kast, D.J., C. Yang, A. Disanza, M. Boczkowska, Y. Madasu, G. Scita, T. Svitkina, and R. Dominguez. 2014. Mechanism of IRSp53 inhibition and combinatorial activation by Cdc42 and downstream effectors. *Nat. Struct. Mol. Biol.* 21:413–22. doi:10.1038/nsmb.2781.

- Keller, R., L. Davidson, A. Edlund, T. Elul, M. Ezin, D. Shook, and P. Skoglund. 2000. Mechanisms of convergence and extension by cell intercalation. *Philos. Trans. R. Soc. Lond. B. Biol. Sci.* 355:897–922. doi:10.1098/rstb.2000.0626.
- Kelley, M.W. 2008. Leading Wnt down a PCP Path: Cthrc1 Acts as a Coreceptor in the Wnt-PCP Pathway. *Dev. Cell.* 15:7–8. doi:10.1016/j.devcel.2008.06.008.
- Kelly, G.M., P. Greenstein, D.F. Erezyilmaz, and R.T. Moon. 1995. Zebrafish Wnt8 and Wnt8B Share a Common Activity But Are Involved in Distinct Developmental Pathways. *Development.* 121:1787–1799.
- Kestler, H.A., and M. Kühl. 2008. From individual Wnt pathways towards a Wnt signalling network. *Philos. Trans. R. Soc. Lond. B. Biol. Sci.* 363:1333–47. doi:10.1098/rstb.2007.2251.
- Kiecker, C., and C. Niehrs. 2001. A morphogen gradient of Wnt/beta-catenin signalling regulates anteroposterior neural patterning in *Xenopus*. *Development.* 128:4189–4201.
- Kikuchi, A., H. Yamamoto, and S. Kishida. 2007. Multiplicity of the interactions of Wnt proteins and their receptors. *Cell. Signal.* 19:659–671. doi:10.1016/j.cellsig.2006.11.001.
- Kikuchi, A., H. Yamamoto, and A. Sato. 2009. Selective activation mechanisms of Wnt signaling pathways. *Trends Cell Biol.* 19:119–129. doi:10.1016/j.tcb.2009.01.003.
- Kikuchi, A., H. Yamamoto, A. Sato, and S. Matsumoto. 2011. New Insights into the Mechanism of Wnt Signaling Pathway Activation. *Int. Rev. Cell Mol. Biol.* 291:21–71. doi:10.1016/B978-0-12-386035-4.00002-1.
- Kim, S.-H., J. Shin, H.-C. Park, S.-Y. Yeo, S.-K. Hong, S. Han, M. Rhee, C.-H. Kim, A.B. Chitnis, and T.-L. Huh. 2002. Specification of an anterior neuroectoderm patterning by Frizzled8a-mediated Wnt8b signalling during late gastrulation in zebrafish. *Development.* 129:4443–4455.
- Kimmel, C.B., W.W. Ballard, S.R. Kimmel, B. Ullmann, and T.F. Schilling. 1995. Stages of embryonic development of the zebrafish. *Dev. Dyn. an Off. public.* 203:253–310. doi:10.1002/aja.1002030302.
- Kinzler, K.W., M.C. Nilbert, L.K. Su, B. Vogelstein, T.M. Bryan, D.B. Levy, K.J. Smith, A.C. Preisinger, P. Hedge, and D. McKechnie. 1991. Identification of FAP locus genes from chromosome 5q21. *Science.* 253:661–665.
- Kitagawa, M., S. Hatakeyama, M. Shirane, M. Matsumoto, N. Ishida, K. Hattori, I. Nakamichi, A. Kikuchi, K. Nakayama, and K. Nakayama. 1999. An F-box protein, FWD1, mediates ubiquitin-dependent proteolysis of beta-catenin. *EMBO J.* 18:2401–2410. doi:10.1093/emboj/18.9.2401.
- Koizumi, K., K. Takano, A. Kaneyasu, H. Watanabe-Takano, E. Tokuda, T. Abe, N. Watanabe, T. Takenawa, and T. Endo. 2012. RhoD activated by fibroblast growth factor induces cytoneme-like cellular protrusions through mDia3C. *Mol. Biol. Cell.* 23:4647–4661. doi:10.1091/mbc.E12-04-0315.
- Komekado, H., H. Yamamoto, T. Chiba, and A. Kikuchi. 2007. Glycosylation and palmitoylation of Wnt-3a are coupled to produce an active form of Wnt-3a. *Genes*

- Cells*. 12:521–534. doi:10.1111/j.1365-2443.2007.01068.x.
- Kondo, S., and T. Miura. 2010. Reaction-diffusion model as a framework for understanding biological pattern formation. *Science*. 329:1616–1620. doi:10.1126/science.1179047.
- Korkut, C., B. Ataman, P. Ramachandran, J. Ashley, R. Barria, N. Gherbesi, and V. Budnik. 2009. Trans-synaptic transmission of vesicular Wnt signals through Evi/Wntless. *Cell*. 139:393–404. doi:10.1016/j.cell.2009.07.051.
- Kornberg, T.B., and S. Roy. 2014. Cytonemes as specialized signaling filopodia. *Development*. 141:729–736. doi:10.1242/dev.086223.
- Kuhl, M., L.C. Sheldahl, C.C. Malbon, and R.T. Moon. 2000a. Ca²⁺/calmodulin-dependent protein kinase II is stimulated by Wnt and Frizzled homologs and promotes ventral cell fates in *Xenopus*. *J. Biol. Chem.* 275:12701–12711.
- Kuhl, M., L.C. Sheldahl, M. Park, J.R. Miller, and R.T. Moon. 2000b. The Wnt/Ca²⁺ pathway: a new vertebrate Wnt signaling pathway takes shape. *Trends Genet.* 16:279–283.
- Kuhnert, F., C.R. Davis, H.-T. Wang, P. Chu, M. Lee, J. Yuan, R. Nusse, and C.J. Kuo. 2004. Essential requirement for Wnt signaling in proliferation of adult small intestine and colon revealed by adenoviral expression of Dickkopf-1. *Proc. Natl. Acad. Sci.* 101:266–271. doi:10.1073/pnas.2536800100.
- Kurayoshi, M., H. Yamamoto, S. Izumi, and A. Kikuchi. 2007. Post-translational palmitoylation and glycosylation of Wnt-5a are necessary for its signalling. *Biochem. J.* 402:515–523. doi:10.1042/BJ20061476.
- Lamb, T.M., A.K. Knecht, W.C. Smith, S.E. Stachel, A.N. Economides, N. Stahl, G.D. Yancopoulos, and R.M. Harland. 1993. Neural induction by the secreted polypeptide noggin. *Science*. 262:713–718.
- Lammi, L., S. Arte, M. Somer, H. Jarvinen, P. Lahermo, I. Thesleff, S. Pirinen, and P. Nieminen. 2004. Mutations in AXIN2 cause familial tooth agenesis and predispose to colorectal cancer. *Am. J. Hum. Genet.* 74:1043–1050. doi:10.1086/386293.
- Langton, P.F., S. Kakugawa, and J.-P. Vincent. 2016. Making, Exporting, and Modulating Wnts. *Trends Cell Biol.* xx:1–10. doi:10.1016/j.tcb.2016.05.011.
- Larson, M.H., L.A. Gilbert, X. Wang, W.A. Lim, J.S. Weissman, and L.S. Qi. 2013. CRISPR interference (CRISPRi) for sequence-specific control of gene expression. *Nat. Protoc.* 8:2180–2196. doi:10.1038/nprot.2013.132.
- Lekven, A.C., C.J. Thorpe, J.S. Waxman, and R.T. Moon. 2001. Zebrafish wnt8 Encodes Two Wnt8 Proteins on a Bicistronic Transcript and Is Required for Mesoderm and Neurectoderm Patterning. *Dev. Cell.* 1:103–114. doi:10.1016/S1534-5807(01)00007-7.
- Li, C., H. Chen, L. Hu, Y. Xing, T. Sasaki, M.F. Villosis, J. Li, M. Nishita, Y. Minami, and P. Minoo. 2008. Ror2 modulates the canonical Wnt signaling in lung epithelial cells through cooperation with Fzd2. *BMC Mol. Biol.* 9:11. doi:10.1186/1471-2199-9-11.
- Lidke, D.S., K.A. Lidke, B. Rieger, T.M. Jovin, and D.J. Arndt-Jovin. 2005. Reaching out for signals: Filopodia sense EGF and respond by directed retrograde transport of activated

- receptors. *J. Cell Biol.* 170:619–626. doi:10.1083/jcb.200503140.
- Lin, X., and N. Perrimon. 1999. Dally cooperates with Drosophila Frizzled 2 to transduce Wntless signalling. *Nature.* 400:281–284. doi:10.1038/22343.
- Liu, Y., J.F. Ross, P.V.N. Bodine, and J. Billiard. 2007. Homodimerization of Ror2 Tyrosine Kinase Receptor Induces 14-3-3 β Phosphorylation and Promotes Osteoblast Differentiation and Bone Formation. *Mol. Endocrinol.* 21:3050–3061. doi:10.1210/me.2007-0323.
- Liu, Y., B. Rubin, P.V.N. Bodine, and J. Billiard. 2008. Wnt5a induces homodimerization and activation of Ror2 receptor tyrosine kinase. *J. Cell. Biochem.* 105:497–502. doi:10.1002/jcb.21848.
- Logan, C., and R. Nusse. 2004. the Wnt Signaling Pathway in Development and Disease. *Annu. Rev. Cell Dev. Biol.* 20:781–810. doi:10.1146/annurev.cellbio.20.010403.113126.
- Lou, E., S. Fujisawa, A. Morozov, A. Barlas, Y. Romin, Y. Dogan, S. Gholami, A.L. Moreira, K. Manova-Todorova, and M.A.S. Moore. 2012. Tunneling nanotubes provide a unique conduit for intercellular transfer of cellular contents in human malignant pleural mesothelioma. *PLoS One.* 7:1–11. doi:10.1371/journal.pone.0033093.
- Lu, F., C. Thisse, and B. Thisse. 2011. Identification and mechanism of regulation of the zebrafish dorsal determinant. *Proc. Natl. Acad. Sci. U. S. A.* 108:15876–15880. doi:10.1073/pnas.1106801108/-/DCSupplemental.www.pnas.org/cgi/doi/10.1073/pnas.1106801108.
- Luz, M., S. Spannli-Müller, G. Zhang, B. Kagermeier-Schenk, M. Rhinn, G. Weidinger, and M. Brand. 2014. Dynamic association with donor cell filopodia and lipid-modification are essential features of Wnt8a during patterning of the zebrafish neuroectoderm. *PLoS One.* 9. doi:10.1371/journal.pone.0084922.
- Madan, B., and D.M. Virshup. 2015. Targeting Wnts at the Source--New Mechanisms, New Biomarkers, New Drugs. *Mol. Cancer Ther.* 14:1087–1094. doi:10.1158/1535-7163.MCT-14-1038.
- Mao, J., S. Fan, W. Ma, P. Fan, B. Wang, J. Zhang, H. Wang, B. Tang, Q. Zhang, X. Yu, L. Wang, B. Song, and L. Li. 2014. Roles of Wnt/ β -catenin signaling in the gastric cancer stem cells proliferation and salinomycin treatment. *Cell Death Dis.* 5:1–9. doi:10.1038/cddis.2013.515.
- Martinez Arias, A., and B. Steventon. 2018. On the nature and function of organizers. *Development.* 145. doi:10.1242/dev.159525.
- Masiakowski, P., and R.D. Carroll. 1992. A novel family of cell surface receptors with tyrosine kinase-like domain. *J. Biol. Chem.* 267:26181–26190.
- Mattes, B., S. Weber, J. Peres, Q. Chen, G. Davidson, C. Houart, and S. Scholpp. 2012. Wnt3 and Wnt3a are required for induction of the mid-diencephalic organizer in the caudal forebrain. *Neural Dev.* 7:12.
- Mattila, P.K., and P. Lappalainen. 2008. Filopodia: Molecular architecture and cellular functions. *Nat. Rev. Mol. Cell Biol.* 9:446–454. doi:10.1038/nrm2406.

- McGough, I.J., and J.-P. Vincent. 2016. Exosomes in developmental signalling. *Development*. 143:2482–2493. doi:10.1242/dev.126516.
- McKinney, M.C., D. A. Stark, T. Jessica, and P.M. Kulesa. 2012. Neural crest cell communication involves an exchange of cytoplasmic material through cellular bridges revealed by photoconversion of KikGR. *Dev Dyn*. 240:1391–1401. doi:10.1002/dvdy.22612.Neural.
- McMahon, A.P., and A. Bradley. 1990. The Wnt-1 (int-1) proto-oncogene is required for development of a large region of the mouse brain. *Cell*. 62:1073–1085.
- McMahon, A.P., and R.T. Moon. 1989. Ectopic expression of the proto-oncogene int-1 in *Xenopus* embryos leads to duplication of the embryonic axis. *Cell*. 58:1075–1084.
- Mentink, R.A., T.C. Middelkoop, L. Rella, N. Ji, C.Y. Tang, M.C. Betist, A. van Oudenaarden, and H.C. Korswagen. 2014. Cell intrinsic modulation of Wnt signaling controls neuroblast migration in *C. elegans*. *Dev. Cell*. 31:188–201. doi:10.1016/j.devcel.2014.08.008.
- Mifflin, R.C., I. V Pinchuk, J.I. Saada, and D.W. Powell. 2011. Intestinal myofibroblasts: targets for stem cell therapy. *Am. J. Physiol. Gastrointest. Liver Physiol*. 300:G684–96. doi:10.1152/ajpgi.00474.2010.
- Mii, Y., and M. Taira. 2009. Secreted Frizzled-related proteins enhance the diffusion of Wnt ligands and expand their signalling range. *Development*. 136:4083–4088. doi:10.1242/dev.032524.
- Mikels, A., Y. Minami, and R. Nusse. 2009. Ror2 receptor requires tyrosine kinase activity to mediate Wnt5A signaling. *J. Biol. Chem*. 284:30167–30176. doi:10.1074/jbc.M109.041715.
- Mikels, A.J., and R. Nusse. 2006. Purified Wnt5a protein activates or inhibits β -catenin-TCF signaling depending on receptor context. *PLoS Biol*. 4:570–582. doi:10.1371/journal.pbio.0040115.
- Minami, Y., I. Oishi, M. Endo, and M. Nishita. 2010. Ror-family receptor tyrosine kinases in noncanonical Wnt signaling: Their implications in developmental morphogenesis and human diseases. *Dev. Dyn*. 239:1–15. doi:10.1002/dvdy.21991.
- Modzelewska, K., A. Lauritzen, S. Hasenoeder, L. Brown, J. Georgiou, and N. Moghal. 2013. Neurons Refine the *Caenorhabditis elegans* Body Plan by Directing Axial Patterning by Wnts. *PLoS Biol*. 11:1–22. doi:10.1371/journal.pbio.1001465.
- Morioka, K., C. Tanikawa, K. Ochi, Y. Daigo, T. Katagiri, H. Kawano, H. Kawaguchi, A. Myoui, H. Yoshikawa, N. Naka, N. Araki, I. Kudawara, M. Ieguchi, K. Nakamura, Y. Nakamura, and K. Matsuda. 2009. Orphan receptor tyrosine kinase ROR2 as a potential therapeutic target for osteosarcoma. *Cancer Sci*. 100:1227–1233. doi:10.1111/j.1349-7006.2009.01165.x.
- Moro, E., G. Ozhan-Kizil, A. Mongera, D. Beis, C. Wierzbicki, R.M. Young, D. Bournele, A. Domenichini, L.E. Valdivia, L. Lum, C. Chen, J.F. Amatruda, N. Tiso, G. Weidinger, and F. Argenton. 2012. In vivo Wnt signaling tracing through a transgenic biosensor fish reveals novel activity domains. *Dev. Biol*. 366:327–340.

doi:10.1016/j.ydbio.2012.03.023.

- Mulligan, K.A., C. Fuerer, W. Ching, M. Fish, K. Willert, and R. Nusse. 2012. Secreted Wntless-interacting molecule (Swim) promotes long-range signaling by maintaining Wntless solubility. *Proc. Natl. Acad. Sci.* 109:370–377. doi:10.1073/pnas.1119197109.
- Munoz-Sanjuan, I., and A.H. Brivanlou. 2002. Neural induction, the default model and embryonic stem cells. *Nat. Rev. Neurosci.* 3:271–280. doi:10.1038/nrn786.
- Nalbant, P., L. Hodgson, V. Kraynov, A. Toutchkine, and K.M. Hahn. 2004. Activation of endogenous Cdc42 visualized in living cells. *Science* (80-.). 305:1615–1619. doi:10.1126/science.1100367.
- Naschberger, A., A. Orry, S. Lechner, M.W. Bowler, D. Nurizzo, M. Novokmet, M.A. Keller, G. Oemer, D. Seppi, M. Haslbeck, K. Pansi, H. Dieplinger, and B. Rupp. 2017. Structural Evidence for a Role of the Multi-functional Human Glycoprotein Afamin in Wnt Transport. *Structure*. 25:1907–1915.e5. doi:10.1016/j.str.2017.10.006.
- Nasevicius, A., and S.C. Ekker. 2000. Effective targeted gene “knockdown” in zebrafish. *Nat. Genet.* 26:216–220. doi:10.1038/79951.
- Neumann, S., D.Y.M. Coudreuse, D.R. van der Westhuyzen, E.R.M. Eckhardt, H.C. Korswagen, G. Schmitz, and H. Sprong. 2009. Mammalian Wnt3a is released on lipoprotein particles. *Traffic*. 10:334–343. doi:10.1111/j.1600-0854.2008.00872.x.
- Niehrs, C. 2012. The complex world of WNT receptor signalling. *Nat. Rev. Mol. Cell Biol.* 13:767–79. doi:10.1038/nrm3470.
- Niemann, S., C. Zhao, F. Pascu, U. Stahl, U. Aulepp, L. Niswander, J.L. Weber, and U. Muller. 2004. Homozygous WNT3 mutation causes tetra-amelia in a large consanguineous family. *Am. J. Hum. Genet.* 74:558–563. doi:10.1086/382196.
- Nieuwkoop, P.D. 1997. Short historical survey of pattern formation in the endo-mesoderm and the neural anlage in the vertebrates: the role of vertical and planar inductive actions. *Cell. Mol. Life Sci.* 53:305–318.
- Nieuwkoop, P.D., and G. v. Nigtevecht. 1954. Neural Activation and Transformation in Explants of Competent Ectoderm under the Influence of Fragments of Anterior Notochord in Urodeles. *J. Embryol. Exp. Morphol.* 2:175 LP-193.
- Nile, A.H., and R.N. Hannoush. 2016. Fatty acylation of Wnt proteins. *Nat. Chem. Biol.* 12:60–69. doi:10.1038/nchembio.2005.
- Nishisho, I., Y. Nakamura, Y. Miyoshi, Y. Miki, H. Ando, A. Horii, K. Koyama, J. Utsunomiya, S. Baba, and P. Hedge. 1991. Mutations of chromosome 5q21 genes in FAP and colorectal cancer patients. *Science*. 253:665–669.
- Nishita, M., M. Enomoto, K. Yamagata, and Y. Minami. 2010a. Cell/tissue-tropic functions of Wnt5a signaling in normal and cancer cells. *Trends Cell Biol.* 20:346–354. doi:10.1016/j.tcb.2010.03.001.
- Nishita, M., S. Itsukushima, A. Nomachi, M. Endo, Z. Wang, D. Inaba, S. Qiao, S. Takada, A. Kikuchi, and Y. Minami. 2010b. Ror2/Frizzled complex mediates Wnt5a-induced AP-1 activation by regulating Dishevelled polymerization. *Mol. Cell. Biol.* 30:3610–

3619. doi:10.1128/MCB.00177-10.

- Nishita, M., S.Y. Park, T. Nishio, K. Kamizaki, Z. Wang, K. Tamada, T. Takumi, R. Hashimoto, H. Otani, G.J. Pazour, V.W. Hsu, and Y. Minami. 2017. Ror2 Signaling regulates Golgi structure and transport through IFT20 for tumor invasiveness. *Sci. Rep.* 7:1–15. doi:10.1038/s41598-016-0028-x.
- Nishita, M., K.Y. Sa, A. Nomachi, S. Kani, N. Sougawa, Y. Ohta, S. Takada, A. Kikuchi, and Y. Minami. 2006. Filopodia formation mediated by receptor tyrosine kinase Ror2 is required for Wnt5a-induced cell migration. *J. Cell Biol.* 175:555–562. doi:10.1083/jcb.200607127.
- Nomachi, A., M. Nishita, D. Inaba, M. Enomoto, M. Hamasaki, and Y. Minami. 2008. Receptor tyrosine kinase Ror2 mediates Wnt5a-induced polarized cell migration by activating c-Jun N-terminal kinase via actin-binding protein filamin A. *J. Biol. Chem.* 283:27973–27981. doi:10.1074/jbc.M802325200.
- Nordstrom, U., T.M. Jessell, and T. Edlund. 2002. Progressive induction of caudal neural character by graded Wnt signaling. *Nat. Neurosci.* 5:525–532. doi:10.1038/nn854.
- Nusse, R., A. Brown, J. Papkoff, P. Scambler, G. Shackelford, A. McMahon, R. Moon, and H. Varmus. 1991. A new nomenclature for int-1 and related genes: the Wnt gene family. *Cell.* 64:231.
- Nusse, R., and H. Clevers. 2017. Wnt/ β -Catenin Signaling, Disease, and Emerging Therapeutic Modalities. *Cell.* 169:985–999. doi:10.1016/j.cell.2017.05.016.
- Nusse, R., and H.E. Varmus. 1982. Many tumors induced by the mouse mammary tumor virus contain a provirus integrated in the same region of the host genome. *Cell.* 31:99–109.
- Nüsslein-Volhard, C., and R. Dahm. 2002. Zebrafish: a practical approach. Oxford University Press, Oxford.
- O’Connell, M.P., J.L. Fiori, M. Xu, A.D. Carter, B.P. Frank, T.C. Camilli, A.D. French, S.K. Dissanayake, F.E. Indig, M. Bernier, D.D. Taub, S.M. Hewitt, and A.T. Weeraratna. 2010. The orphan tyrosine kinase receptor, ROR2, mediates Wnt5A signaling in metastatic melanoma. *Oncogene.* 29:34–44. doi:10.1038/onc.2009.305.
- Obrador-Hevia, A., S.-F. Chin, S. Gonzalez, J. Rees, F. Vilardell, J.K. Greenson, D. Cordero, V. Moreno, C. Caldas, and G. Capella. 2010. Oncogenic KRAS is not necessary for Wnt signalling activation in APC-associated FAP adenomas. *J. Pathol.* 221:57–67. doi:10.1002/path.2685.
- Ohkawara, B., and C. Niehrs. 2011. An ATF2-based luciferase reporter to monitor non-canonical Wnt signaling in xenopus embryos. *Dev. Dyn.* 240:188–194. doi:10.1002/dvdy.22500.
- Oishi, I., H. Suzuki, N. Onishi, R. Takada, S. Kani, B. Ohkawara, I. Koshida, K. Suzuki, G. Yamada, G.C. Schwabe, S. Mundlos, H. Shibuya, S. Takada, and Y. Minami. 2003. The receptor tyrosine kinase Ror2 is involved in non-canonical Wnt5a/JNK signalling pathway. *Genes to Cells.* 8:645–654. doi:10.1046/j.1365-2443.2003.00662.x.
- Okada, A., R. Lansford, J.M. Weimann, S.E. Fraser, and S.K. McConnell. 1999. Imaging

- cells in the developing nervous system with retrovirus expressing modified green fluorescent protein. *Exp. Neurol.* 156:394–406. doi:10.1006/exnr.1999.7033.
- Onfelt, B., S. Nedvetzki, R.K.P. Benninger, M.A. Purbhoo, S. Sowinski, A.N. Hume, M.C. Seabra, M.A.A. Neil, P.M.W. French, and D.M. Davis. 2006. Structurally Distinct Membrane Nanotubes between Human Macrophages Support Long-Distance Vesicular Traffic or Surfing of Bacteria. *J. Immunol.* 177:8476–8483. doi:10.4049/jimmunol.177.12.8476.
- Panáková, D., H. Sprong, E. Marois, C. Thiele, and S. Eaton. 2005. Lipoprotein particles are required for Hedgehog and Wingless signalling. *Nature.* 435:58–65. doi:10.1038/nature03504.
- Pasquier, J., B.S. Guerrouahen, H. Al Thawadi, P. Ghiabi, M. Maleki, N. Abu-Kaoud, A. Jacob, M. Mirshahi, L. Galas, S. Rafii, F. Le Foll, and A. Rafii. 2013. Preferential transfer of mitochondria from endothelial to cancer cells through tunneling nanotubes modulates chemoresistance. *J. Transl. Med.* 11:1. doi:10.1186/1479-5876-11-94.
- Philipp, I., S. Pontasch, M. Jenewein, H. Watanabe, R. Aufschnaiter, S. Ozbek, F. Rentzsch, T.W. Holstein, and B. Hobmayer. 2008. Wnt/ β -Catenin and noncanonical Wnt signaling interact in tissue evagination in the simple eumetazoan Hydra.
- Pinto, D., A. Gregorieff, H. Begthel, and H. Clevers. 2003. Canonical Wnt signals are essential for homeostasis of the intestinal epithelium. *Genes Dev.* 17:1709–1713. doi:10.1101/gad.267103.
- Port, F., and K. Basler. 2010. Wnt Trafficking: New Insights into Wnt Maturation, Secretion and Spreading. *Traffic.* 11:1265–1271. doi:10.1111/j.1600-0854.2010.01076.x.
- Port, F., M. Kuster, P. Herr, E. Furger, C. Banziger, G. Hausmann, and K. Basler. 2008. Wingless secretion promotes and requires retromer-dependent cycling of Wntless. *Nat. Cell Biol.* 10:178–185. doi:10.1038/ncb1687.
- Postlethwait, J.H., I.G. Woods, P. Ngo-Hazelett, Y.L. Yan, P.D. Kelly, F. Chu, H. Huang, A. Hill-Force, and W.S. Talbot. 2000. Zebrafish comparative genomics and the origins of vertebrate chromosomes. *Genome Res.* 10:1890–1902.
- Pröls, F., Sagar, and M. Scaal. 2016. Signaling filopodia in vertebrate embryonic development. *Cell. Mol. Life Sci.* 73:961–974. doi:10.1007/s00018-015-2097-6.
- Qian, D., C. Jones, A. Rzadzinska, S. Mark, X. Zhang, K.P. Steel, X. Dai, and P. Chen. 2007. Wnt5a functions in planar cell polarity regulation in mice. *Dev. Biol.* 306:121–133. doi:10.1016/j.ydbio.2007.03.011.
- Ramírez-Weber, F.A., and T.B. Kornberg. 1999. Cytonemes: Cellular processes that project to the principal signaling center in *Drosophila* imaginal discs. *Cell.* 97:599–607. doi:10.1016/S0092-8674(00)80771-0.
- Rhinn, M., K. Lun, M. Luz, M. Werner, and M. Brand. 2005. Positioning of the midbrain-hindbrain boundary organizer through global posteriorization of the neuroectoderm mediated by Wnt8 signaling. *Development.* 132:1261–1272. doi:10.1242/dev.01685.
- Rhinn, M., A. Picker, and M. Brand. 2006. Global and local mechanisms of forebrain and midbrain patterning. *Curr. Opin. Neurobiol.* 16:5–12. doi:10.1016/j.conb.2006.01.005.

- Ridley, A.J., M.A. Schwartz, K. Burridge, R.A. Firtel, M.H. Ginsberg, G. Borisy, J.T. Parsons, and A.R. Horwitz. 2003. Cell migration: integrating signals from front to back. *Science*. 302:1704–1709. doi:10.1126/science.1092053.
- Roarty, K., A.D. Pfefferle, C.J. Creighton, C.M. Perou, and J.M. Rosen. 2017. Ror2-mediated alternative Wnt signaling regulates cell fate and adhesion during mammary tumor progression. *Oncogene*. 36:5958–5968. doi:10.1038/onc.2017.206.
- De Robertis, E.M. 2006. Spemann’s organizer and self-regulation in amphibian embryos. *Nat. Rev. Mol. Cell Biol.* 7:296–302. doi:10.1038/nrm1855.
- De Robertis, E.M., and H. Kuroda. 2004. Dorsal-ventral patterning and neural induction in *Xenopus* embryos. *Annu. Rev. Cell Dev. Biol.* 20:285–308. doi:10.1146/annurev.cellbio.20.011403.154124.
- Roesch, K., A.P. Jadhav, J.M. Trimarchi, M.B. Stadler, B. Roska, B.B. Sun, and C.L. Cepko. 2008. The transcriptome of retinal Muller glial cells. *J. Comp. Neurol.* 509:225–238. doi:10.1002/cne.21730.
- Roy, S., F. Hsiung, and T.B. Kornberg. 2011. Specificity of *Drosophila* Cytonemes. *Science* (80-.). 354–358. doi:10.1126/science.1198949.
- Rustom, A., R. Saffrich, I. Markovic, P. Walther, and H.H. Gerdes. 2004. Nanotubular Highways for Intercellular Organelle Transport. *Science* (80-.). 303:1007–1010. doi:10.1126/science.1093133.
- Sagar, F. Prols, C. Wiegrefte, and M. Scaal. 2015. Communication between distant epithelial cells by filopodia-like protrusions during embryonic development. *Development*. 142:665–671. doi:10.1242/dev.115964.
- Sailaja, B.S., X.C. He, and L. Li. 2016. The regulatory niche of intestinal stem cells. *J. Physiol.* 594:4827–4836. doi:10.1113/JP271931.
- Sanders, T. a, E. Llagostera, and M. Barna. 2013. Specialized filopodia direct long-range transport of SHH during vertebrate tissue patterning. *Nature*. 497:628–32. doi:10.1038/nature12157.
- Sasai, Y., B. Lu, H. Steinbeisser, D. Geissert, L.K. Gont, and E.M. De Robertis. 1994. *Xenopus* chordin: a novel dorsalizing factor activated by organizer-specific homeobox genes. *Cell*. 79:779–790.
- Sasai, Y., and E.M. De Robertis. 1997. Ectodermal patterning in vertebrate embryos. *Dev. Biol.* 182:5–20. doi:10.1006/dbio.1996.8445.
- Sato, A., H. Yamamoto, H. Sakane, H. Koyama, and A. Kikuchi. 2010. Wnt5a regulates distinct signalling pathways by binding to Frizzled2. *EMBO J.* 29:41–54. doi:10.1038/emboj.2009.322.
- Sato, M., and T.B. Kornberg. 2002. FGF is an essential mitogen and chemoattractant for the air sacs of the *Drosophila* tracheal system. *Dev. Cell*. 3:195–207. doi:10.1016/S1534-5807(02)00202-2.
- Schambony, A., and D. Wedlich. 2007. Wnt-5A/Ror2 Regulate Expression of XPAPC through an Alternative Noncanonical Signaling Pathway. *Dev. Cell*. 12:779–792.

doi:10.1016/j.devcel.2007.02.016.

- Schlessinger, K., A. Hall, and N. Tolwinski. 2009. Wnt signaling pathways meet Rho GTPases. *Genes Dev.* 23:265–277. doi:10.1101/gad.1760809.
- Scholpp, S., A. Delogu, J. Gilthorpe, D. Peukert, S. Schindler, and A. Lumsden. 2009. Her6 regulates the neurogenetic gradient and neuronal identity in the thalamus. *Proc. Natl. Acad. Sci. U. S. A.* 106:19895–19900. doi:10.1073/pnas.0910894106.
- Seaman, M.N.J. 2005. Recycle your receptors with retromer. *Trends Cell Biol.* 15:68–75. doi:10.1016/j.tcb.2004.12.004.
- Shafer, B., K. Onishi, C. Lo, G. Colakoglu, and Y. Zou. 2011. Vangl2 promotes Wnt/planar cell polarity-like signaling by antagonizing Dvl1-mediated feedback inhibition in growth cone guidance. *Dev. Cell.* 20:177–191. doi:10.1016/j.devcel.2011.01.002.
- Smutny, M., Z. Akos, S. Grigolon, S. Shamipour, V. Ruprecht, D. Capek, M. Behrndt, E. Papusheva, M. Tada, B. Hof, T. Vicsek, G. Salbreux, and C.-P. Heisenberg. 2017. Friction forces position the neural anlage. *Nat. Cell Biol.* 19:306–317. doi:10.1038/ncb3492.
- Sougata Roy, T.B.K. 2015. Paracrine signaling mediated at cell-cell contacts. 54:1831–1840. doi:10.1021/acs.biochem.5b00087.
- Souren, M., J.R. Martinez-Morales, P. Makri, B. Wittbrodt, and J. Wittbrodt. 2009. A global survey identifies novel upstream components of the Ath5 neurogenic network. *Genome Biol.* 10:1–16. doi:10.1186/gb-2009-10-9-r92.
- Sowinski, S., C. Jolly, O. Berninghausen, M.A. Purbhoo, A. Chauveau, K. Köhler, S. Oddos, P. Eissmann, F.M. Brodsky, C. Hopkins, B. Önfelt, Q. Sattentau, and D.M. Davis. 2008. Membrane nanotubes physically connect T cells over long distances presenting a novel route for HIV-1 transmission. *Nat. Cell Biol.* 10:211–219. doi:10.1038/ncb1682.
- Spemann, H., and H. Mangold. 2001. Induction of embryonic primordia by implantation of organizers from a different species. 1923. *Int. J. Dev. Biol.* 45:13–38.
- Stanganello, E., A.I.H. Hagemann, B. Mattes, C. Sinner, D. Meyen, S. Weber, A. Schug, E. Raz, and S. Scholpp. 2015. Filopodia-based Wnt transport during vertebrate tissue patterning. *Nat. Commun.* 6:5846.
- Stanganello, E., and S. Scholpp. 2016. Role of cytonemes in Wnt transport. *J. Cell Sci.* 1–8. doi:10.1242/jcs.182469.
- Stern, C.D. 2005. Neural induction: old problem, new findings, yet more questions. *Development.* 132:2007–21. doi:10.1242/dev.01794.
- Stricker, S., V. Rauschenberger, and A. Schambony. 2017. ROR-Family Receptor Tyrosine Kinases. *Curr. Top. Dev. Biol.* 123:105–142. doi:10.1016/BS.CTDB.2016.09.003.
- Surviladze Z , Waller A, J.J. 2010. A Potent and Selective Inhibitor of Cdc42 GTPase
Authors : UNM Center for Molecular Discovery : Zurab Surviladze , Anna Waller , J .
Jacob Assigned Assay Grant #: MH081231-01 Screening Center Name & PI : UNM
Center for Molecular Disco. *Probe Rep.* 1–27. doi:NBK51965 [bookaccession].

- Tada, M., and C.-P. Heisenberg. 2012. Convergent extension: using collective cell migration and cell intercalation to shape embryos. *Development*. 139:3897–3904. doi:10.1242/dev.073007.
- Takada, R., Y. Satomi, T. Kurata, N. Ueno, S. Norioka, H. Kondoh, T. Takao, and S. Takada. 2006. Monounsaturated fatty acid modification of Wnt protein: its role in Wnt secretion. *Dev. Cell*. 11:791–801. doi:10.1016/j.devcel.2006.10.003.
- Takada, S., S. Fujimori, T. Shinozuka, R. Takada, and Y. Mii. 2017. Differences in the secretion and transport of Wnt proteins. *J. Biochem*. 161:1–7. doi:10.1093/jb/mvw071.
- Takeuchi, S., K. Takeda, I. Oishi, M. Nomi, M. Ikeya, K. Itoh, S. Tamura, T. Ueda, T. Hatta, H. Otani, T. Terashima, S. Takada, H. Yamamura, S. Akira, and Y. Minami. 2000. Mouse Ror2 receptor tyrosine kinase is required for the heart development and limb formation. *Genes to Cells*. 5:71–78. doi:10.1046/j.1365-2443.2000.00300.x.
- Takiguchi, G., M. Nishita, K. Kurita, Y. Kakeji, and Y. Minami. 2015. Wnt5a-Ror2 signaling in mesenchymal stem cells promotes proliferation of gastric cancer cells by activating CXCL16-CXCR6 axis. *Cancer Sci*. 1–8. doi:10.1111/cas.12871.
- Tammela, T., F.J. Sanchez-Rivera, N.M. Cetinbas, K. Wu, N.S. Joshi, K. Helenius, Y. Park, R. Azimi, N.R. Kerper, R.A. Wesselhoeft, X. Gu, L. Schmidt, M. Cornwall-Brady, O.H. Yilmaz, W. Xue, P. Katajisto, A. Bhutkar, and T. Jacks. 2017. A Wnt-producing niche drives proliferative potential and progression in lung adenocarcinoma. *Nature*. 545:355–359. doi:10.1038/nature22334.
- Tang, X., Y. Wu, T.Y. Belenkaya, Q. Huang, L. Ray, J. Qu, and X. Lin. 2012. Roles of N-glycosylation and lipidation in Wg secretion and signaling. *Dev. Biol*. 364:32–41. doi:10.1016/j.ydbio.2012.01.009.
- Tassew, N.G., J. Charish, A.P. Shabanzadeh, V. Luga, H. Harada, N. Farhani, P. D’Onofrio, B. Choi, A. Ellabban, P.E.B. Nickerson, V.A. Wallace, P.D. Koeberle, J.L. Wrana, and P.P. Monnier. 2017. Exosomes Mediate Mobilization of Autocrine Wnt10b to Promote Axonal Regeneration in the Injured CNS. *Cell Rep*. 20:99–111. doi:10.1016/j.celrep.2017.06.009.
- Teddy, J.M. 2004. In vivo evidence for short- and long-range cell communication in cranial neural crest cells. *Development*. 131:6141–6151. doi:10.1242/dev.01534.
- Thompson, D.W. 1992. *On Growth and Form*. Cambridge University Press, Cambridge.
- Turing, A. 1952. The chemical basis of morphogenesis. *Philos. Trans. R. Soc. Lond. B. Biol. Sci*. 237:37 LP-72.
- Valenta, T., B. Degirmenci, A.E. Moor, P. Herr, D. Zimmerli, M.B. Moor, G. Hausmann, C. Cantù, M. Aguet, and K. Basler. 2016. Wnt Ligands Secreted by Subepithelial Mesenchymal Cells Are Essential for the Survival of Intestinal Stem Cells and Gut Homeostasis. *Cell Rep*. 15:911–918. doi:10.1016/j.celrep.2016.03.088.
- Veeman, M.T., J.D. Axelrod, and R.T. Moon. 2003. A second canon. Functions and mechanisms of beta-catenin-independent Wnt signaling. *Dev. Cell*. 5:367–377.
- Voloshanenko, O., P. Gmach, J. Winter, D. Kranz, and M. Boutros. 2017. Mapping of Wnt-Frizzled interactions by multiplex CRISPR targeting of receptor gene families. *FASEB*

- J.* 31:4832–4844. doi:10.1096/fj.201700144R.
- Voronkov, A., and S. Krauss. 2013. Wnt/beta-catenin signaling and small molecule inhibitors. *Curr. Pharm. Des.* 19:634–64. doi:10.2174/138161213804581837.
- Waddington, C.H. 1936. Organizers in Mammalian Development. *Nature.* 138:125.
- Wallingford, J.B., and R. Habas. 2005. The developmental biology of Dishevelled: an enigmatic protein governing cell fate and cell polarity. *Development.* 132:4421–4436. doi:10.1242/dev.02068.
- Wallkamm, V., R. Dörlich, K. Rahm, T. Klessing, U. Nienhaus, W. Doris, and D. Gradl. 2014. Live imaging of Xwnt5A-ROR2 complexes. *PLoS One.* 9:1–9. doi:10.1371/journal.pone.0109428.
- Wallkamm, V., K. Rahm, J. Schmoll, L.T. Kaufmann, E. Brinkmann, J. Schunk, B. Kraft, D. Wedlich, and D. Gradl. 2016. Regulation of distinct branches of the non-canonical Wnt-signaling network in *Xenopus* dorsal marginal zone explants. *BMC Biol.* 14:55. doi:10.1186/s12915-016-0278-x.
- Wang, X., and H.H. Gerdes. 2015. Transfer of mitochondria via tunneling nanotubes rescues apoptotic PC12 cells. *Cell Death Differ.* 22:1181–1191. doi:10.1038/cdd.2014.211.
- Wang, X., V. Reid Sutton, J. Omar Peraza-Llanes, Z. Yu, R. Rosetta, Y.-C. Kou, T.N. Eble, A. Patel, C. Thaller, P. Fang, and I.B. Van den Veyver. 2007. Mutations in X-linked PORCN, a putative regulator of Wnt signaling, cause focal dermal hypoplasia. *Nat. Genet.* 39:836–838. doi:10.1038/ng2057.
- Wang, X., M.L. Veruki, N. V. Bukoreshtliev, E. Hartveit, and H.-H. Gerdes. 2010. Animal cells connected by nanotubes can be electrically coupled through interposed gap-junction channels. *Proc. Natl. Acad. Sci.* 107:17194–17199. doi:10.1073/pnas.1006785107.
- Weeraratna, A.T., Y. Jiang, G. Hostetter, K. Rosenblatt, P. Duray, M. Bittner, and J.M. Trent. 2002. Wnt5a signaling directly affects cell motility and invasion of metastatic melanoma. *Cancer Cell.* 1:279–288.
- Willert, K., J.D. Brown, E. Danenberg, A.W. Duncan, I.L. Weissman, T. Reya, J.R. 3rd Yates, and R. Nusse. 2003. Wnt proteins are lipid-modified and can act as stem cell growth factors. *Nature.* 423:448–452. doi:10.1038/nature01611.
- Willert, K., and R. Nusse. 2012. Wnt proteins. *Cold Spring Harb. Perspect. Biol.* 4:1–13. doi:10.1101/cshperspect.a007864.
- Wilson, C., D.C. Goberdhan, and H. Steller. 1993. Dror, a potential neurotrophic receptor gene, encodes a *Drosophila* homolog of the vertebrate Ror family of Trk-related receptor tyrosine kinases. *Proc. Natl. Acad. Sci. U. S. A.* 90:7109–7113.
- Wilson, S.W., and C. Houart. 2004. Early Steps in the Development of the Forebrain. *Cell.* 6:167–181.
- Winkel, A., S. Stricker, P. Tylzanowski, V. Seiffart, S. Mundlos, G. Gross, and A. Hoffmann. 2008. Wnt-ligand-dependent interaction of TAK1 (TGF- β -activated kinase-1) with the receptor tyrosine kinase Ror2 modulates canonical Wnt-signalling. *Cell. Signal.*

20:2134–2144. doi:10.1016/j.cellsig.2008.08.009.

- Witte, F., O. Bernatik, K. Kirchner, J. Masek, A. Mahl, P. Krejci, S. Mundlos, A. Schambony, V. Bryja, and S. Stricker. 2010. Negative regulation of Wnt signaling mediated by CK1-phosphorylated Dishevelled via Ror2. *FASEB J.* 24:2417–2426. doi:10.1096/fj.09-150615.
- Wolpert, L. 1969. Positional information and the spatial pattern of cellular differentiation. *J. Theor. Biol.* 25:1–47.
- Wolpert, L. 1989. Positional information revisited. *Development.* 107 Suppl:3–12.
- Wong, G.T., B.J. Gavin, and A.P. McMahon. 1994. Differential transformation of mammary epithelial cells by Wnt genes. *Mol. Cell. Biol.* 14:6278–6286.
- Wong, H.-C., A. Bourdelas, A. Krauss, H.-J. Lee, Y. Shao, D. Wu, M. Mlodzik, D.-L. Shi, and J. Zheng. 2003. Direct binding of the PDZ domain of Dishevelled to a conserved internal sequence in the C-terminal region of Frizzled. *Mol. Cell.* 12:1251–1260.
- Wright, T.M., A.R. Brannon, J.D. Gordan, A.J. Mikels, C. Mitchell, S. Chen, I. Espinosa, M. van de Rijn, R. Pruthi, E. Wallen, L. Edwards, R. Nusse, and W.K. Rathmell. 2009. Ror2, a developmentally regulated kinase, promotes tumor growth potential in renal cell carcinoma. *Oncogene.* 28:2513–2523. doi:10.1038/onc.2009.116.
- Yamamoto, S., O. Nishimura, K. Misaki, M. Nishita, Y. Minami, S. Yonemura, H. Tarui, and H. Sasaki. 2008. Cthrc1 Selectively Activates the Planar Cell Polarity Pathway of Wnt Signaling by Stabilizing the Wnt-Receptor Complex. *Dev. Cell.* 15:23–36. doi:10.1016/j.devcel.2008.05.007.
- Yan, D., and X. Lin. 2009. Shaping morphogen gradients by proteoglycans. *Cold Spring Harb. Perspect. Biol.* 1:a002493. doi:10.1101/cshperspect.a002493.
- Yan, L., Q. Du, J. Yao, and R. Liu. 2016. ROR2 inhibits the proliferation of gastric carcinoma cells via activation of non-canonical Wnt signaling. *Exp. Ther. Med.* 12:4128–4134. doi:10.3892/etm.2016.3883.
- Yeh, T.C., W. Ogawa, A.G. Danielsen, and R.A. Roth. 1996. Characterization and cloning of a 58/53-kDa substrate of the insulin receptor tyrosine kinase. *J Biol Chem.* 271:2921–2928.
- Yoshikawa, S., R.D. McKinnon, M. Kokel, and J.B. Thomas. 2003. Wnt-mediated axon guidance via the Drosophila Derailed receptor. *Nature.* 422:583–588. doi:10.1038/nature01522.
- Young, T., Y. Poobalan, E.K. Tan, S. Tao, S. Ong, P. Wehner, J. Schwenty-Lara, C.Y. Lim, A. Sadasivam, M. Lovatt, S.T. Wang, Y. Ali, A. Borchers, K. Sampath, and N.R. Dunn. 2014. The PDZ domain protein Mcc is a novel effector of non-canonical Wnt signaling during convergence and extension in zebrafish. *Development.* 141:3505–16. doi:10.1242/dev.114033.
- Yu, J., J. Chia, C.A. Canning, C.M. Jones, F.A. Bard, and D.M. Virshup. 2014. WLS Retrograde transport to the endoplasmic reticulum during Wnt secretion. *Dev. Cell.* 29:277–291. doi:10.1016/j.devcel.2014.03.016.

- Yu, J., and D.M. Virshup. 2014. Updating the Wnt pathways. *Biosci. Rep.* 34:593–607. doi:10.1042/BSR20140119.
- Yuan, Y., C.C. Niu, G. Deng, Z.Q. Li, J. Pan, C. Zhao, Z.L. Yang, and W.K. Si. 2011. The Wnt5a/Ror2 noncanonical signaling pathway inhibits canonical Wnt signaling in K562 cells. *Int. J. Mol. Med.* 27:63–69. doi:10.3892/ijmm.2010.560.
- Zecca, M., K. Basler, and G. Struhl. 1996. Direct and long-range action of a wingless morphogen gradient. *Cell.* 87:833–844.
- Zhu, S., G.S. Victoria, L. Marzo, R. Ghosh, and C. Zurzolo. 2015. Prion aggregates transfer through tunneling nanotubes in endocytic vesicles. *Prion.* 9:125–135. doi:10.1080/19336896.2015.1025189.